



HAL
open science

Role of pyoverdine and pyochelin siderophores in the homeostasis of biological metals different than iron in *Pseudomonas aeruginosa*

Ana Yaiza Carballido Lopez

► **To cite this version:**

Ana Yaiza Carballido Lopez. Role of pyoverdine and pyochelin siderophores in the homeostasis of biological metals different than iron in *Pseudomonas aeruginosa*. Biochemistry [q-bio.BM]. Université de Strasbourg, 2018. English. NNT : 2018STRAJ008 . tel-01820660

HAL Id: tel-01820660

<https://theses.hal.science/tel-01820660>

Submitted on 22 Jun 2018

HAL is a multi-disciplinary open access archive for the deposit and dissemination of scientific research documents, whether they are published or not. The documents may come from teaching and research institutions in France or abroad, or from public or private research centers.

L'archive ouverte pluridisciplinaire **HAL**, est destinée au dépôt et à la diffusion de documents scientifiques de niveau recherche, publiés ou non, émanant des établissements d'enseignement et de recherche français ou étrangers, des laboratoires publics ou privés.

UNIVERSITÉ DE STRASBOURG
École doctorale des Sciences de la Vie et de la Santé
UMR-7242. Métaux et microorganismes: biologie, chimie et applications

THÈSE

Présentée par **Ana Yaiza Carballido López**

Rôle des voies d'import du fer impliquant des sidérophores dans l'homéostasie de métaux biologiques autres que le fer chez *Pseudomonas aeruginosa*

Soutenue le 15 février 2018 pour obtenir le grade de
Docteur de l'Université de Strasbourg
Discipline: Sciences du vivant
Spécialité: Aspects cellulaires et moléculaires de la biologie

Thèse dirigée par:

Dr. Isabelle SCHALK Directeur de Recherche, Université de Strasbourg

Rapporteurs:

Dr. Philippe DELEPELAIRE Directeur de Recherche, Université Paris Diderot
Dr. Romé VOULHOUX Directeur de Recherche, Aix-Marseille Université

Autres membres du jury:

Dr. Agnès RODRIGUE Maître de Conférence, INSA, Lyon
Dr. Myriam SEEMANN Directeur de Recherche, Université de Strasbourg
Dr. Pierre FECHTER Chargé de Recherche, Université de Strasbourg

This Thesis was funded by the IdEx (Initiative of excellence for foreigners) 2014, belonging to the University of Strasbourg.

Acknowledgments

The last three years working on this PhD thesis have been responsible of many 'firsts' to me: the first time living in a foreign country, in my own first apartment, as well as the first work experience... not mentioning the new language. Putting in short, just a completely new life. I came here packed with motivation and enthusiasm, and even though it has been much harder than I could have ever expected, I have been lucky enough not to be alone during this whole process, and both in the laboratory and back home, coming from one country or another, I have received loads of support and advice from you all.

Mes remerciements vont en premier lieu aux membres du jury, au Dr. Philippe Delepelaire et au Dr. Romé Voulhoux pour avoir accepté de juger ce travail, ainsi qu'au Dr. Myriam Seemann et au Dr. Agnès Rodrigue de me faire l'honneur de l'examiner.

Isabelle, si je suis ici c'est grâce à toi. Tu m'as donné l'opportunité de découvrir le monde de la recherche. Merci pour tout le temps que tu m'as consacré. Pierre, tu as toujours été là pour moi. Merci pour ta compréhension, ton soutien et ta patience. Merci pour tout le temps que tu m'as accordé, les réflexions et discussions qu'on a partagé, et pour ton aide. En définitive, merci pour tout. Merci à tous mes collègues du laboratoire, pour les discussions, pour l'aide et pour les bons moments : Olivier, Béatrice, Géraldine, Beata, Véronique, Karl, Valérie, Anne F, Gaëtan, Françoise, Sébastien, Quentin, Anne B, Denis, Nicolas, Mathilde, Gwenaëlle, et bien sûr Aurélie qui est devenue une bonne amie.

No puedo olvidarme de mis amigos, tanto cercanos como lejanos. A todos los que me fueron manteniendo a flote, y con los que he compartido mi vida durante este tiempo. Andrea, qué haría yo sin ti durante estos tres años, has sido de los mejores descubrimientos de este periodo. Gracias a vosotras, mis chicas biólogas, Irene, Alba, Sandra y Grecia, por las risas y los cotilleos, sin olvidarnos de los momentos de desahogo. Mery (my little English helper), Carla, Tere y Jaime, que desde la distancia me habéis mostrado que puedo seguir contando con vosotros.

À miña terra, por permitirme sentir paz e recargar a ialma en cada visita.

Merci Loïc, pour dessiner un sourire sur mon visage tous les jours, et pour les meilleurs câlins du monde entier.

Gracias por supuesto a mi familia, especialmente a mis padres y a mi abuela, sin olvidarme de Gus. Soy la persona que soy a día de hoy gracias a vosotros. Me habéis dado todo el amor y el

apoyo que uno puede pedir, y habéis hecho todo lo que está en vuestra mano para que pueda perseguir mis inquietudes y sueños. Sé que ha sido difícil vivir a más de 1500 km, pero aún en la distancia siempre hemos permanecido juntos.

Table of contents

General introduction	1
Introduction	
Part 1. <i>Pseudomonas aeruginosa</i>	5
1. <i>P. aeruginosa</i> characteristics	6
2. <i>P. aeruginosa</i> as a pathogen	7
3. <i>P. aeruginosa</i> life forms	9
Part 2. Biological metals in bacteria, with focus on <i>P. aeruginosa</i>	11
1. Metals in living organisms	12
2. Importance of transition metals	13
3. Biological metals in bacteria	14
4. Biological metals in <i>P. aeruginosa</i>	17
5. Biological metal uptake strategies used by bacteria, and specifically by <i>P. aeruginosa</i>	20
6. Metal toxicity in bacteria	26
7. Bacterial resistance against metal toxicity	28
Part 3. Siderophores and other metals chelators	35
1. Siderophores	46
2. Siderophores in iron transport.....	47
3. <i>P. aeruginosa</i> siderophores	43
3.1. Pyoverdine (PVD).....	44
3.2. Pyochelin (PCH).....	49
4. Different roles of siderophores	53
5. Other metallophores.....	55
Part 4. Regulation mechanisms of siderophore-mediated iron uptake pathways in <i>P. aeruginosa</i>	57
1. Positive feedback loops.....	58
2. Repression of siderophore expression	63
3. Iron storage	64

4. Other signal inducing siderophore production regulation	65
--	----

<i>Objectives</i>	67
-------------------------	----

<i>Chapter 1. The pathogen <i>P. aeruginosa</i> takes the advantages but avoids the inconveniences of the positive auto-regulation of its major siderophores PVD and PCH production.....</i>	<i>69</i>
--	-----------

1. Introduction	73
2. Results	77
3. Discussion	85
4. Materials and methods	91
5. References	96
6. Figures and graphics	100
7. Tables	105
8. Supplementary material	108

<i>Chapter 2. PVD and PCH siderophores in the homeostasis of biological metals different than iron in <i>P. aeruginosa</i></i>	<i>111</i>
--	------------

1. Results	113
2. Discussion	145
3. Supplementary material	153
4. Material and methods	161

<i>Conclusions</i>	<i>175</i>
--------------------------	------------

<i>References</i>	<i>179</i>
-------------------------	------------

Tables and figures

Introduction

Figure 1. Electron micrograph of biofilm-forming <i>P. aeruginosa</i> bacteria	6
Figure 2. Images of <i>P. aeruginosa</i> cystic fibrosis isolates	6
Figure 3. Percentage (%) of <i>P. aeruginosa</i> MDR in EU/EEA countries	8
Figure 4. Biofilm formation and development	10
Figure 5. Periodic table.....	13
Figure 6. This figure shows (A) the number of atoms per CFU of <i>P. aeruginosa</i> PAO1 cells, and (B) the concentrating factor for each metal in <i>P. aeruginosa</i> PAO1 cells	18
Figure 7. Metal content of <i>P. aeruginosa</i> cells grown in LB, succinate or CAA media as determined by ICP-AES	19
Figure 8. Ferrous iron transport (A) and heme transport by the Phu, the Has and the Hxu heme acquisition systems (B) in <i>P. aeruginosa</i>	22
Figure 9. Proteins involved in the biological transition metals uptake in <i>Pseudomonas spp</i>	25
Figure 10. Fenton reaction.....	25
Figure 11. Mechanism of bacteria protection against metal toxicity	28
Figure 12. Transition metal ions efflux in <i>Pseudomonas spp</i>	30
Figure 13. Families of transcriptional regulators involved in biological metals homeostasis in bacteria.	33
Figure 14. Different families of siderophores	37
Figure 15. Schematic and space filling structures of enterobactin (A) and enterobactin-Fe complex (B).....	38
Figure 16. Structure of the enterobactin TBDT transporter FepA	39
Figure 17. A: Structural model for the TonB complex, which consists of a pentamer of ExbB, a dimer of ExbD, and at least one TonB. B: Ferric iron transport into bacteria (<i>E. coli</i>) via siderophore uptake pathway	40
Figure 18. Different mechanisms and strategies of siderophore-Fe uptake and dissociation in Gram-negative bacteria	42
Figure 19. Structure of PVDI	45
Figure 20. A: Pyoverdine (PVDI) cytoplasmic precursor biosynthesis pathway in <i>P. aeruginosa</i> . B: Steps of PVDI assembling carried out in the siderosome.....	47
Figure 21. PVD iron uptake pathway in <i>P. aeruginosa</i>	49
Figure 22. Structure of PCHI (A) and PCHII (B).....	60
Figure 23. PCH-Fe complex tetra-coordinated with nitrogen (blue) and oxygen (red) groups.	60
Figure 24. Biosynthesis of PCH in <i>Pseudomonas aeruginosa</i>	61
Figure 25. (A) FpyA structure (B) Amino acids of FptA binding site interacting with PCH-Fe....	62

Figure 26. PCH iron uptake pathway in <i>P. aeruginosa</i>	63
Figure 27. Mechanism of regulation of the PVD iron uptake pathway in <i>P. aeruginosa</i>	60
Figure 28. Mechanism of regulation of the PCH iron uptake pathway in <i>P. aeruginosa</i>	62
Table 1. Proteins containing cobalt.....	17
Table 2. Intracellular biological metals concentrations in <i>P. aeruginosa</i> PAO1	19
Table 3. Outer membrane transporters present in <i>P. aeruginosa</i> , associated to the siderophores used by <i>P. aeruginosa</i> to get access to iron.....	44

Chapter 1

Figure 1. PVD and PCH pathways are induced by specific transcription activators included into auto-inducing regulatory loops: the sigma/anti-sigma PvdS/FpvI/FpvR factors for PVD, the transcriptional regulator PchR for PCH.	99
Figure 2. Expression of genes from the PVD pathway in <i>wt</i> and in isogenic mutants.....	100
Figure 3. Expression of genes from the PCH pathway in <i>wt</i> and in isogenic mutants.....	100
Figure 4. Iron effect on the transcription of genes from the PVD and PCH pathways in <i>wt</i> and $\Delta pvdF$ strains.	101
Figure 5. Expression of genes from transcriptional fusion reporters of the PCH pathways in <i>wt</i> and the isogenic $\Delta pchR$ strains.....	101
Figure 6. Iron effect on the expression of genes from the PVD pathway	102
Figure 7. PvdA-eGFP expression in <i>wt</i> and PVD-deficient ($\Delta pvdF$) strains	102
Figure 8. Schematic representation of the regulation of PCH and PVD production.....	103
Figure S1. Production of PCH and PVD in different strains.....	107
Figure S2. Details on the transcriptional reporter constructs used, based on the <i>pvdS</i> , <i>fpvR</i> and <i>pchD</i> promoters	108
Figure S3. Detail on the genomic location of <i>pchR</i> and <i>pchD</i>	108
Figure S4. Schematic representation of the <i>phoPphoQ</i> and PVD positive auto-regulation loops.....	109
Table 1. Strains and plasmids used in this study	104
Table 2. Oligonucleotides used in this study	105

Chapter 2

Figure R1. PVD (A) and PCH (B) production by <i>P. aeruginosa</i> PAO1.....	115
Figure R2. PvdJ expression in <i>pvdJ-mCherry</i> cells grown in CAA medium in the absence and presence of different biological metals.....	117
Figure R3. PchA and FptX expression in <i>pchA-mCherry</i> and <i>fptX-mCherry</i> cells at 7 and 24 h growth in CAA medium in the absence and presence of different biological metals.	118

Figure R4. Transport of metals Fe, Co, Ni, Cu and Zn in complex with PCH in <i>P. aeruginosa</i> cells.....	121
Figure R5. Transport of metals Fe, Co, Ni, Cu and Zn in complex with PVD in <i>P. aeruginosa</i> cells.....	122
Figure R6. Metal transport of Fe, Co and Zn in free state and in complex with PCH in <i>P. aeruginosa</i> cells.....	123
Figure R7. Kinetic of intracellular ⁵⁵ Fe accumulation in <i>P. aeruginosa</i> cells in the presence of PCH ₂ -metal or PVD-metal complexes.	125
Figure R8. A: Affinity chromatogram profile of the MBP-PchR purified using the ‘MBP-Trap HP 5ml’ column in the ÄKTA System.....	126
Figure R9. A: Ionic exchange chromatogram of MBP-PchR purified using the ‘Mono Q™ 5/50 GL’ column in the ÄKTA System.....	127
Figure R10. Fluorescence emission spectra of MBP-PchR in the presence of different concentrations of apo-PCH (A), and PCH ₂ -Fe (B).	128
Figure R11. Stern-Volmer plot for apo-PCH, Fe and PCH ₂ -Fe binding to purified MBP-PchR protein.....	128
Figure R12. Stern-Volmer plot for apo-PCH, PCH ₂ -Fe and the different metals and PCH ₂ -metals tested binding affinities determination of MBP-PchR protein	129
Figure R13. Expression of mCherry in the presence of Fe (panel B and D) or Co (panel A and C) under the effect of different <i>pchD</i> promoter sequences carrying the Fur box and PchR box (blue), or just the Fur box (pink), in the pSEVA631 plasmid.....	132
Figure R14. PCH promoters alignment and identification of conserved sequences belong to the Fur box.....	133
Figure R15. PCH promoters alignment and identification of conserved sequences belong to the PchR box.	133
Figure R16. EMSA results of recognition between Fur-Co and specific DNA fragment, containing the Fur box of the <i>pchD</i> promoter (A), or containing the Fur box and the PchR of the <i>pchD</i> promoter (B).	134
Figure R17. PchR-mCherry expression at 12 h of growth in CAA medium, in the absence and presence of biological metals.	136
Figure R18. Interaction network created using the String tool (https://string-db.org/) including the repressed genes by the effect of Co.	140
Figure S1. PchR expression in <i>mCherry-pchR</i> cells grown in CAA medium, in presence of different concentrations of FeCl ₃ , CoCl ₂ , NiCl ₂ , CuCl ₂ , MnCl ₂ , and ZnCl ₂ added in the culture medium at the beginning of growth.....	154
Figure S2. PchR expression in <i>mCherry-pchR</i> cells grown in CAA medium, in presence of different concentrations of FeCl ₃ , CoCl ₂ , NiCl ₂ , CuCl ₂ , MnCl ₂ , and ZnCl ₂ added in the culture medium at the beginning of growth.....	156
Figure S3. Electrophoresis mobility shift assay (EMSA). Purified MBP-PchR recognition to the <i>pchD</i> promoter containing the PchR box.	159
Figure M1. Schematic representation of siderophore extraction and quantification	163

Figure M2. Scheme of all conditions prepared for the metal detection by ICP-AES	165
Figure M3. Scheme showing all conditions tested for this competition experiment using Co.....	167
Figure M4. Construction of the expression vector pAYC5.....	173
Table R1. Binding constants (K_d) and standard deviation of the apo-PCH (PCH+EDTA at 1:1 relation), different biological metals and the PCH-metal complexes for MBP-PchR.	130
Table R2. <i>pchD</i> promoter sequences introduced into pSEVA631 for the construction of expression plasmids carrying mCherry.	133
Table R3. Expression values from transcriptomic and proteomic analysis of Fe- and Co-dependent proteins that have been down-regulated in presence of these metals.	138
Table R4. Expression values from transcriptomic and proteomic analysis of Co-dependent proteins that have been down-regulated in the presence of Co	142
Table R5. Expression values from transcriptomic and proteomic analysis of Co-dependent proteins that have been up-regulated in presence of Co.....	143
Figure D1. Schematic interactions proposed between Co and the PCH iron uptake pathway, interfering at the level of the PCH ₂ -Fe transport and also in the regulation mechanism of the PCH genes, involving PchR and Fur transcriptional regulators.....	151
Table S1. Bacterial strains used in the different experiments of this study.....	157
Table S2. <i>Primers</i> used in this study.	158
Table S3. Promoter regions cloned into pSEVA631 for the expression analysis.....	158
Table S4. Proteins detected into the purified MBP-PchR sample.	159
Table M1. Buffers used for the purification of the MBP-PchR fusion protein	169

General introduction

Bacterial requirements for growth include sources of energy such as organic carbon (e.g. sugars and fatty acids) and metal ions (e.g. biological metals: iron, zinc, cobalt, nickel, manganese, copper). These metals play a key role by acting as co-factors, contributing to macromolecule structuration, and catalyzing biochemical reactions. They are required for optimal bacterial growth but also become toxic when present in excess. Consequently, the homeostasis of these biological metals has to be finely regulated, and any disequilibrium in their concentration into bacteria could affect cell viability. Important advancements in the understanding of the mechanisms by which bacterial cells acquire adequate amounts of iron have been made in the last decades. However, less is known concerning homeostasis of the other biological metals.

In the frame of this thesis, we have further investigated the molecular mechanisms involved in iron homeostasis in *Pseudomonas aeruginosa* (pathogen bacteria used as a model) involving the two major siderophores produced by this bacterium, pyoverdine (PVD) and pyochelin (PCH), as well as their role in the homeostasis of the biological metals different than iron. Therefore, in this manuscript, it will be first presented in a bibliographic chapter (i) *P. aeruginosa*, then (ii) the importance of biological metals, followed (iii) by a chapter of siderophores, and at last (iv) the regulation of iron homeostasis in bacteria and more specifically in *P. aeruginosa* will be reviewed. This bibliographic chapter will continue with the description of the experimental results obtained during this thesis, presented some of them as a publication (Chapter 1) and others introduced in a dedicated chapter (Chapter 2) including in each chapter the respective discussions, and finally the general conclusions will be presented.



Introduction

Part 1

Pseudomonas aeruginosa

1. *Pseudomonas aeruginosa* characteristics

P. aeruginosa is a gram-negative, rod-shaped, asporogenous, and monoflagellated bacterium, which has an incredible nutritional versatility. It is a rod of about 1-5 μm long and 0.5-1.0 μm wide, and it was first isolated in 1882 by Carle Gessard (Gessard C., 1984). Nowadays more than 120 species were identified into the genus *Pseudomonas* (Yarza et al., 2010; Pascual et al., 2012).

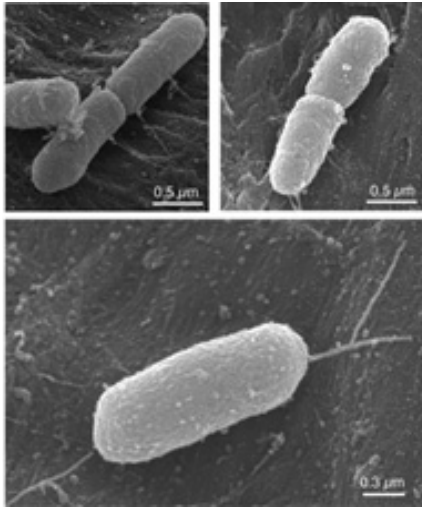


Figure 1. Electron micrograph of biofilm-forming *P. aeruginosa* bacteria grown on a modified surface. Picture from BIFTM programme of Karlsruhe Institute Technology.

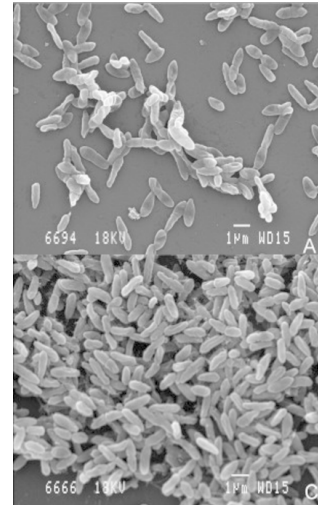


Figure 2. Images of *P. aeruginosa* cystic fibrosis isolates attached to glass surfaces visualized by SEM (Scanning Electron Microscopy) (Deligianni et al., 2010).

P. aeruginosa is a facultative anaerobe that preferentially uses aerobic respiration, and even when the main production of energy is made from a carbon substrate through oxidative catabolism (Suh et al., 2002) it is able to use different carbon compounds as energy source depending on their availability in the medium, such as amino acids or small chain fatty acids. In anaerobic conditions it can survive during a limited period of time changing its metabolism, and doing fermentation from pyruvate (Schreiber et al., 2006) or arginine (Vander Wauven et al., 1984).

The genome size of *P. aeruginosa* PAO1 (the most commonly used *P. aeruginosa* strain in research) is one of the largest bacterial genomes with 6.3 million base pairs (Stover et al., 2000), and a high G/C percentage (66,6%) (www.pseudomonas.com). Its genome encodes more than 520 regulatory proteins, about 150 outer membrane proteins and about 300 internal membrane

proteins. The expression of all these proteins has been mostly studied in laboratory growth conditions, and it is certainly more complex in natural environments (Silby et al., 2011). *P. aeruginosa* can grow between 4 °C and 42 °C (Barbier et al., 2014), (37 °C is its optimal temperature), and it grows at pH between 5,4 and 8,5 (Tsuji et al., 1982). Due to these characteristics, this bacterium is able to colonize and adapt to changing, diverse and extreme environments, thus surviving in a large number of ecological niches. In fact, this ubiquitous microorganism has been found in environments such as soil, water, animals, plants, and hospitals (Lederberg, J., 2000).

2. *P. aeruginosa* as a pathogen

P. aeruginosa is an environmental species but also an opportunist pathogen capable of infecting a large number of organisms, such as mammals (Snouwaert et al., 1992), plants (Rahme et al., 2000), fish (Clatworthy et al., 2009), nematodes (Tan et al., 1999) and insects (Apidianakis and Rahme 2009).

There are two important factors that improve the colonization of the host by *P. aeruginosa*: (i) the efficient uptake of iron, an essential nutrient important for all living organisms but poorly bioavailable, present at very low concentrations in the environment and estimated to be around 10^{-18} M in the body fluids of the host; and (ii) the production of many virulence factors, including the extracellular exotoxin A, extracellular proteases, lipases, phospholipases, and toxins injected *via* the type III secretion system (Coggan and Wolfgang, 2012; Jimenez et al., 2012; Balasubramanian et al., 2013), the production of all these virulence factors being coordinately regulated by the *Quorum Sensing* (Girard and Bloemberg, 2008).

In humans this pathogen is responsible of severe infections in cystic fibrosis patients or immunocompromised individuals (Fig. 2), and it is involved in 10-20 % of nosocomial infections (Carmeli et al., 1999). It can be involved in urinary tract infections, ocular infections, cutaneous lesions, and severe pneumonia (Folkesson et al., 2012), pulmonary infections being the major cause of mortality in cystic fibrosis patients (Cantin et al., 2015). Often these infections are difficult to treat due to the remarkable ability of these bacteria to acquire mechanisms of antibiotic resistance through chemotaxis, enzymatic and mutational mechanisms or the capability to form

biofilms, (Pechère and Köhler, 1999). All these mechanisms may exist simultaneously, conferring combined resistance to multiple groups of antimicrobial agents (McGowan, 2006). The most frequently administered antibiotics that became non-effective due to the development of resistance of several *P. aeruginosa* strains are β -lactams, aminoglycosides and fluoroquinolones (Strateva and Yordanov, 2009). In 2014, the percentage of invasive MDR (multidrug resistant) *P. aeruginosa* isolates was between 10 and 20% in several countries as Spain, France and Italy, and between 25 and 50% in Greece (Surveillance report ECDC, 2014) (Fig. 3). This is the main reason why nowadays *P. aeruginosa* is the protagonist of an important sanitary problem, and the most difficult challenge we face with *P. aeruginosa* is its ability to rapidly develop resistance during the course of treating an infection (Lister et al., 2009). Therefore, there is an urgent need to develop new antibiotics or antibiotherapy strategies against this pathogen, and also change some medical procedures in hospitals, since it was shown that the number of antibiotic treatments has a positive correlation with the number of resistant bacteria detected in the European Union (European Centre for Disease Prevention and Control (ECDC), 2014).

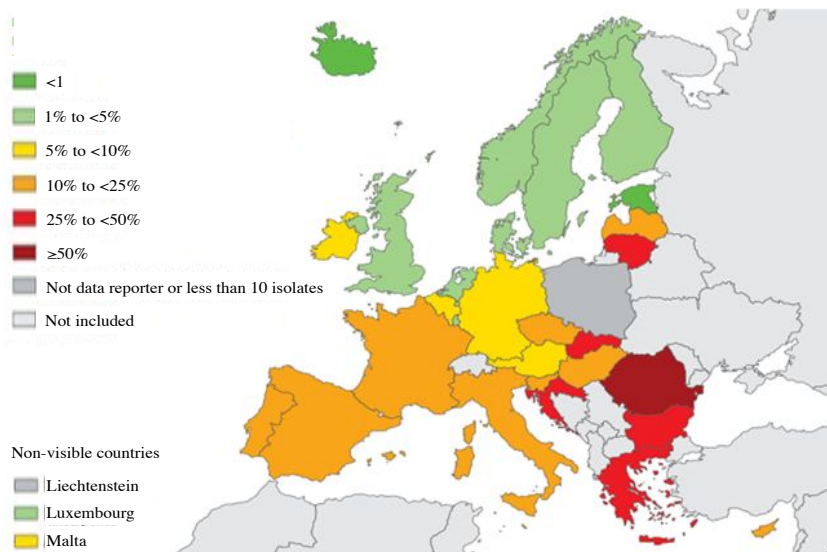


Figure 3. Percentage (%) of *P. aeruginosa* MDR in EU/EEA countries. Representation of invasive isolates with combined resistance (resistance to at least three antibiotics among piperacillin, tazobactam, ceftazidime, fluoroquinolones, aminoglycosides and carbapenems). Surveillance report of the European Centre for Disease Prevention and Control (ECDC), 2014.

3. *P. aeruginosa* life forms

Depending on the environment where it grows, this pathogen can be differently organized to better adapt to external conditions, changing its life form among planktonic, biofilm or dispersive mode. Acute infections with *P. aeruginosa* are usually caused by the bacteria in planktonic form, while it is commonly thought that chronic infections are caused by the bacteria forming a biofilm.

3.1. Planktonic

The planktonic form appears to be the preferential bacteria life form in nutrient-poor conditions, enabling them to move easily to more favorable niches (Madigan, 2012). Moreover, in this form the bacterium has a higher metabolism allowing it to proliferate more rapidly and adapt more specifically to new environments (Madigan, 2012; Nagar and Schwarz, 2015).

P. aeruginosa is able to switch its lifestyle form from planktonic unicellular to a sessile form in biofilms. This switch to biofilm formation and chronic infections involves two conflicting sensor systems, RetS and LadS/GacS (Goodman et al., 2004; Mikkelsen et al., 2011).

3.2. Biofilm

Biofilm formation represents a mode of growth that confers protection from external pressures (Stewart and Costerton, 2001), allowing microorganisms to survive in hostile environments and disperse seeding cells to colonize new niches. Biofilms can form on a variety of surfaces and are prevalent in natural, industrial, and hospital niches. These are physiologically distinct from the free-living planktonic form (Guarner and Malagelada, 2003; English and Gaur, 2010).

Biofilms are microbial communities encased in extracellular polymeric substances (EPS) that hold microbial cells together to a surface in an endless cycle (Donlan, 2002; Karatan and Watnick, 2009) (Fig 4). EPS, also known as matrix, is composed mainly of biomolecules: (i) exopolysaccharides as Psl, Pel, and alginate that have been identified in *P. aeruginosa* to play important roles in structure maintenance and antibiotic resistance of biofilm (Jackson et al., 2004; Ryder et al., 2007; Colvin et al., 2011; Billings et al., 2013), (ii) extracellular DNA (eDNA), and (iii) polypeptides. All components form a highly hydrated polar mixture that contributes to the overall structural scaffold and architecture of the biofilm (Sutherland, 2001; Branda et al., 2005; Flemming and Wingender, 2010). There are also surface appendages such as fimbriae, type IV pili (T4P), and flagellum, considered to be matrix components that play adhesive roles in the cell-to-surface interactions (Ruer et al., 2007; Barken et al., 2008).

The different stages (I-V) of biofilm formation are explained in Figure 4. The stage V (Fig. 4) can be considered as a life form different from biofilm and planktonic lifestyles. In this stage some bacteria are able to disperse from the sessile structure and re-enter in planktonic state to spread and colonize other surfaces (Rasamiravaka et al., 2015), still having the capacity to return to any of these two forms. It was shown that *P. aeruginosa* in stage V has a different physiology from the other two forms, and bacteria are more resistant to the immune system and less susceptible to changes in iron concentrations. They are also more virulent in the infectious *Caenorhabditis elegans* model (Sauer et al., 2004; Chua et al., 2014).

Biofilm formation in *P. aeruginosa* is of particular interest because of its clinical relevance (Donlan & Costerton, 2002). Due to the remarkable ability of *P. aeruginosa* to form biofilms in many environments, it promotes commonly chronic infections (Bjarnsholt, 2013). The number of bacterial infections involving biofilms is high, but it changes according to the reporting agency. The Center for Disease Control (CDC) estimated around 65% of all infections, but according to the National Institutes of Health (NIH) it is 80%.

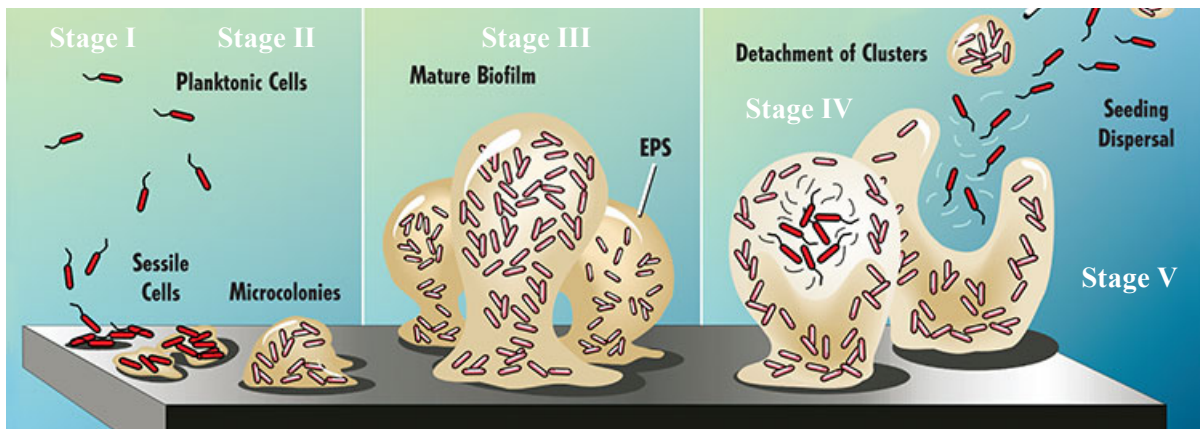


Figure 4. Biofilm formation and development. The biofilm development includes five stages. In stage I, planktonic bacteria initiate attachment to an abiotic surface, which becomes irreversible in stage II. Stage III corresponds to micro-colony formation in the EPS matrix. Progressively, bacterial micro-colonies expand and their confluences lead to a more structured phenotype with non-colonized space. Stage IV corresponds to biofilm maturation and growth of the three-dimensional community. The non-colonized spaces are filled with bacteria, which finally cover the entire surface. Finally, the dispersion occurs in stage V, when planktonic bacteria are released from the biofilm structure to colonize other surfaces (Rasamiravaka et al., 2015). Image belong to the MSU Center For Biofilm Engineering / Peg Dirckx.

Part 2

***Biological metals in bacteria, with focus on P.
aeruginosa***

The present chapter will focus on the importance of biological metals for bacteria and discuss the way bacteria get access to these metals and handle their toxicity.

1. Metals in living organisms

The elements of the periodic table are classified in metals, metalloids and non-metals, according to the physical and chemical properties they share. Metals are chemical elements characterized by their heat and electricity conductance of, and they are usually inclined to form cations through electron loss. This group is divided in alkali metals, alkaline earth metals, transition metals and post-transition metals (Fig. 5); some of them interact with non-metallic ligands and biomolecules, and fulfil essential role for living organisms. Depending on their biological roles, levels of toxicity and concentrations in the living cells, metals can be classified into four groups:

- The first group is composed of sodium (Na), potassium (K), magnesium (Mg) and calcium (Ca) (Fig. 5). They are absolutely necessary for survival and growth of the cells, since they participate in several processes of basic metabolism (Heldal et al., 1985), like the energy production or the maintenance of the stability of the bacterial walls. These metals are present into the cells at high concentrations, in a range of mM concentrations.
- The second group is composed of manganese (Mn), iron (Fe), cobalt (Co), nickel (Ni), copper (Cu) and zinc (Zn), all of them are found in the first row of transition metals in the periodic table (Fig. 5). Even though they are present at μM concentrations range in living cells, they are involved in many biological processes, such as energy production and stabilization of protein structures as metals of the first group, as well as oxido-reduction reactions (Heldal et al., 1985). Because of their importance in biology, these metals are called 'biological metals'.
- The third group includes metals with very poor biological functions, and they are mostly toxic for living organisms. Here are included vanadium (V) and molybdenum (Mo). They are present at similar concentrations than biological metals, around 10^{-7} M (Outten and O'Halloran, 2001).

Metals belong to the second and the third group are toxic at high concentrations despite of their potential biological functions, therefore their accumulation in bacterial cells is highly regulated (Waldron and Robinson, 2009; Guerra and Giedroc, 2012; Braymer and Giedroc, 2014).

- The fourth and last group includes abiotic elements with no biological function that are highly

toxic. Metals like chromium (Cr), silver (Ag) or mercury (Hg) belong to this group. Bacteria or other living cells have developed mechanisms keeping these metals outside the cells, avoiding in this way their high toxic effects (Hobman and Crossman, 2015).

PERIODIC TABLE OF ELEMENTS

GROUP: I IA, 2 IIA, 3 IIIB, 4 IVB, 5 VB, 6 VIB, 7 VIIB, 8, 9, 10, 11 IB, 12 IIB, 13 IIIA, 14 IVA, 15 VA, 16 VIA, 17 VIIA, 18 VIIIA

PERIOD: 1, 2, 3, 4, 5, 6, 7

LANTHANIDE: La (57), Ce (58), Pr (59), Nd (60), Pm (61), Sm (62), Eu (63), Gd (64), Tb (65), Dy (66), Ho (67), Er (68), Tm (69), Yb (70), Lu (71)

ACTINIDE: Ac (89), Th (90), Pa (91), U (92), Np (93), Pu (94), Am (95), Cm (96), Bk (97), Cf (98), Es (99), Fm (100), Md (101), No (102), Lr (103)

www.periodni.com
 (1) Pure Appl Chem, 88, 265-291 (2016)
 Copyright © 2016 Eni Generale

Figure 5. Periodic table. Representation of the chemical elements, ordered by their atomic number and electron configurations, and classified in three major categories: ‘non-metals’ represented in green, the ‘semi-metals’ in red and the ‘metals’ in blue. The metals are subdivided into the highly reactive alkali metals (blue, group 1), through the less reactive alkaline earth metals (group 2), following the transition metals (between group 3 and 12), and ending in the physically and chemically weak post-transition metals (lightest blue). In pink are represented the lanthanides and actinides, often called inner transition metals.

2. Importance of transition metals

Transition metals are *d*-block elements in rows 3-12 of the periodic table defined by the IUPAC in 1990 as "an element whose atom has a partially filled *d* sub-shell, or which can give rise to cations with an incomplete *d* sub-shell". Their characteristics make possible the formation of covalent bonds, Lewis acid-base interaction, between non-metallic ligands. The transition metal can act as Lewis acid, an electron pair acceptor, and the ligand acts as a Lewis base, being the electron pair donor (review Maity and Teets, 2016). As a result, metals and ligands like biomolecules can create specific complexes with relevant biological roles, in the structure of proteins, and also their function. The Lewis acids categorization distinguishes: hard Lewis acids, where Fe^{3+} belongs,

preferring ionic coordination to oxygen-containing ligands; intermediate Lewis acids as Cu^+ , which can coordinate to hard and soft donor ligands with a relative stability (Hobman and Crossman, 2015); and soft Lewis acids, Fe^{2+} , Co^{2+} , Ni^{2+} , Cu^{2+} and Zn^{2+} , that prefer covalent coordination to soft Lewis bases, primarily sulphur and nitrogen ligands.

The relative stabilities of transition metals - biological molecules vary depending on the metal. The Irving–Williams series established that the stability by divalent first-row transition metal ions generally increases across the periodic table: $\text{Mn}^{2+} < \text{Fe}^{2+} < \text{Co}^{2+} < \text{Ni}^{2+} < \text{Cu}^{2+} > \text{Zn}^{2+}$ (Irving and Williams, 1948). This classification shows that divalent Cu has the strongest affinity for biological molecules.

Due to the multiple oxidation states of the transition metals ions (oxido-reduction potential), they became important catalyzing many biochemical reactions. Specifically, the biological metals like Mn, Fe, Co, Ni, Cu, and Zn are often cofactors of enzymes, having structural and catalytic roles in biological processes, including DNA replication, transcription, respiration, and responses to oxidative stress (Palmer and Skaar, 2016). As Crabtree (2009) declared: “Main group organometallics are normally stoichiometric reagents, but transition-metal organics are typically catalysts”, and their ability to easily cycle between these oxidation states contributes to their catalytic properties (Palmer and Skaar, 2016).

2.1. Metalloproteins

Metals became central to cellular function and over 30% of all proteins in the cells are considered as metal-binding proteins, also called metalloproteins. Metals are involved in over 40% of enzymatic reactions, and metalloproteins carry out at least one step in almost all biological pathways (Monosson, 2012). Waldron and Robinson (2009) established that 47% of enzymes studied contained a metal ion, Mg and Zn being by far the most common ions (Monosson, 2012). The next common metal is Fe, which is prevalent in the catalysis of redox reactions, followed by Mn, Co, Mo, Cu and Ni (Andreini et al., 2008).

3. Biological metals in bacteria

Each metal has different physicochemical properties and play a different role in cell metabolism, which also depends on the type of bacteria.

2.1. Iron

Iron is the fourth most abundant element on earth and it is an essential micronutrient for all living organisms (Greenwood and Earnshaw, 1997), except for lactic acid bacteria, which use cobalt and manganese in the place of iron (Weinberg, 1997). Although iron is abundant in nature, it is not usually available in its biologically relevant form, the ferrous form (Fe^{2+}), which in presence of oxygen and under physiological conditions is rapidly oxidized into the ferric form (Fe^{3+}). This second iron form is poorly soluble and precipitates becoming very weakly bioavailable (Krewulak and Vogel, 2008). Conversely, the soluble Fe^{2+} is the most abundant form in anaerobic environments or in micro-aerobic conditions at low pH (Andrews et al., 2003). Therefore, iron is most of the time poorly bioavailable for bacteria, and its concentrations in the different bacterial environments are estimated between 10^{-9} and 10^{-18} M (Raymond et al., 2003). Consequently, bacteria had to develop efficient strategies to get access to iron. Subsequently, during an infection event, pathogen bacteria and host cells have to compete using specific strategies to get access to this limiting metal. This battle involves the use of transferrin and other biological macromolecules like heme, ferritin (iron storage protein) and lactoferrin by the host (Cornelissen and Sparling, 1994; Cornelissen, 2003), and small organic chelators called siderophores or heme binding proteins by the bacteria (Schwyn and Neilands, 1987).

The redox potential of $\text{Fe}^{2+}/\text{Fe}^{3+}$ makes this metal extremely versatile when it is incorporated into proteins. The most important processes in which iron is involved are oxygen transport, ATP generation, photosynthesis, respiration, tricarboxylic acid cycle, cell growth and proliferation, and detoxification. Iron is also an enzyme activator of ribonucleotide reductase, a key enzyme for DNA synthesis, which catalyzes the conversion of ribonucleotides to deoxyribonucleotides (deoxyuridine to thymidine) (Thelander et al., 1983; Krewulak and Vogel, 2008). Iron is also involved in iron-sulfur clusters in various metalloproteins such as ferredoxins, dehydrogenases and nitrogenases (Lill, 2009). Iron-sulfur [Fe-S] enzymes play a key role in a variety of critical biological functions, including electron transfer, substrate binding/activation, regulation of gene expression, and redox and non-redox catalysis (Beinert et al., 1997).

2.2. Zinc

Zinc is stable in the oxidation state Zn^{2+} , thus redox-inactive and not useful for the transfer of electrons. However, this metal plays structural, catalytic and regulatory roles (Maret, 2011). It is useful in the structuring of proteins due to the ability to tie flexible polypeptide chains into a more

rigid confirmation (around a tetrahedral Zn^{2+} complex), and it allows catalysis as a Lewis-acid of a wide variety of hydrolytic reactions (Capdevila et al., 2016). Zinc-binding proteins are around 6 % of all the proteins in bacteria (Andreini et al., 2006).

2.3. Manganese

Manganese is found in two states, Mn^{2+} and Mn^{3+} . Mn^{2+} is the metal cation used by biological systems that can contribute directly to the catalytic detoxification of reactive oxygen species (ROS) protecting bacteria against oxidative stress (Horsburgh et al., 2002; Kehres and Maguire, 2003). In some bacteria, Mn^{2+} can replace the more reactive Fe^{2+} in Fe^{2+} -containing proteins, reducing the oxidative damage (Hood and Skaar, 2012). It was also shown that manganese plays a role in lipid, protein, and carbohydrate metabolism (Porcheron et al., 2013), and it is a cofactor of some superoxide-dismutase (Lisher and Giedroc, 2013).

2.4. Copper

Copper is present in two states, Cu^{2+} and Cu^+ . Cupric copper (Cu^{2+}) is one of the most stable divalent transition metals in aerobic conditions and it has a high affinity for metalloproteins, as it is shown by the Irwin-William series. Under anaerobic conditions, Cu is mainly present in the highly reactive cuprous form (Cu^+) (Porcheron et al., 2013). In contrast to Fe and Zn, the Cu requirements are low in most bacteria. Cu-binding proteins are present in the periplasm or embedded in the cytoplasmic membrane, because the periplasm is more oxidized than the cytosol, stabilizing the cupric form (Tottey et al., 2005). Cu^{2+} is essential to aerobic bacteria, it is a cofactor of enzymes that play a role in electron transfer, oxygen transport as well as in redox reactions of multiple substrates, as the cytochrome oxidase (Solioz et al., 2010; Dupont et al., 2011; Hodgkinson and Petris, 2012).

2.5. Cobalt

Co can exist in oxidation states from Co^{1+} to Co^{4+} , although the last one is not common in nature (Kobayashi and Shimizu, 1999). Cobalt is mainly present as part of vitamin B12 (Moore et al., 2014) and it is an important cofactor in B12-dependent enzymes. Furthermore, it is required as a trace element in prokaryotes and eukaryotes to fulfil a variety of metabolic functions (Table 1), even though it is not a metal frequently found in metalloenzymes in comparison to Fe, Mn, Cu or Zn, (Kobayashi and Shimizu, 1999).

Enzyme or protein		Role	References
Methionine aminopeptidase	<i>Escherichia coli</i>	Hydrolysis	Roderick and Matthews, 1993
Nitrile hydratase	<i>Rhodococcus rhodochrous</i>	H ₂ O activation, CN-triple-bond hydration and protein folding	Brennan et al., 1996
Methylmalonyl-CoA carboxytransferase	<i>Propionibacterium shermanii</i>	Carboxytransferation	Reddy et al., 1998
Lysine-2,3-aminomutase	<i>Clostridium</i> SB4	Mutation	Chirpich et al., 1970
Bromoperoxidase	<i>Pseudomonas putida</i>	Bromination	Itoh et al., 1994
Cobalt-porphyrin-containing protein	<i>Desulphovibrio gigas</i> / <i>D. desulphuricans</i>	Electron carrier	Battersby and Sheng, 1982

Table 1. Proteins containing cobalt. Modified graphic from the original of Kobayashi and Shimizu, 1999.

2.6. Nickel

Nickel is typically found in Ni⁰ or Ni²⁺ state due to the stability of these species in water (Nieminen et al., 2007). In prokaryotic, Ni is an essential component of several enzymes involved in carbon, nitrogen, and oxygen cycles (Mulrooney and Hausinger, 2003; Ragsdale, 2009). Nickel is used as a cofactor of urease, [NiFe] hydrogenase, Ni-superoxide dismutase, carbon monoxide dehydrogenase, acetyl CoA synthase/decarbonylase, acireductone dioxygenase, and methyl coenzyme M reductase, as well as some forms of glyoxalase I (Mulrooney and Hausinger, 2003; Li and Zamble, 2009; Ragsdale, 2009; Kaluarachchi et al., 2010).

4. Biological metals in *P. aeruginosa*

The concentration of metals with potential biological activities in *P. aeruginosa* PAO1 cells was investigated in rich and restricted conditions by our team. Their presence in decreasing order of abundance was: Na - K > Mg >> Ca >> Fe - Zn >> Mn - Mo - Cu - V - Cr - Ni >> Co, independently of the growth medium used (Cunrath et al., 2016). See Figure 6A. K, Na and Mg, the most abundant metals, were present at intracellular concentrations higher than 10⁻¹ M. Fe and Zn were the two most abundant transition metals, with a range of concentration between 10⁻³ and 10⁻⁴ M in function of the growth media. Outten and O'Halloran also established that *E. coli* requires similar concentrations of Fe and Zn into the cells. Cu, Cr, Mn, Mo, Ni and V, metals with less biological functions known, were detected at concentrations ranging between 10⁻⁵ and 10⁻⁴ M, and some of them were not even detected by the ICP-AES technique, like Mn in casamino acid

(CAA) medium, or Ni in Lysogenic broth (LB) medium. Co was not detected in *P. aeruginosa* cells in any of the growth media tested, indicating that *P. aeruginosa* may use very low concentrations of this metal. These values of metal concentrations in *P. aeruginosa* cells are very similar to the values described previously in *E. coli* grown in LB and minimum medium (10^{-4} M of Fe and Zn, 10^{-5} M of Cu and Mn, and nanomolar concentrations of Co) (Outten and O'Halloran, 2001; Ranquet et al., 2007).

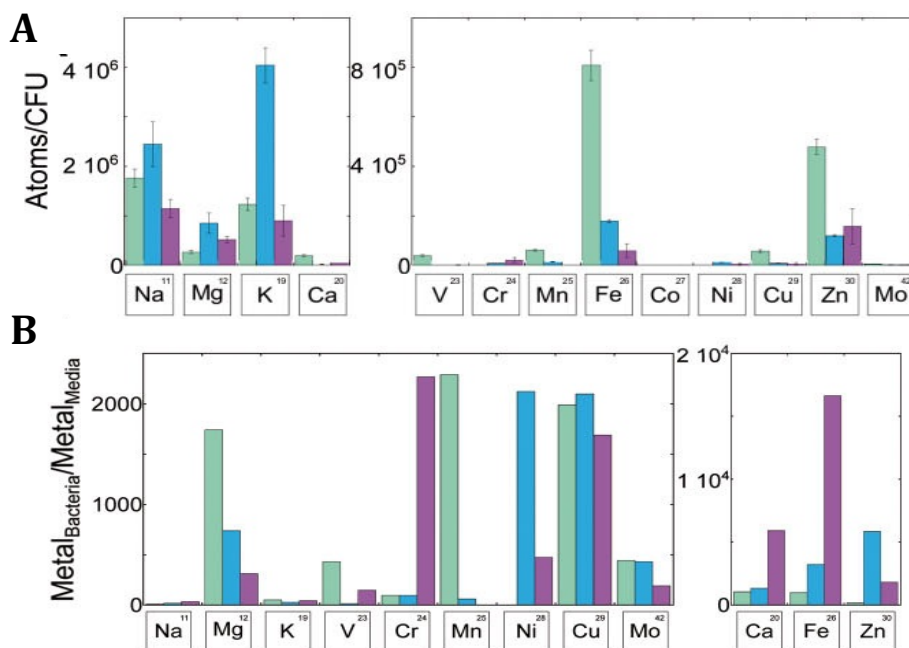


Figure 6. This figure shows (A) the number of atoms per CFU of *P. aeruginosa* PAO1 cells, and (B) the concentrating factor for each metal in *P. aeruginosa* PAO1 cells, which is represented by the ratio between the metal concentration in the bacteria and the metal concentration in the growth media (MetalBacteria/MetalMedia). Green bars represent the values obtained when bacteria were grown in LB medium, blue bars in succinate medium, and purple bars in CAA medium. Graphics from (Cunrath et al., 2016).

Cunrath *et al.* 2016 showed that the concentration of each metal was higher into the bacteria than in the growth media (in both rich and restricted media), indicating that bacteria concentrate all these metals from their environment (Fig. 7). Moreover, it was also shown that these metals were not incorporated from the medium by *P. aeruginosa* cells with the same efficiency (Fig. 6B). Bacteria use different uptake systems to maintain the adequate metal concentration inside the cells

depending on the importance of each metal for their development and survival. The concentrating factors ($[\text{metal concentration in the bacteria}]/[\text{metal concentration in the medium}]$) are very dependent of the metal: this factor is around 10 – 50 for K, 6000 for Ca and reaches 16000 for Fe in CAA medium. Therefore, it exists clearly a stronger effort made by bacteria to incorporate Fe (metal poorly available) than many other biological metals including Co, Ni or Mn. These values give an idea of the energy spent by *P. aeruginosa* cells to concentrate them from the environment (Fig. 6B and Table 2).

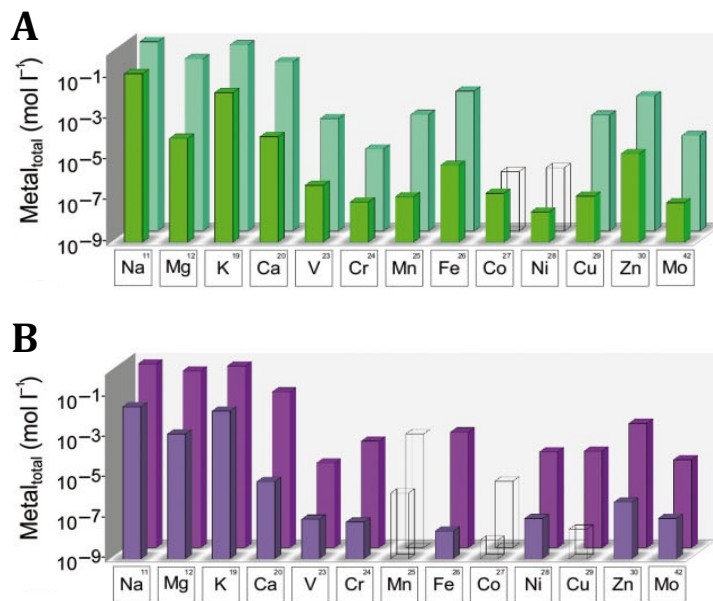


Figure 7. Metal content of *P. aeruginosa* cells grown in LB, succinate or CAA media as determined by ICP-AES. Total content of each metal expressed as moles per volume (log representation) for cells grown in LB (A), and CAA medium (B). Figures from (Cunrath et al., 2016). The bars in the back give the metal concentrations in the bacteria and the bars in the front the metal concentrations in the growth medium. The absent bars are the values under the detection limit of the ICP- AES detector.

Biological metals	LB medium	CAA medium
	Concentration	Concentration
Mn ²⁺	325 μM	-
Fe ³⁺ /Fe ²⁺	4,23 mM	357 μM
Co ²⁺	-	-
Ni ²⁺	-	40,7 μM
Cu ²⁺ /Cu ⁺	302 μM	44,1 μM
Zn ²⁺	2,5 mM	940 μM

Table 2. Intracellular biological metals concentrations in *P. aeruginosa* PAO1. The ‘-’ are the values under the detection limit of the ICP- AES detector. Data from Cunrath et al., 2016.

5. Biological metal uptake strategies used by bacteria, and specifically by *P. aeruginosa*

To get access to the biological metals from the environment, thus making possible their transport across the bacterial wall, bacteria have evolved several metal acquisition systems that are more or less complex or specific, which also depend on the metal bioavailability. Slight bioavailable metals are mostly transported specifically across the outer membrane by TonB-dependent transporters (TBTDs), using energy in the form of proton motive force transduced by the TonB-ExbB-ExbD complex (TonB mechanism is described on section 2.2 of the chapter 3), and across the inner membrane by ABC transporters and P-type ATPases. Other transporters are permeases and porins, which are less selective, used frequently by bioavailable metals. Transport systems play an important role in the maintenance of the biological metal homeostasis, and during metal starvation the expression of these transporters are up-regulated by the action of several regulatory metalloproteins (Wakeman and Skaar, 2012).

5.1. Iron

Most bacteria, including *P. aeruginosa*, have evolved several number of iron scavenging and uptake strategies, including uptake of ferrous iron (Fe^{2+}), uptake of ferric iron (Fe^{3+}) via siderophores and uptake of heme (Cornelis and Dingemans, 2013). This substantial redundancy of iron acquisition systems allows bacteria to better adapt and survive in different iron-limited niches. The iron uptake strategy the most broadly distributed among bacteria is based on the use of siderophores, explained in details in the chapter 3. The other two strategies evolved by bacteria are explain below.

5.1.1. Ferrous iron uptake

In *P. aeruginosa*, Fe^{2+} uptake involves the porin OprG, responsible of the metal diffusion across the outer membrane (McPhee et al., 2009). The FeoABC system, present in many gram-negative bacteria, is involved in the transport of Fe^{2+} through the inner membrane (Fig. 8). This uptake system is composed of the permease FeoB, and the proteins FeoA and FeoC, which function is still unknown (Kammler et al., 1993).

5.1.2. Heme uptake

Heme is one of the most abundant iron sources in the host during infections. 70% of iron in the human body is complexed with heme. *P. aeruginosa* possesses three heme acquisition systems, the Phu, the Has and the Hxu systems (Fig. 8).

- **Phu system:** It is composed of the TonB-dependent transporter PhuR, which recognizes host hemoproteins like myoglobin at the bacterial cell surface (Ochsner et al., 2000). Because of its strong affinity for heme (higher than the affinities for heme of host heme-containing proteins), PhuR extracts heme from hemopexin and myoglobin by interacting directly with these proteins, and transports it into the bacterial periplasm. In this cell compartment heme binds to the periplasmic binding protein PhuT, and is transported across the inner membrane via the ABC transporter PhuUVW (Ochsner et al., 2000). Heme is then transferred to the chaperone PhuS (Bhakta and Wilks, 2006; O'Neill and Wilks, 2013) and degraded by the oxygenase HemO, releasing Fe^{2+} in the cytoplasm (Barker et al., 2012).

- **Has system:** This system, which has been mostly studied in *Serratia marcescens*, involves the secretion of a heme binding protein called the hemophore HasA, able to enter in competition for heme with the host hemoproteins due to its strong affinity for this molecule. The haemophore HasA is secreted into the extracellular medium by the type I secretion system involving HasD (ATPase part), HasE (membrane part) and the TolC / HasF complex. The HasA-heme complex is then recognized at the bacterial cell surface by the HasR TonB-dependent transporter (Létoffé et al., 1999; Ochsner et al., 2000). Heme is transferred from HasA protein to the HasR transporter and transported into the bacterial periplasm (Lefèvre et al., 2008; de Amorim et al., 2013). Afterwards heme is transported across the inner membrane by the PhuUVW ABC transporter (Ochsner et al., 2000).

- **Hxu system:** It has been suggested more recently, that *P. aeruginosa* has also the HxuA/HxuC system to import heme from hemopexin and hemoglobin (Hancock and Speert, 2000). HxuA is a secreted hemophore that binds heme-loaded hemopexin or hemoglobin, and the complex is recognized by HxuC, the TonB-dependent transporter that allows the transport across the outer cellular membrane (Fournier et al., 2011). Heme is then transported from the periplasm into the cytoplasm by the ABC transporter PhuUVW as in the Has and Hxu pathways.

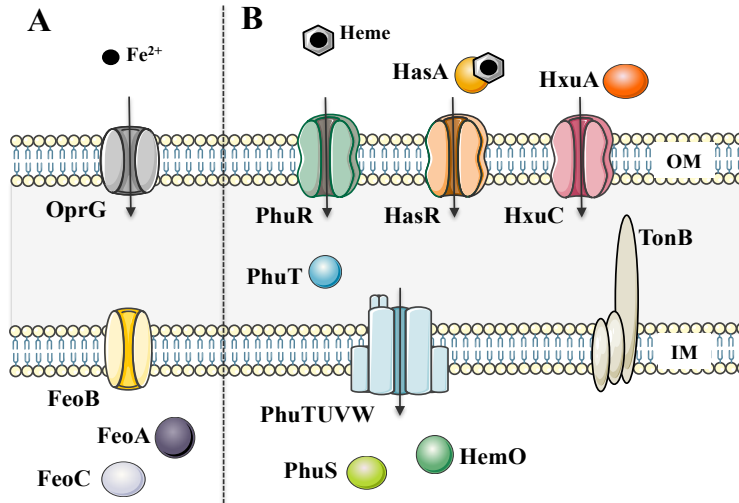


Figure 8. Ferrous iron transport (A) and heme transport by the Phu, the Has and the Hxu heme acquisition systems (B) in *P. aeruginosa*. Fe^{2+} is directly transported into the periplasm by the porin OprG and into the cytoplasm by the permease FeoB. The heme is transported into the periplasm by different TonB-dependent transporters, recognized directly in the case of PhuR, or previously bound to hemophores in the case of the HasR and HxC transporters. Once in the periplasm, the heme transported by PhuR binds to PhuT, and this complex, as well as the other heme incorporated in the periplasm *via* the Has and Hxu systems can be transported across the inner membrane through the ABC transporter PhuTUVW.

5.2. Zinc

Transcriptomic analyses suggest that four TonB-dependent transporters (ZnuD, PA1922, PA2911, PA4837) are involved in Zn uptake across the outer membrane in *P. aeruginosa* (Létoffé et al., 1999; Ochsner et al., 2000). However, no biochemical data are available to confirm the involvement of these transporters in Zn^{2+} acquisition in this pathogen. For the uptake across the inner membrane, different transporters have been identified. The ABC transporter **ZnuABC**, identified in *P. aeruginosa* (D’Orazio et al., 2015), is also able to transport Mn and it is composed of a Zn-binding periplasmic protein ZnuA, an inner membrane permease ZnuB, and an ATPase, ZnuC (Ellison et al., 2013; Pederick et al., 2015). Transcriptomic analysis of *P. aeruginosa* suggested also an implication of three other ABC transporters in Zn acquisition: PA2912-2914 co-transcribed with a putative TonB-dependent transporter (PA2911, already mentioned above), HmtA (PA2435) and PA4063-4066 (Pederick et al., 2015). A Zur site is present in the regulatory elements of these transporter clusters. The PA2911/PA2912-2914 pathway is organized similarly to the ZnuD/ZnuABC pathway, with a TonB-dependent transporter (PA2911) and an ABC transporter for the uptake of the metal across the outer and inner membranes, respectively. It is not known whether this TonB-dependent system works with a specific Zn^{2+} chelator like the ferri-

siderophore uptake pathways. Intracellular metal measurements and transport experiments show that **HmtA** (PA2435) is a P-type ATPase, mediating the uptake of Zn^{2+} (and Cu^{2+}) across the inner membrane in *P. aeruginosa* (Lewinson et al., 2009). Concerning PA4063-4066, it is an ABC transporter with two periplasmic binding proteins associated PA4063 and PA4066. It is still not known how this ABC transporter with these two periplasmic binding proteins handles Zn^{2+} acquisition. More recently, Mastropasqua *et al.* have identified an operon *zrmABCD* regulated by the intracellular Zn concentration that encodes for a metallophore-mediated Zn import system in *P. aeruginosa* (Mastropasqua et al., 2017). This operon includes the genes for an uncharacterized TBDT ZrmA and for a putative nicotinamide synthetase (ZrmB). ZrmB is involved in the synthesis of a metallophore, which is released outside the cell and mediates Zn uptake through ZmrA. Moreover, the thiocarboxylate siderophore pyridine-2,6 (thiocarboxylic acid) (PDTC, a siderophore produced by *Pseudomonas stutzeri*, *P. fluorescens* and *P. putida*) may also be involved in Zn^{2+} uptake in some *Pseudomonads* but not in *P. aeruginosa*: Zn^{2+} chelated by PDTC can be utilized by *P. putida*, but the transport is much less efficient than for PDTC: Fe^{3+} complexes (Leach et al., 2007). *P. stutzeri* and *P. putida* both produce PDTC (Lewis et al., 2000) and two gene products are necessary for iron uptake by this siderophore, the TonB-dependent transporter PdtK (PSF113–2606 in *P. fluorescens* genome) and the proton motive-dependent inner membrane permease PdtE (Leach and Lewis, 2006). Both PdtK and PdtE expression are repressed in response to Zn^{2+} (50 μ M) (Leach et al., 2007).

5.3. Manganese

The proteins and the molecular mechanisms of Mn^{2+} transport across the outer membrane in *P. aeruginosa* have not been identified. The uptake of Mn^{2+} in most bacteria across the inner membrane involves MntH, theoretically present in different species of *Pseudomonas* (www.pseudomonas.com). MntH is a member of the Namrp family of proton-coupled divalent metal ion transporters found also in mammalian macrophages (Chaloupka et al., 2005). MntH is described in many enterobacterial species (Champion et al., 2011; Perry and Fetherston, 2011). In bacteria that need high intracellular Mn^{2+} , this metal is also imported *via* P-type ATPases, like MntA, theoretically present in *Pseudomonas* but not yet identified in *P. aeruginosa* (UniProt and <http://www.pseudomonas.com>). SitABCD, an ABC transporter presents in some pathogenic *E. coli* strains, first described in *S. typhimurium*, is also involved in the uptake of Mn^{2+} (Kehres et al., 2002). SitA and SitB were detected in *P. fluorescens* by comparative analysis.

5.4. Copper

In *P. aeruginosa*, the import of copper through the outer membrane requires a TonB-dependent transporter OprC which has a high affinity for Cu (Yoneyama and Nakae 1996) and the uptake through the inner membrane involves certainly the ABC transporter of type-P HmtA, also involved in Zn²⁺ transport (Lewinson et al., 2009). Methanotropic bacteria need large amounts of copper, and they produce a small Cu-chelating molecule called chalkophore to chelate this metal. The Cu-chalkophore is transported by a TonB-dependent transporter into the bacterial periplasm (Balasubramanian et al., 2011; Kenney and Rosenzweig, 2012). Nevertheless, there is no evidence that *P. aeruginosa* produces such a Cu chelator and uses a chalkophore-dependent uptake system. Beside this system, CopA is a Cu⁺-dependent ATPase present in a variety of bacteria (Odermatt et al., 1993; Rensing et al., 2000; Mandal et al., 2002), and also been identified in *Pseudomonas spp.* (www.pseudomonas.com).

5.5. Cobalt

Cobalt can be transported as metal cation and as cobalamin (vitamin B12). Cobalamin is transported through the outer membrane into the periplasm by the TonB dependent transporter BtuB (Bassford and Kadner, 1977; Chimento et al., 2003), and across the inner membrane into the cytoplasm by the ABC transporter BtuCDF, present in several *Pseudomonas spp.*. In the bacterial periplasm, cobalamin binds BtuF, a periplasmic high affinity binding protein (Cadieux et al., 2002), and is further transported into the cytosol by the ATP-dependent permease BtuCD (Borths et al., 2002). Concerning the metal cation alone (without cobalamin), it can be transported across the inner membrane by one of the following transporters: ABC transporters; Cbi, an energy-coupled factor (ECF) transporter (Rodionov et al., 2006); P-type ATPases transporters (Axelsen and Palmgren, 1998) or Ni-Co (NiCoT) permeases lacking ATPase activity (Komeda et al., 1997). The Cbi system is the most widely distributed Co²⁺ transporter described to date, but it can also transport Ni at a very low affinity (Da et al., 2006). The NiCoT transporters, also identified in *P. aeruginosa* (Haritha et al., 2008)([pseudomonas.com](http://www.pseudomonas.com)), constitute a class of Co²⁺ and Ni²⁺ importers (Eitinger et al., 2005). Nothing is known about the uptake of Co or cobalamins across the inner membranes of *P. aeruginosa*. The CorA Co²⁺/Mn²⁺ transporter was described in *E. coli* (Smith et al., 1993), but it is proposed PA5268 to be the homolog in *P. aeruginosa* (www.pseudomonas.com).

5.6. Nickel

Ni is probably able to diffuse across the outer membrane *via* porins. No data are available in the literature about the Ni²⁺ requirements of *Pseudomonads* growth, or virulence or about the strategies used by these bacteria to get access to this metal. Ni²⁺ uptake has been mostly studied in *E. coli* and *Helicobacter pilori*. The ABC transporter identified in *E. coli* to import Ni into the cytoplasm is NikABCDE; it transports preferentially Ni, even though it transports Co at low affinity (Da et al., 2006; Rodionov et al., 2006). Moreover, NiCoT already mentioned above for Co import, transports both Ni and Co cations (Rodionov et al., 2006; Gogada et al., 2015), and it is ubiquitously present in bacteria and also Archaea. At last, Ni can also be transported by the Cbi system (energy-coupling factor transporter family) like Co, also mentioned above (Rodionov et al., 2006).

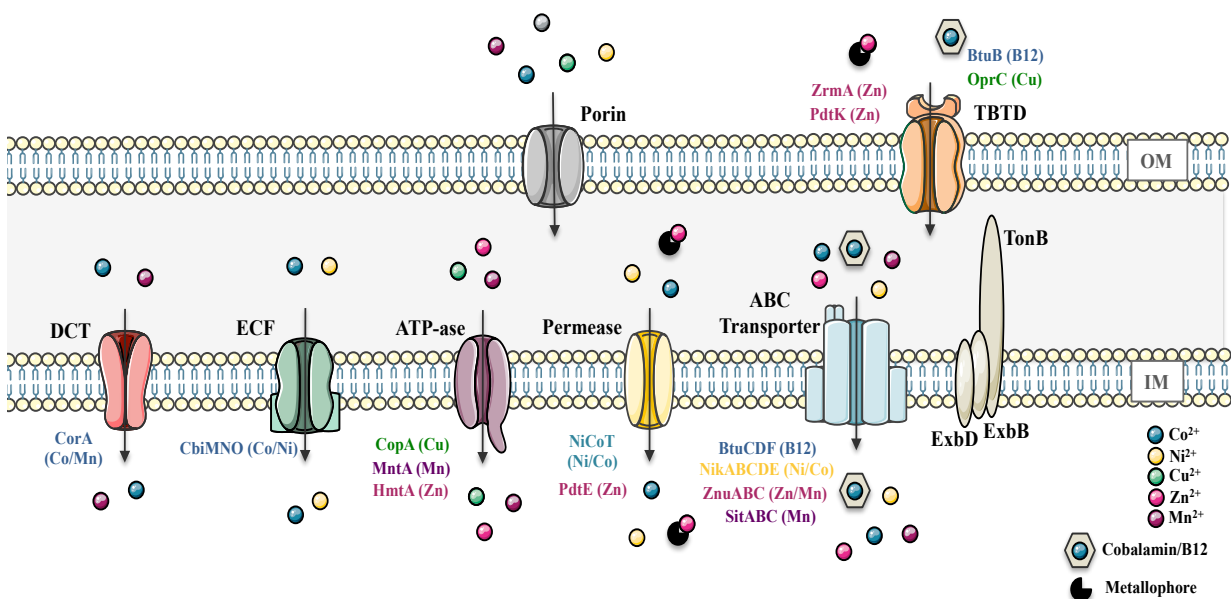


Figure 9. Proteins involved in the biological transition metals uptake in *Pseudomonas spp.* Metals can be transported in the free state or associated to metal quelators, as cobalamin in the case of Co, transported through TonB-dependent transporters (TBDT) across the outer membrane, and by ABC transporters or permeases across the inner membrane. Biological metals cations can be transported unselectively via porins or more specifically via other transporter families: Energy-coupled factor transporters (ECF), ABC transporters, permeases, ATP-ases, and divalent cation transporters (DCT). The color names represent the different transporters involved in metal uptake for one or more specific metals.

6. Metal toxicity in bacteria

As it was explained above, biological metals (Mn, Fe, Co, Ni, Cu and Zn) serve catalytic and structural functions, and they are required for a number of diverse physiological processes, ranging from gene transcription to respiration (Silva and Williams, 2001). However, despite their essential roles and ubiquitous presence, all of these metals at high concentrations are toxic causing deleterious effects in bacterial cells. This is why these transition metals may also be considered as toxic metals, and they can be classified for the toxicity levels according to two different ways, the Irving-Williams or the Lewis acids classifications. The Irving-Williams series represent the affinity of the first-row transition metals for biological molecules: $\text{Ca} < \text{Mg} < \text{Mn} < \text{Fe} < \text{Co} < \text{Ni} < \text{Cu} > \text{Zn}$. This classification shows that divalent Cu has a strong affinity for biological molecules, suggesting that it can displace others first-row transition metals from them (Waldron and Robinson, 2009). Moreover, most toxic metals are soft Lewis acids, because of their capacity to displace intermediate and hard Lewis acids from cysteine thiols due to their higher affinity for these groups (Hobman and Crossman, 2015). Intermediate Lewis acids, as Cu^+ , can also be toxic due to the ability to coordinate to hard and soft donor ligands with a relative stability (Hobman and Crossman, 2015).

Some transition metals have been used for their antimicrobial properties for thousands of years. For example, vessels made of Cu and Ag have been used for water disinfection and food preservation since the time of the Persian kings, a practice adopted by the Phoenicians, Greeks, Romans and Egyptians (Alexander, 2009). Over the past two centuries physicians have also used Cu and Hg salts to treat diseases such as tuberculosis, gonorrhoea and syphilis (Tilles and Wallach, 1996; Djoko et al., 2015a; Dalecki et al., 2015).

Biological metals can exert toxic effects in a number of different ways. Some metals can lead to protein dysfunction, interfering in normal enzyme functions and cellular processes as nutrient assimilation; lead to the production of reactive oxygen species (ROS) and depletion of antioxidants, resulting genotoxic (Nies, 1999; review Lemire et al., 2013; Hobman and Crossman, 2015).

6.1. Protein dysfunction

Some metals can displace others in the active sites of enzymes with as consequence a dysfunction of the enzymes. A clear example is provided by Cu, which may interact with polypeptide

backbones, interferes with the binding of some cofactors to specific amino acids, and that way disrupts protein structures by forming thiolate bonds with iron-sulfur clusters (Dupont et al., 2011; Hodgkinson and Petris, 2012). Another example is Co: its toxicity was also attributed to a competition between Fe and Co as these metals have the same biologically relevant oxidation states (2+/3+) and similar radii², which facilitates their interference (Okamoto and Eltis, 2011). It was proposed that Co at elevated concentrations could bind Fe-S proteins in a kinetically stable form, mediated by the Fe-S cluster assembly machineries. It was shown that the holo-form of IscU, a scaffold protein involved in formations of Fe-S clusters, can incorporate cobalt and lose its iron content *in vitro* (Ranquet et al., 2007). Moreover, the IscU containing Co had the capacity to transfer mixed (Co, Fe)-S clusters to apo-targets *in vitro*, as the carrier protein SufA (Ranquet et al., 2007). Moreover, the excess of Co in the growth medium induces the production of cobalt protoporphyrin, which has the ability to be incorporated into heme proteins, resulting in a decrease of 85 % in the cellular oxygen utilization (Okamoto and Eltis, 2011), thus promoting a change in the bacteria metabolism. The last example includes Gallium, which interferes with Fe binding sites of proteins that belong to iron acquisition pathways, inhibiting Fe uptake and interfering with iron sensing, inducing iron starvation (Kaneko et al., 2007).

6.2. ROS production

Fe²⁺ and Cu²⁺ are highly toxic due to their high oxidative potential, increasing intracellular Reactive Oxygen Species (ROS) (Rizvi et al., 2015). This toxicity involves the Fenton reaction, where free Fe²⁺ or Cu²⁺ catalyzes the formation of highly reactive compounds, as hydroxyl radical (OH[•]) (See Fig. 10), that causes damage to the macromolecular components of the cells, including DNA and proteins (Imlay et al., 1988; Nunoshiba et al., 1999; Aisen et al., 2001). Moreover, Cu also degrades iron-sulfur clusters, increasing free iron concentrations into the cells, and therefore generating oxidative stress (Macomber and Imlay, 2009).

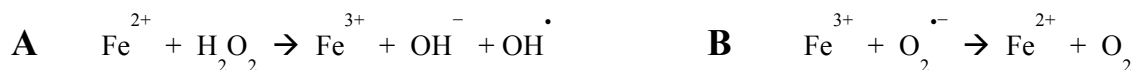


Figure 10. Fenton reaction. Fenton reaction is initiated by products of aerobic respiration, such as hydrogen peroxide (H₂O₂) and superoxide (O₂^{•-}). **A:** H₂O₂ oxidizes Fe²⁺ to produce hydroxide (OH⁻) and hydroxyl radical (OH[•]), which is highly reactive. **B:** *In vitro* work has demonstrated that O₂^{•-} can reduce the oxidized metal released by the Fenton reaction (Lemire et al., 2013).

7. Bacterial resistance against metal toxicity

Metal toxicity in bacterial cells can be due to excess of a biological metal or to the presence of purely toxic metals. Because of the different physiochemical properties of the metals, bacteria have not evolved one single strategy that provides universal resistance to all toxic metals, but have evolved different mechanisms of resistance. All these different strategies try to maintain and control the homeostasis of the different metals through the coordinated action of proteins involved in the efflux and metal transport, proteins and molecules involved in metal sequestering and storage, proteins playing a role in the reparation of molecules, and metal-responsive transcriptional regulators activity (Osman and Cavet, 2008; Ma et al., 2009; Argüello et al., 2012; Lemire et al., 2013). See Fig. 11.

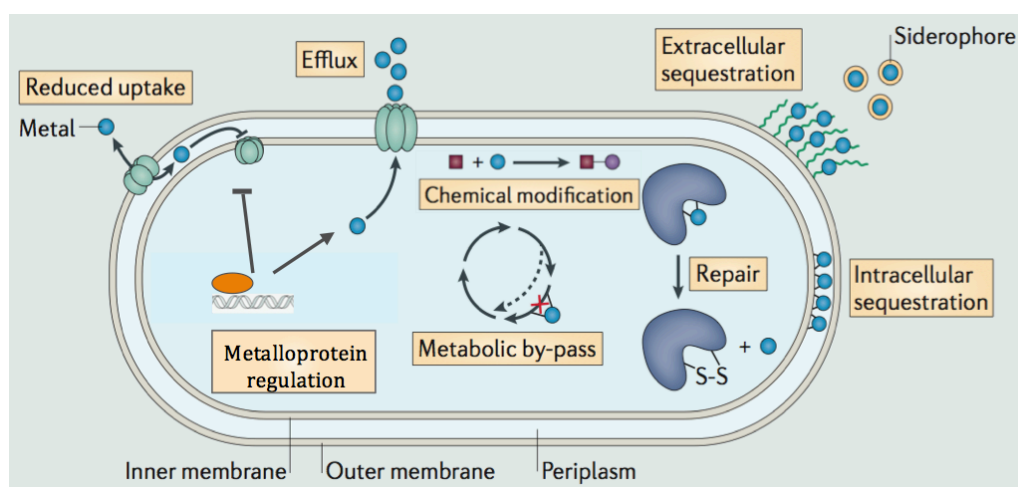


Figure 11. Mechanism of bacteria protection against metal toxicity. Figure modified from Lemire et al., 2013.

7.1. Capture and sequestration of metals

In the presence of excess of biological metals or of toxic metals, some microorganisms are able to upregulate the production of polymers at the surface, promoting the formation of biofilm, which can trap metals, decreasing their acquisition (Harrison et al., 2007). Siderophore, small organic iron chelators produced by bacteria in order to get access to iron, also play a significant role in metal resistance. They are able to chelate many metals other than iron like heavy metals, sequestering them in the extracellular medium, and thus reducing their diffusion *via* porins in bacterial cells (Braud et al., 2010; Chaturvedi et al., 2014; Hannauer et al., 2012). Moreover, the

storage of biological metals in the bacterial cells decreases their toxicity, and at the same time serves as metal reservoir in case of future deficiency. An example is the cytoplasmic protein Dps2 from *Deinococcus radiodurans*, involved in storage of iron and manganese (Santos et al., 2015). Many microorganisms can also precipitate toxic metals at the cytoplasmic membrane as metallic oxides or sulfides (Zannoni et al., 2008).

7.2. Repair, chemical modification and metabolic by-pass.

Cellular molecules with redox-sensitive functional groups, that are vulnerable to oxidation due to the Fenton reaction, can be repaired by cellular chaperones, enzymes or antioxidants (Harrison et al., 2009). Another strategy is to chemically modify the redox potential of the metal, making it less toxic (Silver and Phung, 1996). In the case of a protein altered by a metal, cells can circumvent metabolic pathways in which this protein play a role, by producing alternative proteins with catalytic cores that do not bind to the toxic metal ligand (Lemire et al., 2010).

7.3. Change the transport rates

Another common strategy used by living cells to prevent damage caused metals reside in the regulation of metal uptake proteins in order to decrease the import of the metals, or efflux proteins, to increase their export out of the cells. The expression of these different transport proteins is under the control of metal-binding proteins, which control metal homeostasis.

7.3.1. Biological metals efflux

Metal transport by efflux pumps is a way to control metal homeostasis through the export of toxic metals. Resistance-nodulation-division (RND)-type efflux pumps transport metals from the cytoplasm directly to the extracellular medium through an inner-membrane component belonging to the RND superfamily, a channel-forming outer membrane factor (OMF), and a periplasmic membrane fusion protein (MFP) (Minagawa et al., 2012). RND are responsible for the extrusion of a broad range of compounds, including antibiotics (Piddock, 2006) (Nikaido and Pagès, 2012). Moreover P-type ATPases, cation diffusion facilitator (CDF) transporters (Fig. 12), and major facilitator superfamily (MFS) transporters catalyze metal translocation across the inner membrane, from the cytoplasm to the periplasm (Klein and Lewinson, 2011). See Figure 12.

The most extensively characterized bacterial CDF is YjiP from *E. coli*, which exports Fe and Zn (Grass et al., 2005a). RcnA is proposed to be a member of the MFS family of membrane permeases, which is able to export Co and Ni cations (Rodrigue et al., 2005), identified in *P.*

syningae and *P. fluorescens* (www.pseudomonas.com). CnrCBA belongs to the RND superfamily and exports Co and Ni (Grass et al., 2005b). Other RND is CzcCBA, able to transports Zn but also Co (www.pseudomonas.com)(Dieppois et al., 2012). CusCFBA, present in several enterobacteria as *E. coli* and probably in *Pseudomonas spp.* (Uniprot) is a member of the RND protein superfamily and exports Zn (Franke et al., 2003). Cu efflux has been shown to be mediated also by the Cu (I)-specific P-type ATPase CopA in *E. coli* (Fan and Rosen, 2002; Argüello et al., 2011) and *P. syringae*. The efflux of cellular Zn in prokaryotes is also carried out by P-type ATPase transporters, like ZntA, and cation diffusion facilitator transporters, as the case of ZitB (Nies, 1995). ZntA was identified in *P. fluorescens* or *P. pseudoalcaligenes*, but not in *P. aeruginosa*.

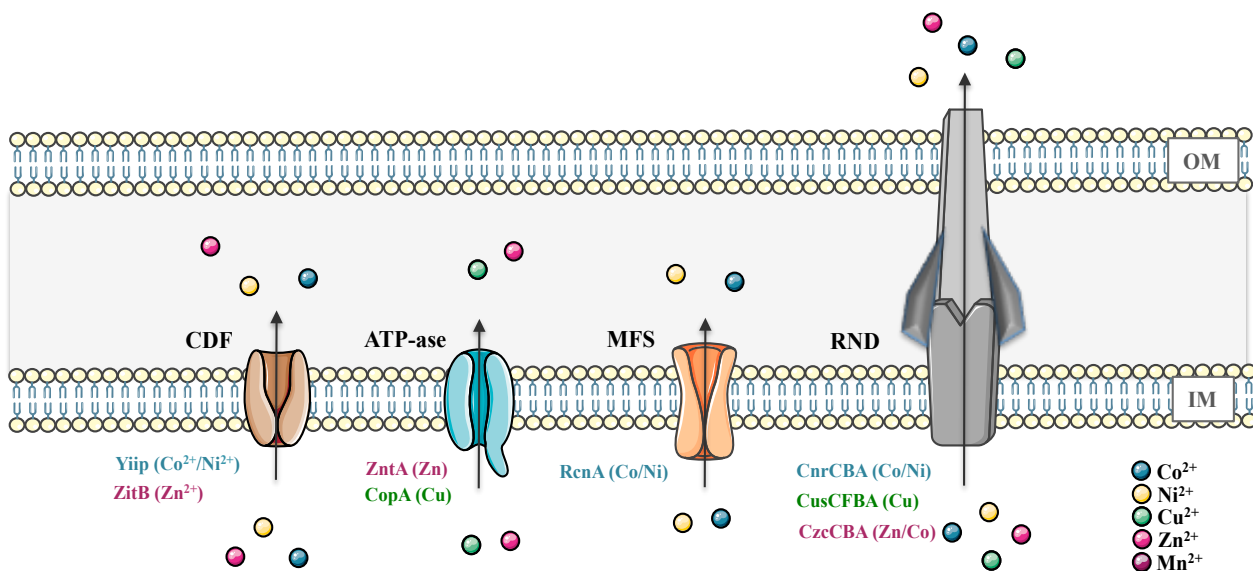


Figure 12. Transition metal ions efflux in *Pseudomonas spp.* Different families of transporters were identified in *Pseudomonas* to export biological metals across the bacterial membranes: cation diffusion facilitator (CDF), P-type ATPases, major facilitator superfamily (MFS) transporters, and Resistance-nodulation-division (RND)-type efflux pumps, transporting the last one metals from the cytoplasm directly to the extracellular medium. Each color name represent the transporter belong to a specific family that transport a specific metal or metals. Light blue: Co²⁺ and Ni²⁺; green: Cu²⁺; pink: Zn²⁺; and purple: Mn²⁺. See text for more details.

7.3.2 Regulation and metal homeostasis

The metal homeostasis was defined by Ma et al., 2009 as ‘the maintenance of an optimal bioavailable concentration, mediated by the balancing of metal uptake and intracellular trafficking with efflux/storage processes’. Extensive regulatory and protein machineries are devoted to

maintain the homeostasis of biologically required metal ions and underscores the essentiality of this process for cell viability, acting to regulate uptake, efflux, intracellular trafficking within compartments, and storage (Waldron et al., 2009). Seven major families of high affinity transcriptional regulators involved in metal homeostasis have been identified in different bacteria and functionally or structurally characterized: ArsR, CsoR/RncR, MerR, CopY, Fur, NikR, and DtxR (Giedroc and Arunkumar 2007, Braymer and Giedroc 2014).

There are two mechanisms of action for these regulators. ArsR, CsoR/RncR, MerR and Cop, bind to the DNA repressing, gene expression, but once the metal binds them, the regulator is released and allows the access of the promoter region to the transcription machinery, inducing the expression of genes usually involved in metal efflux. These four families (ArsR, CsoR/RncR, MerR, and Cop) are able to bind and sense biological and non-biological metals (Giedroc and Arunkumar 2007). See Fig. 13A.

- **ArsR:** The ArsR family (or ArsR/SmtB) is a large and functionally diverse metalloregulatory family extensively studied, involved in the regulation of biological metals as well as high toxic ones: Co, Ni, Cu, Zn, As, Bi, Cd and Pb (Zhang et al., 2009).
- **MerR:** MerR proteins have a structural diversity in the C-terminal region that allows binding of different metals: Cu, Zn, Ag, Cd, Au, Hg and Pb.
- **CsoR/RcnR:** The CsoR/RcnR family encloses *M. tuberculosis* CsoR, a Cu¹⁺ sensor regulator (Liu et al., 2007), and RcnR, that regulates the expression of the efflux protein RcnA involved in the Ni and Co efflux under induced cobalt stress (Rodrigue et al., 2005; Blériot et al., 2011).
- **CopY:** It represents a family of copper-specific metalloregulatory proteins regulating the transcription of the *copYZBA* operon which encodes the specific P-type ATPases CopA involved in copper efflux (Ma et al., 2009).

For the second block of family regulators (Fur, DtxR and NikR), the metal activates the repressor activity of Fur, DtxR and NikR, through a conformational change of the regulatory protein. These proteins then bind to specific DNA sequences, blocking the DNA transcription. These three families, (Fur, DtxR and NikR) are specific to biological metals, and usually repress the expression of genes involved in metal acquisition (Giedroc and Arunkumar, 2007). See Fig. 13B.

- **NikR:** this family of regulator was initially characterized in *E. coli*, is composed of transcriptional regulators described as a dimer of dimers (Chivers and Sauer, 1999), and

repress the expression of proteins involved in nickel uptake and of nickel-dependent enzymes (De Pina et al., 1999). For example, NikR regulates the expression of the ABC transporter NikABCDE decreasing its synthesis in abundant nickel concentrations, and therefore reducing the metal uptake into the cell (Rowe et al., 2005).

- **DtxR:** The DtxR family of metalloregulatory proteins includes two major subfamilies. One is the DtxR-like Fe²⁺ sensing repressor subfamily regulating genes that encode for proteins mediating iron uptake and storage (Andrews et al., 2003). These genes are constitutively expressed under iron-limiting conditions. MntR-like Mn²⁺, the second sensing repressors subfamily, regulates the transcription of the high affinity manganese uptake systems encoded by the *mntABCD* and *mntH*. MntR represses the expression when cytosol Mn²⁺ levels are high (Schmitt, 2002).
- **Fur:** The Fur protein (Ferric Uptake Regulator), belongs to the FUR superfamily. This protein was first identified in *E. coli* and is the prototype of this growing family of metalloregulatory proteins (Escolar et al., 1999), which acts as a repressor controlling the expression of the vast majority of genes involved in iron acquisition. Fur acts as a repressor with a dimer conformation, containing for each monomer a DNA binding domain, in the N-terminal domain, and a dimerization domain in the C-terminal domain. When the intracellular concentration of iron is elevated, Fe²⁺ binds to Fur, resulting in a conformational change that allows the protein to bind to a specific DNA sequence called the Fur-Box, in the promoter region of genes involved in iron homeostasis. A dimer of Fur binds on each sides of the DNA double helix preventing the RNA polymerase binding, and consequently the repression of the genes (Fillat, 2014). Fur responds *in vivo* to iron, but there are five other regulatory proteins belonging to this superfamily that respond to other different biological metals: Zur (zinc uptake regulator) responds to Zn; Nur (nickel uptake regulator) that responds to nickel; Wall (Manganese uptake regulator); PerR (Peroxide stress regulator) and Irr (Heme regulator regulator) (Fillat, 2014). In *P. aeruginosa*, Fur and Zur were identified (Ellison et al., 2013; Fillat, 2014). They are no example yet of cross-recognition of DNA targets among these different regulators, suggesting that they control mutually exclusive regulons (Herbig and Helmann, 2002)

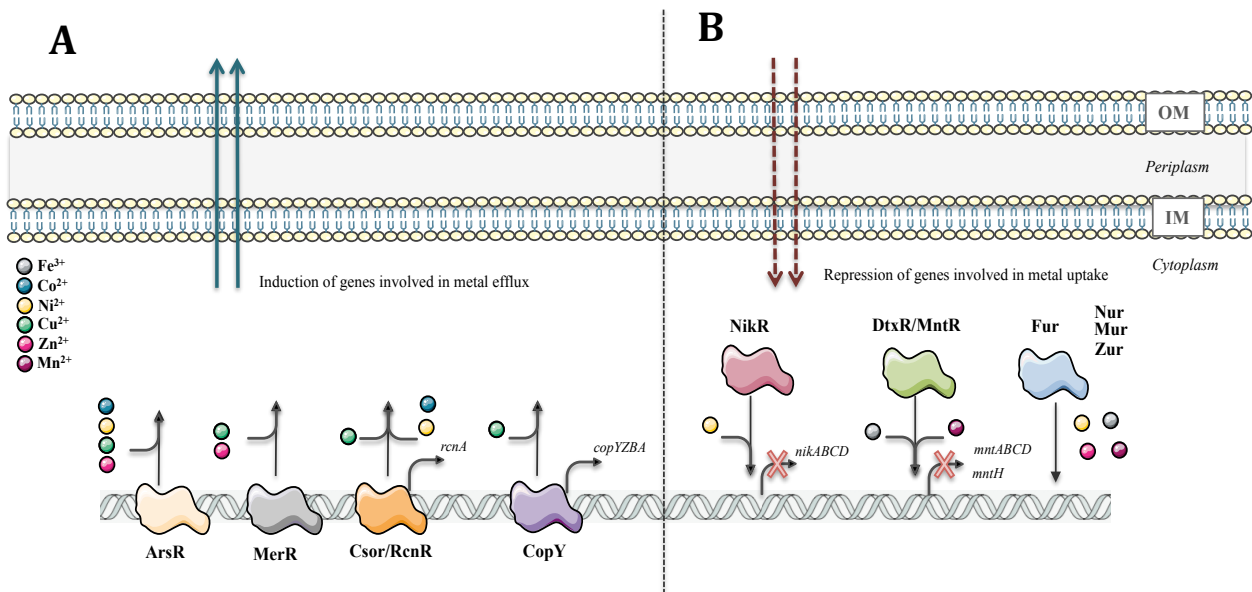


Figure 13. Families of transcriptional regulators involved in biological metals homeostasis in bacteria. A: Transcriptional activators that allow the DNA transcription when they are activated by specific metal or different metals, promoting the expression of bacterial genes involved in metal efflux. **B:** Transcriptional repressors that block the DNA expression once they are activated by the metal or metals, promoting the repression of genes involved in metal uptake. See text for more details.

Part 3

Siderophores and other metal chelators

1. Siderophore

Siderophores are small organic chelators with low weights (200–2000 Da) produced by microorganisms (Schwyn and Neilands, 1987), fungi (Haas et al., 2008) and plants (Kloepper et al., 1980), called in this case phytosiderophores. Their main function is to scavenge ferric iron (Fe^{3+}) from environments, transporting it into the cells via specific iron uptake pathways, and making this essential nutrient bioavailable for bacteria. Siderophores have extremely high affinities for Fe^{3+} with stability constants between 10^{10} to 10^{49} M^{-1} (Boukhalfa and Crumbliss, 2002), although they are generally around 10^{30} M^{-1} (Albrecht-Gary et al., 1994; Raymond et al., 2003). Enterobactin is the siderophore with the highest affinity for this metal (Miethke and Marahiel, 2007). Since the discovery of microbial siderophores in the 1950s by Lankford with the identification of mycobactin, over 500 different other siderophores have been identified, of which 270 have been structurally characterized (Boukhalfa and Crumbliss, 2002; Hider and Kong, 2010).

Each siderophore is specifically produced by one or a few bacteria *spp.* Most bacteria *spp.* are able to produce different siderophores, and many are even capable of using siderophores produced by other bacteria. In this last case, the siderophores are called xenosiderophores. This allows a better adaptation of the bacteria to the environment by extracting iron from diverse sources (Brock et al., 1991; Valdebenito et al., 2006).

Siderophores can also be used to identify and characterize microbial strains by a process called siderotyping, based on the chemical structures and characteristics of the siderophores produced (Meyer et al., 1998; Fuchs et al., 2001). For example, *Pseudomonas* produce over 50 different pyoverdines (Boukhalfa and Crumbliss, 2002), family of siderophores all composed of a chromophore linked to a peptide of 8 to 12 amino acids. The peptide chain of the fluorescent pyoverdines varies among the different species and this variability can be easily used to determine the relatedness of these species. Siderotyping could become a powerful tool in environmental research to provide a quick and unambiguous identification of microbes at the species level (Meyer et al., 2002; Meyer, 2010).

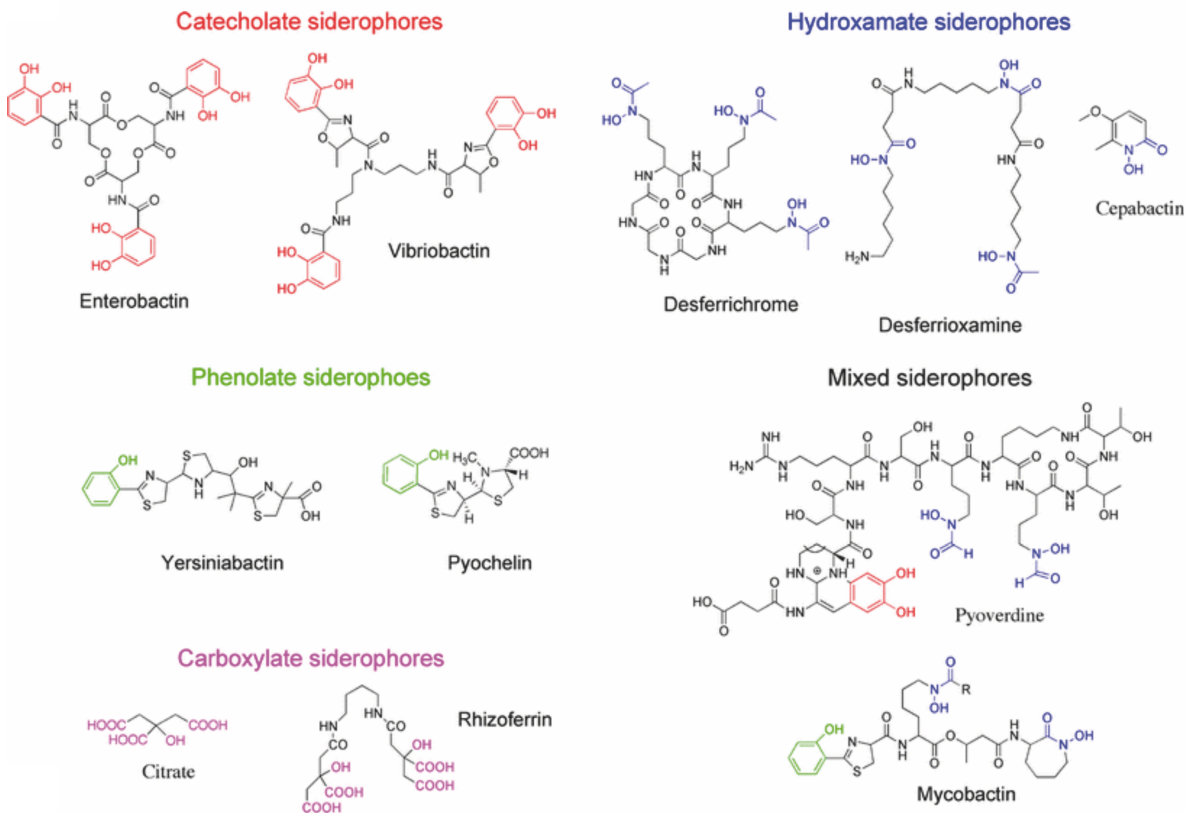


Figure 14. Different families of siderophores (Schalk and Guillon, 2013a). The different groups in colour indicate the groups of each siderophore family involved in the chelation of ferric iron.

2. Siderophores in iron transport

2.1. Siderophore-Fe coordination

Siderophores have up to six oxygen or nitrogen electron donor atoms, which can bind the iron cations. This is the case of the enterobactin (Fig. 15) and the pyoverdine. Since iron preferentially forms a hexacoordinated complex, some siderophores possess three dentates for the coordination of metal. In the case of siderophores that only have two or one dentate, they chelate iron with a stoichiometry of two or three siderophores for one ferric ion, as pyochelin does (Tseng et al., 2006).

Siderophores can be classified in four major families, depending on their motifs involved in iron chelation: catecholates are the most common (e.g. enterobactin), carboxylates (e.g. rhizobactin), phenolates (e.g. pyochelin or yersiniabactin), and hydroxamates (e.g. cepabactin). However, there

are also some types of bacterial siderophores that contain a mix of chelating groups, like pyoverdine produced by *P. aeruginosa* (Cornelis, 2010) (Fig. 14).

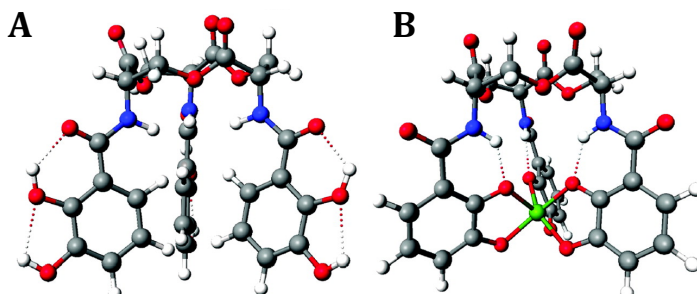


Figure 15. Schematic and space filling structures of enterobactin (A) and enterobactin-Fe complex (B). The B structure is considered to be a close model of the Fe^{3+} complex. The structure A is a computer-generated structure of uncomplexed enterobactin based on the trilactone structure of Seebach et al., 1992. The oxygen atoms are depicted in red, the nitrogen atoms in blue, the carbon atoms in grey, the hydrogen atoms in white, and the metal ion (Fe^{3+}) is labelled in green (Raymond et al., 2003).

2.2. Siderophore-Fe transport into bacteria

Once iron is chelated by the siderophore in the extracellular medium, the siderophore-Fe complex formed is transported across the outer membrane into the periplasm *via* a TonB-dependent transporter (TBDT). Afterwards, some classes of siderophores release Fe in the bacterial periplasm and some others deliver this metal in the bacterial cytoplasm. In this second case, ferri-siderophore complexes are transported further across the inner membrane by ABC transporters or proton motive dependent permeases (Schalk and Guillon, 2013a). Fe is released from siderophores in the bacterial periplasm or cytoplasm by mechanisms involving mostly a Fe reduction step coupled often to a chemical modification or degradation of the siderophore.

TBDTs are embedded in the outer membrane and recognize at the bacterial cell surface specific siderophore-Fe complexes (Krewulak and Vogel, 2008), transporting them into the periplasm. The energy necessary for this transport is provided by the proton-motive force (pmf) of the inner membrane, which is transferred to the TBDT by the inner membrane TonB complex, composed of three proteins TonB, ExbB and ExbD (Schalk, 2008; Noinaj et al., 2010) (Fig. 17A). TonB–ExbB–ExbD complex is composed of a pentamer of ExbB, a dimer of ExbD, and at least one TonB (Celia et al., 2016).

All known TBDTs share a general structure consisting of a C-terminal 22-stranded β -barrel

embedded in the outer membrane and a N-terminal plug domain, also known as the ‘cork domain’ and located in the lumen of the β -barrel (Fig. 16) (Postle and Larsen, 2007; Noinaj et al., 2010). The siderophore-Fe binding site is located on the extracellular face of the transporter and is composed of residues of the plug and the barrel domains (Schalk et al., 2012). At the N-terminal region, after the cork domain, on the periplasmic face of the protein, is located a conserved region called the TonB box of 5 to 7 residues (Fig. 17) (Schramm et al., 1987; Noinaj et al., 2010). This region is essential for the interaction between the TBDTs and the TonB protein and therefore critical for energy transduction and transport. When the siderophore-Fe complex interacts with its binding site on the TBDT, conformational changes in the plug domain occur and make possible the formation of a stable physical interaction between the N-terminal TonB box of the transporter and the inner membrane TonB protein (Noinaj et al., 2010; Schalk et al., 2012). This protein interaction allows energy transduction from the TonB–ExbB–ExbD complex to the TBDT, which causes further conformational changes in the plug domain and allows the transport of the siderophore-Fe complexes into the periplasm. The exact mechanism of translocation of ferri-siderophore complexes through TBDT or the mechanism of channel formation in these transporters has not been elucidated yet. However, recently were suggested two mechanisms to explain how the TonB complex harnesses the pmf: the electrostatic piston model, where the trans-membrane helix of ExbD moves in a translational way within the trans-membrane pore of ExbB, creating a piston-like motion; and the rotational model, where the trans-membrane helix of ExbD rotates within the trans-membrane pore of ExbB, creating rotational motion, a combination of both mechanisms may also be possible (Celia et al., 2016).

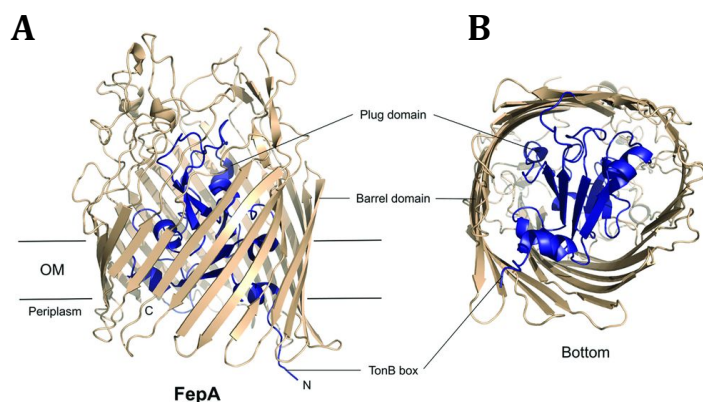


Figure 16. Structure of the enterobactin TBDT transporter FepA. (A) Crystal structure of FepA embedded in the outer membrane from a lateral view (Buchanan et al., 1999). (B) View from the periplasm of the TBDT, showing the C-terminal 22-stranded β -barrel and the N-terminal plug domain. The barrel domain is shown in tan, and the plug domain in blue (Neumann et al., 2017).

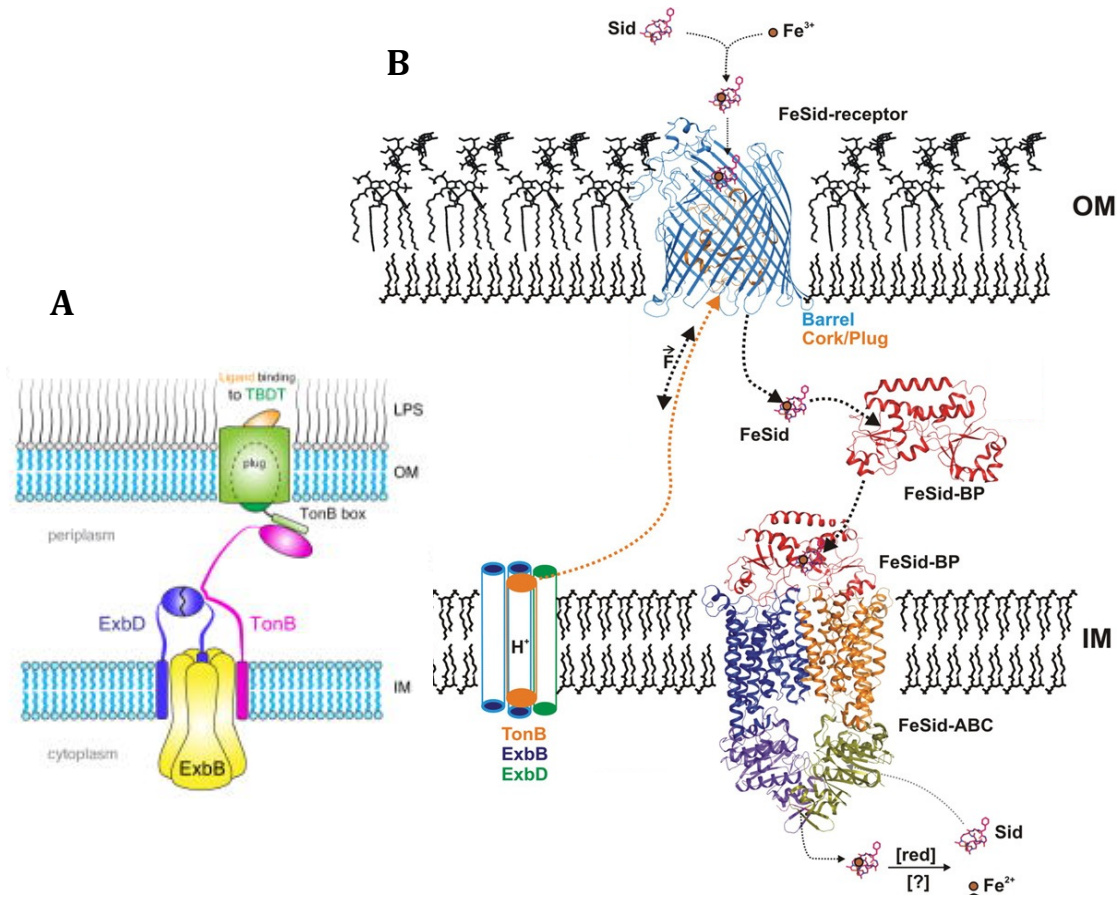


Figure 17. A: Structural model for the TonB complex, which consists of a pentamer of ExbB, a dimer of ExbD, and at least one TonB (Celia et al., 2016). B: Ferric iron transport into bacteria (*E. coli*) via siderophore uptake pathway. 'FeSid' represents the complex siderophore-Fe³⁺, originally formed in the extracellular medium. The 'FeSid-receptor' is the outer membrane specific transporter, a TonB-dependent transporter (TBDT) that recognizes with high affinity the complex FeSid. Once FeSid is bound to the TBDT, its N-terminus is activated and the protein make possible the transport of FeSid into the periplasm from the extracellular medium using the energy delivered from the TonB complex. Then FeSid is generally associated to a periplasmic binding protein (PBP) also called binding protein (BP), which will present FeSid to the inner membrane transporter, an ABC transporter-type, delivering FeSid into the cytoplasm. Once in the cytoplasm, a reducer environment, Fe³⁺ is released from the siderophore by different mechanisms, and it is reduced to Fe²⁺. Siderophore can be then recycled or degraded. Modified figure from Zeth, 2012.

For the transport of siderophore-Fe complexes across the inner membrane into the cytoplasm, two families of transporters can be involved either ABC transporters or proton motive dependent permeases. In the case of the ABC transporters, once the ferri-siderophore is in the periplasm, it binds to the siderophore-periplasmic binding protein (PBP) component of the ATP-binding cassette (ABC) transporter. The ferrisiderophore is then transferred to the permease part of the transporter and imported into the cytoplasm (Hvorup et al., 2007). See Fig. 17B. ATP hydrolysis is

coupled to this transport. Bacterial ABC transporters involved in ferri-siderophore import commonly consist of five structural domains: a periplasmic binding protein, two transmembrane polypeptides that form a channel through which the ferrisiderophore is transported and two nucleotide binding subunits that hydrolyse ATP. It is the case of ABC transporters FepBCDE and FhuBCDE involved in ferrichrome-Fe and enterobactin-Fe uptake in *E. coli* (Koster and Braun, 1989; Staudenmaier et al., 1989; Chenault and Earhart, 1991; Koster, 1991; Köster, 1997; Braun and Herrmann, 2007). More recently, it has been shown that uptake of siderophore-Fe complexes across the bacterial inner membranes can also be carried out by proton motive dependent permeases. This is the case of the pyochelin-Fe pathway in *P. aeruginosa* (Reimann, 2012), and the rhizobactin-Fe pathway in *Sinorhizobium meliloti* (Cuív et al., 2004).

Concerning iron release from the siderophores three different mechanisms have been proposed: siderophore hydrolysis, chemical modification, and/or iron reduction (Schalk and Guillon, 2013a). All three mechanisms involve a decrease of the siderophores affinity for iron. Iron release from siderophores occurs either in the cytoplasm or periplasm, depending of the siderophores and the bacteria. For example, in the case of pyochelin-Fe and ferrichrome-Fe pathways in *P. aeruginosa* and in *E. coli* respectively (Fig. 18A&B), iron dissociation from the siderophores occurs in the bacterial cytoplasm (Schalk and Guillon, 2013a). In the case of the pyoverdine-Fe, citrate-Fe and enterobactin-Fe pathways in *P. aeruginosa*, this step occurs in the bacterial periplasm (Schalk and Guillon, 2013a and unpublished data of the team) (Fig. 18C). However, there are some exceptions for these schemes with the case of the salmochelin-Fe pathway in *Salmonella sp.* In this iron uptake pathway, the siderophore-Fe complex undergoes a first hydrolysis in the periplasm and a second in the cytoplasm coupled to an iron reduction step allowing complete release of iron from the siderophore (Lin et al., 2005; Zhu et al., 2005). Moreover, this chemical modification of the siderophores can be a complete hydrolyses of the siderophore as for enterobactin, or just a chemical modification in order to decrease its affinity for iron, like an acetylation of the siderophore in the ferrichrome pathway in *E. coli* and *P. aeruginosa* (Hannauer et al., 2010a). For some siderophore-dependent iron uptake pathway, as for iron uptake by pyoverdine in *P. aeruginosa*, the siderophore needs not to be chemically modified to be able to release iron. In all cases, the siderophore or the hydrolysed or chemically modified siderophores are recycled into the extracellular medium by efflux systems. In the case of pyoverdine, the siderophore is recycled via the efflux pump PvdRT-OpmQ (Fig. 18C).

In contrast, in gram-positive bacteria (e.g. *Bacillus sp.*), where the outer membrane is lacking, the

outer membrane TonB-dependent transporters are absent. Therefore, the siderophore-Fe complexes are caught from the bacterial environment by periplasmic siderophore binding proteins that are anchored to the cell membrane (Fukushima et al., 2013). Afterwards the siderophore-Fe complexes are transferred to the permeases of ABC transporters as in gram-negative bacteria (Braun and Hantke, 2011).

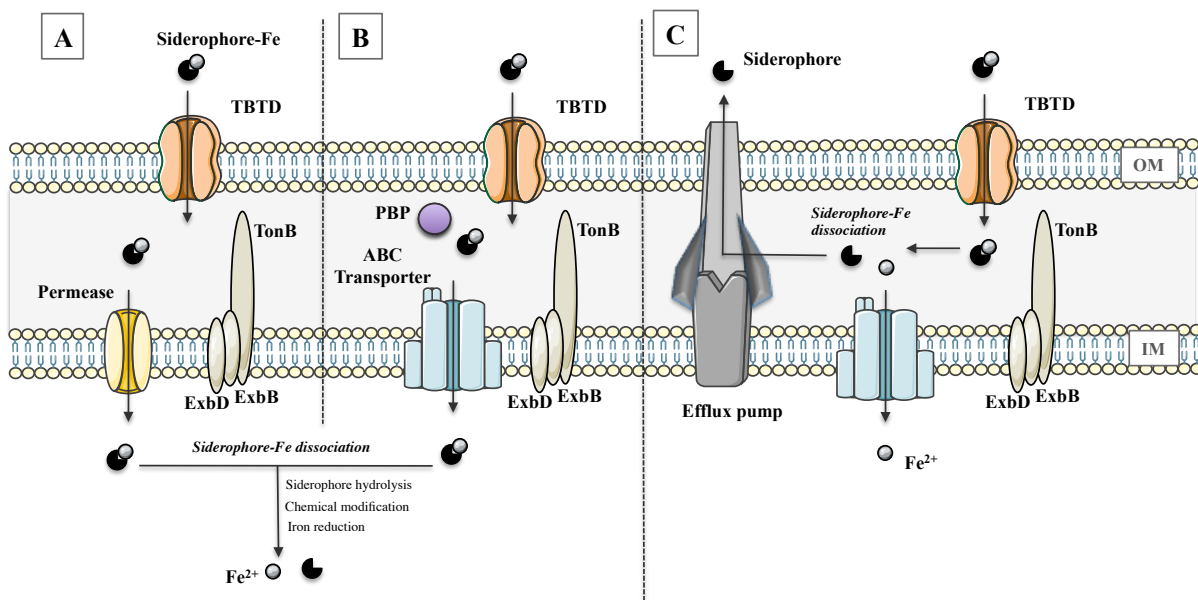


Figure 18. Different mechanisms and strategies of siderophore-Fe uptake and dissociation in Gram-negative bacteria. Siderophore-Fe uptake across the outer membrane always involves a specific TonB-dependent transporter (TBTD). Siderophore-Fe transport across the inner membrane involves either specific ABC transporters (B) or specific permeases (A). Depending on the siderophores, iron may be released from the chelator either in the cytoplasm (A and B) or periplasm (C). Different mechanisms can be involved in iron release from siderophores: siderophore hydrolysis, chemical modification of the siderophore and/or iron reduction. Modified figure from Schalk et al., 2011.

3. *Pseudomonas aeruginosa* siderophores

P. aeruginosa produces two major siderophores to get access to iron: pyoverdine (PVD) (Cox and Adams, 1985) and pyochelin (PCH) (Cox, 1980). PVD is a siderophore with a high affinity for iron (10^{31} M^{-1}) (Albrecht-Gary et al., 1994), and PCH with a lower affinity (10^{28} M^{-2}) (Brandel et al., 2012). It was shown that PVD is more effective transporting iron into bacteria, and it could seem that PCH production is superfluous, but there are evidences supporting the importance of the PCH for *P. aeruginosa*.

It is known that *P. aeruginosa* is able to switch between both siderophore iron uptake pathways, and choose one over the other depending on the environmental conditions, with the objective to improve the iron uptake efficiency. It is proposed that such switching could potentially emerge from interactions between the respective negative and positive feedback loops, which are part of the mechanisms of regulation of these pathways and are a response to the environmental conditions of the bacteria (Cornelis and Dingemans, 2013; Dumas et al., 2013). See Regulation mechanisms in 'Part 4'. In high iron restricted conditions, *P. aeruginosa* produces PVD and in less iron-restricted media, it will produce PCH (Cunrath et al., 2016).

P. aeruginosa can also get access to iron using siderophores produced by other bacteria *spp.* called xenosiderophores, such as PVDs from other pseudomonads (Greenwald et al., 2009), enterobactin (Poole et al., 1990), cepabactin (Mislin et al., 2006), mycobactin and carboxymycobactin (Llamas et al., 2008), ferrichrome (Hannauer et al., 2010a), deferrioxamines (Llamas et al., 2006) and desferrichrysin, desferricrocin, coprogen (Meyer, 1992), aerobactin and its analogue rhizobactin (O'Cuiv et al., 2006) and citrate (Cox, 1980; Harding and Royt, 1990). The ability to use these different siderophores is allowed thanks to the expression in *P. aeruginosa* cells of specific import proteins for each of these siderophores as shown in Table 3.

Moreover, *P. aeruginosa* can also import Fe^{2+} via the FeoABC inner membrane transporter (Kammler et al., 1993). At last, *P. aeruginosa* can import heme as an iron source via the TonB-dependent transporter FhuR, HasR or HxuR, transporting directly the heme or complexing it previously to a hemophore protein HasAp (Letoffe et al. 1999; Lefevre et al. 2008; de Amorim et al. 2013).

Siderophores	Outer membrane transporters
Pyoverdine	FpvA, FpvB
Pyochelin	FptA
Citrate	FecA
Ferrichrome, ferrioxamine	FiuA, FoxA
Enterobactin, proteochelin, azotochelin	PfeA
Mycobactin, carboxymycobactin	FemA
Rhizobactin, aerobactin, schizokinen	ChtA
Vibriobactin	FvbA
Cepabactin	?
Coprogen, desferrichrysin, desferricrocin,	?

Table 3. Outer membrane transporters present in *P. aeruginosa*, associated to the siderophores used by *P. aeruginosa* to get access to iron.

3.1. Pyoverdine (PVD)

PVD is the yellow-green, water-soluble, fluorescent pigment produced by all fluorescent *Pseudomonas* species. PVD was discovered in 1892 but it was originally described using different names, fluorescein, or pseudobactin in soil isolates, and its function in iron transport was conclusively established only in the late 1970s (Meyer and Abdallah, 1978).

More than 50 different types of PVD are produced by different strains and species of *Pseudomonas* (Budzikiewicz, 2004), but all of them are composed of the same three parts: a chromophore, derived of quinoline (2,3-diamino-6,7-dihydroxyquinoline); a variable peptide of 6-12 amino acids linked at the position C1 of the chromophore; and a side chain located at the C3 of the chromophore, that can be a dicarboxylic acid or a di-carboxylic amide (Meyer, 2000; Ravel and Cornelis, 2003a). The chromophore moiety confers the yellow-green characteristic colour of PVD and makes this molecule fluorescent under UV exposure with a maximum of emission of fluorescent at 450 nm when excited at 400 nm (Folschweiller et al., 2002).

P. aeruginosa strains produce three PVDs, which differ in the sequence and length of their peptide chains (Schalk and Guillon, 2013b). Each of these three PVD (PVDI, PVDII and PVDIII) is associated to a specific TonB dependent transporter (TBDT, FpvAI, FpvAII and FpvAIII) (Cornelis et al., 1989). The PVD produced by *P. aeruginosa* PAO1 is PVDI (Fig. 19), and FpvAI is its specific outer membrane transporter.

PVDI structure has been solved by mass spectrometry and NMR (Demange et al., 1990), and it has been demonstrated that it is composed of a partially cyclized octapeptide attached to the 2,3-diamino-6,7-dihydroxyquinoline-based chromophore. It chelates iron with a stoichiometry of 1:1 (PVDI:Fe³⁺), *via* the catechol group of the chromophore and the two hydroxyornithines of the peptide moiety, with an affinity of 10^{30,8} M⁻¹ (Albrecht-Gary et al., 1994). Only the PVDI iron uptake pathway of *P. aeruginosa* has been investigated at the molecular level and not PVDII and PVDII pathways.

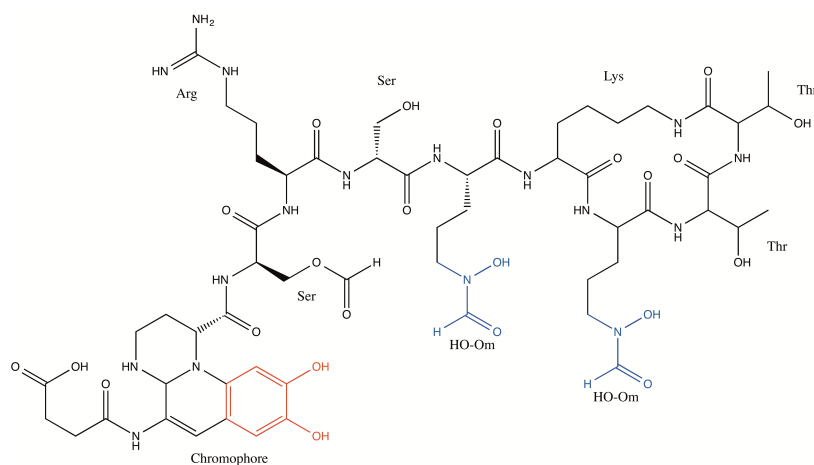


Figure 19. Structure of PVDI. Catechol group in red and hydroxyornithines groups in blue, which coordinate with ferric iron.

3.1.1. PVDI biosynthesis

PVDI biosynthesis is a complex process starting in the bacterial cytoplasm and ending in the periplasm. It requires numerous synthesis and maturation steps, and amino acid modifications, involving at least eleven different enzymes (Schalk and Guillon, 2013b; Cézard et al., 2015). See Fig. 20. The backbone of PVDI is a peptide of 11 amino acids, with the sequence L-Glu – L-Tyr – D-Dab – L-Ser – L-Arg – L-Ser – L-fOHOrn – L-Lys – L-fOHOrn – L-Thr – L-Thr and which is assembled as a precursor in the bacterial cytoplasm. The first amino acid of the peptide (L-Glu) is the precursor of the α -ketoglutaric acid, succinamide or malamide side chains bound on C3 of the PVDI chromophore. The adjacent L-Tyr and D-Dab (D-amino butyric acid) residues form the chromophore and the other eight residues the peptide moiety. This PVDI precursor is assembled in the cytoplasm from the N- to the C-terminal end by the coordinated action of four nonribosomal peptide synthetases (NRPSs): PvdL, PvdI, PvdJ, and PvdD (Mossialos et al., 2002; Ackerley et al., 2003; Ravel and Cornelis, 2003). These proteins are multienzymatic complexes working as

'assembly chains' in which the different basic elements of the siderophore are successively assembled. The biosynthesis also involves PvdA, PvdF and PvdH, three cytoplasmic enzymes that participate in the synthesis of atypical amino acids present in the PVDI backbone. It has been shown that all these 7 enzymes are partially associated with the inner leaflet of the cytoplasmic membrane, forming a siderosome (Imperi and Visca, 2013) that are concentrated rather at the poles of the bacterium. The siderosome is considered as a multi-protein complex associated to the cytoplasmic membrane and composed of all the biosynthesis proteins of a specific siderophore. Therefore, the different siderophore precursors move from the binding site of one enzyme to the next one in the biosynthesis pathway without leaving the siderosome. Such an organization limits the diffusion of the precursors of the siderophore in the cytoplasm, which could be toxic to the bacterium because of iron or other metal chelation (Schalk and Guillon, 2013b).

Consistent with the existence of this siderosome, it has been shown that the cytoplasmic PVDI precursor has a myristic or myristoleic acid chain bound to the first residue of the peptide backbone (Glu) probably keeping the cytoplasmic PVDI precursor bound to the inner membrane during its assembling. Indeed, this fatty acid chain is linked to the first amino acid of PVDI backbone at the beginning of the siderophore biosynthesis. This cytoplasmic PVDI precursor has an unformed chromophore and is apparently transported across the inner membrane by the export ABC transporter PvdE (McMorran et al., 1996). Once in the periplasm, the myristic chain is removed by PvdQ and the chromophore cyclized by PvdP (Nadal-Jimenez et al., 2014). At last, PvdN is involved in the transformation of the N-terminal glutamic acid to a succinamide (Ringel et al., 2016). The newly synthesized PVDI is stored all over the periplasm (Yeterian et al., 2010).

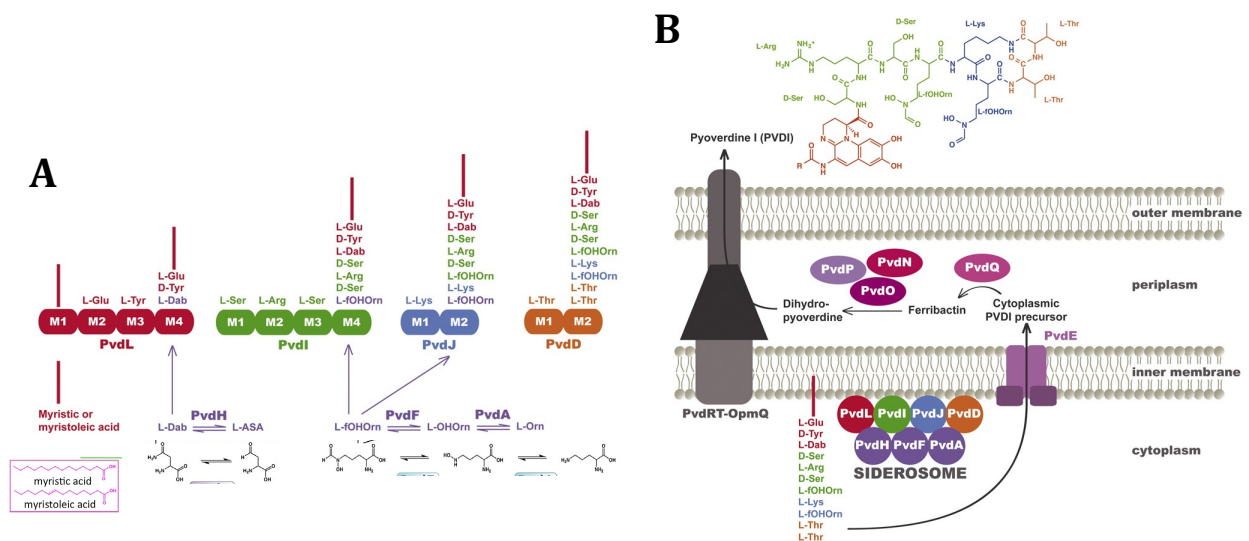


Figure 20. A: Pyoverdine (PVDI) cytoplasmic precursor biosynthesis pathway in *P. aeruginosa*. B: Steps of PVDI assembling carried out in the siderosome. Read main text for details. Modified figure from Gasser et al., 2015.

3.1.2. PVDI secretion

It has been demonstrated that PvdRT-OpmQ efflux pump is involved in the secretion of newly synthesized PVDI after the final steps of biosynthesis in the periplasm (Fig. 20B) (Hannauer et al., 2010b; Hannauer et al., 2012). This efflux pump is predicted to have the same organization as other bacterial efflux pumps (Nikaido and Takatsuka, 2009) with PvdT, an ATP-dependent inner membrane protein, PvdR a periplasmic adaptor protein and OpmQ porin-like β -barrel located in the outer membrane with a large periplasmic extension (Schalk and Guillon, 2013b). In the absence of this efflux system, PVDI accumulates in the bacterial periplasm and its secretion is partially decreased, supposing that another efflux system can carry out secretion (Hannauer et al., 2010b; Schalk and Guillon, 2013b).

3.1.4. PVDI-Fe uptake

PVDI-Fe complex is recognized and transported into the bacterial periplasm by two possible TonB-dependent outer membrane transporters FpvAI and FpvB. Only the structure of FpvAI has been solved in different siderophore loading status: without PVDI, loaded with PVDI-Fe and in interaction with other PVDs. FpvAI has the general structure of the TBDT, involving a β -barrel, a plug domain inserted in the barrel domain, followed by the TonB box and at last an additional domain not present in all TonB-dependent transporters called the signalling domain. This last N-

terminal domain located in the bacterial periplasm interacts with the sigma FpvR regulator inserted in the internal membrane (Cobessi et al., 2005; Brillet et al., 2007). The PVDI-Fe binding site of FpvAI is located on the extracellular part of the protein and is mostly composed by hydrophobic amino acids belonging to the plug and the barrel domains. The process of recognition between FpvAI and PVDI-Fe is siderophore specific (Greenwald et al., 2009), with nanomolar affinities (Schalk et al., 2001; Clément et al., 2004). The PVDI-Fe transport is possible due to the induction of a conformational change in FpvAI *via* the TonB machinery, allowing the formation of a channel, through which PVDI-Fe is translocated into the periplasm. See Fig. 21.

3.1.5. PVDI-Fe dissociation and recycling

Once in the periplasm, iron is released from PVDI by a mechanism involving iron reduction and no chemical modification or hydrolysis of the siderophore (Greenwald et al., 2007). This PVDI-Fe mechanism of dissociation involves first an interaction of PVDI-Fe with two periplasmic binding proteins FpvC and FpvF able to form an FpvF-FpvC-PVDI-Fe complex (Brillet et al., 2012). FpvC and FpvF belong to two different sub-groups of periplasmic binding proteins: FpvC appears to be a metal-binding protein whereas FpvF has homology with ferrisiderophore binding proteins (Brillet et al., 2012). Iron reduction involves the inner membrane complex FpvGHJK, where FpvG acts as a reducer (Ganne et al., 2017). Fe^{2+} is then released from PVDI and probably still in complex with FpvC, which brings the ferrous iron to the ABC transporter FpvDE for the transport of the free metal into the cytoplasm (Brillet et al., 2012). The metal-free PVDI is probably still in interaction with FpvF (Brillet et al., 2012) and brings the siderophore to the PvdRT-OpmQ efflux pump to be recycled to the extracellular medium (Schalk et al., 2002; Greenwald et al., 2007; Imperi et al., 2009), where it can then re-start a new cycle of Fe^{3+} uptake. See Fig. 21.

3.1.6. PVD and virulence factors

PVD is also involved in the expression of different virulence factors, such as exotoxin A and protease PrpL (Lamont et al., 2002). The production of virulence factors enables *P. aeruginosa* to adhere to tissue surfaces, to damage tissue for dissemination and nutrition supply in order to increase its survival rate (Coggan and Wolfgang, 2012; Jimenez et al., 2012; Balasubramanian et al., 2013). Exotoxin A (PE) is an enzyme belonging to the mono-ADP-ribosyltransferase family (Liu, 1974) and PrpL is an extracellular endoproteinase with elastolytic activity that contributes to infection in a rat lung model (Wilderman et al., 2001). In the presence of iron ions, PVDI-Fe

complex interacting with FpvAI was found to activate a signalling pathway for the up-regulation of PE and PrpL expression (Lamont et al., 2002; Cornelis and Dingemans, 2013).

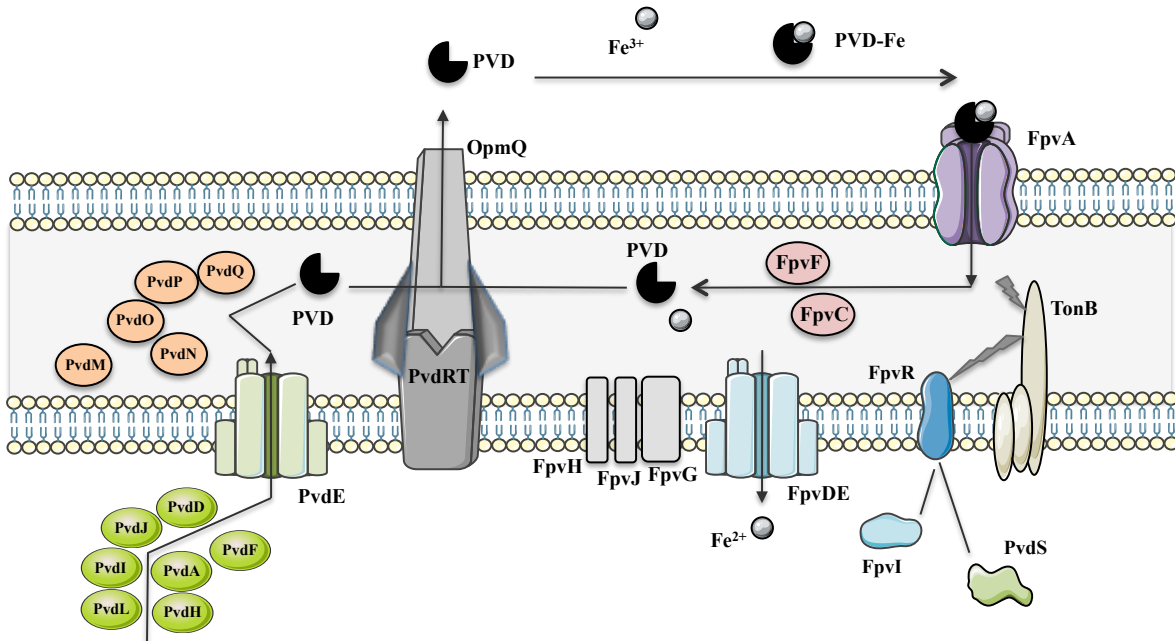


Figure 21. PVD iron uptake pathway in *P. aeruginosa*. Representation of the different processes of the PVD pathway to achieve the Fe acquisition: the biosynthesis, involving cytoplasmic and periplasmic enzymes, and the ABC transporter PvdE; the export to the extracellular medium by PvdRT-OpmQ; the Fe quelenation in relation 1:1 and the complex (PVD-Fe) recognition by the outer membrane transporter FpvA, which activate FpvR and release the sigma factors PvdS and FpvI for the regulation; the complex dissociation in the periplasm, allowing the recycling of PVD into the extracellular medium via PvdRT-OpmQ, and the Fe^{2+} import into the cytoplasm by the action of the ABC transporter FpvDE. From some non-published results from the laboratory we saw that FpvG interacts to FpvH, FpvF and FpvC, being involved in the reduction of the PVD-Fe complex.

3.2. Pyochelin (PCH)

PCH is the second major siderophore produced by *P. aeruginosa* and was characterized for the first time in the latest 1970 (Liu and Shokrani, 1978). This siderophore is a thiazoline derivative [2(2-o-hydroxy-phenyl-2-thiazolin-4-yl)-3-methylthiazolidine-4-carboxylic acid] (Cox et al., 1981), which binds ferric iron (Fe^{3+}) with a stoichiometry of 2:1 (PCH to Fe^{3+}) (Tseng et al., 2006) and an affinity of $10^{28} M^{-2}$ (Brandel et al., 2012). *P. aeruginosa* produce two different isoforms of this siderophore, PCHI and PCHII (PCH has three chiral centers at positions C4', C2'' and C4'') (Mislin et al., 2006). See Fig. 22.

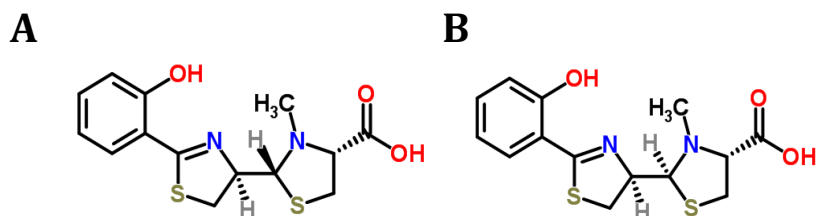


Figure 22. Structure of PCHI (A) and PCHII (B). Figures from Chempider.

PCH has been shown to increase the levels of reactive oxygen species (ROS) and inflammation, especially in the presence of pyocyanin, another *P. aeruginosa* extracellular compound (Adler et al., 2012; Jayaseelan et al., 2014). Therefore, the production of PCH could play a role in the sustained inflammatory response in chronic infections, which is known to produce tissue damage (Lyczak et al., 2002; Kiraly et al., 2015).

PCH has four groups that are able to chelate Fe^{3+} . Therefore, one molecule of PCH provides a tetra-dentate coordination of Fe^{3+} (Fig. 23), while a second molecule binds bidentately to complete the hexacoordinate octahedral geometry of ferric iron (Tseng et al., 2006). Consequently PCH chelates iron with a 2:1 (PCH:Fe) stoichiometry (Tseng et al., 2006) and an affinity of 10^{28} M^{-2} (Brandel et al., 2012).

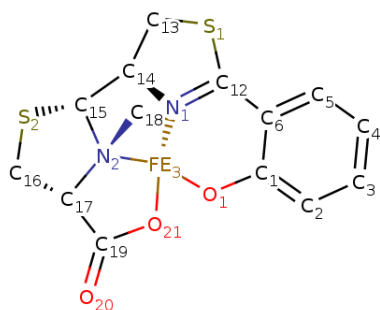


Figure 23. PCH-Fe complex tetra-coordinated with nitrogen (blue) and oxygen (red) groups. Image from RCBS protein data bank.

3.2.1. PCH biosynthesis

Like the majority of siderophores, PCH is synthesized by non-ribosomal peptide syntheses (NRPS) (Crosa and Walsh, 2002). The process of biosynthesis takes place in the cytoplasmic and involves seven biosynthetic enzymes organized in two operons, *pchDCBA* and *pchEFGHI* (Serino

et al., 1997; Reimmann et al., 1998) and according to the current knowledge of PCH biosynthesis, neither *pchH* nor *pchI* genes appears to be essential for PCH biosynthesis (Reimmann et al., 2001). PCH is the condensation product of salicylate and two molecules of cysteine (Youard et al., 2011). The isochorismate synthetase PchA and the isochorismate pyruvate-lyase PchB enzymes convert chorismate to salicylate *via* isochorismate (Gaille et al., 2002; Meneely et al., 2013). Salicylate is then linked to two molecules of L-cysteine by a thiotemplate mechanism involving the salicylate-adenylating enzyme PchD (Serino et al., 1997), the two NRPS PchE and PchF and the reductase PchG (Reimmann et al 1998, Quadri et al., 1999, Reimmann et al., 2004).

3.2.2. PCH secretion

The proteins and mechanisms involved in PCH secretion are still unknown, It has been suggested that PchI and PchH could be involved in the secretion of this sideriophore (Feinbaum et al., 2012), but unpublished data of our group have shown that deletion of these genes had no effect on PCH secretion.

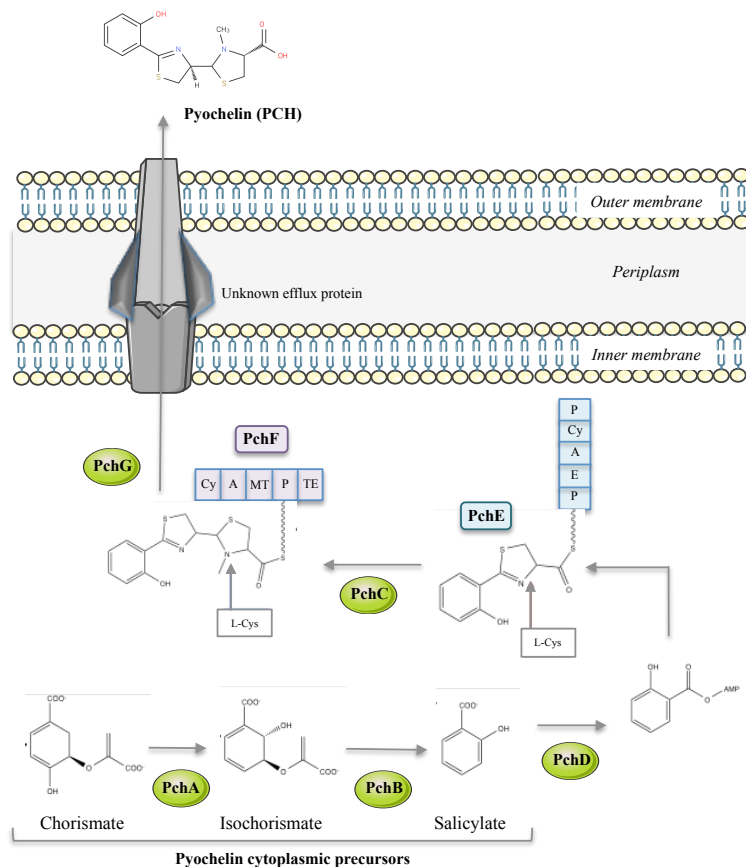


Figure 24. Biosynthesis of PCH in *P. aeruginosa*. See text for more information.

3.2.3. PCH₂-Fe uptake

After its formation, the PCH₂-Fe complex is recognized at the surface of *P. aeruginosa* cells and transported into the periplasm by the TonB-dependent transporter FptA (Cobessi et al., 2005) and then across the inner membrane into the cytoplasm by the proton motive dependent permease FptX.

The outer membrane transporter FptA is a TonB-dependent transporter, with a typical TBDT's structure, a C-terminal 22-stranded β -barrel embedded in the outer membrane and a N-terminal plug domain (Fig. 25A), followed by the TonB-box (Cobessi et al., 2005). FptA has not a signalling domain allowing an interaction with an anti-sigma factor, as FpvA (Cobessi et al., 2005). PCH₂-Fe binding site on FptA is composed of hydrophobic residues of the plug and barrel domains (Cobessi et al., 2005) and binds ferri-PCH with an affinity in the nM range. FptA binding site, like for all TBDTs, is highly siderophore-specific and even enantio-specific, because only one enantiomer of PCH is recognized (PCH has three asymmetric centers) (Hoegy et al., 2009). Moreover, only the PCH providing the tetradentate coordination of iron is necessary for recognition by FptA, the second PCH involved in the bidentate coordination does not interact with the transporter.

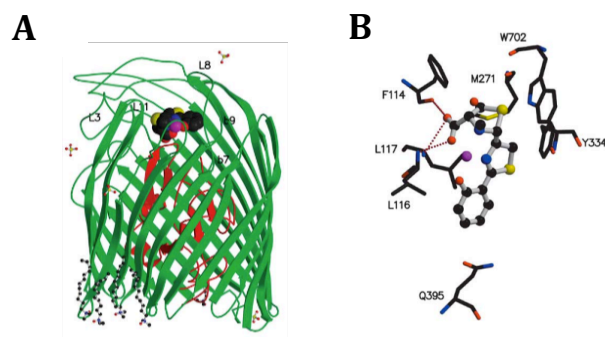


Figure 25. (A) FpyA structure (B) Amino acids of FptA binding site interacting with PCH-Fe.

Once in the periplasm, PCH₂-Fe complex is transported across the inner membrane into the cytoplasm by FptX permease (Michel et al., 2007; Youard et al., 2011; Cunrath et al., 2015). FptX is not enantiospecific like FptA, it can transport the ferric forms of PCH and its enantiomer (Reimmann, 2012). The energy necessary for this transport is provided by the proton motive force of the inner membrane. Iron is released from PCH in the bacterial cytoplasm by a so far unknown mechanism.

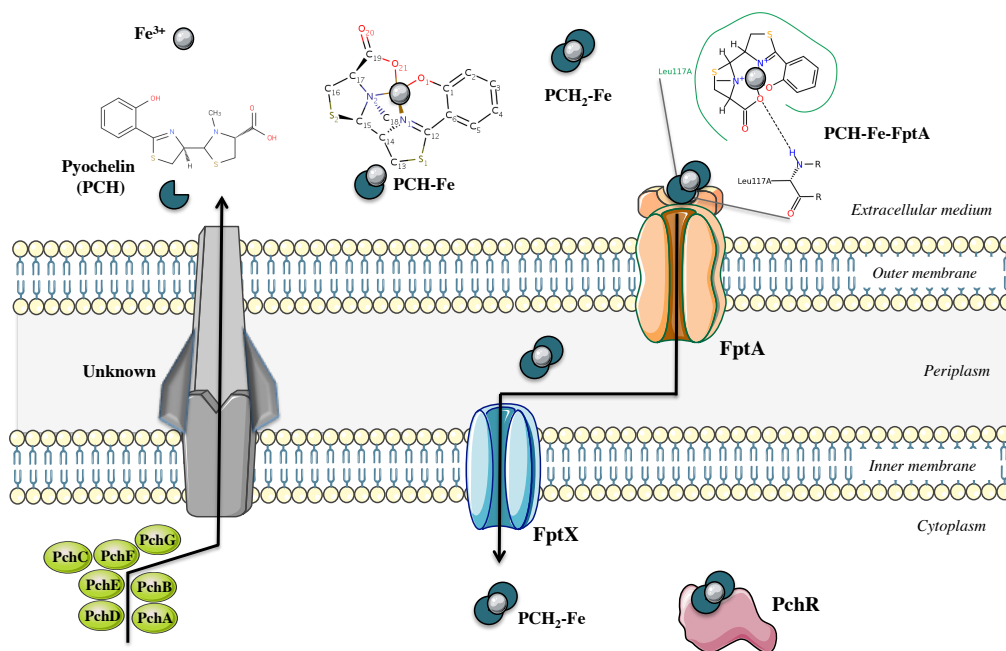


Figure 26. PCH iron uptake pathway in *P. aeruginosa*. The different processes representation of the PCH pathway to achieve the Fe acquisition: the PCH biosynthesis involves seven enzymes located in the cytoplasm; the secretion is still unknown; PCH chelates Fe^{3+} in the extracellular medium (2:1); $\text{PCH}_2\text{-Fe}$ transport involves the TBDT FptA in the outer membrane and the permease FptX in the inner membrane; once in the cytoplasm, $\text{PCH}_2\text{-Fe}$ complex activates the transcriptional regulator of this pathway, PchR.

4. Different roles of siderophores

The main function of any siderophore is the uptake of ferric iron into the cells, but these chelators can also be involved in other biological processes of bacteria.

4.1. Increase of heavy metal resistance in bacteria

Siderophores can also form stable complexes with metal cations other than iron (Hernlem et al., 1996; Neubauer et al., 2000). For example, the formation constants for the hydroxamate siderophore desferrioxamine B with Ga^{3+} , Al^{3+} and In^{3+} are between 10^{20} and 10^{28} M^{-1} , whereas that with Fe^{3+} is 10^{30} M^{-1} (Evers et al., 1989; Hernlem et al., 1996). Screening with sixteen different metals (Ag^+ , Al^{3+} , Cd^{2+} , Co^{2+} , Cr^{2+} , Cu^{2+} , Eu^{3+} , Ga^{3+} , Hg^{2+} , Mn^{2+} , Ni^{2+} , Pb^{2+} , Sn^{2+} , Tb^{3+} , Tl^+ and Zn^{2+}), carried by our team, revealed that PVD and PCH, the two major siderophores produced by *P. aeruginosa* are able to chelate all these metals (Braud et al., 2009a, 2009b). All metals can be transported into the cell *via* the porins, and this is the most common way toxic metals enter the periplasm of Gram-negative bacteria (Lutkenhaus, 1977; Pugsley and Schnaitman,

1978). Our group has shown in 2010, that the *P. aeruginosa* capable of producing PVD and PCH were more resistant to metal toxicity than strains unable to produce these siderophores. ICP-AES analyses of bacteria producing and none-producing siderophores grown in the presence of toxic metals showed that PVD and PCH are able to sequester toxic metals in the extracellular medium preventing their diffusion across the bacterial membranes.

4.2. Ability of siderophores to chelate and transport metals other than iron

Increasing evidence in the literature indicate that siderophores could be implicated in the homeostasis of other metals. Stable complexes are formed between siderophores and metal cations other than iron (Hernlem et al., 1996; Neubauer et al., 2000). Screening with sixteen different metals (Ag^+ , Al^{3+} , Cd^{2+} , Co^{2+} , Cr^{2+} , Cu^{2+} , Eu^{3+} , Ga^{3+} , Hg^{2+} , Mn^{2+} , Ni^{2+} , Pb^{2+} , Sn^{2+} , Tb^{3+} , Tl^+ and Zn^{2+}) revealed that PVD and PCH are able to chelate all these metals (Braud et al., 2009a; Braud et al., 2009b). However, competition experiments between iron and other metals for PVD showed a clear preference for iron indicating a lower affinity of this siderophore for these other biological metals (Braud et al., 2009b). Indeed, formation constants for PVD with Zn^{2+} , Cu^{2+} and Mn^{2+} are between 10^{17} and 10^{22} M^{-1} , whereas that with Fe^{3+} is 10^{32} M^{-1} (Chen et al., 1994). The formation constants for the hydroxamate siderophore desferrioxamine B with Ga^{3+} , Al^{3+} and In^{3+} are between 10^{20} and 10^{28} M^{-1} , whereas that with Fe^{3+} is 10^{30} M^{-1} (Evers et al., 1989; Hernlem et al., 1996).

What about the uptake of metals other than iron by siderophores? A screening study with 16 metals showed that PCH is able to import Co^{2+} , Ga^{3+} and Ni^{2+} in *P. aeruginosa* cells, but with uptake rates 23- to 35-fold lower than for PCH-Fe (Braud et al., 2009a). Equivalent data have been obtained for the PVD pathway: Cu^{2+} , Ga^{3+} , Mn^{2+} and Ni^{2+} in complex with PVD accumulated into the cells but with lower uptake rates compared to PVD-Fe (7- to 42-fold lower). In both assays, metal uptakes were dependent on the presence of the siderophore and were TonB-dependent, suggesting that they occurred *via* the siderophores and their corresponding TBDT. All the metals transported are biological metals except Ga^{3+} . No accumulation of toxic metals suggests that the import of Co^{2+} , Cu^{2+} , Mn^{2+} and Ni^{2+} could have a biological significance. Moreover, the efflux pump PvdRT-OmQ has been described as being able to efflux all unwanted PVD-metal complexes: when this efflux system is expressed less PVD-metal complexes other than PVD-Fe accumulate in the bacteria (Hannauer et al., 2012). PvdRT-OpmQ seems to play a key role in the control of the specificity of iron acquisition by the PVD pathway (Hannauer et al., 2012).

Moreover, metals other than iron are also able to stimulate or inhibit siderophore production in a number of bacteria, even in the presence of high iron concentrations, suggesting also that siderophores may be involved somehow in homeostasis of metal other than iron. In iron-limited succinate medium, PVD production is induced by 10 μM Al^{3+} , Cu^{2+} , Ga^{3+} , Mn^{2+} and Ni^{2+} (Braud et al., 2009b). Still under iron-limited conditions, exposure to 10 mM Cu^{2+} up-regulates genes involved in the synthesis of PVD and down-regulates those involved in the synthesis of PCH (Teitzel et al., 2006). Interestingly, even in the presence of iron (100 μM), PVD production is increased by 10 and 100 μM Cu^{2+} and Ni^{2+} (290 and 380 % respectively) and to a lesser extent by 100 μM Cr^{2+} (134 %) (Braud et al., 2010). No activation of PCH production was observed, but a repression for 10 μM Co^{2+} and 100 μM Cu^{2+} , Mo^{+6} and Ni^{2+} in iron-limited medium (Visca et al., 1992). Such regulating effects have also been observed for other siderophores and bacteria. For instance, the presence of molybdenum in the environment of *Azotobacter vinelandii* regulates the production of azotochelin, a catecholate siderophore able to chelate this metal: at concentrations up to 100 μM of molybdenum, azotochelin production is activated, whereas at higher metal concentrations the synthesis of the siderophore is completely repressed (Duhme et al., 1998). High concentrations of aluminum increase the production of schizokinen and N-deoxyschizokinen (two hydroxamate siderophores) in iron-limited cultures but not iron-replete cultures of *Bacillus megaterium* (Hu and Boyer, 1996). Probably, as for iron, siderophore production can be both activated and inhibited by many of these metals, depending on their concentrations. However, further studies are necessary to better understand the role of siderophores in the uptake of metals other than iron.

5. Other metallophores

Bacteria produce also specific chelators for other metals. For example, the fact that Cu, like Fe, is poorly bioavailable in various bacterial environments raises the question of how *P. aeruginosa* and other microorganisms adapt to copper limitation. Methanotropic bacteria, organisms able to metabolize methane as their only source of carbon and energy, need large amounts of Cu. They produce a small Cu-chelating molecule, or chalkophore, called methanobactin (Kenney and Rosenzweig, 2012). Chalkophores have a similar function to siderophores for iron: they chelate and scavenge Cu^{2+} or Cu^{+} from the bacterial environment and shuttle them into the bacterial cells. The transport across the outer membrane probably involves a TBDT (Balasubramanian et al.,

2011) as for the uptake of Fe by siderophores. Methanobactins from different methanotrophs have different chemical compositions (Kenney and Rosenzweig, 2012). *P. aeruginosa* has a lower need than methanotropic bacteria for Cu, but very little is known about how it manages Cu acquisition.

In vitamin B12, the central Co ion is chelated by a ligand that can also be considered as a metallophore that belongs to the same prosthetic group family as heme and chlorophyll. The Co coordination involves four pyrrole nitrogen ligands of a corrin and the 5,6-dimethylbenzimidazole provides a fifth ligand to the Co. The sixth ligand differs depending on the cobalamin: cyanocobalamin, methylcobalamin, hydroxocobalamin and adenosylcobalamin (Okamoto and Eltis, 2011; Randaccio et al., 2010). The corrin macrocycle stabilizes oxidation states of Co¹⁺ to Co³⁺ and the toxicity of cobalamin is significant lower than that of the free Co ion. The uptake of cobalamin across bacterial outer membranes involves a TVDT BtuB, found in *P. aeruginosa*.

A metallophore has also highly been suggested for Ni acquisition in *Helicobacter pylori*. The crystal structures of NikA (the periplasmic protein of the ABC transporter NikABCDE) (Cherrier et al., 2005, 2008, 2012; Heddle et al., 2003) strongly suggest that this periplasmic binding protein is not able to bind free Ni²⁺, but that a chelating ligand (a nickelophore) is required to complete the coordination environment of the metal ion (Cherrier et al., 2008). This Ni²⁺-chelating compound could be either a small organic ligand (Cherrier et al., 2008) or (L-His)₂ (Chivers et al., 2012; Lebrette et al., 2013). *NikABCDE* genes have been found in the genomes of *P. putida*, *P. fluorescens*, *P. syringae*, but not in any *P. aeruginosa* genome.

At last, metallophores have also been described recently for Zn acquisition. The thiocarboxylate siderophore pyridine-2,6 (thiocarboxylic acid) (PDTC, a siderophore produced by *Pseudomonas stutzeri*, *P. fluorescens* and *P. putida*) may be involved in Zn²⁺ uptake in some *Pseudomonads* but not in *P. aeruginosa* (Leach et al., 2007). *P. stutzeri* and *P. putida* both produce PDTC (Lewis et al., 2000) and two gene products are necessary for Fe uptake by this siderophore, the TonB-dependent transporter PdtK (PSF113–2606 in *P. fluorescens* genome) and the proton motive force dependent inner membrane permease PdtE (Leach and Lewis, 2006). More recently Mastropasque et al. have shown that *P. aeruginosa* synthesis of a nicotinamide related metallophore, which is released outside the cell and mediates Zn uptake through the TBDT ZrmA (Mastropasqua et al., 2017). This nicotinamide metallophore seems to have a similar function to siderophores for iron. This compound is also produced by *Staphylococcus aureus* and called Staphylopine and was described as being involved in Ni, Co, Zn, Cu, and Fe acquisition, depending on the growth conditions (Ghssein et al., 2016).

Part 4

Regulation mechanisms of siderophore-mediated iron uptake pathways in P. aeruginosa

According to their genome, bacteria have the possibility to express several iron acquisition pathways. In the case of *P. aeruginosa*, proteomic approaches have shown that this pathogen is able to get access to iron *via* heme and Fe^{2+} import and is able to produce two siderophores PVD and PCH and use several xenosiderophores for Fe^{3+} scavenging and uptake. All these pathways are not used simultaneously by *P. aeruginosa*. They are all expressed at a basal level, and the pathogen will induce *via* a positive feedback loop only the expression of the most efficient pathway(s) in iron acquisition depending on the bacterial environments. Indeed, the bacteria may have the ability to switch from one to another one in function of their environment. These expressions are regulated by different strategies like sigma/antisigma factors, AraC regulators or two-component systems.

Moreover, iron at high concentration becomes toxic and bacteria have developed regulating negative feedback loops to avoid a high intracellular iron concentration. The major actor in this control of intracellular iron concentrations is the regulator Fur, a repressor activated by Fe^{2+} that inhibits the expression of all iron acquisition pathways.

1. Positive feedback loops

1.1. Sigma and anti-sigma regulating systems

Positive feedback loops involving sigma and anti-sigma factors have been mostly investigated for the Fe and the PVD-Fe uptake pathways in *E. coli* and *P. aeruginosa* respectively. In the frame of this thesis, we will focus on the PVD pathway. PVD is considered as the major siderophore produced by *P. aeruginosa*, because of its higher affinity for Fe^{3+} compared to PCH, and probably also because the production of PVD can be easily followed with the naked eyes (characteristic yellow-green colour), which is not the case of the PCH production. Dumas *et al.* in 2013 have shown that there is a difference in iron sensitivity for both siderophore pathways. PVD is the predominant siderophore produced in more restricted iron concentrations while PCH become the predominant siderophore at intermediate iron concentration. The authors have seen that PVD synthesis was strongly repressed in presence of high amounts of iron, whereas the synthesis of PCH prevailed relatively high in a wide range of iron concentrations. This difference of sensitivity is certainly linked to the different affinities between PVD and PCH for iron (Albrecht-Gary *et al.*, 1994; Brandel *et al.*, 2012).

The expression of the genes of the PVD pathway is positively regulated by a signalling cascade involving the TBDT transporter FpvAI, the anti-sigma factor located at the inner membrane FpvR, and two sigma factors in the cytoplasm, PvdS and FpvI, that belong to the extracytoplasmic function (ECF) sigma factors family (Lamont et al., 2002; Edgar et al., 2014). See Fig. 27. These small regulatory sigma factors play key roles at different stages of initiation of transcription: in the RNA polymerase direct recognition of promoter elements (Helmann, 2002), stabilisation of polymerase and DNA complex, interaction with transcription activators, and in the scape of the promoter (Saecker et al., 2011). This PVD pathway-regulating cascade is initiated by the binding of PVD-Fe complex to FpvAI binding site at the bacterial surface, an interaction that induces a change of conformation in FpvAI, changing the position of the N-terminal periplasmic signalling domain. This movement has been observed in the FpvAI-PVD-Fe X-ray structure and it was identified as TonB dependent (Brillet et al. 2007). The periplasmic globular signalling domain is essential for the interaction between FpvAI and the periplasmic region of the anti-sigma factor FpvR, which then allows the release of PvdS and FpvI into the cytoplasm, two proteins that maintain an interaction with FpvR in the absence of FpvAI-PVD-Fe stimulation (Lamont et al., 2002; Beare et al., 2003). The two sigma factors recruit the RNA polymerase on the consensus sequence called iron-starvation (IS) box (TAAAT-N16 / 17-CGT) (Ochsner et al., 2002), present in the promoter region of the twelve operons required in the synthesis of PVD (Cunliffe et al., 1995; Lamont and Martin, 2003; Ravel and Cornelis, 2003), inducing the expression of the PVD pathway genes. FpvI is responsible of the expression of the TBDT *fpvA* gene, involved in PVDI-Fe import (Beare et al., 2003), whereas PvdS is responsible of the induction of the expression of all genes involved in PVD biosynthesis (Cunliffe et al., 1995; Ochsner et al., 2002), and it is also required for maximal expression of two secreted virulence factors not related with the iron uptake pathway, the exotoxin A (Ochsner et al., 1996; Helmann, 2002) and the PrpL protease (Wilderman et al., 2001). In the absence of PVD-Fe recognition by FpvA, the signalling cascade is not started, and the two sigma factors stay in interactions with FpvR on the inner leaflet of the cytoplasmic membrane, thus not interacting with iron-starvation (IS) boxes in the PVD locus (Potvin et al., 2008; Llamas et al., 2014).

This kind of signal transduction system is commonly used to control the expression of a large number of genes encoding siderophore-Fe transporter proteins in several Gram negative bacteria *spp.* (Visca et al., 2002; Mahren, et al., 2005; Llamas et al., 2014). Nevertheless, PVD cell-surface signalling pathway is the only in which a single anti-sigma factor, FpvR, regulates two different

sigma factors, PvdS and FpvI (Beare et al., 2003), providing an effective mechanism of post-translational control of protein activity (Edgar et al., 2014).

Other iron uptake pathways in *P. aeruginosa* have their expression regulated by sigma and antisigma factors: ferrichrome (FiuA/FiuR/FiuI), ferrioxamin (FoxA/FoxR/FoxI), ferri-citrate (FecA/FecR/FecI) and heme (HasR/HasS/HasI) uptake pathways (Llamas et al., 2014). For all these iron acquisition pathways, the TBDT involved has this additional N-terminal domain called the “signalling domain” and which is necessary for the interaction in the bacterial periplasm with the anti-sigma factor. *P. aeruginosa* will be able to sense the presence of the ferric forms of these xenosiderophores thanks to this signalling cascades involving as a first step the binding of these siderophore-Fe complexes to their corresponding TBDT. Consequently the bacteria will “switch on” the expression of these pathways to get access to iron.

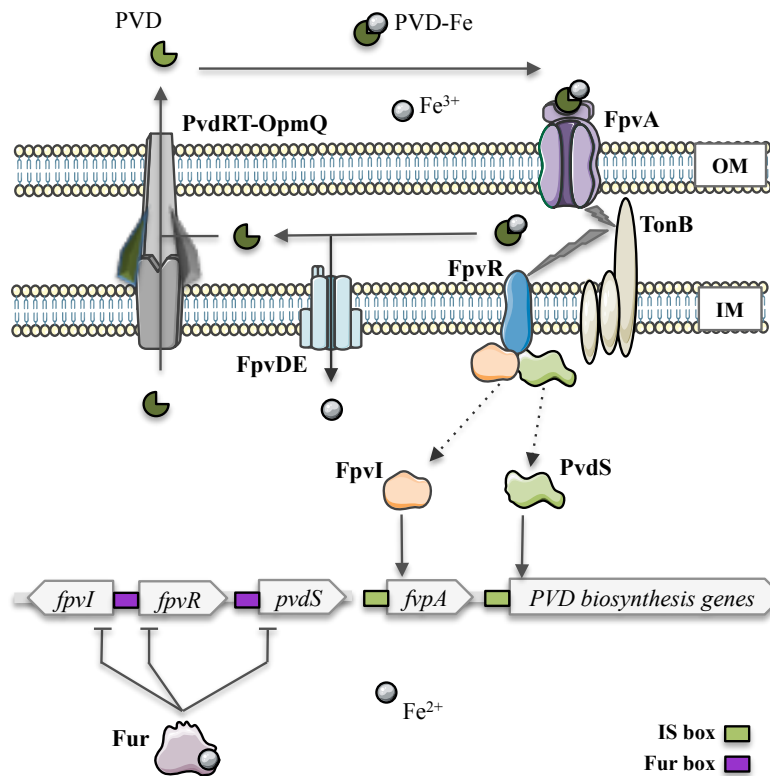


Figure 27. Mechanism of regulation of the PVD iron uptake pathway in *P. aeruginosa*. Expression of the PVD pathway is positively regulated through a signalling cascade initiated by the binding of PVD-Fe complex to the FpvAI transporter in the extracellular medium, a binding that induces a conformational change of this protein in a TonB-dependent process, making possible an interaction to the anti-sigma factor FpvR, which allows the release of the sigma factors PvdS and FpvI into the cytoplasm. They recruit the RNA polymerase on the consensus sequence called iron-starvation (IS) box, located in the promoter region of the PVD biosynthesis operons, which is identified by PvdD, and located in the promoter of *fvpA*, being identified by FpvI, inducing in this way the PVD pathway genes expression. The transcriptional regulator Fur represses this pathway once it is activated by Fe^{2+} . Fur recognizes the Fur boxes in the promoter region of the sigma and anti-sigma factors, repressing their expression.

1.2. AraC regulator in the regulation of the PCH pathway

Positive feedback loops involving AraC regulators implies different mechanisms from those described above involving sigma factors. The archetype among AraC regulators is PchR, that belong to the PCH pathway in *P. aeruginosa*. The transcriptional regulator PchR is the cytoplasmic protein responsible of the up-regulating of all the genes coding for proteins involved in the PCH pathway. This positive feedback loop requires that the PCH₂-Fe complex is transported into *P. aeruginosa* cytoplasm first by the outer membrane transporter FptA and afterwards by the inner membrane permease FptX. Once in the cytoplasm, PCH₂-Fe binds to PchR (Heinrichs and Poole, 1993 and 1996; Michel et al., 2007) and consequently PchR-PCH₂-Fe complex is able to bind conserved and specific sequences motif called ‘PchR-box’, located in the promoter region of genes involved in the PCH biosynthesis (operon *pchDCBA* and *pchEFGHI*), but also involved in the PCH₂-Fe uptake (operon *fptAB(CX)*) (Michel et al., 2005; Michel et al., 2007; Youard et al., 2011). See Fig. 28. The sequences recognized by PchR were determined by Michel et al., 2005, based on the alignments of promoter regions of the operons *pchDCBA*, *pchEFGHI*, and *fptAB(CX)*. They proposed a consensus sequence of 32 bp, which consists of two identical heptameric consensus sequences, ATCGAAA, separated by 14 nucleotides: CTGCATCGAAAGAAAAAGCCCC/GGCAATCGAAA. It is located between 70 and 105 bp upstream of the ATGs. Further, *pchR* and *pchD* genes are encoded on the same locus, but in opposite direction. Their promoter regions overlap, so that the PchR box of the *pchD* promoter lies in the ORF of *pchR*. Michel et al., 2005 showed that while the PchR box is required for the induction of *pchD* expression, it is at the same time involved in the repression of *pchR*. Thus, PchR is also able to repress its own expression in a PCH-dependent way.

In general, the transcriptional regulators of the AraC family are organized in two different domains, the C-terminal domain highly conserved with two helix-turn-helix motifs involved in the DNA recognition and binding to the specific target promoters (PchR-box) (Cass and Wilcox, 1986; Michel et al., 2005), and the weakly conserved N-terminal domain responsible for the effector (ligand) recognition (Tobes and Ramos, 2002). This second domain consists of about 150 amino acids that confers siderophore specificity (Youard and Reimann, 2010), and it is probably also involved in protein dimerization (Ruiz et al., 2003). Several regulators are active in a dimer conformation, probably PchR as well, but unlike other proteins from the same family, it seems that no DNA looping is formed, and only one binding site is present in the promoter regions (Schleif, 2003). It was suggested that PCH₂-Fe activates PchR by binding to the N-terminal domain of the

protein (Youard and Reimann, 2010), and this binding occurs only when the siderophore is in complex with iron (Lin et al., 2013). PCH is a siderophore with three asymmetric centers, and enantiospecificity studies have shown that PchR can be activated by PCH as well as by its enantiomer, enantio-PCH (Youard et al., 2011; Lin et al., 2013).

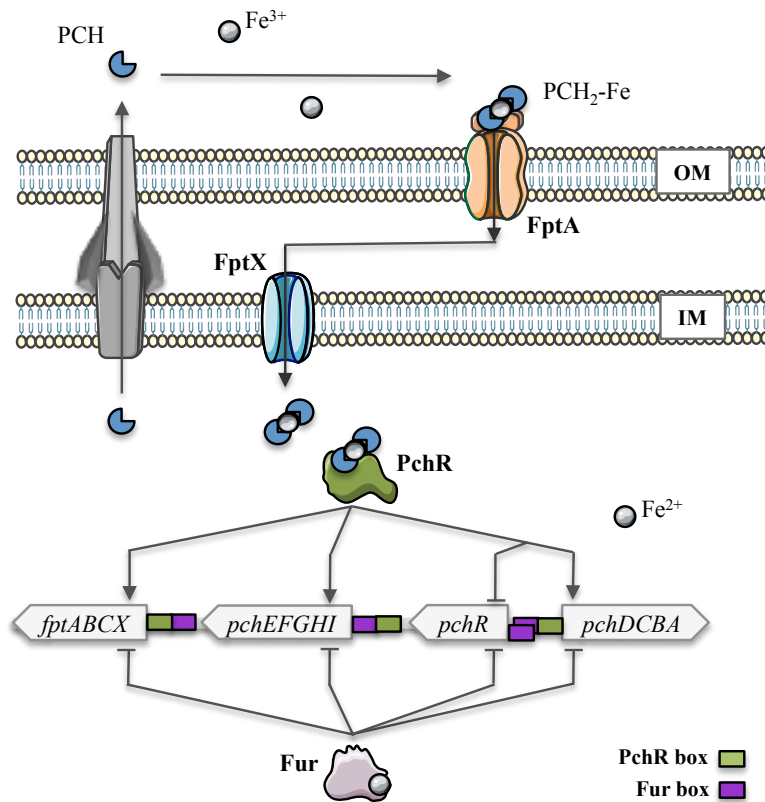


Figure 28. Mechanism of regulation of the PCH iron uptake pathway in *P. aeruginosa*. The PCH pathway is induced by auto-inducing regulatory loop through the action of the transcriptional regulator PchR. The PCH₂-Fe is imported back into the periplasm via the specific outer transporter FptA, and into the cytoplasm through the permease FptX. Once in the cytoplasm, the PCH₂-Fe complex binds and activates the transcriptional regulator PchR, which recognizes the PchR boxes located in the promoter regions of the PCH genes operons involved in the PCH biosynthesis (*pchEFGHI* and *pchDCBA*) and transport (*fptABCX*), inducing their expression. The transcriptional regulator Fur represses this pathway. Once Fur is activated by Fe²⁺, it recognizes the Fur boxes located in the promoter of all the PCH operons, also including the *pchR* gene.

1.3. Two-component systems

At last, some iron uptake pathway expressions are also regulated by two component systems, like the enterobactin pathway in *P. aeruginosa* as well as the expression of the TBDT PirA for which the natural siderophore transported has not been identified yet. This kind of positive feedback loop are composed of a membrane-bound histidine kinase that senses a specific environmental stimulus

and a regulator that mediates the cellular response, mostly through differential expression of target genes. Two-component systems accomplish signal transduction through the phosphorylation of the response regulator by the histidine kinase: upon detecting a particular change in the extracellular environment, the histidine kinase performs an autophosphorylation reaction, transferring a phosphoryl group from adenosine triphosphate (ATP) to a specific histidine residue. The cognate response regulator then catalyzes the transfer of the phosphoryl group to an aspartate residue on the response regulator's receiver domain. This typically triggers a conformational change that activates the response regulator's effector domain, which in turn produces the cellular response to the signal, by stimulating (or repressing) expression of target genes.

For the enterobactin pathway of *P. aeruginosa*, Dean and Poole have shown that two genes, *pfeS* and *pfeR* (located immediately upstream from *pfeA*), encode the sensor kinase and response regulator, respectively, of a two-component system involved in regulating *pfeA* expression in response to enterobactin (Dean and Poole, 1993; Rodrigue et al., 2000). The sequence of PfeS suggests that it is an inner membrane protein (Dean and Poole, 1993), and further studies are required to gain insight into the mechanism of stimulus perception by this protein: do the catechol compounds interact with this protein only after their transport into the bacterial periplasm or is another mechanism involved? Our group has shown that the presence of enterobactin in *P. aeruginosa* environment induces the “switch on” for the expression of the proteins involved in iron acquisition by this siderophore and represses the expression of the proteins of the PCH pathway (Gasser et al., 2016).

2. Repression of siderophore expression

The ferric uptake regulator Fur is the transcriptional repressor that controls the expression of PVD and PCH pathways in response to iron availability by negative feedback as well as any gene coding for proteins involved in iron homeostasis. Concerning these two pathways of *P. aeruginosa*, the expression of *pvdS* and *pchR* are under the control of Fur, thus the PVD biosynthesis genes (Fig. 27), as well as the genes involved in the biosynthesis and uptake of PCH (Fig. 28); including the production of exotoxin A and PrpL (Venturi et al., 1995; Crosa, 1997).

Fur proteins become active by binding Fe^{2+} in the bacterial cytoplasm. Afterwards, the Fur-Fe complex binds to a conserved nucleotide sequence, the Fur box, located in the promoter regions of iron-regulated genes, blocking the RNA polymerase, thus the gene transcription (Guerinot, 1994;

Escolar et al., 1999). This Fur box was initially identified in *E. coli*, and it is composed in *E. coli* and *P. aeruginosa* of a palindromic consensus sequence of 19 nucleotides GATAATGATAATCATTATC (Ochsner et al., 1995). Fur-boxes are present in the promoters of the *fptAB(CX)*, *pchEFGHI*, *pchDCBA*, *pvdS* and *pchR* (Michel et al., 2005). Expression studies have demonstrated Fur-dependent repression of these genes in iron-replete conditions (Heinrichs and Poole 1993; Ochsner et al. 1995; Serino et al. 1997; Reimann et al. 1998). As mentioned above, *pchR* and *pchD* are overlapping genes, and it was shown that their Fur box overlap as well (Ochsner et al., 1995; Serino et al., 1997).

Under iron starvation conditions, when the concentration of this metal decreases in the bacterial cytoplasm, less Fur-Fe complexes are formed, as a consequence, the occupancy of the Fur boxes is reduced, allowing the expression of the genes coding for the synthesis of proteins involved in iron uptake.

Fur metal binding site is located in the C-terminal part of the protein and the DNA binding site in the N-terminal region (Coy and Neilands, 1991; Stojiljkovic and Hantke, 1995). When the metal is bound, a conformational change occurs allowing the binding of the N-terminal part of the protein to the Fur box. The C-terminal domain also contains the dimerization site (Stojiljkovic and Hantke, 1995). Even though Fe^{2+} is the cofactor of this regulator, it was demonstrated that other divalent cations with a similar size, as Co^{2+} or Mn^{2+} can also associate with Fur, and in fact, Fur-Co and Fur-Mn were able to bind the 25 oligomer DNA containing the consensus iron-box sequence during the gel retardation assay in *E. coli* (Adrait et al., 1999). It has been also shown that Fur of *P. aeruginosa* was able to bind the *pchR* promoter in presence of Co^{2+} , Ni^{2+} and Mn^{2+} (Ochsner et al., 1995).

3. Iron storage

To avoid the toxic effect of iron, *P. aeruginosa* has to inhibit the expression of its iron uptake systems when iron concentration increases, but it has also evolved storage mechanisms that participate to the global regulation of iron availability, and thus to the expression of the siderophore pathways. *P. aeruginosa* produces two ferritins, the bacterioferritin (Rui et al., 2012), and another bacterial ferritin FtnA (Yao et al., 2011). These proteins assemble in multimers allowing the storage of thousands of iron atoms (Yao et al., 2011). Different proteins using iron as co-factors are also overexpressed at high iron concentration, and most of these proteins are

positively regulated by Fur. Thus, Fur is not only a transcriptional repressor, but also a transcriptional activator. This activation of gene expression can be indirect, through the repression of non-coding RNAs for example. Indeed, Fur repress the expression of at least two non-coding RNAs, PrrF1, 2, known to inhibit the expression of proteins involved in iron homeostasis (Wilderman et al., 2004). In other bacteria, Fur also directly activates the expression of some genes (Gilbreath et al., 2012).

4. Other signal inducing siderophore production regulation

If iron concentration remains the main signal involved in the regulation of siderophore production, other signals affect this production, linked to oxidative stress (Vinckx et al., 2008), lipid signalling cascades (Funken et al., 2011), alginate synthesis (Ambrosi et al., 2005), di-cyclic GMP (Frangipani et al., 2014; Chen et al., 2015), temperature (Barbier et al., 2014), *Quorum sensing* (Stintzi et al., 1998), AmpR signalling cascade (Balasubramanian et al., 2014). For most of them, the regulation mechanisms have not been deciphered. Nevertheless, all these regulation potentials play for an extensive interplay between iron import and virulence pathways, or metabolism stress. In such complex network, small changes in the regulation nodes may have important consequences in the whole network expression. The characterisation of these interactions and regulations would be important to fully understand the adaptation of siderophore production in ever changing environment.

Objectives

In the frame of this thesis, I was interested in two aspects of biological metals homeostasis in *P. aeruginosa*:

- Previous work in our laboratory shown that a PVD and PCH-deficient strain had still the expression of the PVD and PCH pathways activated despite the absence of production of these two siderophores in strong iron restricted conditions. These data highly suggested that PVD and PCH are not essential to activate the expression of their corresponding pathways *via* FpvR/FpvI/PvdS or PchR, respectively. We have investigated during this thesis the different molecular levels involved in the regulation of the PVD and PCH pathways in the presence of different iron concentrations, to highlight the differences between both types of regulation and their dynamic.
- In parallel, we have also investigated how other biological metals than iron (Co, Cu, Ni, Mn, and Zn) interfere with the PVD and PCH iron uptake pathways in *P. aeruginosa* cells. We have studied the effect of these metals on siderophore production, their ability to be transported by these two siderophores, as well as their ability to interact with the transcriptional regulator PchR.



Chapter 1

The pathogen *Pseudomonas aeruginosa* takes the advantages but avoids the inconveniences of the positive auto-regulation of its major siderophores pyoverdine and pyochelin production

1 **The pathogen *Pseudomonas aeruginosa* takes the advantages but avoids the**
2 **inconveniences of the positive auto-regulation of its major siderophores pyoverdine and**
3 **pyochelin production**

4

5 Cunrath Olivier^{1, 2, 3}, Carballido-López Ana¹, Perard Julien⁴, Forster Anne^{1,2}, Seguin
6 Cendrine⁵, Godet Julien⁶, Michaud-Soret Isabelle⁴, Schalk Isabelle^{1,2}, Fechter Pierre^{1,2*}

7 ¹Université de Strasbourg, UMR7242, ESBS, Bld Sébastien Brant, F-67413 Illkirch,
8 Strasbourg, France

9 ²CNRS, UMR7242, ESBS, Bld Sébastien Brant,
10 F-67413 Illkirch, Strasbourg, France

11 ³Present address : Focal Area Infection Biology, Biozentrum, University of
12 Basel, Basel, Switzerland.

13 ⁴Laboratoire de Chimie et Biologie des Métaux, UMR 5249 CNRS, Grenoble, France.

14 ⁵Laboratoire de Conception et Application de Molécules Bioactives, UMR 7199 CNRS,
15 Université de Strasbourg, Faculté de Pharmacie, Illkirch, France.

16 ⁶Laboratoire de Biophotonique et Pharmacologie, UMR 7213 CNRS, Université de
17 Strasbourg, Faculté de Pharmacie, Illkirch, France.

18

19 * Corresponding author: P.Fechter@unistra.fr

20 **Abstract**

21

22 Siderophores are iron chelators produced by bacteria to get access to iron, an essential
23 nutriment. The pathogen *Pseudomonas aeruginosa* produces two siderophores, pyoverdine
24 (PVD) and pyochelin (PCH). The production of both siderophores is tightly regulated,
25 repressed by the global iron sensitive regulator Fur, and activated through specific positive
26 auto-regulation loops. We investigated the dynamic properties of the production of PVD and
27 PCH by *P. aeruginosa* PAO1 cells. Our data shown that in strong iron uptake difficulties,
28 bacterial cells manage to by-pass the dependence of their siderophore production on the
29 positive auto-regulation loops at steady state levels. Nevertheless, the auto-regulation loop is
30 activated, and responsible for a surge notably of PVD production that may be critic to speed
31 up the adaptation of the cell to adverse environments. When the iron concentration increases,
32 both positive auto-regulation loop gain importance, but having different dynamics. Thus, the
33 cells manage to benefit from the peculiar properties of such regulation loop, but also manage
34 to avoid its disadvantages. Altogether, these results allow to understand how *P. aeruginosa*
35 adapts the production of its endogenous siderophores according to environment stresses, such
36 as iron depletion, competition with other organisms, or presence of toxic metals.

37

38 **Introduction**

39 Iron is absolutely required for growth of most living organisms, because this trace element is
40 a cofactor for many enzymes involved in fundamental biological processes. However, iron
41 availability in various bacterial environments is severely limited: iron(II) is rapidly oxidized
42 to iron(III) in the presence of oxygen and precipitates as a polymeric oxyhydroxide.
43 Consequently, bacteria have developed efficient strategies to get access to this essential
44 element. One of the most commonly used strategies involves the synthesis of siderophores
45 and their release into the bacterial environment (Miethke and Marahiel, 2007; Saha et al.,
46 2016; Llamas et al., 2014). Siderophores chelate iron(III) in the extracellular medium, and the
47 resulting ferric-siderophore complex is then transported back into the bacteria.

48 *P. aeruginosa* produces two major endogenous siderophores, pyoverdine (PVD) and
49 pyochelin (PCH), with different affinities for iron ($K_a = 10^{32} \text{ M}^{-1}$ compared to 10^{28} M^{-1} for
50 pyochelin) (Albrecht-Gary et al., 1994; Brandel et al., 2012). Beside its endogenous
51 siderophores, *P. aeruginosa* is also able to use siderophores produced by other bacteria
52 (xenosiderophores), like enterobactin produced by *Escherichia coli*, different ferrichromes, or
53 heme produced by the host (Cornelis and Dingemans, 2013). Considering the plethora of iron
54 import strategies, the expression of all these pathways, and especially those dedicated to the
55 production of the endogenous siderophores, have to be finely tuned to allow iron import, but
56 avoiding its toxic effect.

57 The regulation of the expression of the two endogenous iron import pathways (PVD and PCH
58 pathways) is submitted to repression by the major iron sensitive transcription regulator Fur
59 (Cornelis et al., 2009; Troxell and Hassan, 2013), and to induction by specific transcription
60 activators included into auto-inducing regulatory loops: the iron-loaded siderophores are
61 required for the expression of their own pathway (enzymes involved in its biosynthesis and

62 transport proteins) (Lamont et al., 2002; Beare et al., 2003; Michel et al., 2005) (See Figure
63 1).

64 The PVD pathway is induced by two sigma factors, PvdS and FpvI (Llamas et al., 2014)
65 (Figure 1). While FpvI only induces the expression of the outer membrane transporter, FpvA,
66 PvdS induces the expression of most other proteins of the pathway. Concerning iron
67 acquisition by PVD, once excreted in the environment, PVD chelates iron, and ferri-PVD is
68 imported back into the periplasm via the specific outer membrane transporter FpvA
69 (Folschweiller et al., 2000). Iron dissociates from PVD in the periplasm, the metal is imported
70 further into the cytoplasm by the ABC transporter PvdE (Schalk et al., 2002; Greenwald et al.,
71 2007; Ganne et al., 2017), and the apo-PVD is recycled back into the extracellular medium
72 (Imperi et al., 2009; Yeterian et al., 2010). Ferri-PVD uptake via FpvA induces also in
73 parallel, via a TonB dependent mechanism (Brillet et al., 2007), a conformational change of
74 the anti-sigma factor FpvR embedded in the cytoplasmic membrane, which binds the two
75 sigma factors, PvdS and FpvI at the inner leaflet of this inner membrane (Edgar et al., 2014).
76 The conformational change of FpvR induces the release of PvdS and FpvI into the cytoplasm,
77 that can consequently activate the expression of the PVD pathway (Llamas et al., 2014). See
78 Figure 1A. This mechanism induces a positive auto-regulation, and is supposed to allow the
79 synthesis of the siderophore only when the bacterial cells are able to import it back.

80 The PCH pathway expression is induced by one transcription factor, PchR, that belongs to the
81 AraC-type of transcription factor (Figure 1B). Once excreted in the environment, PCH
82 chelates iron, and the ferri-PCH is imported back into the periplasm *via* the specific outer
83 transporter FptA (Cobessi et al., 2005), and into the cytoplasm through the permease FptX
84 (Cunrath et al., 2014). Once in the cytoplasm, ferri-PCH complex binds and activates the
85 transcription regulator PchR (Michel et al., 2005; Lin et al., 2013). Again, this positive auto-

86 regulation loop allows the synthesis of the siderophore only when the bacteria is able to
87 import it back.

88 Both pathways are repressed by the global iron responsive regulator Fur. While Fur inhibits
89 only the expression of the PVD sigma or anti-sigma factors PvdS, FpvR and FpvI, a Fur box
90 has been identified in the promoter of *pchR*, but also in different promoters of genes from the
91 PCH pathways (Michel et al., 2005) (Figure 1).

92 It is known that both siderophores are not used similarly by the cell, which adapts the
93 expression of these two pathways to its iron requirement (Cornelis and Dingemans, 2013).
94 Nevertheless, the interconnection between all these modules, the dynamic of their regulation
95 has not been studied. Such studies would be important to understand how *P. aeruginosa*
96 accommodates its iron import strategies when facing changing environments, or how it
97 challenges the presence of other bacteria or iron acquisition in the host during infection.
98 Moreover, different anti-bacteria strategies focuses on iron homeostasis, either by looking for
99 inhibitors of iron import, or through Trojan Horse strategies by designing hybrid molecules
100 between iron siderophore derivatives and antibiotic (Mislin and Schalk, 2014). The
101 development of these strategies also requires to understand how the expression of the iron
102 uptake pathways is modulated in the presence of these new molecules.

103 Finally, different genetic constructions have evolved to trigger auto-regulation, and their
104 properties studied in some examples (Smits et al., 2006; Mitrophanov and Groisman, 2008;
105 Brautaset et al., 2009). These systems present some advantages over linear circuits, and are
106 used in biological systems to build new blocks of regulatory nodes, taking advantages of these
107 peculiar properties. In *P. aeruginosa*, the juxtaposition of two such circuits, encompassing
108 differences in their genetic constructions is an opportunity to further characterize such

109 circuits, and understand how to combine them to build regulatory networks with further
110 complexity.

111 In the present work, we investigated the dynamic properties of the production of PVD and
112 PCH by *P. aeruginosa* PAO1 cells, depending on the iron concentrations in the growth media.
113 Our data show that when facing strong difficulties in getting access to iron, bacterial cells
114 manage to decrease the dependence of their siderophore production by the positive auto-
115 regulation loops. In slightly lower iron restricted conditions, only PVD is dispensable for its
116 own production. The auto-regulation loop is nevertheless activated, and responsible for a
117 burst of PVD production that may be critic to speed up the adaptation of the cell to adverse
118 environments. When the iron concentration increases, the PVD positive auto-regulation loop
119 gains importance. Thus, the cells manage to benefit from the peculiar properties of such
120 regulation loop, but also manage to avoid its disadvantages. We further showed that the global
121 transcription repressor Fur plays a role not only in the repression of the transcription
122 regulators expression of both pathways, but also in the dynamic of the PVD positive auto-
123 regulation loop, as well as in fine tuning the repression of PCH effector genes expression.
124 Altogether, taking into account those results we propose different scenario for *P. aeruginosa*
125 endogenous siderophore production, according to environment stresses, like iron depletion,
126 competition with other organisms, or presence of toxic metals.

127

128 **Results**

129

130 **PVD is not required for its own production in strong iron depleted conditions**

131 To study the dynamic of the positive PVD auto-regulation loop, a PVD-deficient strain *pvdF*,
132 (PvdF being an enzyme involved in PVD biosynthesis) was grown in CAA, a strongly iron-
133 depleted medium, ([Fe] = 50 nM, (Cunrath et al., 2016). The inability of this strain to produce
134 PVD was confirmed by monitoring the characteristic absorbance of PVD at 400 nm (Figure
135 S1). The effect of this deletion on the expression of different genes involved in PVD pathway
136 was then measured by RT-qPCR in PAO1 and $\Delta pvdF$ (Figure 2A). The expression of several
137 genes was studied: *pvdA* and *pvdJ* involved in the biosynthesis of PVD, *fpvA*, involved in the
138 import of ferri-PVD, the sigma/anti-sigma factors *pvdS*, *fpvI*, and *fpvR*, as well as the house
139 keeping gene *uvrD*, which was used for normalization. RT-qPCR shown that the expression
140 of all these genes was only weakly affected (< 2.5 fold changes). We confirmed these results
141 by measuring the expression of a chromosomal *pvdJ*-mCherry fusion in the two backgrounds
142 (*wt* and $\Delta pvdF$, Figure 2B). mCherry signal measured over time was not significantly
143 diminished in the $\Delta pvdF$ mutant. These data showed that the presence of PVD is not essential
144 to get expression of the genes belonging to the PVD pathway in bacteria grown in CAA
145 medium.

146 The expression of the PVD pathway is under the control of the sigma factors PvdS and FpvI.
147 Our results highlighted that either PVD is not essential for gene activation by PvdS and FpvI
148 in such drastic iron depleted conditions, or that another transcription factor could play a role
149 in the expression of the proteins of this pathway. To settle this question, *pvdS* gene was
150 deleted to generate $\Delta pvdS$. In this background, neither PVD was produced (Figure S1) nor any

151 of the genes under the control of PvdS (*pvdA*, *pvdJ* and *fpvA* in Figure 2A) were expressed.
152 These results were further confirmed by measuring the expression of the PvdJ-mCherry
153 fusion in the $\Delta pvdS$ background (Figure 2B). The data show that no other transcription factor
154 can replace PvdS.

155

156 **PCH is not required for its own production in drastic iron uptake difficulties**

157 To study the dynamic of the positive auto-regulation of the PCH pathway, a PCH-deficient
158 strain $\Delta pchA$ (*pchA* being a gene coding for an enzyme involved in the first step of PCH
159 synthesis) was used as well as a PVD- and PCH-deficient strain $\Delta pchA\Delta pvdF$ unable to
160 produce both endogenous siderophores. The strains were grown in CAA and the absence of
161 PCH production by these mutants was confirmed by monitoring the characteristic absorbance
162 of PCH at 320 nm (Figure S1). The expression of different genes from the PCH pathway was
163 then measured by RT-qPCR in PAO1 and in the two mutants: the mRNAs encoding for *pchE*,
164 a gene encoding for an enzyme involved in PCH synthesis, *fptA* and *fptX*, the two transporters
165 involved in the import of the ferri-PCH complex, and the transcription factor *pchR*. As
166 expected from the literature (Michel et al., 2005), no genes belonging to the PCH pathway
167 were expressed in the absence of PCH, except *pchR*, in the $\Delta pchA$ strain (Figure 3A).
168 Surprisingly, in a PVD-and PCH-deficient strain ($\Delta pchA\Delta pvdF$), which has more drastic
169 difficulties to get access to iron, the genes belonging to the PCH pathways were expressed
170 with the same expression rates as in the *wt* strain (Figure 3A). This observation was
171 confirmed at the protein level by measuring the expression of a chromosomal *pchE*-mCherry
172 fusion. While PchE was indeed not expressed in the single $\Delta pchA$ mutant, it became
173 expressed in the double $\Delta pchA\Delta pvdF$ mutant (Figure 3B). In that context, the cells do not
174 require PCH to induce the expression of the PCH pathway.

175 As for the PVD pathway, the expression of the PCH genes in such drastic conditions could
176 involve another transcription factor. To discard this possibility, we generated the single
177 mutant $\Delta pchR$, and a double mutant $\Delta pchR\Delta pvdS$. In both contexts PCH was not produced,
178 and in the double mutant, PVD was not produced as well (Figure S1). None of the tested
179 genes from the two pathways (*pchE*, *fptX* and *fptA*) were expressed, neither in the single
180 $\Delta pchR$ mutant, nor in the double $\Delta pchR\Delta pvdS$ mutant (Figure 3A). These results were
181 confirmed at the protein level by measuring the expression of a chromosomal *pchE*-mCherry
182 fusion in both contexts (Figure 3B). In conclusion, PchR is always required for the expression
183 of the PCH genes in all conditions tested.

184

185 **PvdS and PchR expression at increasing iron concentration**

186 Previous studies have shown that in strongly depleted iron conditions, *P. aeruginosa* produces
187 larger amounts of PVD compared to PCH, whereas at milder iron-restricted conditions, the
188 ration of production between both siderophores changes (Dumas and Kümmerli, 2012; Ross-
189 Gillespie et al., 2015). PVD having a higher affinity for iron than PCH (Albrecht-Gary et al.,
190 1994; Brandel et al., 2012), this siderophore will be more efficient than PCH in scavenging
191 iron when this metal becomes very rare, and consequently the PCH pathway is less efficiently
192 activated. At milder iron-restricted conditions, PVD is less expressed, and thus the PCH
193 siderophore is produced in higher amounts (Dumas and Kümmerli, 2012; Ross-Gillespie et
194 al., 2015). We show here for the first time, that this decrease in PVD production when the
195 concentration of iron increases is due to another layer of regulation involving a difference in
196 the expression levels of PchR and PvdS/FpvI. Indeed, the expression of the two types of
197 transcription regulators is not similarly affected by the intracellular iron concentration. RT-
198 qPCR experiments showed that while the level of *pvdS* and *fpvI* mRNA expression decreases

199 quickly with iron addition, that of *pchR* mRNAs decreases with a slower kinetic (Figure 4 A
200 and B). Consequently also, the expression of the genes of both pathways (*pvdA*, *fpvA*, *pchE*)
201 followed the same pattern of expression than *pvdS/fpvI* and *pchR* (Figure 4 A and B),
202 confirming the key role of the two types of regulators in regulating the expression of the two
203 pathways under different iron conditions. In conclusion, our data demonstrate for the first
204 time a different level of expressions between the regulators of the PCH and PVD pathways
205 explaining that the production of PCH takes over the production of PVD in *P. aeruginosa*
206 cells grown in the moderated iron restricted conditions, despite the higher affinity for PVD in
207 regard to iron compared to PCH.

208

209 **Fur fine tunes the repression of PCH effectors**

210 qRT-PCR measurement performed on *pchR* shown that its expression was similarly affected
211 by iron concentration than that of *pchE* (Figure 4B). Repression of *pchR* expression seems
212 thus to be the main route to repress the expression of the genes from the PCH pathway. It was
213 nevertheless reported that Fur boxes were not only found in front of the *pchR* gene, but also in
214 front of other genes of the pathway, like *pchD*, or *fptA* (Figure S2). To further understand the
215 relative importance of both regulators on these genes, plasmid transcriptional fusion were
216 created with the mCherry ORF fused to the promoter of *pchD* that contains either only the Fur
217 box, or the Fur box plus the PchR box (Figure S2). We first validated that the promoter
218 containing only the Fur box was negatively sensitive to iron concentration. The measurement
219 of mCherry fluorescence shown indeed a decrease in fluorescence when the concentration of
220 iron increases: the expression of this construction is under iron negative regulation, probably
221 due to Fur repression (Figure 5A). It was nevertheless not possible to study this regulation in a
222 PAO1 mutant with a Fur deletion, since Fur becomes essential when the concentration of iron

223 increases and its absence induces pleiotropic effect on protein expression. Nevertheless,
224 electro mobility shift assay (EMSA) experiments confirmed that Fur was able to bind DNA
225 sequences containing only this Fur box (Figure 5B). The effect of iron on the expression of
226 these plasmid reporters is thus likely due to Fur. These results imply that there is a
227 competition between the PchR activation of these effectors and the Fur repression. In poor
228 iron growth conditions, in which PchR is highly expressed and Fur poorly activated, the
229 importance of the induction of the PCH effectors expression by PchR may outcompete Fur
230 repression. Indeed, the measurement of mCherry fluorescence showed that the absence of a
231 PchR box reduces more than 50-fold the expression of the transcriptional reporter in CAA
232 (Figure 5A). Nevertheless, when iron concentration is increased, with lower PchR expression
233 and higher level of activated Fur, the absence of this PchR box reduces the expression of
234 mCherry only of 3-fold (at 5 μ M of iron). In these conditions, the competition between
235 activation and repression becomes more important. The repression by Fur might thus
236 contribute to speed up the repression of PCH production at increasing iron concentrations.

237 An analysis of the sequences of *pchD*, but also *fptA* promoters shown that the PchR box also
238 contained some of the determinants required for a repression by Fur (Figure S2). Would this
239 box also be recognized by Fur? In that case, Fur could also directly compete with PchR to
240 bind the same sequence. In order to check if the PchR box could also play a role in the
241 repression of the pathway when iron concentration increases, the two transcriptional reporters
242 were used to transform the $\Delta pchR$ strain, in order to check a possible repression of the PchR
243 box in absence of any competition by PchR. The decrease of mCherry expression when iron
244 concentration increases was more important for the construct with the promoter containing the
245 Fur and PchR boxes, than for the construct with the promoter containing only the Fur box. Fur
246 may thus bind to a second site located on the PchR box, and enhance the repression (Figure

247 5A). To validate the role of Fur in this repression, EMSA were performed between Fur and
248 the two fragments encompassing the *pchD* promoter sequence, containing only the Fur box, or
249 the Fur box with the PchR box (Figure 5B and C). While only one shift is observed when Fur
250 is bound to the small fragment containing only the Fur box, two shifts are observed with the
251 long fragment.

252 In conclusion, all these data together shown for the first time that the presence of two Fur
253 boxes in the promoter of several effector genes from the PCH pathway may help to finely
254 tune the expression of this pathway, avoiding any leaky expression conditions, and/or
255 tightening the repression of the system in iron-replete conditions.

256

257 **Different repression by Fur of the PVD sigma / anti-sigma factors**

258 In order to understand why *P. aeruginosa* cells are able to express PVD pathway even in the
259 absence of the corresponding siderophore in strongly iron-restricted conditions, we compared
260 by RT-qPCR the expression levels of the sigma factors *pvdS* and *fpvI* of the PVD pathway
261 together with their corresponding anti-sigma factor *fpvR*. Surprisingly, while the expression of
262 *pvdS* mRNAs followed the same pattern than the expression of the enzyme *pvdA*, the
263 expression of the anti-sigma factor *fpvR* mRNA remained mostly stable, whatever the
264 concentration of iron used (Figure 4A). The expression of these factors does not depend on
265 the production of PVD, since similar results were obtained in a *wt* strain and the $\Delta pvdF$ strain
266 (or even slight overproduction in the $\Delta pvdF$ strain, Figure 4A). These intriguing results were
267 confirmed by measuring the expression of mCherry from a plasmid encompassing a
268 transcriptional reporter fusion between the promoter of *pvdS* or *fpvR* and the ORF of mCherry
269 (constructs are detailed in Figure S2). While mCherry was similarly expressed in both

270 constructs in CAA medium, the addition of iron inhibited the expression of mCherry coupled
271 to the *pvdS* promoter more efficiently than the expression of mCherry coupled to the *fpvR*
272 promoter (Figure 6A).

273 Since the expression of these regulators are under the control of Fur, EMSA experiments were
274 performed to measure the binding of Fur to DNA fragments encompassing either the *pvdS* or
275 *fpvR* promoter sequences (Figure S2). While almost all *pvdS* DNA fragments were bound to
276 Fur before 125 nM, as already described (Ochsner et al., 1995) free *fpvR* DNA fragments
277 could still be seen at 500 nM of Fur (Figure 6B). These results proved an important
278 difference of affinity of Fur for the two promoters that can explain a more important
279 repression of *pvdS* mRNA expression than of *fpvR* mRNAs at increasing iron concentration.
280 These results may be also applied for FpvI. Indeed, the expression of *fpvI*, measured by RT-
281 qPCR, decreased also quickly at 500 nM even if it appears to be less sensitive to further
282 iron concentration increase (Figure 4A).

283

284 **Importance of the PVD positive auto-regulation loop at different iron concentration**

285 As a consequence of the quicker decrease of PvdS expression, probably the ratio PvdS/FpvR
286 decreases upon iron concentration increases, inducing a shift of the equilibrium
287 $PvdS_{free}/PvdS_{b-FpvR}$ ($PvdS_{b-FpvR}$: PvdS bound to FpvR) toward the bound state. At low iron
288 concentrations, most of PvdS may be in the free state, whereas at higher iron concentrations,
289 it is preferentially bound to FpvR. As a consequence, at low iron concentration, the expression
290 of the PVD pathway (depending on free PvdS) is poorly dependent on a dissociation of PvdS
291 from FpvR, whereas at higher iron concentration, the expression of the PVD pathway is more
292 dependent on this dissociation, and thus on the amount of extracellular ferri-PVD. To validate

293 the importance of this mechanism on the expression of the PVD pathway, we compared the
294 relative expression of *pvdA* and *fpvA* mRNAs in the PVD-deficient $\Delta pvdF$ strain, versus the
295 wt strain, at different iron concentration (Figure 4A). It appears indeed, that the expression of
296 *pvdA* and *fpvA* was more important in the wt strain versus $\Delta pvdF$ when the iron concentration
297 was increased to 500 nM or 5 μ M. These results confirm that the presence of PVD become
298 more important to get expression of the genes of the PVD pathway at increasing iron
299 concentration.

300

301 **The positive auto-regulation loop induces a burst of PVD production**

302 Even if dispensable for PVD production at low iron concentrations, this regulatory loop is
303 activated, and may thus still play a role. Positive auto-regulation loops are a peculiar type of
304 positive feed-forward loops. These regulatory motifs can promote different behaviours, the
305 most frequent being to speed up the expression of the final product, or to induce a bi-stable
306 expression of the final product, e.g. to set two populations of cells expressing different levels
307 of the product (Mitrophanov and Groisman, 2008; Brautaset et al., 2009). These peculiar
308 properties were looked for in the case of the PVD positive auto-regulation.

309 Fluorescence emission by the cells has been monitored by FACS on wt cells, as well as on the
310 PVD-deficient mutant $\Delta pvdF$ cells, after 4 h, 8 h or 16 h of growth in CAA. Both strains were
311 expressing a chromosomal fusion between the enzyme PvdA involved in PVD biosynthesis
312 and eGFP. After 4 h of growth in CAA, wt cells were expressing almost 50 % more PvdA-
313 eGFP than $\Delta pvdF$ (Figure 7A and B). Then, this difference diminished gradually at 8 h and 16
314 h of growth (Figure 7B). To study the effect of the positive auto-regulation loop on the
315 establishment of a bi-stable population, especially at 4h of growth, cells from these two

316 strains were also visualized by microscopy. 25 images were recorded for each strain, all
317 showing only one population of cells which express PvdA-eGFP (Figure 7C). Altogether,
318 even at low iron concentrations, the auto-regulatory loop is important, inducing a burst in the
319 production of PVD that could play a role in the rapid adaptation of the cell to new
320 environments.

321

322 **Discussion**

323 The positive auto-regulation loop allows to speed up siderophore production only if the cells
324 are able to import the ferri-siderophore back. Further, PVD shares also some virulence factor
325 characteristics. In that aspect, the positive auto-regulation loop allows the system to function
326 like a *Quorum sensing* system: the cell will produce PVD only when enough cells are present
327 to combat the host, or other competitors. Altogether, the presence of such positive auto-
328 regulation loop presents different crucial advantages. Nevertheless, such iron import strategy
329 presents also serious weakness. Under such regulatory mode, the competition between
330 different bacteria for iron will be always won by the bacteria that produce the siderophore
331 with the best affinity for this metal. Further, in extremely iron-depleted conditions, under
332 continuous flow conditions, or in contexts of low cell density, like in ocean, the positive auto-
333 regulation mode of siderophore production may not be activated (the low concentration of
334 siderophore-Fe complexes may be lost for the bacteria due to important diffusion in the
335 environment). Under such drastic conditions, can really the bacteria spare the use of its major
336 iron uptake mechanisms?

337 The ratio between the sigma factor free and bound to the anti-sigma factor (under non induced
338 conditions) that depends on the production of both proteins and on their affinity, determine

339 the importance of the positive auto-regulation loop for the siderophore production. In most
340 systems, but PVD, the two genes are located adjacent onto the chromosome (Braun et al.,
341 2003), that probably allows a coupled transcription of both genes: they are expressed in the
342 same ratio, whatever the environmental conditions are, so the importance of the regulation
343 loop in the production of siderophore may be similar in all conditions. In the case of PVD, the
344 genes encoding for *pvdS* and *fpvR* are located on different locus, and may thus be submitted
345 to a different regulation by Fur. The EMSA experiments confirmed indeed that Fur binds
346 more efficiently the promoter sequence of *pvdS* than that of *fpvR*. Consequently, the
347 repression of transcription by Fur of *pvdS* is more efficient than that of *fpvR*, and may allow
348 a quicker repression of *pvdS* expression once iron concentration increases. This hypothesis
349 was verified at the mRNA and protein levels, by qRT-PCR, and by the measure of mCherry
350 expression, which ORF was cloned in a plasmid under the control of each promoter. The
351 expression of the *pvdS* mRNA, as well as the expression of mCherry under the control of the
352 *pvdS* promoter, decrease more quickly than that of the *fpvR* counterparts when the
353 concentration of iron increases. As a consequence, the concentration of free PvdS should be
354 the highest at low iron concentration. In such conditions, the positive auto-regulation through
355 the sigma/anti-sigma complex plays a less important role than at higher iron conditions.
356 Indeed, in CAA medium, the absence of PVD production (in the $\Delta pvdF$ strain) affected
357 weakly (less than 2-fold) the expression of most genes from the PVD pathway. By increasing
358 the concentration of iron in the medium, the difference in the expression of genes from the
359 PVD pathway increased. The cells become more dependent on the sigma/anti-sigma positive
360 auto-regulation system. Since such sigma/anti-sigma systems are widely used in bacteria, the
361 results presented here advocate that the regulation of gene expression through such system

362 may not be linear, but could depend on the environment, and that the chromosomal location of
363 both genes could be an indication of such complexity.

364 Such complex dynamic through positive auto-regulation may be more broadly shared by
365 different positively auto-regulated systems. For example, the *phoPphoQ* system is a
366 particularly well characterized auto-regulated two component system in bacteria (Kato et al.,
367 2008). PhoQ is a membrane protein whose activity is modulated by various environmental
368 signals, including Mg^{2+} . The transcription of the *phoPphoQ* system is controlled by a
369 constitutive promoter and a PhoP-dependent promoter. The presence of two promoters (one
370 constitutive and one inducible) is widespread across genetic circuit with positive feedback:
371 the constitutive promoter ensures the production of sufficient amounts of the regulatory
372 proteins, so that the cell can respond to an activating signal when it appears. Once activated,
373 PhoQ auto-phosphorylates, and transfers its phosphoryl group to PhoP. In *E. coli*, or
374 *Salmonella enterica*, phosphorylated PhoP positively regulates the expression of multiple
375 genes, including the *phoPphoQ* system (Figure S4). Mitrophanov *et al.* (2010) modelled this
376 circuit to understand its behaviour (Mitrophanov et al., 2010). They shown that if the
377 constitutive promoter is weak compared to the inducible promoter, the impact of the positive
378 feedback is stronger than if the constitutive promoter is strong (Figure S4). In the case of
379 PVD, even if the system diverges, the resulting phenotype is similar. The *pvdS* promoter is
380 Fur-sensitive: it is transcribed until Fur binds its promoter and represses its transcription.
381 Through this genetic construct, *P. aeruginosa* combines two situations. When iron
382 concentration is low (e.g. in CAA medium), Fur repression is low and PvdS efficiently
383 expressed. In that case we showed that the contribution of PVD auto-regulation was low.
384 When iron concentration is high, Fur repression is more efficient, and the positive auto-
385 regulation system gain importance (Figure S4). Further, since PhoP binds multiple promoters

386 with different affinities, the amount of PhoP generated when the auto-regulation is OFF will
387 suffice to induce the expression of genes from high affinity promoters, but genes from low
388 affinity promoters will only be induced when the auto-regulation is ON and allows to generate
389 high levels of PhoP (Zwir et al., 2012). The role of the auto-regulation circuit in the induction
390 of other genes under the control of PvdS (Swingle et al., 2008) has still not been tested.
391 Nevertheless, it would not be surprising to find that the auto-regulation plays a role in a
392 possible hierarchized induction among different PvdS controlled genes. Finally, Shin et al.
393 (2006) revealed that the *phoPphoQ* system induces a surge in PhoP production at early time of
394 induction, a property that is also shared by the PVD system as shown by FACS analyses.
395 Altogether, these comparisons showed that similar properties of the positive auto-regulation
396 can be retrieved in different types of auto-regulatory circuits, even if their genetic
397 construction diverges widely.

398 The regulatory cascade leading to PCH production seems less complex. It is based on a
399 ‘classical’ AraC type of transcription factor, which requires an inducer. It was previously
400 shown that the ferri-PCH, not the apo-PCH, was the co-factor (Michel et al., 2005).
401 Nevertheless, the regulation of this system proved to be more complex. Under strong
402 difficulties in iron uptake (e.g. when both siderophores are not produced anymore), the cell
403 manage to overcome the requirement of PCH for its own synthesis. This capability of the
404 bacteria could be important in specific conditions. Fur repression of *pchR* expression, that
405 remains the key step in the repression of the PCH pathway at higher iron concentration, is
406 further tightened by several other control mechanisms. It was previously shown that the ferri-
407 PCH bound to PchR, if inducing the expression of most genes from the PCH pathway, was
408 also involved in its own repression (Michel et al., 2005), probably through an interference
409 mechanism: since *pchD* and *pchR* are encoded on the same locus, but in opposite direction,

410 the binding of PchR on the promoter of *pchD* could interfere with the polymerisation of *pchR*
411 mRNAs (Figure S3). This would cap the production of PCH. Further, a Fur box has been
412 identified in the promoter of different genes from the PCH pathways, and not only in the
413 promoter of *pchR*. The EMSA experiments confirmed that Fur is indeed able to bind the
414 promoter of *pchD*. At increasing iron concentration, we nevertheless did not observed a strong
415 increase of the repression of the *pchD* promoter containing only this Fur box, through the
416 transcriptional reporters: Fur plays only a minor role in the repression of *pchD* mRNA
417 expression. The absence of *pchD* expression at higher iron concentration is more linked to the
418 absence of induction by PchR (see Figure 8). Further, while only one shift is observed when
419 using the sequence corresponding to the Fur box, we saw a second shift when we used a
420 longer sequence, comprising the PchR box. Fur can thus bind the PchR box of the *pchD*
421 promoter *in vitro*. *In vivo*, we also showed that this PchR box, even in the absence of PchR,
422 was indeed sensitive to iron concentration. The expression of mCherry cloned under the
423 promoter of *pchD* that contains either only the Fur box, or the Fur and PchR boxes were
424 compared in a strain deleted of *pchR* (Figure8). In that strain, the expression of mCherry
425 under the promoter containing the two motifs was more dependent on iron concentration than
426 the construct with only the Fur box. Finally, the alignment of the Fur box sequences of *pvdS*,
427 *fpvR*, *pchD* and the PchR box of the *pchD* gene confirmed the presence of some determinants
428 required for a recognition by Fur (Seo et al., 2014) in the PchR box (Figure S2). Altogether,
429 even if the two Fur boxes identified in the PCH effector genes do not represent the main
430 regulation routes involved in the regulation of these genes, they still allow to fine tune their
431 expression. In iron replete conditions, Fur may be able to compete with the low level of PchR-
432 PCH-Fe and to bind the two sites on the PCH genes to speed up their repression and/or to
433 avoid any noisy transcription of these genes.

434 Altogether, these results allow to understand how the cell finely adapts the production of its
435 siderophores under different iron situations (Figure 8). In drastically iron depleted conditions,
436 both siderophores are produced, even if sufficient ferri-siderophore cannot be imported back.
437 Under iron depleted conditions, PVD is produced mostly independently of the positive auto-
438 regulation, whereas PCH production still requires ferri-PCH import. Under these conditions,
439 PchR represses also its own expression: this mechanism participates to the lower production
440 of PCH over PVD. When iron becomes more concentrated, both positive auto-regulation
441 modes become important for the production of PVD and PCH. Nevertheless, since Fur
442 represses more tightly *pvdS* expression than *pchR*, the production of PVD decreases more
443 quickly than that of PCH. At higher iron concentration, both systems are tightly repressed
444 through at least two mechanisms to avoid any leaky production of siderophore. While both
445 *pvdS* and *pchR* expression are repressed by Fur, any noisy expression of PvdS will be silent
446 by its binding to FpvR. In such conditions, the few PVD molecules that have been produced
447 may not be sufficient to induce the positive auto-regulation loop. The binding of Fur on the
448 PCH effector promoters (Fur and PchR promoters) may also help to tightly control the
449 repression of the PCH pathway when the concentration of iron increases. These regulatory
450 schemes may also explain other observations. The presence of enterobactin in the culture
451 medium (iron depleted medium CAA), a siderophore produced by *E. coli* with a high affinity
452 for iron ($K_a = 10^{43} \text{M}^{-1}$) (Carrano and Raymond, 1979) compared to PVD and PCH (10^{32}M^{-1}
453 and 10^{28}M^{-2} respectively) has been shown to induce a strong repression of PCH production,
454 but only faintly of PVD (Gasser et al., 2016). Likely, the strong chelation of iron by
455 enterobactin inhibits the two positive auto-regulation loops, but in CAA the production of
456 PVD depends only faintly on this regulation loop. This explains why the PCH pathway is
457 strongly repressed, and the PVD pathway only weakly. It was known that in the presence of

458 enterobactin, *P. aeruginosa* express a transporter system (Pfe system) that specifically
459 transports enterobactin: it allows the bacteria to hijack the competitor's siderophore, and
460 deprive it from its iron source. The PVD production mechanism underlined here suggests that
461 *P. aeruginosa* does not base its iron uptake strategy when facing competitors only on other's
462 siderophore hijacking. On a virulence point of view, this mechanism further allows *P.*
463 *aeruginosa* to still benefit from the virulence properties of PVD in the presence of bacterial
464 competitors or host.

465 Further, both *P. aeruginosa* siderophores chelate several toxic metals, and participate to the
466 protection of the cell against their toxic effect (Braud et al., 2010; Schalk et al., 2011). While
467 these metal chelated by PCH do not enter into the cells, the metal-PVD could enter into the
468 periplasm, but were then exported back into the extra-cellular environment. In this context,
469 several metal have been shown to induce a repression of the production of PCH, but not of
470 PVD, with even an induction by a few of them (Braud et al., 2009a, 2009b). Again, if the
471 metal-PCH does not enter into the cytoplasm, the positive auto-regulation loop is not
472 activated, and the pathway repressed. On the opposite, the import of some PVD-metal into the
473 periplasm may not affect the regulation loop, and in that case the PVD is still produced
474 independently of the auto-regulation loop. It is possible that in some cases, the metal-PVD
475 complex could still induce a conformational change of FpvR, leading to an activation of the
476 positive auto-regulation loop and an increase of the production of PVD.

477

478 **Materials and Methods**

479 *Strains used and growth conditions*

480 The *P. aeruginosa* and *E. coli* strains and plasmids used in this study are listed in Table 1. *E.*
481 *coli* strains were routinely grown in LB (Difco) at 37°C. *P. aeruginosa* strains were first
482 grown overnight at 30°C in LB broth and were then washed, re-suspended and cultured
483 overnight at 30°C in iron-deficient CAA medium (composition: 5 g l⁻¹ casamino acids
484 (Difco), 1.46 g l⁻¹ K₂HPO₄·3H₂O (Carlo Erba), 0.25 g.l⁻¹ MgSO₄·7H₂O (Merck)). When
485 required, tetracyclin (100 mg.ml⁻¹), carbenicillin (150 µg.ml⁻¹) or gentamycin (30 mg.ml⁻¹)
486 were added to *P. aeruginosa* cultures. The cells were then pelleted by centrifugation and re-
487 suspended in fresh CAA medium, and the resulting suspension was diluted to the OD_{600 nm}
488 required.

489

490 *Mutant construction*

491 All enzymes for DNA manipulation were purchased from Fermentas and were used in
492 accordance with the manufacturer's instructions. *Escherichia coli* strain TOP10 (Invitrogen)
493 was used as the host strain for all plasmids. The DNA fragments from *P. aeruginosa* used for
494 cloning were amplified from the genomic DNA of the PAO1 strain with Phusion High-
495 Fidelity DNA polymerase (ThermoFisher Scientific). The primers used are listed in Table 2.
496 Mutations in the chromosomal genome of *P. aeruginosa* were generated by transferring
497 suicide vectors from *E. coli* TOP10 strains into the PAO1 strain and allowing the plasmid to
498 integrate into the chromosome, with selection for tetracycline resistance. The suicide vectors
499 contained either 700 bp flanking sequences on either side of the gene to be deleted or 700 bp
500 flanking the stop codon of the gene of interest with the sequence of the open reading frame of
501 mCherry in between for reporter fusion construction. A second crossing-over event excising
502 the vector was achieved by enrichment for tetracycline-sensitive cells to generate the

503 corresponding mutants (Ye et al., 1995). All gene deletion mutants were verified by PCR and
504 sequencing.

505 For the construction of transcriptional reporter plasmids, the promoters of the genes of interest
506 were amplified from the chromosomal DNA of *P. aeruginosa* PAO1 by PCR with specific
507 primers (Table 2) allowing an overlapping with a second PCR fragment encompassing the
508 open reading frame of mCherry. A second PCR was generated using the two first PCR
509 fragment as template to obtain of the transcriptional reporter fragment. This fragment was
510 trimmed by digestion with *EcoRI* and *HindIII* or *BamHI* and inserted between the sites for
511 these enzymes in pSEVA631 (<http://seva.cnb.csic.es>), and bacteria were transformed with this
512 vector.

513

514 *Real-time quantification of fluorescence intensity*

515 The cells were cultured overnight in CAA medium, pelleted by centrifugation and re-
516 suspended in fresh CAA medium, and the resulting suspension was diluted to obtain an OD₆₀₀
517 nm of 0.01 units. 200 µl of the suspension per well were dispensed into a 96-well plate
518 (Greiner, U-bottomed microplate). The plate was incubated at 30°C, with shaking, in a
519 TECAN microplate reader (Infinite M200, TECAN) for measurements of OD_{600 nm} and
520 mCherry (excitation/emission wavelengths: 570 nm/610 nm) fluorescence at 30 min intervals,
521 for 24 to 40 h. When required, iron (500 nM or 5 µM), or gentamycin (30 mg/ml) was added.

522

523 *Siderophore production*

524 Overnight cultures of strains grown in LB or CAA medium were pelleted, re-suspended and
525 diluted in fresh medium to obtain an OD_{600nm} of 0.1. The cells were then incubated in the

526 presence or absence iron, with vigorous shaking, at 30°C for 8 h. The OD_{600 nm} was taken to
527 measure cell growth. The OD_{400 nm} was also taken from 1 ml of supernatant to measure the
528 production of PVD ($e_{\text{pvd}} = 19000 \text{ M}^{-1} \cdot \text{cm}^{-1}$). PCH was then extracted twice from 1ml of
529 supernatant (acidified with 50 ml of citric acid 1M) with 500 ml of dichloromethane. The
530 absorbance at 320 nm was taken, and the PCH concentration calculated ($e_{\text{PCH}} = 4300 \text{ M}^{-1} \cdot \text{cm}^{-1}$).
531 ¹).

532

533 *Quantitative real-time PCR*

534 Specific gene expression was measured by RT-qPCR, as previously described (Gross and
535 Loper, 2009). Briefly, overnight cultures of strains grown in LB or CAA medium were
536 pelleted, re-suspended and diluted in fresh medium to obtain an OD_{600 nm} of 0.1 units. The
537 cells were then incubated in the presence or absence iron, with vigorous shaking, at 30°C 8 h.
538 An aliquot of 2.5×10^8 cells from this culture was added to two volumes of RNAprotect
539 Bacteria Reagent (Qiagen). Total RNA was extracted with an RNeasy Mini kit (Qiagen),
540 treated with DNase (RNaseFree DNase Set, Qiagen) and purified with an RNeasy Mini Elute
541 cleanup kit (Qiagen). We then reverse transcribed 1 µg of total RNA with a High-Capacity
542 RNAtc-cDNA Kit, in accordance with the manufacturer's instructions (Applied Biosystems)
543 with oligonucleotides described in Table 2. The amounts of specific complementary DNAs
544 were assessed in a StepOne Plus instrument (Applied Biosystems) with Power Sybr Green
545 PCR Master Mix (Applied Biosystems) and the appropriate primers (Table 2), with the *uvrD*
546 messenger RNA used as an internal control. The transcript levels for a given gene in a given
547 strain were normalized with respect to those for *uvrD* and are expressed as a ratio (fold
548 change) relative to the reference conditions.

549

550 FACS and microscopy

551 The cells were cultured overnight in CAA medium, pelleted by centrifugation, re-suspended
552 in fresh CAA medium, and the resulting suspensions were diluted in falcons 50 ml to obtain
553 10 ml of cells at an OD_{600nm} of 0.1 units. These suspensions were then incubated at 30°C
554 with shaking for 4h, 8h, or 16h. 1ml of cells at an OD_{600nm} adjusted to 1 were centrifuged
555 washed with PBS and fixed for 16h at 4°C with paraformaldehyde 4%. Cells were washed
556 once again in PBS, and diluted to 10⁶cells/ml prior FACS analysis or 10⁸ cells/ml prior
557 microscopic visualization. GFP expression was monitored by flow cytometry on a
558 FACScalibur (BD, Franklin Lakes, NJ) and data were analysed with FlowJo Software
559 (FLOWJO LLC, Ashland, Oregon).

560

561 **References**

- 562 Albrecht-Gary, A.-M., Blanc, S., Rochel, N., Ocaktan, A.Z., and Abdallah, M.A. (1994).
563 Bacterial Iron Transport: Coordination Properties of Pyoverdin PaA, a Peptidic Siderophore
564 of *Pseudomonas aeruginosa*. *Inorg. Chem.* *33*, 6391–6402.
- 565 Beare, P.A., For, R.J., Martin, L.W., and Lamont, I.L. (2003). Siderophore-mediated cell
566 signalling in *Pseudomonas aeruginosa*: divergent pathways regulate virulence factor
567 production and siderophore receptor synthesis. *Mol. Microbiol.* *47*, 195–207.
- 568 Brandel, J., Humbert, N., Elhabiri, M., Schalk, I.J., Mislin, G.L.A., and Albrecht-Gary, A.-M.
569 (2012). Pyochelin, a siderophore of *Pseudomonas aeruginosa*: Physicochemical
570 characterization of the iron(III), copper(II) and zinc(II) complexes. *Dalton Trans.* *41*, 2820–
571 2834.
- 572 Braud, A., Hoegy, F., Jezequel, K., Lebeau, T., and Schalk, I.J. (2009a). New insights into the
573 metal specificity of the *Pseudomonas aeruginosa* pyoverdine-iron uptake pathway. *Environ.*
574 *Microbiol.* *11*, 1079–1091.
- 575 Braud, A., Hannauer, M., Mislin, G.L.A., and Schalk, I.J. (2009b). The *Pseudomonas*
576 *aeruginosa* pyochelin-iron uptake pathway and its metal specificity. *J. Bacteriol.* *191*, 3517–
577 3525.
- 578 Braud, A., Geoffroy, V., Hoegy, F., Mislin, G.L.A., and Schalk, I.J. (2010). Presence of the
579 siderophores pyoverdine and pyochelin in the extracellular medium reduces toxic metal
580 accumulation in *Pseudomonas aeruginosa* and increases bacterial metal tolerance. *Environ.*
581 *Microbiol. Rep.* *2*, 419–425.
- 582 Braun, V., Mahren, S., and Ogierman, M. (2003). Regulation of the FecI-type ECF sigma
583 factor by transmembrane signalling. *Curr. Opin. Microbiol.* *6*, 173–180.
- 584 Brautaset, T., Lale, R., and Valla, S. (2009). Positively regulated bacterial expression systems.
585 *Microb. Biotechnol.* *2*, 15–30.
- 586 Brillet, K., Journet, L., Célia, H., Paulus, L., Stahl, A., Pattus, F., and Cobessi, D. (2007). A β
587 Strand Lock Exchange for Signal Transduction in TonB-Dependent Transducers on the Basis
588 of a Common Structural Motif. *Structure* *15*, 1383–1391.
- 589 Carrano, C.J., and Raymond, K.J. Ferric ion sequestering agents. 2. Kinetics and mechanism
590 of iron removal from transferrin by enterobactin and synthetic tricatechols. *J. Am. Chem. Soc.*
591 *121*, 5401–5404.
- 592 Cobessi, D., Celia, H., and Pattus, F. (2005). Crystal Structure at High Resolution of Ferric-
593 pyochelin and its Membrane Receptor FptA from *Pseudomonas aeruginosa*. *J. Mol. Biol.* *352*,
594 893–904.
- 595 Cornelis, P., and Dingemans, J. (2013). *Pseudomonas aeruginosa* adapts its iron uptake
596 strategies in function of the type of infections. *Front. Cell. Infect. Microbiol.* *3*.
- 597 Cornelis, P., Matthijs, S., and Van Oeffelen, L. (2009). Iron uptake regulation in
598 *Pseudomonas aeruginosa*. *Biometals Int. J. Role Met. Ions Biol. Biochem. Med.* *22*, 15–22.

599 Cunrath, O., Gasser, V., Hoegy, F., Reimann, C., Guillon, L., and Schalk, I.J. (2014). A cell
600 biological view of the siderophore pyochelin iron uptake pathway in *Pseudomonas*
601 *aeruginosa*. *Environ. Microbiol.* *17*, 171–185.

602 Cunrath, O., Geoffroy, V.A., and Schalk, I.J. (2016). Metallome of *Pseudomonas aeruginosa*:
603 a role for siderophores. *Environ. Microbiol.* *18*, 3258–3267.

604 Dean, C.R., and Poole, K. (1993). Expression of the ferric enterobactin receptor (PfeA) of
605 *Pseudomonas aeruginosa*: involvement of a two-component regulatory system. *Mol.*
606 *Microbiol.* *8*, 1095–1103.

607 Dumas, Z., and Kümmerli, R. (2012). Cost of cooperation rules selection for cheats in
608 bacterial metapopulations. *J. Evol. Biol.* *25*, 473–484.

609 Edgar, R.J., Xu, X., Shirley, M., Konings, A.F., Martin, L.W., Ackerley, D.F., and Lamont,
610 I.L. (2014). Interactions between an anti-sigma protein and two sigma factors that regulate the
611 pyoverdine signaling pathway in *Pseudomonas aeruginosa*. *BMC Microbiol.* *14*, 287.

612 Enz, S., Mahren, S., Stroehel, U.H., and Braun, V. (2000). Surface signaling in ferric citrate
613 transport gene induction: interaction of the FecA, FecR, and FecI regulatory proteins. *J.*
614 *Bacteriol.* *182*, 637–646.

615 Folschweiller, N., Schalk, I.J., Celia, H., Kieffer, B., Abdallah, M.A., and Pattus, F. (2000).
616 The pyoverdine receptor FpvA, a TonB-dependent receptor involved in iron uptake by
617 *Pseudomonas aeruginosa* (review). *Mol. Membr. Biol.* *17*, 123–133.

618 Ganne, G., Brillet, K., Basta, B., Roche, B., Hoegy, F., Gasser, V., and Schalk, I.J. (2017).
619 Iron Release from the Siderophore Pyoverdine in *Pseudomonas aeruginosa* Involves Three
620 New Actors: FpvC, FpvG, and FpvH. *ACS Chem. Biol.* *12*, 1056–1065.

621 Gasser, V., Baco, E., Cunrath, O., August, P.S., Perraud, Q., Zill, N., Schleberger, C.,
622 Schmidt, A., Paulen, A., Bumann, D., et al. (2016). Catechol siderophores repress the
623 pyochelin pathway and activate the enterobactin pathway in *Pseudomonas aeruginosa*: an
624 opportunity for siderophore-antibiotic conjugates development. *Environ. Microbiol.* *18*, 819–
625 832.

626 Greenwald, J., Hoegy, F., Nader, M., Journet, L., Mislin, G.L.A., Graumann, P.L., and
627 Schalk, I.J. (2007). Real Time Fluorescent Resonance Energy Transfer Visualization of Ferric
628 Pyoverdine Uptake in *Pseudomonas aeruginosa* A ROLE FOR FERROUS IRON. *J. Biol.*
629 *Chem.* *282*, 2987–2995.

630 Guillon, L., Altenburger, S., Graumann, P.L., and Schalk, I.J. (2013). Deciphering protein
631 dynamics of the siderophore pyoverdine pathway in *Pseudomonas aeruginosa*. *PloS One* *8*,
632 e79111.

633 Imperi, F., Tiburzi, F., and Visca, P. (2009). Molecular basis of pyoverdine siderophore
634 recycling in *Pseudomonas aeruginosa*. *Proc. Natl. Acad. Sci. U. S. A.* *106*, 20440–20445.

635 Kato, A., Groisman, E.A., and Howard Hughes Medical Institute (2008). The PhoQ/PhoP
636 regulatory network of *Salmonella enterica*. *Adv. Exp. Med. Biol.* *631*, 7–21.

637 Kirby, A.E., Metzger, D.J., Murphy, E.R., and Connell, T.D. (2001). Heme Utilization in

- 638 Bordetella aviumIs Regulated by RhuI, a Heme-Responsive Extracytoplasmic Function
639 Sigma Factor. *Infect. Immun.* *69*, 6951–6961.
- 640 Koster, M., van Klompenburg, W., Bitter, W., Leong, J., and Weisbeek, P. (1994). Role for
641 the outer membrane ferric siderophore receptor PupB in signal transduction across the
642 bacterial cell envelope. *EMBO J.* *13*, 2805–2813.
- 643 Lamont, I.L., Beare, P.A., Ochsner, U., Vasil, A.I., and Vasil, M.L. (2002). Siderophore-
644 mediated signaling regulates virulence factor production in *Pseudomonas aeruginosa*. *Proc.*
645 *Natl. Acad. Sci. U. S. A.* *99*, 7072–7077.
- 646 Lin, P.-C., Youard, Z.A., and Reimann, C. (2013). In vitro-binding of the natural
647 siderophore enantiomers pyochelin and enantiopyochelin to their AraC-type regulators PchR
648 in *Pseudomonas*. *Biometals Int. J. Role Met. Ions Biol. Biochem. Med.* *26*, 1067–1073.
- 649 Llamas, M.A., Imperi, F., Visca, P., and Lamont, I.L. (2014). Cell-surface signaling in
650 *Pseudomonas*: stress responses, iron transport, and pathogenicity. *FEMS Microbiol. Rev.* *38*,
651 569–597.
- 652 Marena, M., Brito, B., Callard, D., Genin, S., Barberis, P., Boucher, C., and Arlat, M.
653 (1998). PrhA controls a novel regulatory pathway required for the specific induction of
654 *Ralstonia solanacearum* hrp genes in the presence of plant cells. *Mol. Microbiol.* *27*, 437–453.
- 655 Michel, L., González, N., Jagdeep, S., Nguyen-Ngoc, T., and Reimann, C. (2005). PchR-
656 box recognition by the AraC-type regulator PchR of *Pseudomonas aeruginosa* requires the
657 siderophore pyochelin as an effector. *Mol. Microbiol.* *58*, 495–509.
- 658 Miethke, M., and Marahiel, M.A. (2007). Siderophore-based iron acquisition and pathogen
659 control. *Microbiol. Mol. Biol. Rev. MMBR* *71*, 413–451.
- 660 Mislin, G.L.A., and Schalk, I.J. (2014). Siderophore-dependent iron uptake systems as gates
661 for antibiotic Trojan horse strategies against *Pseudomonas aeruginosa*. *Met. Integr. Biometal*
662 *Sci.* *6*, 408–420.
- 663 Mitrophanov, A.Y., and Groisman, E.A. (2008). Positive feedback in cellular control systems.
664 *BioEssays News Rev. Mol. Cell. Dev. Biol.* *30*, 542–555.
- 665 Mitrophanov, A.Y., Hadley, T.J., and Groisman, E.A. (2010). Positive autoregulation shapes
666 response timing and intensity in two-component signal transduction systems. *J. Mol. Biol.*
667 *401*, 671–680.
- 668 Ochsner, U.A., Vasil, A.I., and Vasil, M.L. (1995). Role of the ferric uptake regulator of
669 *Pseudomonas aeruginosa* in the regulation of siderophores and exotoxin A expression:
670 purification and activity on iron-regulated promoters. *J. Bacteriol.* *177*, 7194–7201.
- 671 Ross-Gillespie, A., Dumas, Z., and Kümmerli, R. (2015). Evolutionary dynamics of
672 interlinked public goods traits: an experimental study of siderophore production in
673 *Pseudomonas aeruginosa*. *J. Evol. Biol.* *28*, 29–39.
- 674 Saha, M., Sarkar, S., Sarkar, B., Sharma, B.K., Bhattacharjee, S., and Tribedi, P. (2016).
675 Microbial siderophores and their potential applications: a review. *Environ. Sci. Pollut. Res.*
676 *Int.* *23*, 3984–3999.

677 Schalk, I.J., Abdallah, M.A., and Pattus, F. (2002). Recycling of pyoverdinin on the FpvA
678 receptor after ferric pyoverdinin uptake and dissociation in *Pseudomonas aeruginosa*.
679 *Biochemistry (Mosc.)* 41, 1663–1671.

680 Schalk, I.J., Hannauer, M., and Braud, A. (2011). New roles for bacterial siderophores in
681 metal transport and tolerance. *Environ. Microbiol.* 13, 2844–2854.

682 Seo, S.W., Kim, D., Latif, H., O’Brien, E.J., Szubin, R., and Palsson, B.O. (2014).
683 Deciphering Fur transcriptional regulatory network highlights its complex role beyond iron
684 metabolism in *Escherichia coli*. *Nat. Commun.* 5, ncomms5910.

685 Smits, W.K., Kuipers, O.P., and Veening, J.-W. (2006). Phenotypic variation in bacteria: the
686 role of feedback regulation. *Nat. Rev. Microbiol.* 4, 259–271.

687 Stover, C.K., Pham, X.Q., Erwin, A.L., Mizoguchi, S.D., Warrener, P., Hickey, M.J.,
688 Brinkman, F.S., Hufnagle, W.O., Kowalik, D.J., Lagrou, M., et al. (2000). Complete genome
689 sequence of *Pseudomonas aeruginosa* PAO1, an opportunistic pathogen. *Nature* 406, 959–
690 964.

691 Swingle, B., Thete, D., Moll, M., Myers, C.R., Schneider, D.J., and Cartinhour, S. (2008).
692 Characterization of the PvdS-regulated promoter motif in *Pseudomonas syringae* pv. tomato
693 DC3000 reveals regulon members and insights regarding PvdS function in other
694 pseudomonads. *Mol. Microbiol.* 68, 871–889.

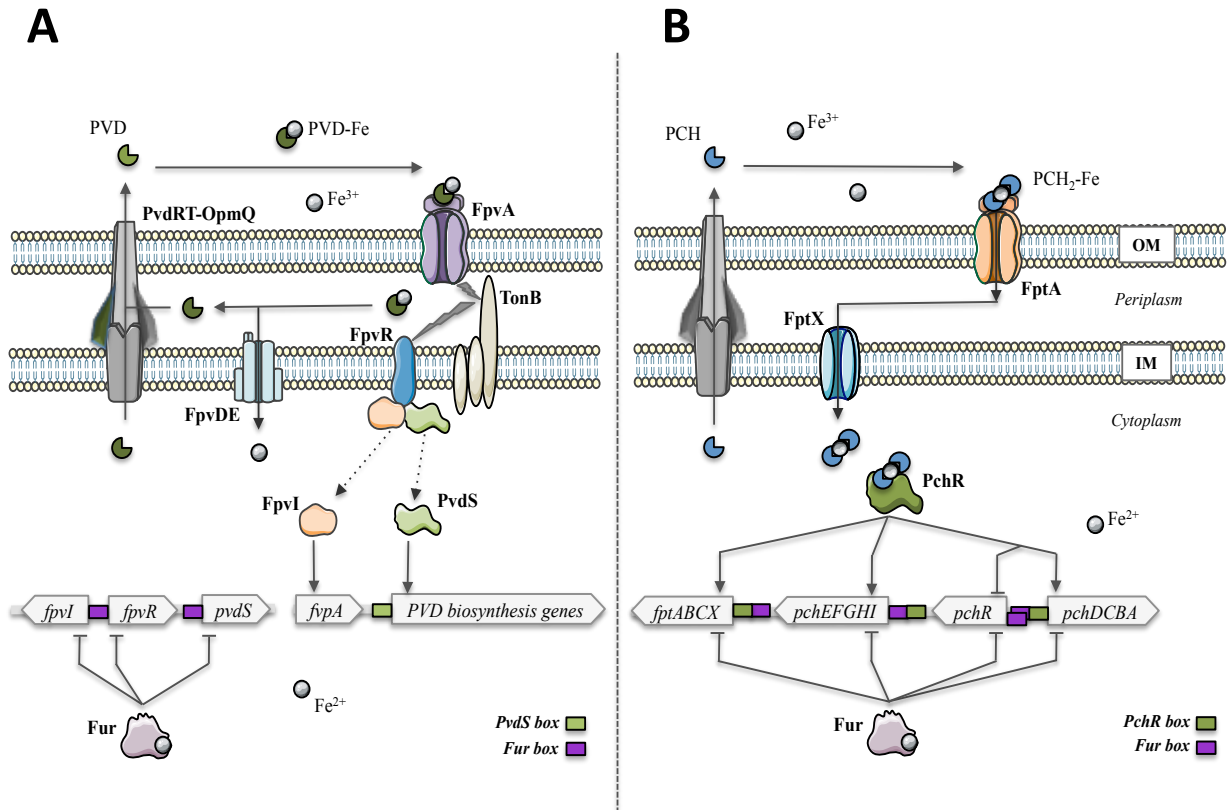
695 Troxell, B., and Hassan, H.M. (2013). Transcriptional regulation by Ferric Uptake Regulator
696 (Fur) in pathogenic bacteria. *Front. Cell. Infect. Microbiol.* 3, 59.

697 Visca, P., Leoni, L., Wilson, M.J., and Lamont, I.L. (2002). Iron transport and regulation, cell
698 signalling and genomics: lessons from *Escherichia coli* and *Pseudomonas*. *Mol. Microbiol.*
699 45, 1177–1190.

700 Yeterian, E., Martin, L.W., Lamont, I.L., and Schalk, I.J. (2010). An efflux pump is required
701 for siderophore recycling by *Pseudomonas aeruginosa*. *Environ. Microbiol. Rep.* 2, 412–418.

702 Zwir, I., Latifi, T., Perez, J.C., Huang, H., and Groisman, E.A. (2012). The promoter
703 architectural landscape of the *Salmonella* PhoP regulon. *Mol. Microbiol.* 84, 463–485.

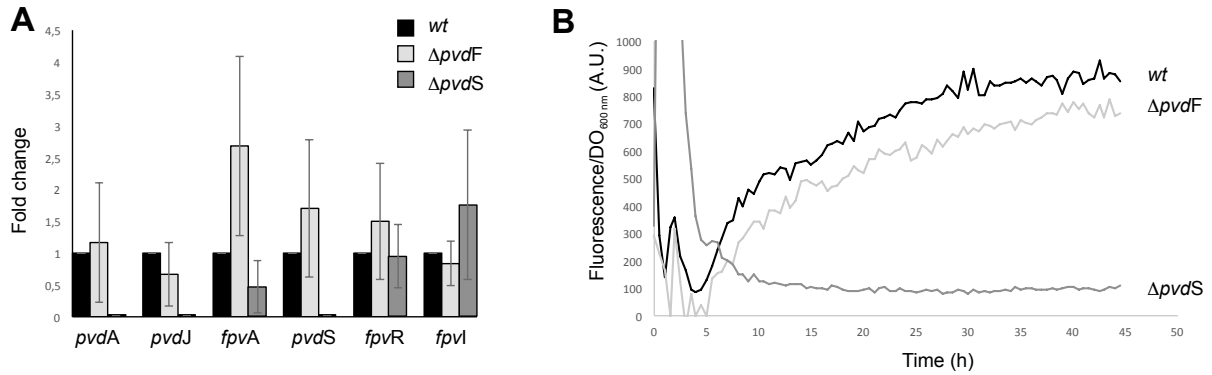
704



707

708 **Figure 1. PVD and PCH pathways are induced by specific transcription activators included**
 709 **into auto-inducing regulatory loops: the sigma/anti-sigma PvdS/FpvI/FpvR factors for PVD,**
 710 **the transcriptional regulator PchR for PCH. (A)** Concerning the PVD pathway, the Ferri-PVD
 711 uptake trough FpvA induces a conformational change of the anti-sigma factor FpvR, *via* a TonB
 712 dependent mechanism, releasing PvdS and FpvI into the cytoplasm, and consequently activating
 713 the expression of the PVD pathway. **(B)** The ferri-PCH is imported back into the periplasm *via*
 714 the specific outer transporter FptA, and into the cytoplasm through the permease FptX. Once in the
 715 cytoplasm, the ferri-PCH complex binds and activates the transcription regulator PchR, which binds
 716 to the PchR boxes inducing all promoters' genes expression of this pathway. The transcriptional
 717 regulator Fur represses both PVD and PCH pathways. Nevertheless, whereas in the PVD pathway
 718 Fur inhibits the expression of the sigma and anti-sigma factors PvdS, FpvR and FpvI (A), in the PCH
 719 pathway Fur inhibits directly *pchR*, but also the different promoters of genes involved in the PCH
 720 biosynthesis (*pchEFGHI* and *pchDCBA*) and transport (*fptABCX*).

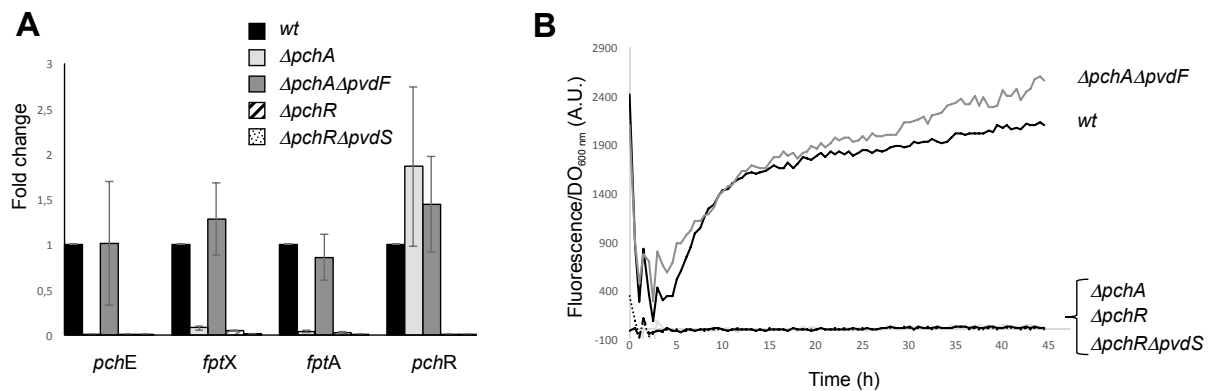
721



722

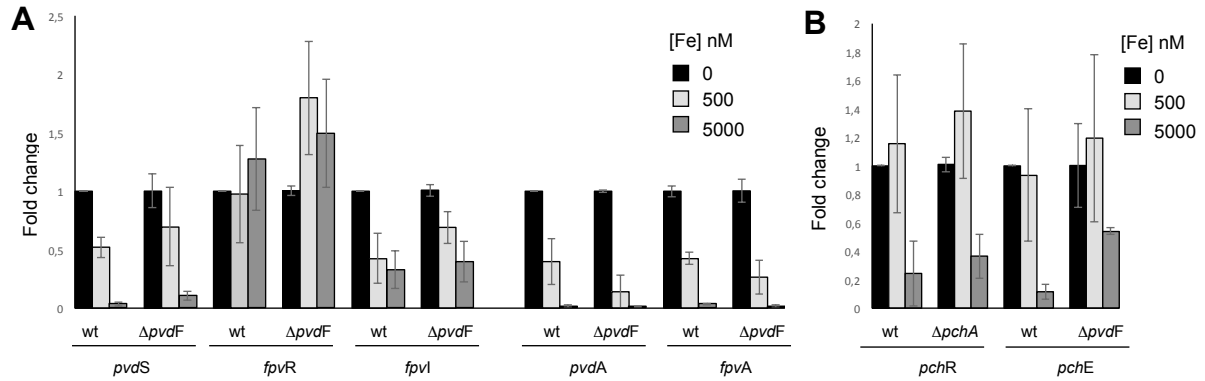
723 **Figure 2. Expression of genes from the PVD pathway in wt and in isogenic mutants. (A)**
 724 Analysis of changes in transcription for the genes *pvdA*, and *pvdJ* encoding a nonribosomal
 725 peptide synthetases involved in PVD biosynthesis, *fpvA* encoding the outer membrane transporters
 726 of PVD-Fe, *pvdS* and *fpvI*, the two sigma factors of the PVD pathway, as well as *fpvR*, their
 727 corresponding anti-sigma factor. Reverse transcription qPCR was performed on *P. aeruginosa*
 728 PAO1 *wt* and its isogenic mutants $\Delta pvdF$, and $\Delta pvdS$, grown in CAA medium. Results are given as
 729 a ratio between the values obtained from the mutant over those obtained in the *wt* strain **(B)**
 730 Monitoring of PvdJ-mCherry fluorescence (PvdJ is a nonribosomal peptide synthetase involved in
 731 PVD biosynthesis) during bacterial growth in CAA in the *wt* and its isogenic mutants $\Delta pvdF$, and
 732 $\Delta pvdS$.

733



734

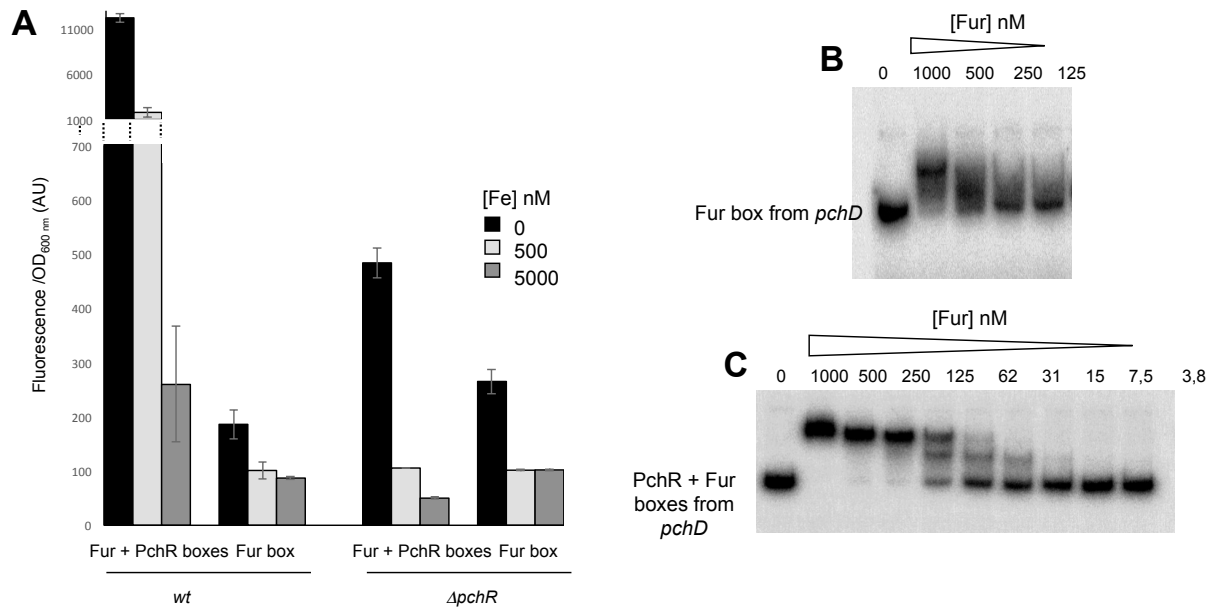
735 **Figure 3. Expression of genes from the PCH pathway in wt and in isogenic mutants. (A)**
 736 Analysis of changes in transcription for the genes *pchE* encoding a nonribosomal peptide
 737 synthetase involved in PCH biosynthesis, *fptA* and *fptX* encoding the outer and inner membrane
 738 transporters of PCH-Fe, respectively, and *pchR*, the transcriptional regulator of the PCH pathway.
 739 Reverse transcription qPCR was performed on *P. aeruginosa* PAO1 *wt* and its isogenic mutants
 740 $\Delta pchA$, $\Delta pchA\Delta pvdF$, $\Delta pchR$ and $\Delta pchR\Delta pvdS$ grown in CAA medium. Results are given as a
 741 ratio between the values obtained from the mutants over those obtained in the *wt* strain. Values
 742 below 0,05 are barely seen (most values from $\Delta pchR$ and $\Delta pchR\Delta pvdS$ strains). **(B)** Monitoring of
 743 PchE-mCherry fluorescence (PchE is a nonribosomal peptide synthetase involved in PCH
 744 biosynthesis) during bacterial growth in CAA in the *wt* and its isogenic mutants $\Delta pchA$,
 745 $\Delta pchA\Delta pvdF$, $\Delta pchR$ and $\Delta pchR\Delta pvdS$.



746

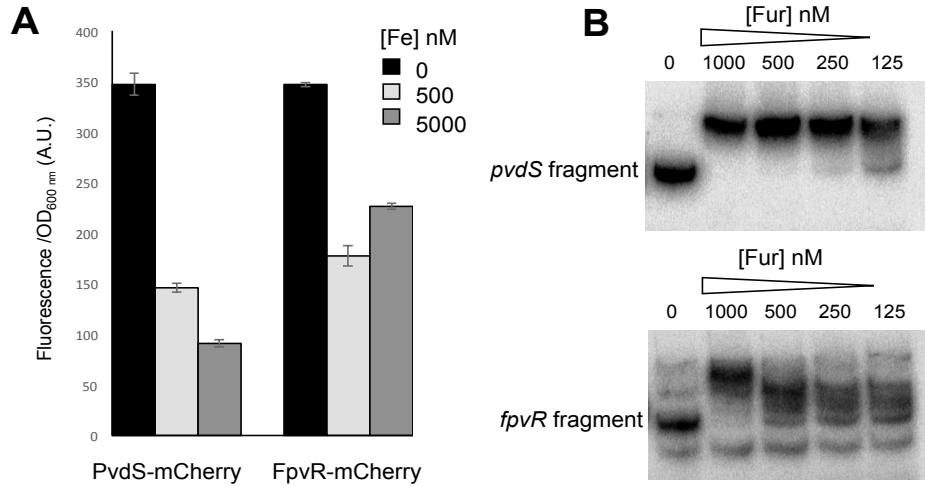
747 **Figure 4. Iron effect on the transcription of genes from the PVD and PCH pathways in wt**
 748 **and $\Delta pvdF$ strains.** Analysis of changes in transcription for the genes *pvdS*, *fpvR*, *fpvI*, *pvdA*, and
 749 *fpvA* (A); *pchR* and *pchE* (B). Reverse transcription qPCR was performed on *P. aeruginosa* PAO1
 750 wt grown in CAA medium supplemented with iron. Results are given as a ratio between the values
 751 obtained from the strain grown in CAA supplemented with iron over those obtained in the same
 752 strain grown in CAA.

753



754

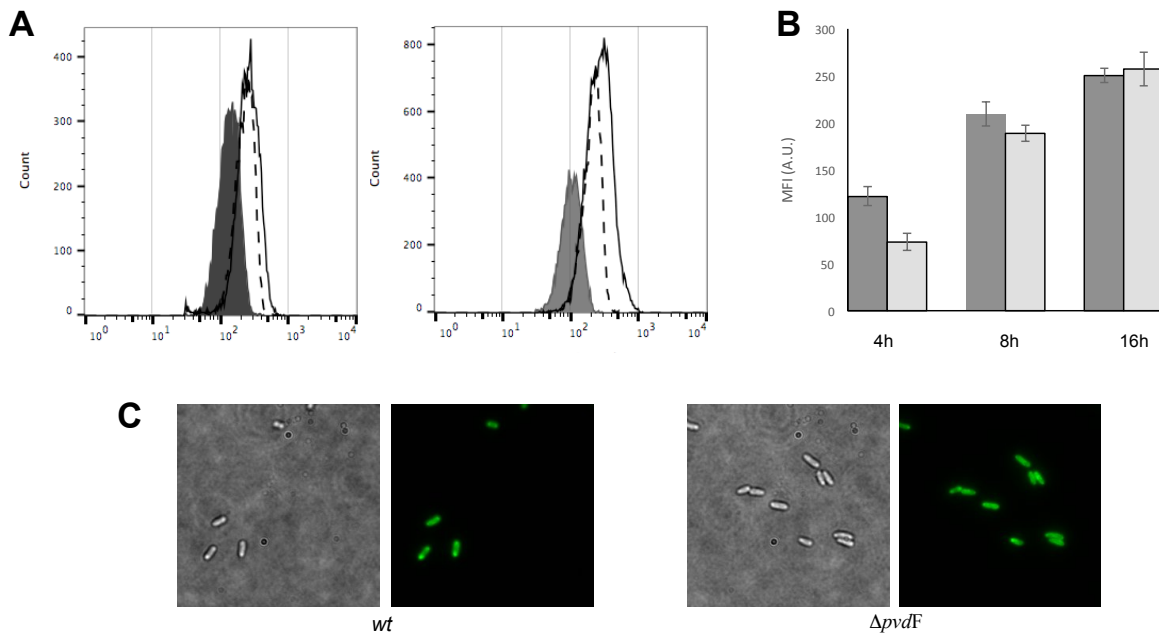
755 **Figure 5. Expression of genes from transcriptional fusion reporters of the PCH pathways in**
 756 **wt and the isogenic $\Delta pchR$ strains.** (A) Monitoring of mCherry fluorescence after 20 h of growth
 757 (late exponential phase) in CAA or CAA supplemented with iron of a wt and a $\Delta pchR$ strain
 758 transformed with a transcriptional reporter encoding the mCherry ORF under the control of the
 759 *pchD* promoter, containing either the PchR + Fur boxes, or only the Fur box. (B) EMSA
 760 experiment with a DNA fragment encompassing the sequence of the Fur box of the *pchD* promoter
 761 labelled with ^{32}P [ATP] and increasing concentration of Fur protein. (C) EMSA experiment with a
 762 DNA fragment encompassing the Fur and PchR boxes of the *pchD* promoter labelled with
 763 ^{32}P [ATP] and increasing concentration of Fur protein.



764

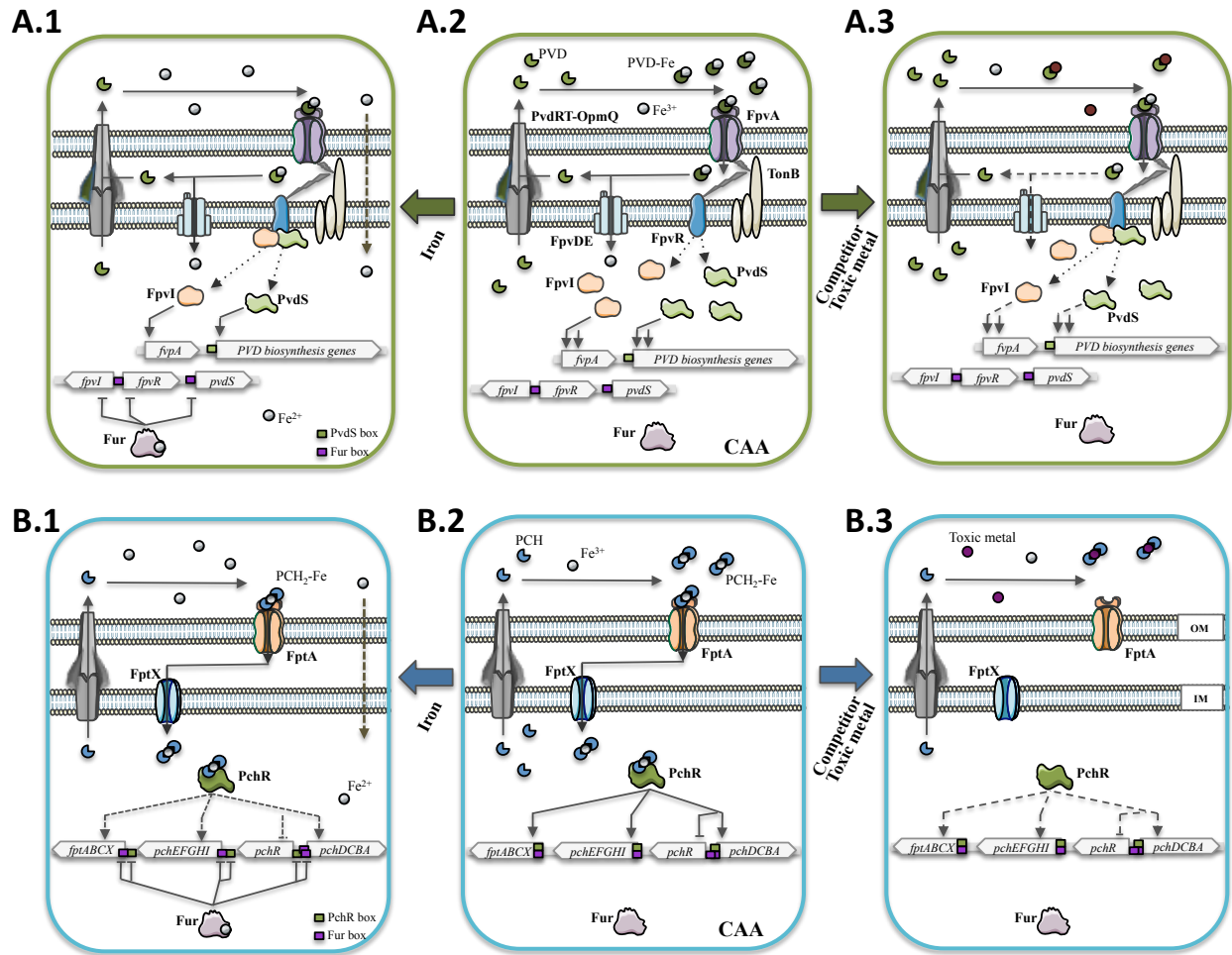
765 **Figure 6. Iron effect on the expression of genes from the PVD pathway. (A)** Monitoring of
 766 mCherry fluorescence after 20 h of growth (late exponential phase) in CAA or CAA supplemented
 767 with iron of a wt strain transformed with a transcriptional reporter encoding the mCherry ORF
 768 under the control of the *pvdS* promoter or the *fpvR* promoter. **(B)** EMSA experiment with the
 769 sequence of the *pvdS*, or the *fpvR* promoter labelled with ³²P[ATP] and increasing concentration of
 770 Fur protein.

771



772

773 **Figure 7. PvdA-eGFP expression in wt and PVD-deficient (*ΔpvdF*) strains. (A)** PAO1 wt (left)
 774 and *ΔpvdF* (right) cells have been grown in CAA for different times (4h, filled grey areas; 8h, dotted
 775 delimited areas; and 16h, dark delimited areas) and cells analysed by flow cytometry. One experiment
 776 representative of 4. **(B)** Geometric mean fluorescence intensity values of PvdA-eGFP expression in
 777 the *wt* (dark grey) and the *ΔpvdF* mutant (light grey) at these different collecting times are given. **(C)**
 778 Image of *wt* (left) and *ΔpvdF* (right) cells after 4h of growth.



779

780 **Figure 8. Schematic representation of the regulation of PCH and PVD production.** In CAA,
 781 ferri-PVD is not essential to the expression of the PVD pathway (A.2), while ferri-PCH is required
 782 for the PCH pathway expression (B.2). Different regulation scheme are then proposed according to
 783 changes in the environment (in iron concentration, toxic metal or presence of competitive
 784 siderophores). In presence of high iron concentration the positive-regulation loops are important, but
 785 the effect of Fur become stronger, binding the Fur boxes and repressing the sigma and anti-sigma
 786 factors PvdS/FpvI/FpvR thus the PVD production (A.1), and possibly the Fur box and also the PchR
 787 box of the PCH pathway to increase the efficient of the repression of this pathway (B.1). The
 788 presence of toxic metal leads to the same phenotype than the presence of competitive siderophores:
 789 less *P. aeruginosa* siderophores are becoming charged with iron, therefore, less ferri-PVD binds
 790 FpvA thus less induce the PvdS and FpvI release (A.3), and less ferri-PCH can be transported into the
 791 cytoplasm to induce the PchR (B.3).

792

793 **Tables**

794

795 **Table 1.** Strains and plasmids used in this study

Strains and plasmids	Relevant characteristics	References
Strains		
<i>E. coli</i> Top10	F- mcrA Δ (mrr-hsdRMS-mcrBC) ϕ 80lacZ Δ M15 Δ lacX74 nupG recA1 araD139 Δ (ara-leu)7697 galE15 galK16 rpsL(StrR) endA1 λ	Invitrogen
PAO1 wt ATCC15692		(Stover et al., 2000)
PAO1 <i>pchEmCherry</i>	PAO1; mCherry fused to 3' of <i>pchE</i>	(Cunrath et al., 2014)
PAO1 <i>pvdJmCherry</i>	PAO1; mCherry fused to 3' of <i>pvdJ</i>	(Gasser et al., 2015)
PAO1 <i>pvdAegfp</i>	PAO1; egfp fused to 3' of <i>pvdA</i>	(Guillon et al. 2013)
Δ <i>pvdF</i>	PAO1; <i>pvdF</i> chromosomally deleted	This study
Δ <i>pchA</i>	PAO1; <i>pchA</i> chromosomally deleted	(Cunrath et al., 2014)
Δ <i>pvdF</i> Δ <i>pchA</i>	PAO1; <i>pvdF</i> and <i>pchA</i> chromosomally deleted	(Gasser et al., 2015)
Δ <i>pvdS</i>	PAO1; <i>pvdS</i> chromosomally deleted	This study
Δ <i>pchR</i>	PAO1; <i>pchR</i> chromosomally deleted	This study
Δ <i>pchR</i> Δ <i>pvdS</i>	PAO1; <i>pchR</i> and <i>pvdS</i> chromosomally deleted	This study
Δ <i>pvdF</i> <i>pchEmCherry</i>	PAO1; <i>pvdF</i> chromosomally deleted, mCherry fused to 3' of <i>pchE</i>	This study
Δ <i>pchA</i> <i>pchEmCherry</i>	PAO1; <i>pchA</i> chromosomally deleted, mCherry fused to 3' of <i>pchE</i>	(Cunrath et al., 2014)
Δ <i>pvdF</i> Δ <i>pchA</i> <i>pchEmCherry</i>	PAO1; <i>pvdF</i> and <i>pchA</i> chromosomally deleted, mCherry fused to 3' of <i>pchE</i>	This study
Δ <i>pvdS</i> <i>pchEmCherry</i>	PAO1; <i>pvdS</i> chromosomally deleted, mCherry fused to 3' of <i>pchE</i>	This study
Δ <i>pchR</i> <i>pchEmCherry</i>	PAO1; <i>pchR</i> chromosomally deleted, mCherry fused to 3' of <i>pchE</i>	This study
Δ <i>pchR</i> Δ <i>pvdS</i> <i>pchEmCherry</i>	PAO1; <i>pchR</i> and <i>pvdS</i> chromosomally deleted, mCherry fused to 3' of <i>pchE</i>	This study
Δ <i>pvdF</i> <i>pvdJmCherry</i>	PAO1; <i>pvdF</i> chromosomally deleted, mCherry fused to 3' of <i>pvdJ</i>	(Gasser et al., 2015)
Δ <i>pchA</i> <i>pvdJmCherry</i>	PAO1; <i>pchA</i> chromosomally deleted, mCherry fused to 3' of <i>pvdJ</i>	This study
Δ <i>pvdF</i> Δ <i>pchA</i> <i>pvdJmCherry</i>	PAO1; <i>pvdF</i> and <i>pchA</i> chromosomally deleted, mCherry fused to 3' of <i>pvdJ</i>	(Gasser et al., 2015)
Δ <i>pvdS</i> <i>pvdJmCherry</i>	PAO1; <i>pvdS</i> chromosomally deleted, mCherry fused to 3' of <i>pvdJ</i>	This study
Δ <i>pchR</i> <i>pvdJmCherry</i>	PAO1; <i>pchR</i> chromosomally deleted, mCherry fused to 3' of <i>pvdJ</i>	This study
Δ <i>pchR</i> Δ <i>pvdS</i> <i>pvdJmCherry</i>	PAO1; <i>pchR</i> and <i>pvdS</i> chromosomally deleted, mCherry fused to 3' of <i>pvdJ</i>	This study
Δ <i>pvdF</i> <i>pvdAegfp</i>	PAO1; <i>pvdF</i> chromosomally deleted, egfp fused to 3' of <i>pvdA</i>	This study

Plasmids	Collection ID		
pME deltapvdS	pLG4	Suicide vector to delete <i>pvdS</i>	(Guillon et al., 2013)
pME3088deltapchR	pOC8	Suicide vector to delete <i>pchR</i>	(Cunrath et al., 2014)
pME3088 delta pchA	pOC6		(Cunrath et al., 2014)
pME3088 delta pvdF	pVEGA1		(Gasser et al., 2015)
pEXG2pvdJmCherry	pAF6	Suicide vector to add mCherry at the 3' of <i>pvdJ</i>	This study
pME3088PchE-mCherry	pOC3	Suicide vector to add mCherry at the 3' of <i>pchE</i>	(Cunrath et al., 2014)
pSEVA631 pchD_fur-mCherry	pAYC6	<i>pchD</i> promoter containing only the Fur box fused to mCherry ORF	This study
pSEVA631_pchD_Fur PchR-mCherry	pAYC5	<i>pchD</i> promoter containing the Fur box and PchR box fused to mCherry ORF	This study
pSEVA631 FpvI-mCherry	pPF1	<i>fpvI</i> promoter containing the Fur box fused to mCherry ORF	This study
pSEVA631 FpvR-mCherry	pPF2	<i>fpvR</i> promoter containing the Fur box fused to mCherry ORF	This study
pSEVA631 PvdS-mCherry	pPF3	<i>pvdS</i> promoter containing the Fur box fused to mCherry ORF	This study

796

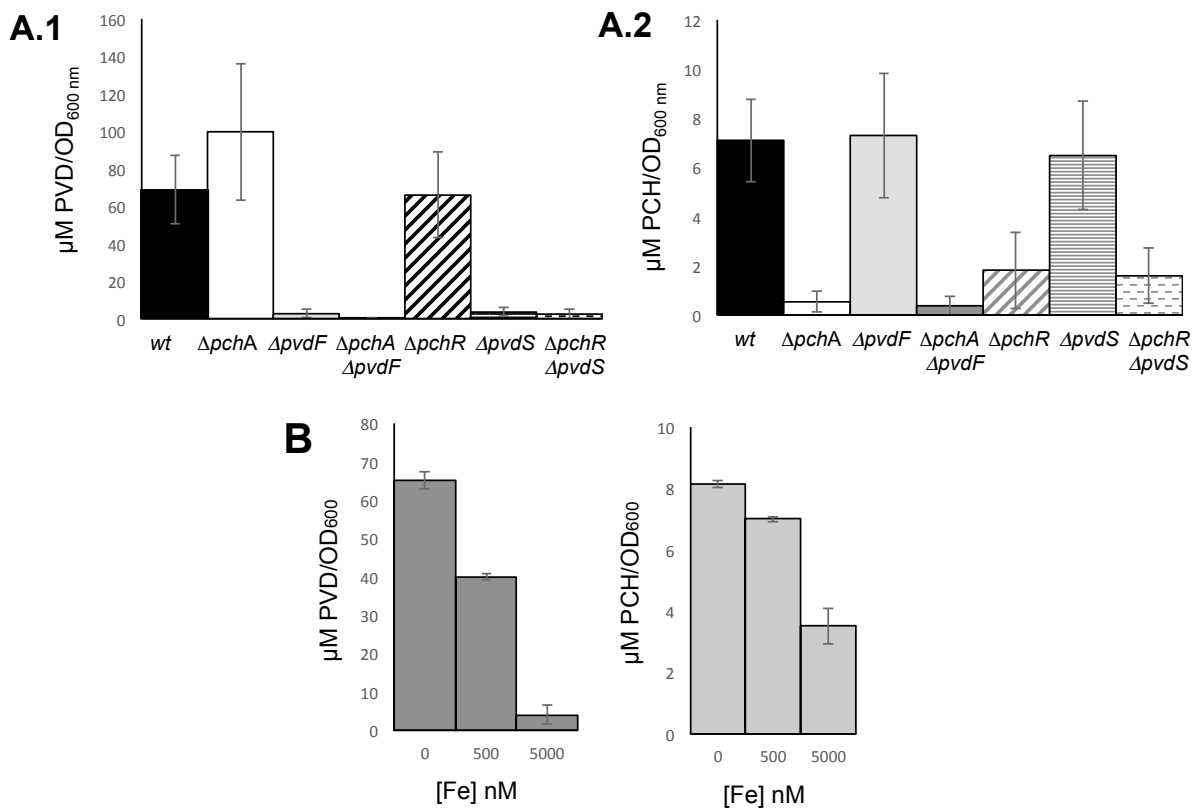
797 Table 2. Oligonucleotides used in this study

Oligonucleotides	Sequences 5'-3'	Final construct
Cloning		
<i>pchD</i> Fur box Fwd	CAAAGAATTCGCCGCCGCAATGATAATAAATCTC ATTTC	pAYC6
<i>pchD</i> Fur box. Rev	CCATGTTATCCTCCTCGCCCTTGCTCAC CATGCGATCTCCGTGGATGCGG	pAYC6
<i>pchD</i> PchR box & Fur box Fwd	CAAAGAATTCGACAAAGCGCCCTGCACTCCG	pAYC5
<i>pchD</i> PchR box & Fur box Rev	CATGTTATCCTCCTCGCCCTTGCTCAC CATGCGATCTCCGTGGATGCG	pAYC5
<i>pvdS</i> large Fur box Fwd	CAAAGAATTCGAAACGCCGAAGAATTTCTCCCTC	pPF3
<i>pvdS</i> Fur box Rev	GAAGGCATAA CTGGAACCCT CGATGGTGAG CAAGGGCGAG GAGGATAACA TGG	pPF3
<i>fpvR</i> large Fur box Fwd	CAAAGAATTCGGATAATGGTTTTCCAAGACGACTCC	pPF2
<i>fpvR</i> large Fur box Rev	CCATGTTATCCTCCTCGCCCTTGCTCACCATCGAGGG TTCCAGTTATGCCTTC	pPF2
<i>fpvI</i> Fur box Fwd	ATATATGAATCCAAGGGTGTGCTGCTGCG	pPF1
<i>fpvI</i> Fur box Rev	CCATGTTATC CTCCTCGCCC TTGCTCACCA T GACGACTCC TGCTCGCT	pPF1
mCherry Fwd	GTGAGCAAGGGCGAGGAGGATAACATG	pAY and pPF series
mCherry Rev HindIII	CTCCAAGCTTTTACTTGTACAGCTCGTCCATGCCGC	pAY5, pAY6, pPF3
mCherry Rev BamHI	CTCCGGATCCTTACTTGTACAGCTCGTCCATGCCGC	pPF2, pPF1
qRT-PCR		
FpvR F1	GGTCGAACTGGACCTCAATAC	

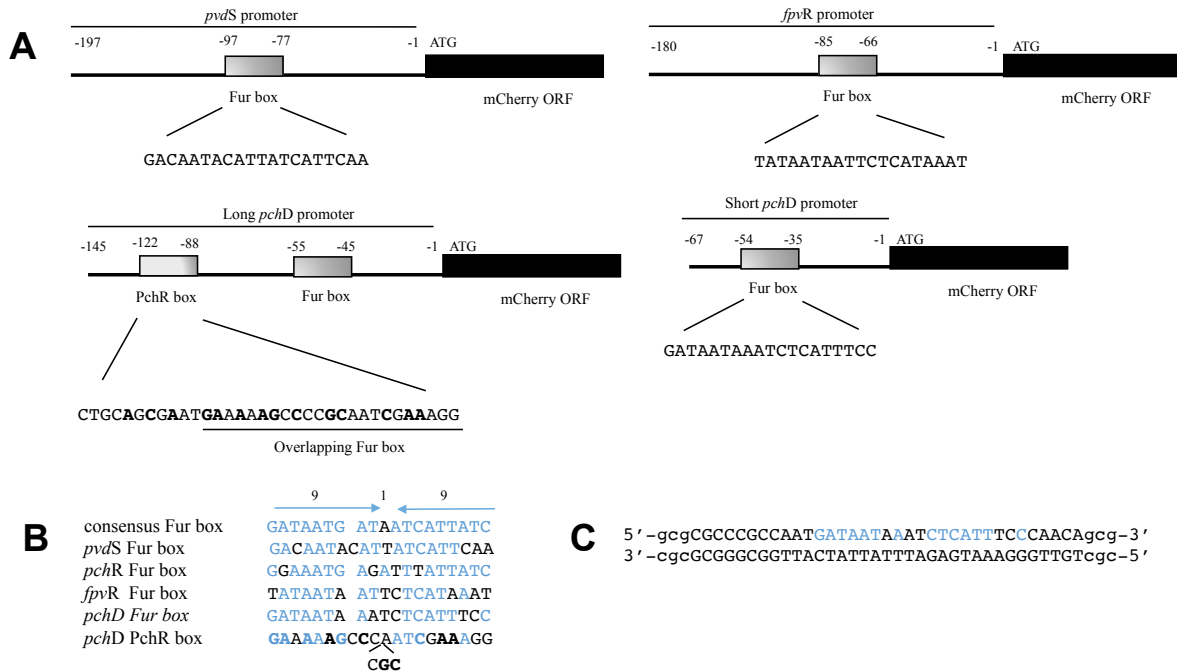
FpvR R1	CGTGGGTGACATGGAAGTAG
PvdS F1	CAGGCGCTCGAACAGAAATA
PvdS R1	CGTAGTTGATGTGCGAGGTT
FpvI F1	CAGATCGCCGAACATCTCAATA
FpvI R1	CACCCGACAGTGCTTCATC
uvrD F	CTACGGTAGCGAGACCTACAACAA
PvdA R qRT	TGGTATTCGCGCAGCAAAC
PvdA F qRT	CGCCGAAGTTCACCGATCT
fpvA R qRT	TGCCGTAATAGACGCTGGTTT
fptA F qRT	GCGCCTGGGCTACAAGATC
pchA F qRT	CGCGAAACCTGCCTTAAGC
pchA R qRT	GTCCAGGCCGCTATGG
fptX F qRT	CCCTGGGTGGTCAAGTTCCT
fptX R qRT	CGGCGCGACCAGTGA
pvdJ F qRT	CGTGGCCGCGATATGG
pvdJ R qRT	CTCTTCAGGCTGACTTCGATACC
4 F	CCGACATGGCGTTGTTCTCT
4 R	TACCTGGACTTCGCCGATCT
qRTPCR-PchR-Fwd	CGGCTTTCGCAAGGTGTT
qRTPCR-PchR-Rev	AGGCGGTATTCTGCAGGTA
EMSA	
Short <i>pchD</i> prom sens	GCGCGCCCGCCAATGATAATAAATCTCATTCCCAA CAGCG
Short <i>pchD</i> prom antisens	CGCTGTTGGGAAATGAGATTTATTATCATTGGCGGG CGCGC
<i>pchD</i> PchR box & Fur box Fwd	CAAAGAATTCGACAAAGCGCCCTGCACTCCG
<i>pchD</i> PchR box & Fur box Rev	CATGTTATCCTCCTCGCCCTTGCTCAC CATGCGATCTCCGTGGATGCG
<i>pvdS</i> large Fur Box Fwd	CAAAGAATTCGAAACGCCGAAGAATTCTCCCCTC
<i>pvdS</i> Fur box Rev	GAAGGCATAACTGGAACCCTCGATGGTGAG CAAGGGCGAG GAGGATAACATGG
<i>fpvR</i> large Fur Box Fwd	CAAAGAATTCGATAATGGTTTTCCAAGACGACTCC
<i>fpvR</i> large Fur Box Rev	CCATGTTATCCTCCTCGCCCTTGCTCACCATCGAGGG TTCCAGTTATGCCTTC

798

799



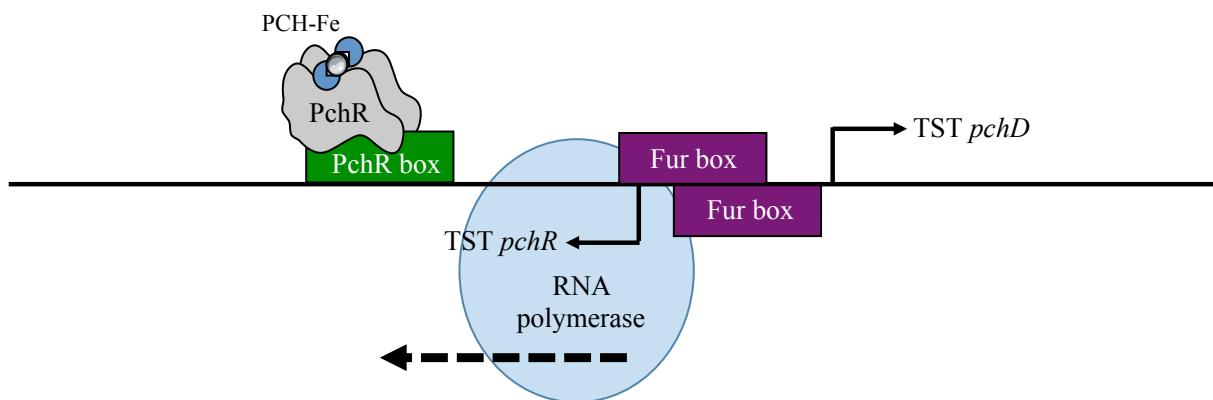
803 **Figure S1. Production of PCH and PVD in different strains.** (A) PVD (A.1) and PCH (A.2)
 804 production have been monitored after 8 h of growth in CAA. PVD production has directly been
 805 estimated from the $\text{OD}_{400 \text{ nm}}$ of culture supernatants, while PCH monitoring required first an
 806 organic extraction prior $\text{OD}_{320 \text{ nm}}$ measurement. (B) Iron effect on PVD (dark grey bars) and PCH
 807 (light grey bars) production in the wt strain.



808

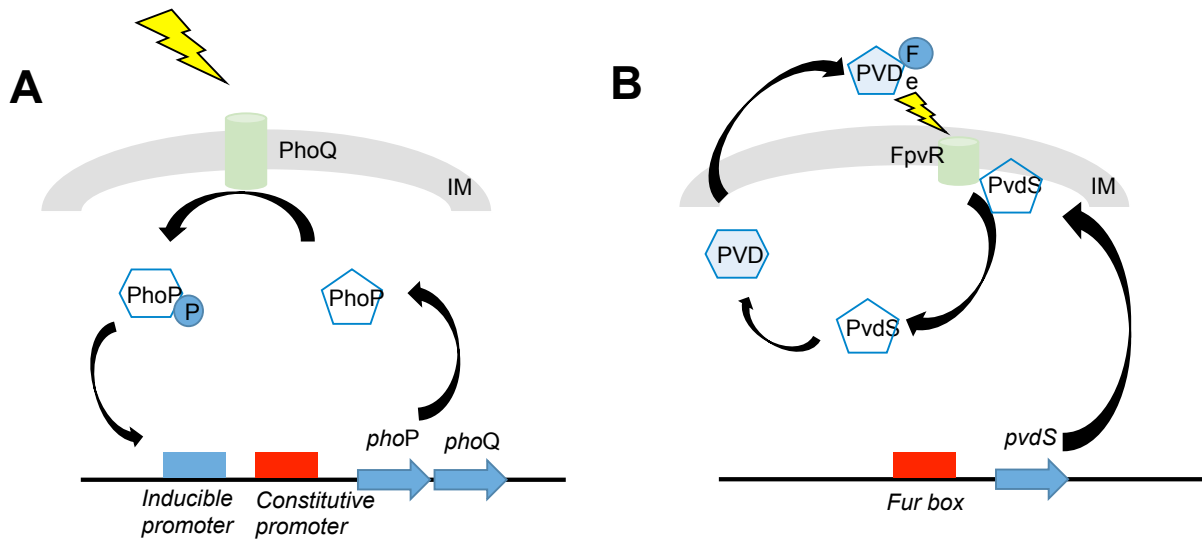
809 **Figure S2. Details on the transcriptional reporter constructs used, based on the *pvdS*, *fpvR* and**
810 ***pchD* promoters.** (A) The length of the promoter sequence cloned is given, and the -1 corresponds to
811 the last nucleotide before the start codon. The sequences of the Fur and PchR boxes are given. In bold
812 are the nucleotides corresponding to the consensus sequence of the PchR box, as characterized by
813 Michel et al. 2005 (B) The Fur boxes have been aligned and compared to the *E. coli* Fur box
814 consensus sequence. The nucleotides corresponding to the consensus are highlighted in blue. (C)
815 Sequence of the two primers mimicking the *pchD* Fur box and used for the EMSA experiments. The
816 nucleotides corresponding to the consensus sequence are in blue.

817



818

819 **Figure S3. Detail on the genomic location of *pchR* and *pchD*.** The two genes are encoded in
820 opposite direction. Both promoters contain a Fur box, that overlaps. Thus, if the ternary complex
821 ferri-PCH-PchR binds this box, it could interfere with transcription of the *pchR* mRNA. This would
822 avoid any overexpression of PchR. TST stands for Transcription Start Site.



824

825 **Figure S4. Schematic representation of the *phoPphoQ* and PVD positive auto-regulation loops.**
 826 (A) The *phoPphoQ* system comprises two promoters, one constitutive and one inducible. When the
 827 constitutive promoter is strong, PhoP and PhoQ are synthesized efficiently, and the effect of the
 828 global contribution of the induction through PhP phosphorylation may be low. When the promoter is
 829 weak, this positive auto-regulation gains importance. (B) *pvdS* contains only one promoter, sensitive
 830 to Fur repression. When iron loads are low, PvdS is efficiently produced, resulting in high free PvdS
 831 in the cytoplasm. The global contribution of the PVD auto-induction loop is thus lowered. When iron
 832 loads are high, PvdS expression is lower, more bound to FpvR, and thus the positive auto-regulation
 833 gains importance. IM: inner membrane.



Chapter 2

Pyoverdine and pyochelin siderophores in the homeostasis of biological metals different than iron in *Pseudomonas aeruginosa*

Results

1. Effect of the biological metals on PVD and PCH production

To investigate the possible role of PVD and PCH, the two siderophores produced by *P. aeruginosa*, in the homeostasis of biological metals other than iron, we first focused on the effects of the metals on the production of both siderophores in highly iron-restricted conditions (Casamino acids -CAA- medium). According to ICP-AES measurements, this medium contains 21 nM of Fe, a really low concentration in comparison to LB Broth medium containing 4,3 μM (Cunrath et al., 2016). PAO1 was grown in CAA medium in the absence and presence of 1,5 μM , 15 μM and 150 μM of the different biological metals tested (Fe^{3+} , Co^{2+} , Ni^{2+} , Cu^{2+} , Mn^{2+} and Zn^{2+}). During the 24 h cultures, bacterial growth was monitored at $\text{OD}_{600 \text{ nm}}$ and PVD production at 400 nm (this siderophore has a typical absorbance at 400 nm at neutral pH with an ϵ_{PVD} of 19 000 $\text{L mol}^{-1} \text{ cm}^{-1}$). PCH has a characteristic absorbance at 320 nm, but unlike PVD, this siderophore cannot be detected directly in the bacterial growth medium ($\epsilon_{\text{PCH}} = 4300 \text{ L mol}^{-1} \text{ cm}^{-1}$). Therefore, PCH was extracted after 24 h cultures from the supernatant and concentrated (Cunrath et al., 2016) before monitoring the absorbance at 320 nm.

In our growth conditions and in the absence of any biological metal, PAO1 cells produced twice more PVD compared to PCH: $116,5 \pm 30,7 \mu\text{M}/\text{OD}_{600 \text{ nm}}$ and $51,7 \pm 3,1 \mu\text{M}/\text{OD}_{600 \text{ nm}}$ for PVD and PCH respectively (Fig. R1), as also previously described (Cunrath et al., 2016). In the presence of these biological metals, different effects were observed on siderophore production:

- Fe^{3+} , as expected and demonstrated in Chapter 1, repressed completely PVD production at 1 μM and PCH production at a higher concentration (15 μM) (Fig. R1A).
- Co^{2+} is the only other metal able to repress as Fe the production of both siderophores. 41,1 %, 48,5 % and 61,4 % repression of PVD production were observed with 1,5 μM , 15 μM and 150 μM Co^{2+} respectively (Fig. R1A). Concerning PCH production (Fig. R1B), Co^{2+} (at 1 μM) was even more efficient than Fe^{3+} in repressing the production of this siderophore: 76,7 % of repression for Co^{2+} while 63,7 % for Fe^{3+} .
- Ni^{2+} had no effect on PVD production and only affected PCH biosynthesis at 150 μM , repressing 42 % the production.
- Mn^{2+} and Zn^{2+} had no significant effect on both PVD and PCH production.
- At last, Cu^{2+} had no effect on PCH production but seemed to be able to induce slightly PVD production, 26,8%.

According to these results, PVD production is impacted by the presence of Fe^{3+} and at a lower extent by Co^{2+} , whereas PCH production is affected in an equivalent manner by Fe^{3+} and Co^{2+} , and at a lower level by the presence of Ni^{2+} .

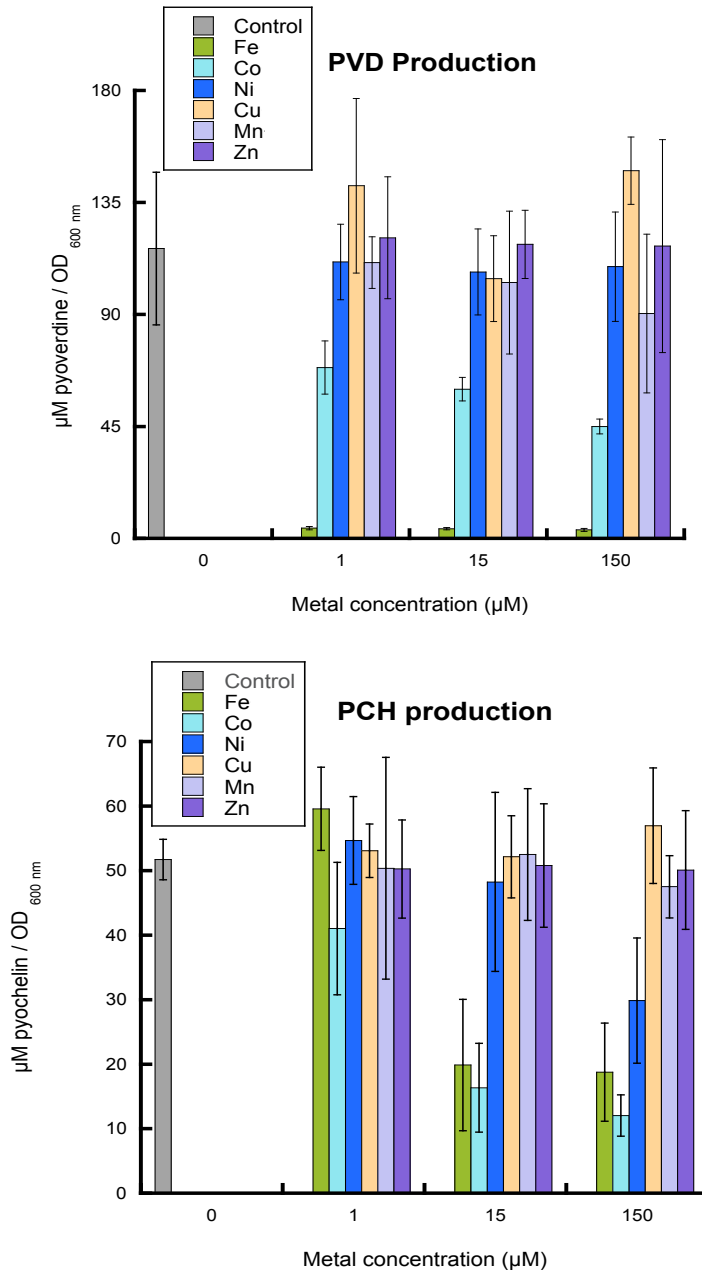


Figure R1. PVD (A) and PCH (B) production by *P. aeruginosa* PAO1. Bacteria were growing 24 h in CAA medium in the absence or presence of 1 µM, 15 µM and 150 µM of biological metals. No metal: grey; FeCl_3 : green; CoCl_2 : light blue; NiCl_2 : dark blue; CuCl_2 : yellow, MnCl_2 : light purple and ZnCl_2 : dark purple. The concentration of PVD and PCH ($\mu\text{M}/\text{OD}_{600\text{ nm}}$) was monitored after 24 h cultures and calculated as described in ‘Material and Method’.

2. Biological metals effect on the expression of proteins belonging to the PVD and PCH pathways

In order to further investigate how the different biological metals impact siderophore production, we followed the expression of different proteins of both PVD and PCH pathways during bacterial growth in the absence and presence of Fe^{3+} , Co^{2+} , Ni^{2+} , Cu^{2+} , Mn^{2+} and Zn^{2+} in iron restricted CAA medium. For this purpose, we used strains expressing fluorescent fusion proteins between mCherry and studied proteins. For the PVD pathway, a strain expressing fluorescent-tagged PvdJ, an enzyme involved in the biosynthesis of PVD (*pvdJ-mCherry*, Table S1) was used (Gasser et al., 2015). For the PCH pathway, we had available strains expressing fluorescent-tagged PchA, an enzyme involved in the biosynthesis of PCH (*pchA-mCherry*, Table S1), and also FptX, the inner membrane transporter of PCH-Fe (*fptX-mCherry*, Table S1) (Cunrath et al., 2014). All these proteins were tagged with mCherry at the N-terminal end, and the tag was introduced at the level of the chromosome. Moreover, for all these strains it has been shown by RT-qPCR that the presence of the tag does not affect the expression levels of the proteins and their biological activities (siderophore production or ferri-siderophore uptake). Bacterial growth, monitored at $\text{OD}_{600 \text{ nm}}$, and the expression of the fluorescent fusion proteins, following the fluorescence at 610 nm (with excitation at 570 nm) detecting the mCherry signal, were measured using a TECAN spectrophotometer plate reader. See also Fig. S1.

The data concerning the PVD pathway (Fig. R2) have been carried out by Olivier Cunrath during his thesis. Concerning the PCH pathway, the complete growth kinetics data for all conditions tested are presented in the Fig. S1. In this chapter are detailed the expression levels of the different proteins at 7 h (exponential phase) and 24 h (stationary phase) of culture in presence of the different metals.

For the PVD pathway (Fig. R2), only Fe^{3+} repressed significantly mCherry-PvdJ expression. Co^{2+} and Ni^{2+} repressed mCherry-PvdJ expression between 20-35 %. No significant effect was observed with any other metal tested. These results are in line with previous ones, that showed no or weak effect of these metals on PVD production (Fig. R1A), and also by previous publications (Braud et al., 2009; Visca et al., 1992).

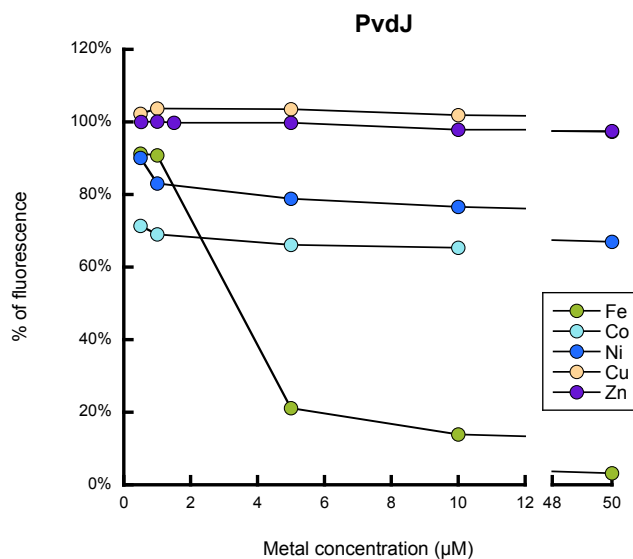


Figure R2. PvdJ expression in *pvdJ-mCherry* cells grown in CAA medium in the absence and presence of different biological metals. The metals were added at the beginning of growth, and the data represent the percentage of fluorescence between the culture in the presence (F_{metal}) of metals compared to the culture in the absence ($F_{\text{no-metal}}$) of metals after 24 h culture. Data in the presence of FeCl_3 : green; CoCl_2 : light blue; NiCl_2 : dark blue; ZnCl_2 : purple; CuCl_2 : yellow.

Concerning the proteins of the PCH pathway (Fig. R3), a clear and significant repression of both PchA-mCherry and FptX-mCherry fusion proteins were observed in presence of Fe^{3+} and Co^{2+} with a quite similar concentration dependency, except that the repression was total with Fe already at 7 h of culture and became total with Co^{2+} only at stationary phase (24 h culture). In addition, 60 % of repressions of FptX-mCherry and PchA-mCherry expressions were also observed with Ni^{2+} and Mn^{2+} at 24 h cultures (the effect were not significant at 7h, in the exponential phase). For the other metals, Cu and Zn^{2+} , no significant impact has been observed on the fluorescent-tagged PchA and FptX proteins. Repression effect of the different metals on PchA-mCherry and FptX-mCherry expression can be classified as followed: $\text{Fe}^{+3} \approx \text{Co}^{+2} > \text{Ni}^{+2} > \text{Mn}^{+2} \gg \text{Cu}^{+2} = \text{Zn}^{+2}$. It is also important to precise that the repression effects of Fe^{3+} , Co^{2+} , Ni^{2+} and Mn^{2+} are equivalent on the expression of both, proteins involved in PCH synthesis (PchA) and proteins involved in PCH- Fe^{3+} import (FptX).

In conclusion, the expression of the proteins belonging to the PCH pathway is more affected by the presence of biological metals (others than iron), than the expression of the proteins of the PVD

pathway. The metal having the highest effect is in addition to Fe^{3+} , Co^{2+} ; however Ni^{2+} and Mn^{2+} seem to affect as well this pathway at a lower extent.

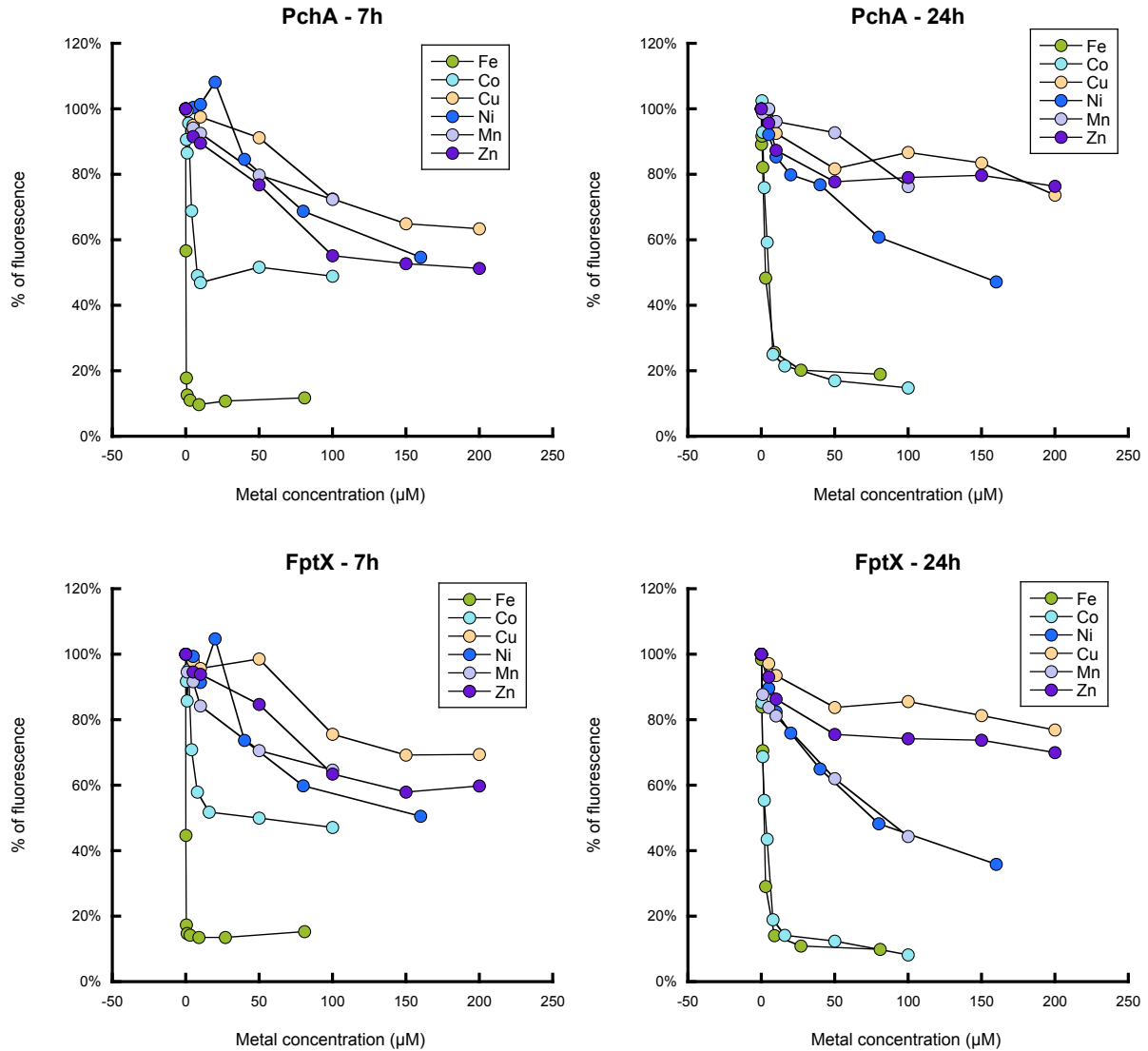


Figure R3. PchA and FptX expression in *pchA-mCherry* and *fptX-mCherry* cells at 7 and 24 h growth in CAA medium in the absence and presence of different biological metals. The metals were added at the beginning of growth, and the data represent the percentage of fluorescence between the culture in the presence (F_{metal}) of metals compared to the culture in the absence ($F_{\text{no-metal}}$) of metals after 24 h culture. Data in the presence of FeCl_3 : green; CoCl_2 : light blue; NiCl_2 : dark blue; CuCl_2 : yellow; Mn: light purple, and ZnCl_2 : dark purple.

3. Ability of different PCH- and PVD-metal complexes to be transported *via* the PCH uptake pathway or the PVD uptake pathway respectively

To better understand the biological link of Co^{2+} , Ni^{2+} and Mn^{2+} with the PCH pathway, we evaluated the ability of these metals and the other biological metals to be transported into *P. aeruginosa* cells in a PCH- or PVD-dependent way. Metal accumulation in the bacteria was followed using ICP-AES (Inductively Coupled Plasma Atomic Emission Spectroscopy), which allows the detection of metals at the trace amount levels. In order to control the nature of the siderophore and its concentration in the assay, the PVD and PCH-deficient strain ($\Delta pvdF\Delta pchA$, Table S1) was used. The importance of the PCH pathway is evaluated by the use of the *fptA* (PCH-Fe outer membrane transporter) mutant strain $\Delta pvdF\Delta pchA\Delta fptA$ (Table S1) and the importance of the PVD pathway by using the *fpvA* and *fpvB* (both PVD-Fe outer membrane transporter) mutant strain $\Delta pvdF\Delta pchA\Delta fpvA\Delta fpvB$ (Table S1). The siderophores were pre-incubated with the metals in the following concentrations: 4 μM of metal and 4 μM PVD (1:1) or 8 μM PCH (1:2); and the mixture was added to bacterial suspensions.

Concerning Fe^{3+} , if we compare the amount of this metal inside bacteria between the $\Delta pvdF\Delta pchA$ and $\Delta pvdF\Delta pchA\Delta fptA$ strains, it is possible to observe that 46,5% less $\text{PCH}_2\text{-Fe}$ was imported at 30 min of incubation, showing that $\text{PCH}_2\text{-Fe}$ is recognized and transported specifically by FptA (Fig. R4). We can also observe that the transport of this metal is more efficient when it is complexed to PCH ($\text{PCH}_2\text{-Fe}$) than in its free state (Fig. R6), reaffirming again the role of siderophores and the efficiency of PCH in iron acquisition in *P. aeruginosa*. However, Fe^{2+} accumulation into the cells in the presence and absence of PCH, also indicate that another pathway can take over the uptake of this metal in the absence of PCH and PVD production. Concerning Co^{2+} , we have observed that the uptake of $\text{PCH}_2\text{-Co}$ decreased in the $\Delta pvdF\Delta pchA\Delta fptA$ cells compared to $\Delta pvdF\Delta pchA$, indicating that like $\text{PCH}_2\text{-Fe}$, the outer membrane transporter FptA can transport $\text{PCH}_2\text{-Co}$. It has been shown previously that $\text{PCH}_2\text{-Co}$ was able to interact with FptA binding site with an affinity really close to the one of $\text{PCH}_2\text{-Fe}$, $K_i = 14,6$ nM and $K_i = 13,6$ nM respectively, (Braud et al., 2009a). This previous study also highlighted that Ni^{2+} , Mn^{2+} , Cu^{2+} and Zn^{2+} were able to interact as well with FptA binding site the bacterial cell surface but with lower affinities (Braud et al., 2009a). However, no PCH- dependent uptake has been observed for Ni^{2+} ,

Cu^{2+} and Zn^{2+} . For Cu^{2+} an accumulation has been observed but which is not linked to the expression of FptX.

It is also interesting to underline that PCH₂-Co transport is less efficient than the import of siderophore-free Co^{2+} in *P. aeruginosa* cells (Fig. R6). As well for Zn^{2+} , the presence of PCH reduces Zn^{2+} diffusion into *P. aeruginosa* cells, decreasing the intracellular accumulation of the metal. These data illustrate again that siderophores can also protect bacteria against the presence of toxic metals.

Concerning the uptake of these biological metals by the PVD pathway, no FpvA/FpvB dependent uptake or metal accumulation had been observed in *P. aeruginosa* cells except for PVD-Fe (Fig. R5), despite the ability of FpvA to bind with different affinities the different PVD-metal complexes (Braud et al., 2009b). Previous studies of our group have shown that the efflux system PvdRT-OpmQ controls the metal selectivity of the uptake for the PVD pathway. Any unwanted PVD-metal complex transported by FptA/PVD is excreted from the periplasm into the extracellular medium by the efflux system PvdRT-OpmQ, avoiding that way PVD-metal accumulation in *P. aeruginosa* cells other than PVD-Fe (Hannauer et al., 2012). Such an efflux system controlling the metal selectivity for metal uptake *via* PCH has not been identified and may not exist, which may explain that metals other than Fe (Co^{2+}) can accumulate in the bacterial cells via the PCH pathway.

In conclusion, only Co^{2+} could be transported and accumulated in *P. aeruginosa* cells in a PCH/FptA dependent way. No biological metal accumulation could be observed via the PVD pathway, probably because in this pathway the efflux pump PvdRT-OpmQ controls the metal selectivity of the transport in this pathway (Hannauer et al., 2012).

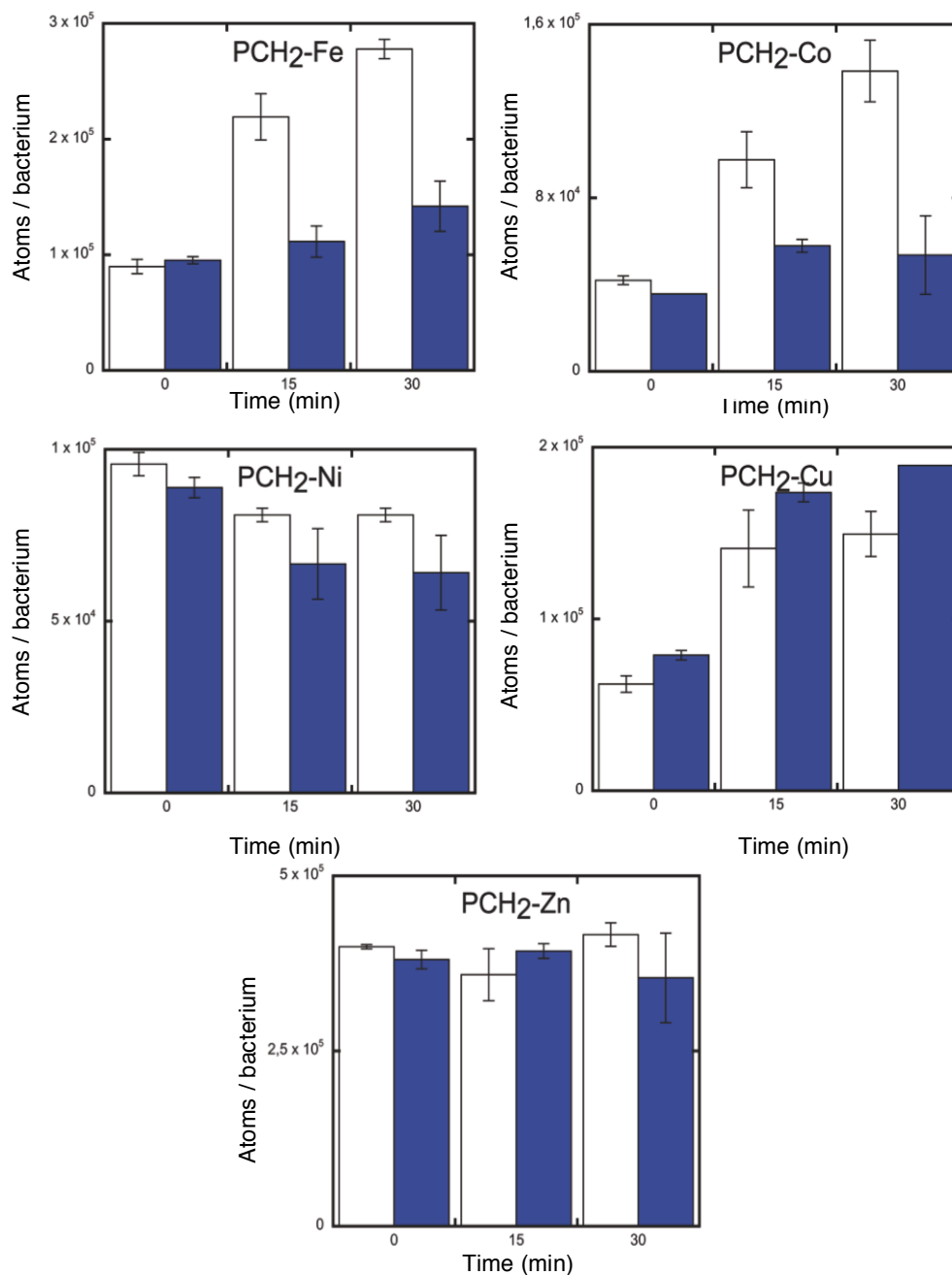


Figure R4. Transport of metals Fe, Co, Ni, Cu and Zn in complex with PCH in *P. aeruginosa* cells. $\Delta pvdF\Delta pchA$ and $\Delta pvdF\Delta pchA\Delta fptA$ strain at an $OD_{600\text{ nm}}$ of 1 in CAA medium have been incubated in the presence of PCH-metal complexes at a concentration of 8 μM PCH and 4 μM of metal. After incubation, bacteria have been pelleted, washed and the amount of metal monitored by ICP-AES.

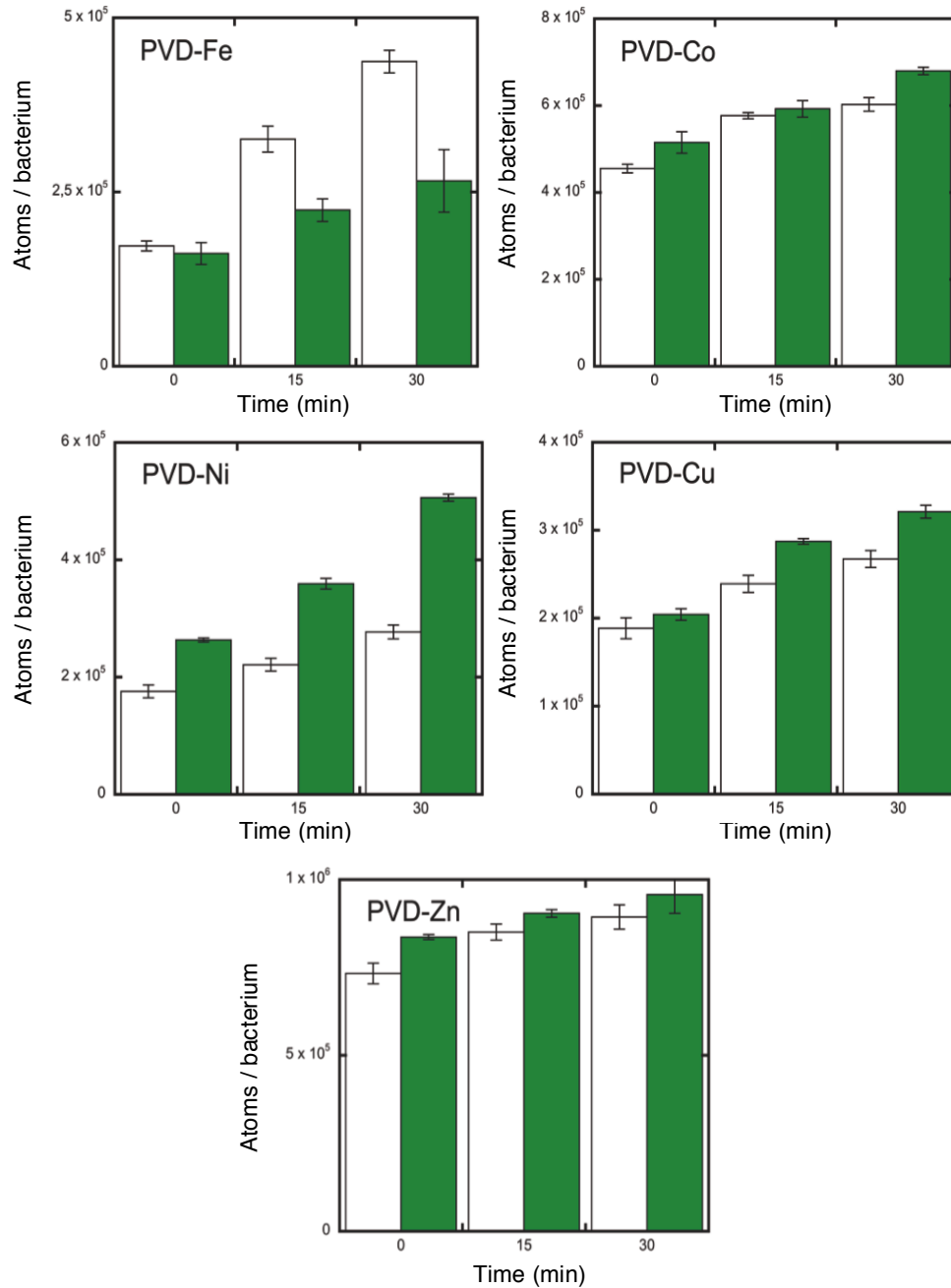


Figure R5. Transport of metals Fe, Co, Ni, Cu and Zn in complex with PVD in *P. aeruginosa* cells. $\Delta pvdF\Delta pchA$ and $\Delta pvdF\Delta pchA\Delta pvnA\Delta pvnB$ strains at an $OD_{600\text{ nm}}$ of 1 in CAA have been incubated in the presence of PVD-metal complexes at a concentration of 4 μM PVD and 4 μM of metal. After incubation, bacteria have been pellet, washed and the amount of metal monitored by ICP-AES.

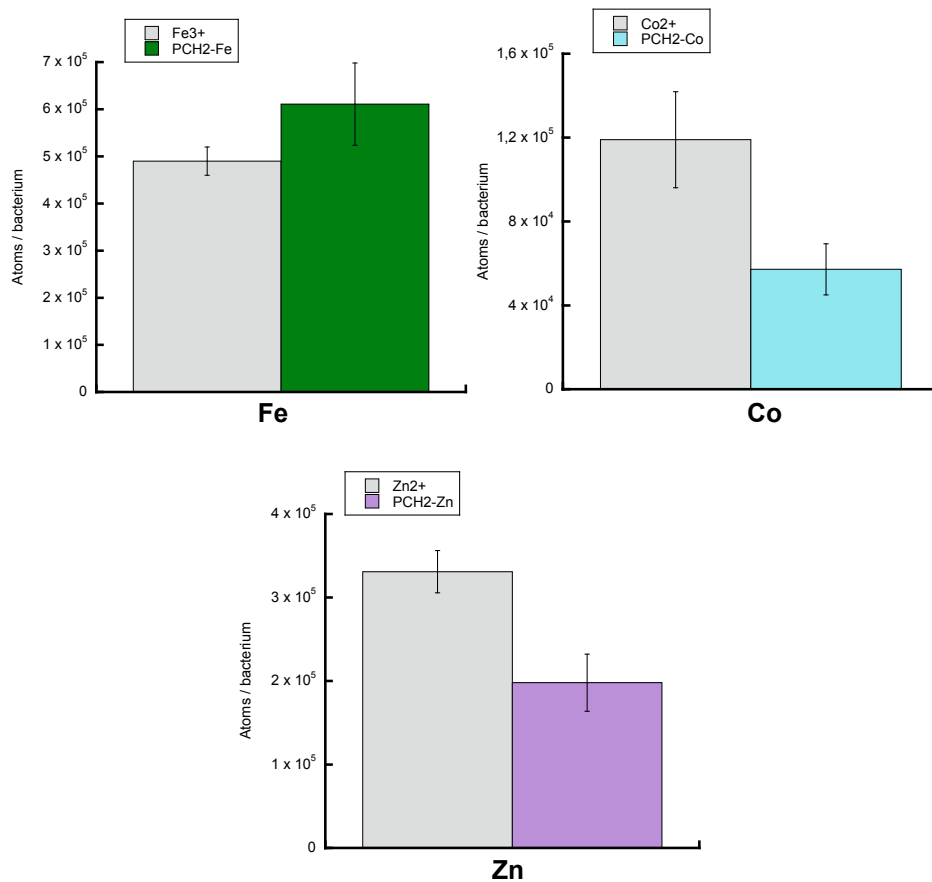


Figure R6. Metal transport of Fe, Co and Zn in free state and in complex with PCH in *P. aeruginosa* cells. Concentration of metal (mg/kg = ppm) transported inside *P. aeruginosa* $\Delta pvdF\Delta pchA$ (non-producing siderophores), in presence of 4 μ M of metal cation or 4 μ M of PCH₂-metal after 30 min of incubation at initial OD₆₀₀ = 1.5. Measures by ICP-AES.

4. PCH₂-Co enters in competition with PCH₂-Fe uptake

We have tested the ability of PCH₂-metal and PVD-metal complexes to inhibit the uptake of PCH₂-⁵⁵Fe and PVD-⁵⁵Fe respectively. In order to control the nature of the siderophore and its concentration in the assay, the PVD and PCH-deficient strain ($\Delta pvdF\Delta pchA$) was again used. The strain was incubated in the presence of 0,2 μ M PCH-⁵⁵Fe or PVD-Fe and in the absence or presence of 0,2 μ M and 2 μ M (10-fold excess) of PCH₂-metal or PVD-metal complexes. At different times of incubations, aliquots were removed, bacteria separated from the growth medium and the radioactivity incorporated into the bacteria (⁵⁵Fe transported) was counted. The metals chosen in this experiment were Co²⁺ and Ni²⁺, which have a strong effect on PCH genes expression, and Zn, a metal with no effect on PCH genes expression. To evaluate the uptake linked to the PCH pathway from any other uptake, we used the *fptA* deleted strain $\Delta pvdF\Delta pchA\Delta fptA$ and the $\Delta pvdF\Delta pchA$ strain treated with CCCP (carbonyl cyanide-m-chlorophenylhydrazone), an inhibitor of the proton motive force of bacterial cells, inhibiting any TonB-dependent transport. Having no *fpvA* and *fpvB* deleted strain, we only used for the assays with PVD a control with $\Delta pvdF\Delta pchA$ bacteria treated with CCCP.

When bacteria were incubated in the presence of PCH₂-⁵⁵Fe alone, an uptake of 99 pmol of ⁵⁵Fe per cell per minutes was observed. A 70 % inhibition of this uptake was observed when a 10-fold excess of PCH₂-Co was added to the solution (Fig. R7). The competition assay with PCH₂-Zn or PCH₂-Ni complexes gave rise to less than 10% of inhibition of ⁵⁵Fe uptake *via* PCH.

For the uptake assays carried out in the presence of PVD-⁵⁵Fe, very similar results were observed as for the assays with PCH-⁵⁵Fe. ⁵⁵Fe accumulation in the absence of any other metal reached a value of 93 pmol of ⁵⁵Fe transported per min and per bacteria. Accumulation of ⁵⁵Fe decreased to 50 % in the presence of 10-fold excess of PVD-Co compared to the experiment with PVD-⁵⁵Fe alone. No significant inhibition was observed when the experiment was carried out in the presence of PVD-Ni or PVD-Zn complexes.

In conclusion, only PVD-Co and PCH₂-Co complexes were able to compete with PVD-Fe and PCH₂-Fe complexes respectively during iron acquisition, decreasing their transport and accumulation into the cells.

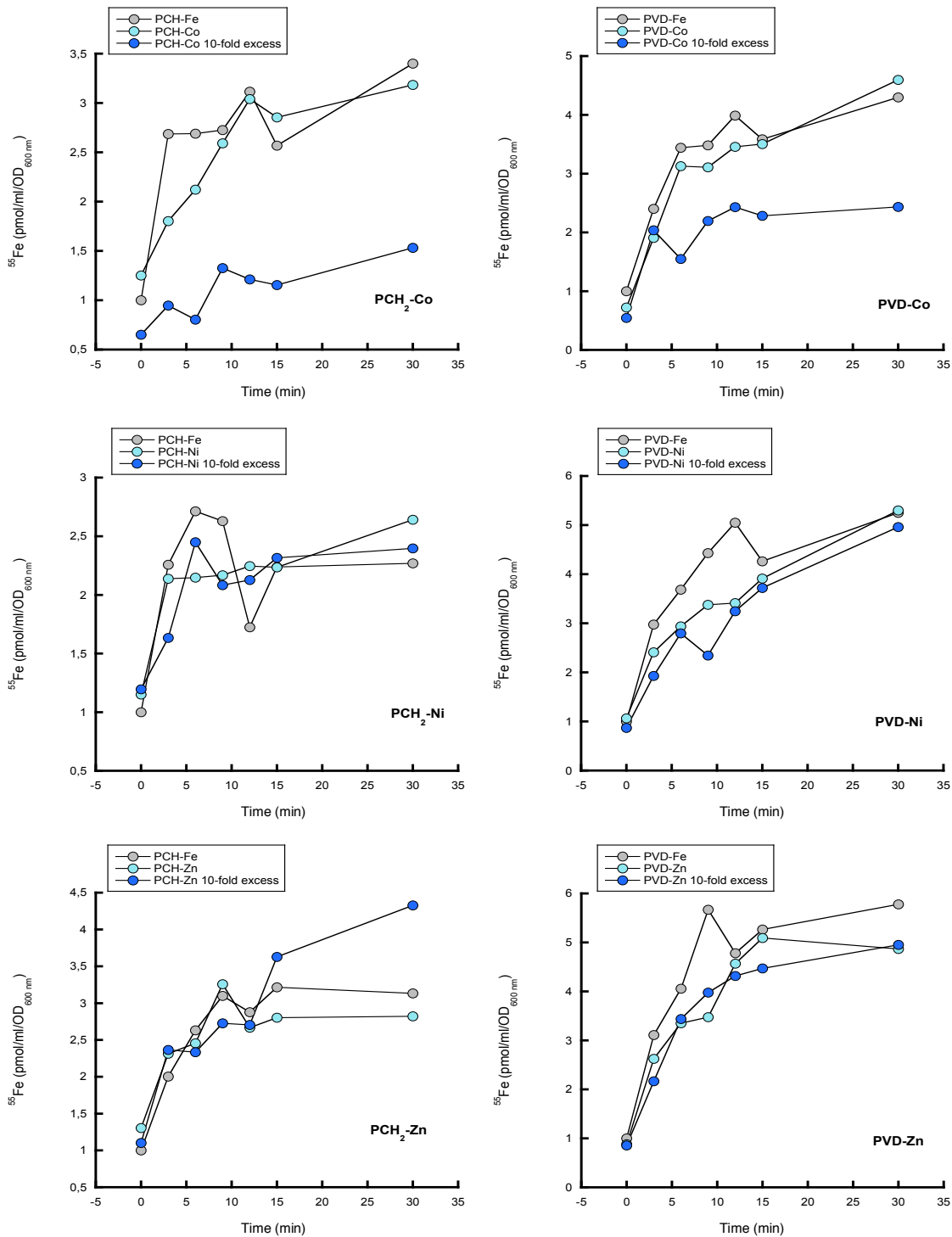


Figure R7. Kinetic of intracellular ⁵⁵Fe accumulation in *P. aeruginosa* cells in the presence of PCH₂-metal or PVD-metal complexes. $\Delta pvdF\Delta pchA$ cells at an OD_{600 nm} = 1 were incubated in the presence of 0,2 μ M PCH-⁵⁵Fe or PVD-⁵⁵Fe and in the absence or presence of 0,2 μ M and 2 μ M (10-fold excess) PCH-metal or PVD-metal complexes respectively. At different times (3 min, 6 min, 9 min, 12 min, 15 min and 30 min) aliquots were removed and the radioactivity in the cells monitored. The values were normalized using the ppm of fluorescence obtained in the PCH₂-⁵⁵Fe or PVD-⁵⁵Fe transport with no other complex. Grey: siderophore-Fe; light blue: 1-fold siderophore-metal; dark blue: 10-fold siderophore-metal.

5. Interaction between the transcriptional regulator PchR and different ligands: biological metals, apo-PCH and PCH₂-metal complexes

Since the presence of Co²⁺, Ni²⁺ and Mn²⁺ in the culture media of *P. aeruginosa* had a sensible effect on the PCH pathway, we investigated further the way biological metals can affect the expression of the enzymes involved in the biosynthesis of PCH and consequently the production of this siderophore. Binding assays between purified PchR, the transcriptional regulator responsible of PCH genes expression, and the different PCH-metal complexes were carried out. These binding assays were based on a spectroscopy approach using the fluorescent properties of the tryptophans (Trp) of PchR. For this purpose, the laboratory of C. Reimann in Lausanne provided us with an *E. coli* strain (*DH5α-pME7180*) overproducing MBP fused PchR (Table S1). The protein was first purified on the amylose resin column ‘MBPTrap HP’ (Fig. R8), followed by an anion exchange chromatography on a ‘Mono QTM 5/50 GL’ column (Fig. R9). See ‘Material and methods’ for details.

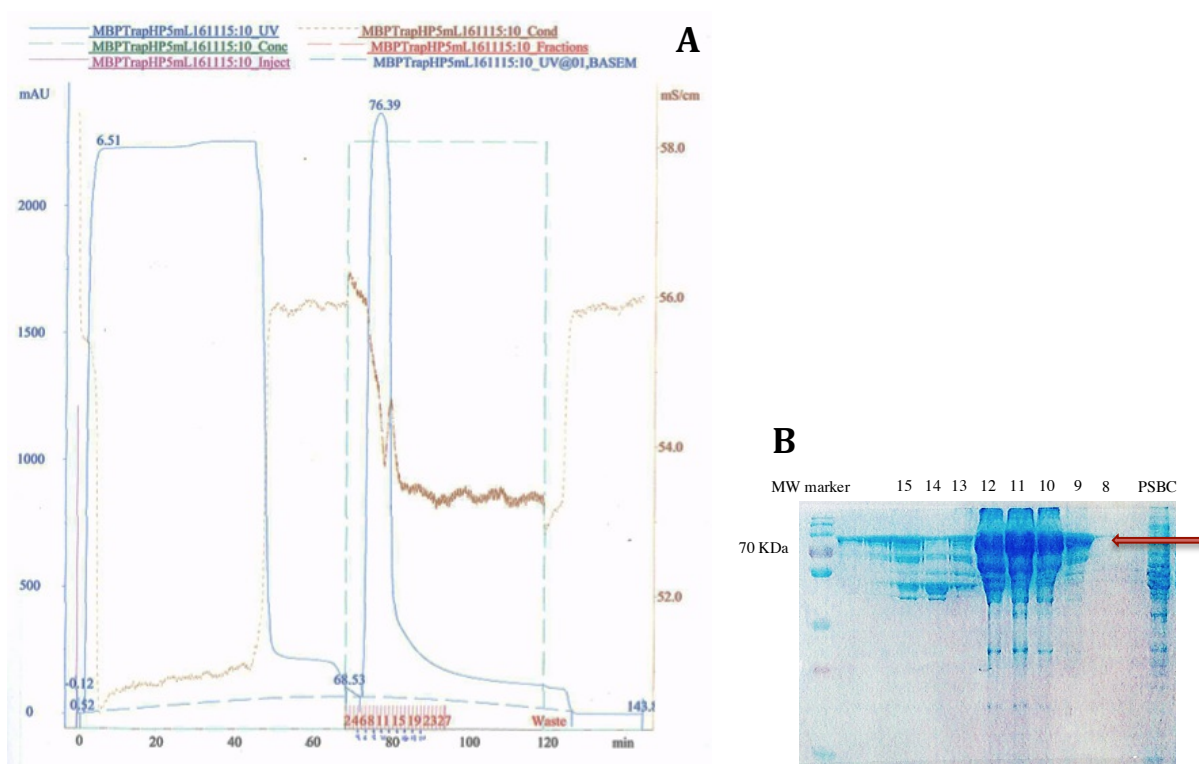


Figure R8. A: Affinity chromatogram profile of the MBP-PchR purified using the ‘MBP-Trap HP 5ml’ column in the ÄKTA System. MBP-PchR was eluted after the addition of maltose by competition. B: SDS-PAGE revealing with coomassie blue the protein content in the fractions (8-17), where the overproduced MBP-PchR (75 KDa) was eluted. PSBC: protein solution before chromatography.

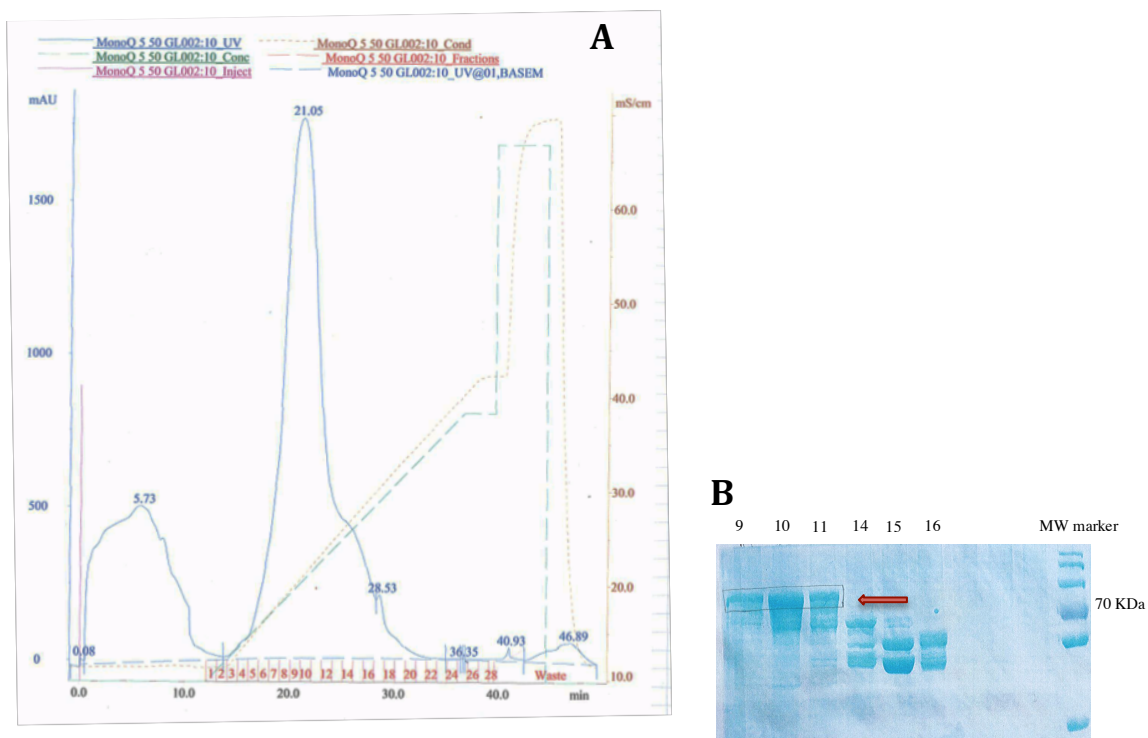


Figure R9. A: Ionic exchange chromatogram of MBP-PchR purified using the ‘Mono Q™ 5/50 GL’ column in the ÄKTA System. MBP-PchR was eluted by NaCl₂ gradient. **B: SDS-PAGE** revealing with coomassie blue the protein content in several elution fractions, where the purified MBP-PchR (75 KDa) was present in the elutions 9-11, and separated from other proteins. This chromatography in addition to the previous affinity chromatography, allowed to increase the purity of MBP-PchR.

When MBP-PchR is excited at 280 nm, the tryptophans present in the protein emit intrinsic fluorescence with a maximal intensity at 340 nm. Upon addition of ligand, fluorescence is quenched (Li et al. 2013) (Fig R10). Taking advantage of this quenching, the affinity of the protein for its natural ligand can be determined by plotting the relative fluorescence intensity, F_0/F , against the concentration of ligands (Fig. R11 and R12), being F_0 the fluorescence emitted by MBP-PchR without ligand, and F the fluorescence emitted by MBP-PchR once a specific concentration of ligand was added. Afterwards the K_d values determined using the Stern-Volmer representation and a linear regression from which a K_d value can be calculated. The ligands tested were different concentrations of siderophore-free metals (Fe^{+3} , Co^{+2} , Ni^{+2} , Cu^{+2} and Zn^{+2}), apo-PCH, and PCH-metal complexes (PCH-Fe, PCH-Co, PCH-Ni, PCH-Cu and PCH-Zn). See Material and Methods.

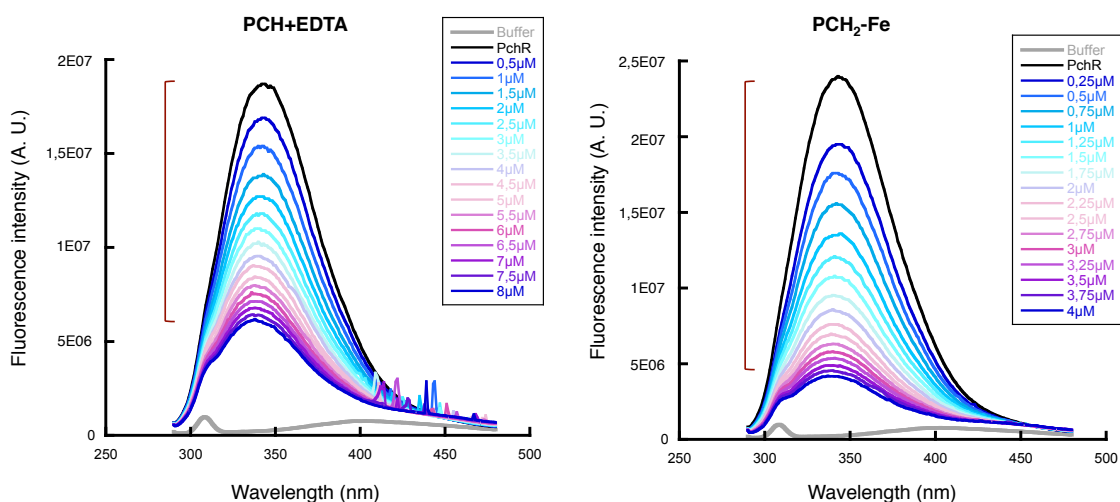


Figure R10. Fluorescence emission spectra of MBP-PchR in the presence of different concentrations of apo-PCH (A), and PCH₂-Fe (B). 10 μM of purified MBP-PchR was incubated with 10 mM DTT at 25°C for 10 min, and the fluorescence emission spectrum was monitored at 340 nm with an excitation at 290 nm (excitation wavelength of the tryptophans) (black line). Increasing concentrations of apo-PCH in solution with EDTA (1:1 ratio) or PCH-Fe were added to the MBP-PchR solution and the fluorescence spectra was monitored (coloured spectra). For the experiment with apo-PCH, EDTA was added to the siderophore to avoid the formation of PCH-metal complexes with any trace metal present in the solution. In grey is represented the emission fluorescence spectra of the buffer without the protein. The same experiments have been carried out with all the biological metals alone and with the different PCH-metal complexes (data not shown).

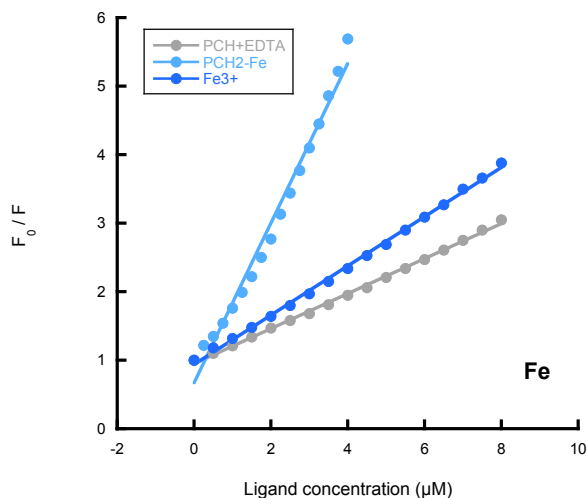


Figure R11. Stern-Volmer plot for apo-PCH, Fe and PCH₂-Fe binding to purified MBP-PchR protein. Relative fluorescence intensity of MBP-PchR (F_0/F), being F_0 the initial MBP-PchR emission fluorescence at 340 nm, and F , the fluorescence emitted after the addition of the ligand, represented in function of the concentration of each ligand. Dark blue represents the PCH₂-Fe values, light blue the Fe values, and grey the PCH + EDTA values.

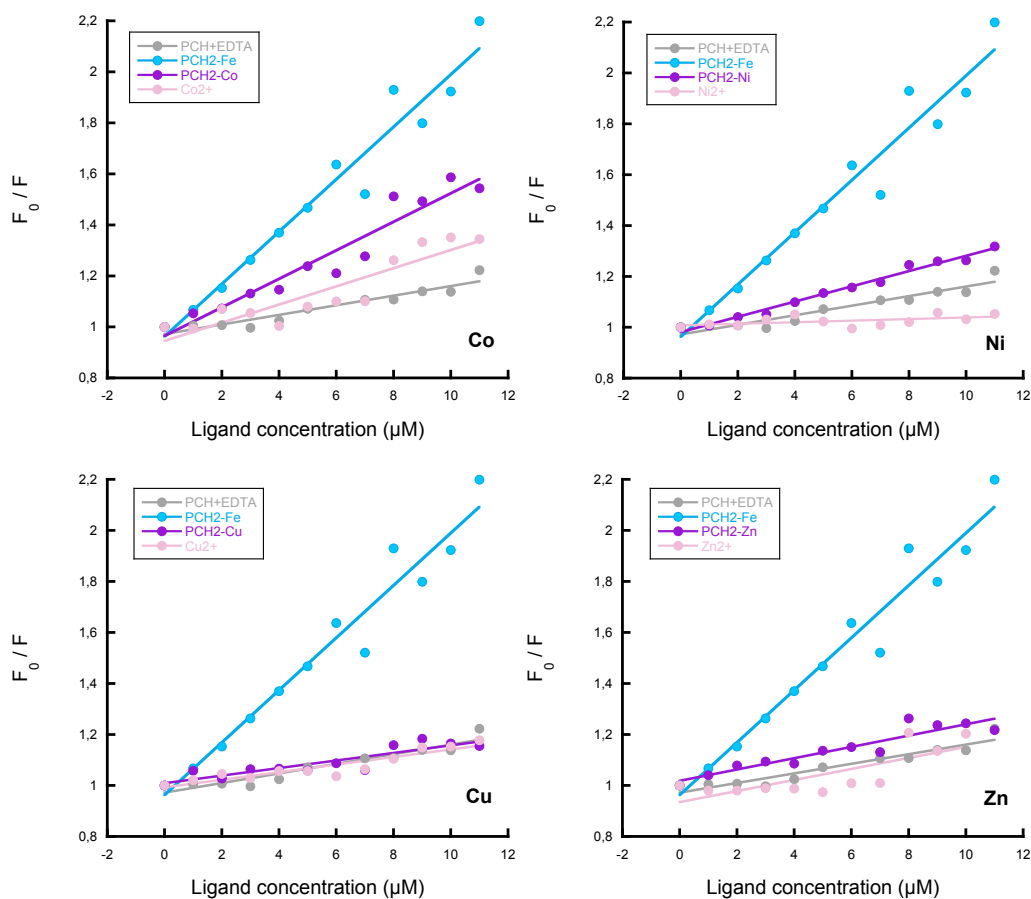


Figure R12. Stern-Volmer plot for apo-PCH, PCH₂-Fe and the different metals and PCH₂-metals tested binding affinities determination of MBP-PchR protein. Relative fluorescence intensity of MBP-PchR (F_0/F), being F_0 the initial MBP-PchR emission fluorescence at 340 nm, and F , the fluorescence emitted after the addition of the ligand, represented in function of the concentration of each ligand. The different colours represent the values obtained for PCH₂-Fe (blue), apo-PCH (grey), the different PCH₂-metal complexes (purple), and the biological metals (pink).

With this approach we were able to determine an affinity of PCH₂-Fe ($K_d = 5,82 \pm 2,84 \mu\text{M}$) for MBP-PchR (Table R1) stronger than the one described previously $K_d \text{PCH}_2\text{-Fe} = 41 \pm 5 \mu\text{M}$ (Lin et al., 2013). Surprisingly, in our experimental conditions, we were also able to visualize an affinity of apo-PCH for PchR ($K_d = 31,01 \pm 3,06 \mu\text{M}$), which is in contradiction with the data published by the group of C. Reimann (Lin et al., 2013). Indeed, this group has observed no binding between apo PCH and PchR. In our experimental approach, apo-PCH was in solution with 1 equivalent of EDTA to avoid any binding between PCH and any iron of biological metal ion present in the solution. Therefore, the binding we observed must be due to an interaction between PchR and apo PCH and not with any PCH-metal complex. Furthermore, PCH₂-Co as well was able to bind to

PchR, but with a 3-fold lower affinity compared to PCH₂-Fe and a better affinity than apo PCH (Table R1). Co²⁺ alone was also able to bind PchR with a similar affinity than PCH₂-Co. Fe, without siderophore, binds also to MBP-PchR but with clearly a lower affinity than PCH₂-Fe. Considering the K_d values and the corresponding standard deviation, Ni²⁺, Zn²⁺ or Cu²⁺ alone were unable to bind to MBP-PchR, however, the different PCH₂-Cu, PCH₂-Zn complexes were also able to bind to MBP-PchR but with a affinities much lower than PCH₂-Fe and PCH₂-Co complexes.

In conclusion, ligands recognized by the non-conserved N-terminal domain of PchR can be classified as followed in regard to their affinity for MBP-PchR: PCH₂-Fe > PCH₂-Co > Co⁺² > Fe⁺³ > PCH >> PCH-Ni, PCH-Zn, PCH-Cu. All these results suggest that PCH₂-Co can bind and potentially activates PchR. In conditions of high Co concentrations, this interaction may become effective, promoting changes on the expression of the genes regulated by PchR.

	K _d (μM)	Standard deviation
apo-PCH	31,01	3,06
PCH ₂ -Fe	5,82	2,84
Fe ⁺³	28,87	8,87
PCH ₂ -Co	13,95	3,37
Co ²⁺	16,07	9,25
PCH ₂ -Ni	42,00	35,49
Ni ²⁺	118,94	172,68
PCH ₂ -Cu	77,00	9,50
Cu ²⁺	161,55	94,05
PCH ₂ -Zn	47,40	2,20
Zn ²⁺	240,00	217,00

Table R1. Binding constants (K_d) and standard deviation of the apo-PCH (PCH+EDTA at 1:1 relation), different biological metals and the PCH-metal complexes for MBP-PchR. Values determined from the data presented in Figures R11 and R12. See Material and methods for the K_d calculations.

6. Role of PchR and Fur in the repression of the PCH pathway in presence of Co

To go further in the understanding of the mechanism of PCH pathway regulation by Co^{2+} via PchR, we have constructed expression plasmids carrying mCherry sequence and the promoter of the *pchDCBA* operon responsible of the PCH biosynthesis, containing the PchR box and the Fur box, or just the Fur box (Table R2). The strains carrying these constructions were grown in CAA medium supplemented or not with 0,5 and 5 μM of Co^{2+} or Fe^{3+} . mCherry signal was monitored at 610 nm (excitation at 570 nm).

In CAA medium without addition of Fe^{3+} or Co^{2+} , an increase of fluorescence corresponding to mCherry expression was observed only when both boxes, Fur box and PchR box, were present in front of mCherry gene. mCherry expression was completely repressed in restricted iron and cobalt conditions when only the Fur box was present, consequently we can conclude that the presence of the PchR box makes possible mCherry expression (Fig. R13). These results are congruent with the transcriptomic and proteomic analysis showing no expression of the genes of the PCH pathway in the $\Delta pchR$ strain (*pchR* deletion) (Table R3). According to what is known from the literature concerning the role of PchR, in Fe-restricted medium, probably trace amounts of Fe are scavenged by PCH produced by the bacteria and the formed PCH-Fe complex interacts with PchR in the bacterial cytoplasm activating the transcription of mCherry.

In the presence of increasing concentrations of Fe^{3+} , when both boxes were present on the plasmid, a decrease of fluorescence corresponding to a decrease in the expression levels of mCherry was observed, being consistent with the literature: in the bacteria that have acquired enough iron, the PCH pathway as well as mCherry expression is repressed. This repression is certainly due to Fur-Fe complexes interacting with the promoter region. Consistent with this conclusion, in the strains carrying the plasmid with just de Fur box, a slight repression of mCherry expression was observed in presence of Fe^{3+} , confirming that Fe has an effect on the Fur activity (Fig. R13D).

In the presence of increasing concentrations of Co^{2+} , a decrease of the expression levels of mCherry is also observed but with a lower efficiency compared to the presence of Fe^{3+} : higher concentrations of Co^{2+} are necessary to have an effect equivalent to the one observed with Fe^{3+} . Two scenarios may explain this observation. Either Co^{2+} is able like Fe^{2+} to interact in the bacterial cytoplasm with Fur and the formed Fur-Co complex binds to the Fur boxes to represses the expression of the genes regulated by Fur. However, Fig R13C shows no decrease of fluorescence in the presence of increasing concentrations of Co^{2+} as observed for Fe^{3+} , suggesting that Fur-Co is

not able to regulate mCherry expression in our assay. The other possibility is that the increasing concentration of PCH₂-Co complexes in the bacterial cytoplasm has as a consequence an increase of PchR-PCH-Co complexes at the expense of PchR-PCH-Fe complexes, the only one able to activate the transcription of the PCH pathway genes.

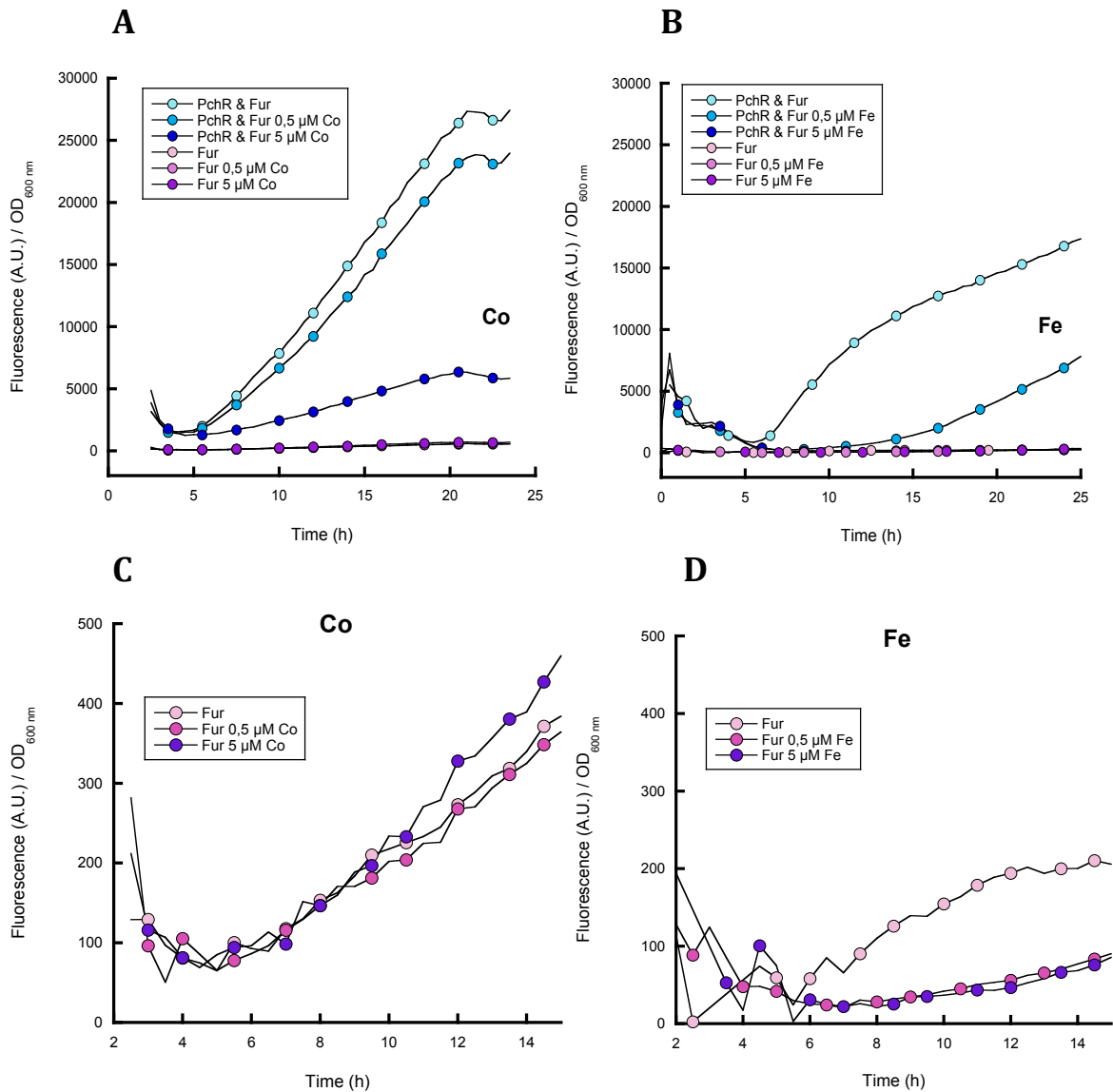


Figure R13. Expression of mCherry in the presence of Fe (panel B and D) or Co (panel A and C) under the effect of different *pchD* promoter sequences carrying the Fur box and PchR box (blue), or just the Fur box (pink), in the pSEVA631 plasmid. PAO1 wt cells containing these plasmids were incubated without metal (lightest blue and pink), in presence of 0,5 μM of Co or Fe (darker blue and pink), and in presence of 5 μM of Co or Fe (darkest blue and pink). The fluorescence was followed at 610 nm with an excitation at 570 nm to follow mCherry expression. Panels C and D are zoom of panels A and B respectively.

Gene	Promoter boxes	Promoter sequence	Genome location	Plasmid collection
<i>pchD</i>	PchR box, Fur box	5'GACAAAGCGCCCTGCACTCCGCCCTG CAGCGAATG AAAAAGC CCCGAATCGAA AGGCGGGCTTGC GGGT CCCTGCCGCCCGCCAA TGATAATAAATCTCA TTTCCCAACAATGG CAATCGACCGCATCCACGGAGATCGCATG 3'	4742278 – 4742426 [+]	pAYC5
	Fur box	5'GCCGCCCGCCAA TGATAATAAATCTCA TTTCCCAACAATGGCA ATCGACCGCATCCACGGAGATCGCATG 3'	4742356 – 4742426 [+]	pAYC6

Table R2. *pchD* promoter sequences introduced into pSEVA631 for the construction of expression plasmids carrying mCherry. See ‘Material and methods’. Purple sequences correspond to the PchR box, and blue sequences to the Fur box. The genome location in PAO1 is according to pseudomonasaeruginosa.com.

PCH Operon Promoters

fptA ATTT**CTTCAT****AA****TGATAAG****CAT****TAT****CAAA****TC**--**GTATA****TCCCCC****GAGGCT****G****TCGA****AC****GATG**
pchEFG TAAG**GT****TCGC****ATT****TGATAA****TCG****TTG****CCAGGAA****CTGG****CA****CCGACCT****CAGAT****GCTT****GCC****CTAGGG****GAGCCCC****CATG**
pchDCBA GCC**GCCCG****CCAA****TGATAA****TAAAT****CT****CATT****TCCCA****CA****AT****TGGCA****ATCG****ACC****G****CAT****CCA****CGG****GAGAT****CGCATG**
Consensus cgtcgc.aa**TGATAA**tcatT.tCA..tcc.g.caAtcgccctcggtGcttgcaCg

Complementary: ACTATTAg**TAA****AGT** (7-1-7) Palindromic Sequence

Consensus Fur box: TGATAATCATTATCA (15bp, 40-60bp upstream of operon start codon)

Figure R14. PCH promoters alignment and identification of conserved sequences belong to the Fur box. The nucleotides under dark blue were conserved in all the sequences, whereas in light blue, only in two of the three sequences aligned.

PCH Operon Promoters

fptA **CGAC****CG****GT****CG****TG****GAT****CG****AT****AG****AG****AG****CCG****CA****AT****CG****AAA****AAG****CCCG****G****AG****AC****CG****ATT****CT****TCA****TAA****T**
pchEFG **GGAT****G****AC****CG****CT****GC****AT****CT****A****CG****AA****C****AG****T****CC****GG****CT****G****T****C****T****AA****AG****CA****T****T****CC****CG****CC****AG****GC****CT****CC****AG****CA****AG****T****G****A****T****A****AG****T****CG****C****A****T****T**
pchDCBA **CT****CC****CG****CC****CG****CT****CG****AT****GA****AT****G****AA****AG****CC****CG****CA****AT****CG****AAA****G****CG****CG****GG****CT****T****GC****CG****GG****TC****CT****G****CC****G****CC****CG****CC****CA****T**
Consensus acG.cccTgCAtC.Aa.**GAA**AaAG.CCgGCaa**TGAAA**g...cgcgg

Consensus PchR box: TGCATCNAANGAAAAAGNCCGGCAATCGAAA (27-47bp upstream of Fur box).

Figure R15. PCH promoters alignment and identification of conserved sequences belong to the PchR box. The nucleotides under dark purple were conserved in all the sequences, whereas in purple, only in two of the three sequences aligned.

It is published that Fur can bind DNA sequences containing a Fur box by interacting with other metals than Fe (Ochsner et al., 1995). Thus to confirm if *P. aeruginosa* Fur-Co complex is able to bind or not the *pchD* promoter containing the Fur box, experiments of EMSA (electrophoretic mobility shift assay) were performed with the collaboration of the laboratory of Dr Isabelle

Michaud-Soret (CEA, Grenoble). This group is able to overexpress and purify Fur protein of *P. aeruginosa* (Adrait et al., 1999).

EMSA experiments show that Fur-Co can bind to the *pchD* promoter sequence (Fig. R16A & 16B), and it seems that this protein can form two different complexes, suggesting that Fur-Co binds in two different locations: to the two overlapped Fur box proposed to be on this operon, one affecting the *pchD* expression and the other, the *pchR*, or may be also to the PchR box (the PchR boxes having some characteristics of the Fur box). EMSA was also performed using the *pvdS* promoter belong to the PVD pathway (Fig. R16C), which contains only one Fur box, and two complexes with Fur were also obtained. Therefore, this different DNA binding complexes using the *pvdS* promoter as the *pchD* promoter may be by the Fur dimer or tetramer recognition. The EMSA experiments highly suggest that Fur-Co can regulate the expression of the PCH pathway, but it cannot be totally confirmed, since the Fig R13C and R13D show different effects on mCherry expression for Co and Fe. Further studies will be necessary to clearly understand how Co^{2+} regulates the expression of the PCH pathway.

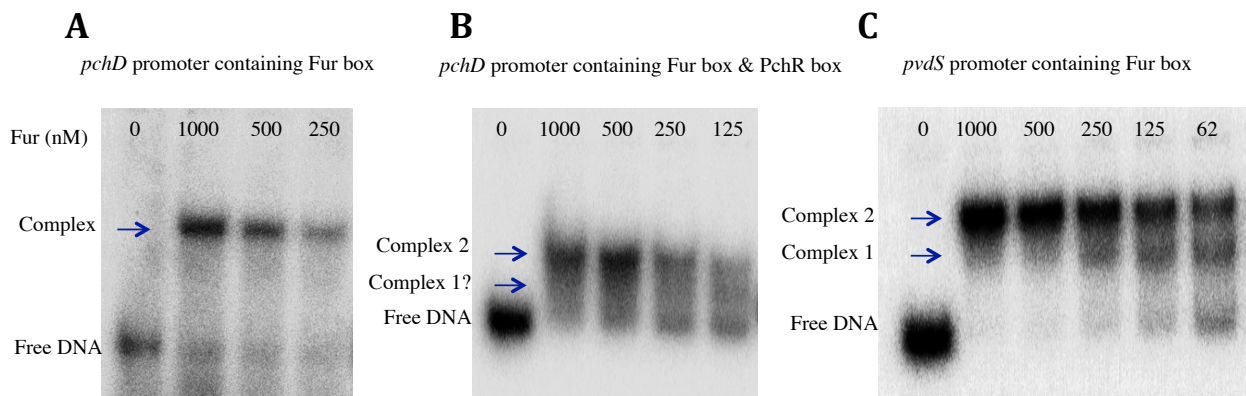


Figure R16. EMSA results of recognition between Fur-Co and specific DNA fragment, containing the Fur box of the *pchD* promoter (A), or containing the Fur box and the PchR of the *pchD* promoter (B). The specific DNA fragments used are represented in the Table R2.

We have also tried to carry out EMSA experiments between the purified MBP-PchR protein and the *pchD* promoter containing the PchR box, but without success. We cannot exclude that the MBP tag may be a problem for the interaction between PchR with its PchR box. The experiments need to be repeated with a PchR protein having no tag.

7. The effect of biological metals on *pchR* expression

PchR expression is regulated by Fur-Fe: when bacteria have acquired sufficient amounts of Fe^{2+} , the expression of *pchR*, as well as of all other genes of PCH regulons, is repressed by the Fur-Fe complex. To further understand how Co^{2+} interferes with the PCH pathway expression, we also investigated the effect of this metal on PchR expression. For this purpose, we used a *P. aeruginosa* strain (*mCherry-pchR*, Table S1) expressing a mCherry-tagged PchR protein. The tag has been introduced at the chromosomal level, at the C-terminal end of PchR (Cunrath et al., 2014), and qRT-PCR controls showed that the presence of this tag had no effect on the expression levels of the regulator. The *mCherry-pchR* strain was grown in CAA medium in the presence of increasing concentrations of Fe^{3+} or Co^{2+} . The other biological metals (Ni^{2+} , Cu^{2+} , Mn^{2+} , and Zn^{2+}) were also tested in this assay to evaluate their possible effect. mCherry-PchR expression was followed by monitoring the emission of fluorescence of mCherry at 610 nm (excitation 570 nm) during bacterial growth.

The results in the Figure R17 represent mCherry-PchR expression at 12 h of growth, during the exponential phase. Fe^{3+} is the only metal that repressed significantly the expression of the transcriptional regulator PchR. Co^{2+} , Ni^{2+} , Cu^{2+} , Mn^{2+} and Zn^{2+} induce it slightly, 35% by Zn^{2+} and 40% by Co^{2+} at the concentrations that caused repression effects on the expression of the genes of the biosynthesis of PCH (PchA) and transport (FptX) (16 μM of Co^{2+} , and 200 μM of Zn^{2+}). Ni^{2+} , Cu^{2+} , and Mn^{2+} induced less the *pchR* expression (30 % induction). In all cases the level of fluorescence (after 15 h) increased progressively and did not reach in the saturation phase (Fig. S2). It is a different pattern comparing to the expression of PchA and FptX in presence of the different biological metals (Fig. S1).

In our experimental conditions, Co^{2+} had no effect on PchR expression, suggesting that the Fur-Co complex is unable to interact with the fur box of *pchR* gene.

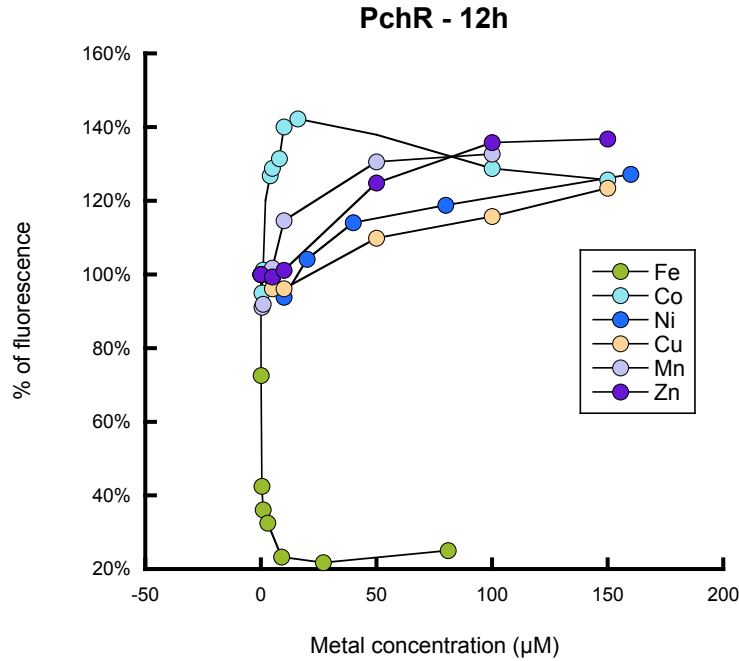


Figure R17. PchR-mCherry expression at 12 h of growth in CAA medium, in the absence and presence of biological metals. The data represented here are the percentage of fluorescence calculated from the ratio between the fluorescence in the culture in the absence ($F_{\text{no-metal}}$) and presence (F_{metal}) of metals ($F_{\text{no-metal}}/F_{\text{metal}}$), establishing at 100 % the values of expression in metal absence. FeCl_3 : green; CoCl_2 : light blue; NiCl_2 : dark blue; CuCl_2 : yellow; Mn: light purple, and ZnCl_2 : dark purple.

8. Proteomic and transcriptomic approach

To further investigate the impact of the presence of Co^{2+} in the environment on *P. aeruginosa*, we carried out proteomic and transcriptomic analyses. Proteomic studies are more affordable, easier to set up, and give results at the protein level, which are the effectors of the cells. Nevertheless, some proteins are more difficult to analyse, such as membrane proteins, proteins that are weakly expressed, small peptides, or proteins poor in Lys or Arg (less prone to trypsin digestion). Thus, transcriptomic analyses can help in some instances to cover the analyses of the whole genome, even if results are only at the RNA level.

We investigated the effect of non-toxic concentrations of Co^{2+} (10 μM) on the genomic expression of *P. aeruginosa*. Even if under such mild conditions, the response of the cell might be mild as well, we also avoided any confusion between a specific response of the cell toward Co^{2+} , and the global response of the cell toward any agent given at toxic concentrations. Cells were grown for 8 h in the presence of 10 μM of Co^{2+} and then pelleted and treated for protein or RNA extractions. Changes in gene expression are given as log2 ratio between *P. aeruginosa* grown in the presence or absence of Co^{2+} , and the p-values indicated.

As usually observed when comparing proteomic and transcriptomic data, the two analyses do not totally recover each other. We thus consider mostly the genes which expression varies in the two analyses.

8.1. Co affects the expression of the PCH pathway, but not the PVD pathway.

As already shown earlier on a few examples (PchA, FptX), most genes of the PCH pathway except PchR are repressed in the presence of Co^{2+} , whereas almost no effect has been observed on the expression of the PVD pathway. The repression of several PCH proteins has been observed in the presence of Fe^{3+} and Co^{2+} , showing a similar effect of both metals on their expression (Table R3). Contrarily, regarding the PVD pathway, a repression in all genes detected belonging to this pathway in presence of Fe^{3+} was observed, and but no significant values were obtained in presence of Co^{2+} . We could only confirm the strong PCH repression due to Co^{2+} , showing no PVD proteins repressed significantly under 10 μM of Co^{2+} (Table R3).

		<i>wt Fe3+</i>				<i>wt Co2+</i>			
		Transcriptome		Proteome		Transcriptome		Proteome	
ID		log2 fc	p-value	log2 ratio	p-value	log2 fc	p-value	log2 ratio	p-value
PA4218	fptX	-7,51	0	-2,08	2,22E-02	-3,75	2,86E-300	-1,88	1,70E-02
PA4221	fptA	-7,88	0	-2,91	1,56E-04	-3,68	3,02E-108	-3,16	1,05E-04
PA4222	pchI	-7,51	0	-2,45	7,30E-04	-3,83	1,98E-170	-2,45	7,67E-04
PA4223	pchH	-7,29	0	-1,32	6,24E-03	-4,21	0	-2,62	2,25E-04
PA4224	pchG	-7,34	0	-	-	-4,12	2,54E-116	-1,45	1,74E-03
PA4225	pchF	-7,41	0	-1,53	3,25E-03	-4,30	2,48E-257	-2,87	1,45E-04
PA4226	pchE	-7,46	0	-2,87	6,30E-05	-4,38	1,02E-235	-2,75	1,74E-04
PA4227	pchR	-5,37	0	-	-	-4,41	7,46E-282	0,48	7,93E-02
PA4228	pchD	-6,12	0	-1,26	1,54E-03	-4,40	2,88E-194	-1,93	2,41E-04
PA4229	pchC	-6,37	7,75E-308	1,26	3,55E-03	-3,40	0	-	-
PA4230	pchB	-6,60	0	-5,31	1,08E-04	-3,95	0	-3,04	7,45E-06
PA4231	pchA	-6,58	0	-2,04	2,12E-03	-3,82	9,10E-271	-2,80	1,14E-04
PA2385	pvdQ	-9,42	0	-1,46	9,88E-04	-	-	-	-
PA2386	pvdA	-10,23	0	-2,42	1,72E-04	-	-	-	-
PA2389	pvdR	-7,64	0	-1,37	2,37E-03	-	-	-	-
PA2390	pvdT	-7,62	0	-	-	-	-	-	-
PA2391	opmQ	-7,69	0	-2,27	1,03E-03	-	-	-	-
PA2392	pvdP	-7,72	0	-3,52	1,22E-05	-	-	-	-
PA2394	pvdN	-9,61	0	-2,03	3,32E-04	-	-	-	-
PA2395	pvdO	-8,86	0	-2,46	5,53E-05	-	-	-	-
PA2396	pvdF	-6,78	0	-3,18	2,66E-05	-	-	-	-
PA2397	pvdE	-9,98	0	-2,77	8,45E-04	-	-	-	-
PA2398	fpvA	-8,93	0	-2,26	2,01E-04	-	-	-	-
PA2399	pvdD	-6,94	0	-0,62	3,85E-02	-	-	-	-
PA2400	pvdJ	-6,81	0	-2,17	1,74E-04	-	-	-	-
PA2404	fpvH	-5,16	2,37E-288	-	-	-	-	-	-
PA2405	fpvJ	-5,25	0	-2,24	1,16E-02	-	-	-	-
PA2406	fpvK	-5,53	2,25E-163	-	-	-	-	-	-
PA2407	fpvC	-4,93	4,77E-135	-	-	-	-	-	-
PA2408	fpvD	-4,92	3,87E-117	-2,07	7,52E-03	-	-	-	-
PA2410	fpvF	-4,34	3,30E-163	1,63	2,00E-02	-	-	-	-
PA2413	pvdH	-6,70	0	-2,82	7,27E-05	-	-	-	-
PA2424	pvdL	-9,33	0	-1,75	1,71E-04	-	-	-	-
PA2426	pvdS	-9,93	0	-	-	-	-	-	-

Table R3. Expression values from transcriptomic and proteomic analysis of Fe- and Co-dependent proteins that have been down-regulated in presence of these metals. PCH genes are represented in blue and PVD genes in green. log2 fc: log2 fold change. ‘-’ indicates a difference in expression: $-1 < \log_2 \text{fold change} < 1$.

8.2. Pathways affected in the presence of Co

Several other genes (not of the PCH pathway) were repressed significantly (\log_2 ratio < -1 and a p-value $< 0,02$) in the presence of Co^{2+} (Table R4). To identify the global pathways affected by the presence of Co^{2+} , we used the STRING software (<https://string-db.org/>) to visualize whether regulated genes may take part to functional networks. Four functional networks were down-regulated by the addition of Co^{2+} (Fig. R18). These functional networks were linked to PCH biosynthesis (Table R4 blue), *Quorum sensing* (Table R4 green) related to the quinolone-based intracellular signalling (PQS) (Lee and Zhang, 2015), oxydo-reduction reactions (Table R4 brown), sulfur/cysteine metabolism (Table R4 orange), and the type VI secretion system (Table R4 red). None of the genes already known to affect Co^{2+} transport were found down-regulated in the two analyses. Some proteins like Cmax (a CorA-like Mg protein, known to transport Co^{2+} and Mg^{2+} from the periplasm to the cytoplasm) have been observed repressed in the proteomic analysis, but not in the transcriptomic one. It can nevertheless still not be excluded that the expression of some transporters may be regulated at the post-transcriptional level.

If the repression effect on the PCH pathway was expected, the down-regulation of the other functional networks were not, and we thus studied the role of these genes in the response to Co^{2+} . Since sulfur and cysteine are required as precursors in the PCH synthesis, we also analysed the proteome of a mutant affected in PCH production, the $\Delta pchR$ mutant (Table R4). Interestingly, in this mutant, the networks linked to PCH production, sulfur/cysteine metabolism, oxydo-reduction, and *Quorum sensing* were down-regulated as well. The only specific down-regulated pathway to the addition of Co^{2+} is linked to the T6SS. This secretion system is often associated to the formation of biofilm. This system is regulated by the *Quorum sensing*, but through Las and Rhl, and not by the *Quorum sensing* PQS detected in our analysis.

Further, a non-coding RNA, ErsA, has been found up-regulated in the presence of Co^{2+} . ErsA is known to inhibit the expression of AlgC, an enzyme required for the synthesis of alginate, which is involved in the formation of biofilm as well.

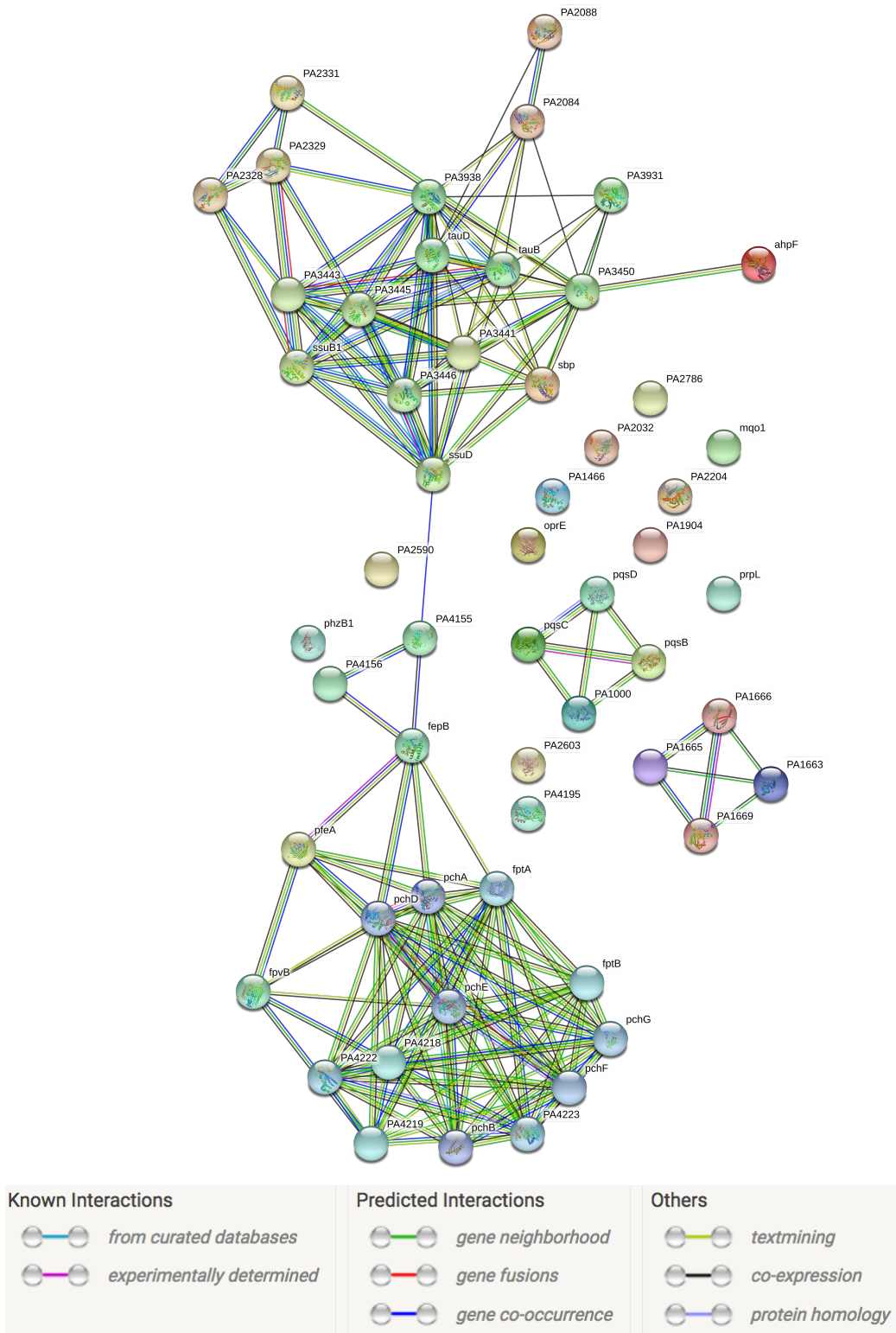


Figure R18. Interaction network created using the String tool (<https://string-db.org/>) including the repressed genes by the effect of Co. The filled nodes indicates that some 3D structure is known or predicted.

		Down-regulated proteins					
		Transcriptome		Proteome			
		PAO1 wt		PAO1 wt		$\Delta pchR$	
ID		log2 fold change	p-value	log2 ratio	p-value	log2 ratio	p-value
PA0283	sbp	-5,327	5,68E-181	-1,423	9,28E-04	-4,585	1,84E-06
PA0291	oprE	-1,775	2,19E-44	-1,007	5,47E-03	-1,133	7,68E-04
PA0997	pqsB	-4,937	3,13E-35	-1,337	1,02E-03		
PA0998	pqsC	-4,323	6,84E-23	-1,633	3,82E-03		
PA0999	pqsD	-3,478	1,14E-23	-3,170	7,72E-02	-2,375	2,11E-02
PA1000	pqsE	-3,276	6,74E-20	-2,986	3,83E-04	-1,28	1,78E-02
PA1466	-	-2,135	2,65E-52	-2,772	4,03E-02		
PA1663	sfa2	-1,71	1,62E-11	-1,759	2,41E-01		
PA1665	fha2	-1,742	1,58E-11	-1,433	3,92E-03		
PA1666	lip2	-1,932	2,21E-13	-1,470	2,28E-03		
PA1669	icmF2	-1,625	2,87E-12	-1,510	5,11E-03		
PA1904	phzF2	-2,228	1,41E-15	-1,886	2,10E-03	-1,230	1,58E-02
PA2084	yucB	-1,703	5,44E-23	-2,871	1,94E-01	-3,634	1,13E-01
PA2088	-	-4,743	3,65E-95	-3,127	7,32E-02	-5,70	8,38E-07
PA2204	-	-5,818	3,29E-225	-1,771	3,70E-03	-3,838	5,86E-05
PA2328	-	-1,651	1,77E-41	-1,580	7,46E-02	-3,553	1,60E-05
PA2329	-	-1,354	2,60E-15	-1,107	1,46E-03	-2,052	1,63E-03
PA2331	-	-1,331	1,21E-09	-1,236	3,68E-02	-2,133	5,03E-04
PA2590	-	-1,243	1,65E-07	-1,860	1,44E-01	-1,722	1,20E-02
PA2603	-	-2,736	1,60E-202	-2,105	4,05E-03	-3,777	6,04E-04
PA2688	pfeA	-1,288	8,52E-31	-1,778	8,21E-02		
PA2786	-	-4,522	0	-1,172	5,26E-02	-1,303	3,55E-02
PA3441	ssuF	-5,786	0	-1,566	2,19E-02	-5,218	5,31E-05
PA3442	ssuB	-4,189	2,95E-107	-3,635	1,15E-05	-4,28	4,62E-05
PA3443	ssuC	-4,874	3,19E-122	-4,770	4,40E-04	-8,36	1,82E-04
PA3444	ssuD	-4,88	2,66E-259	-6,828	4,45E-04	-6,28	4,88E-05
PA3445	-	-5,421	1,53E-201	-1,907	3,67E-03	-5,800	7,60E-06
PA3446	ssuE	-4,167	3,28E-129	-6,964	3,49E-04	-6,08	8,44E-03
PA3450	lsfA	-5,809	9,79E-165	-1,857	9,51E-05	-4,579	2,29E-07
PA3452	mqaA	-1,337	1,64E-32	-1,136	8,01E-02		
PA3931	-	-3,978	2,34E-114	-1,542	4,82E-04	-3,617	8,56E-05
PA3935	tauD	-5,149	1,67E-208	-1,261	1,29E-02	-4,675	1,09E-05
PA3937	-	-5,135	6,74E-297	-5,951	1,60E-01	-12,047	8,05E-03
PA3938	tauA	-4,798	9,03E-189	-1,683	6,37E-04	-3,425	3,77E-06

PA4155	-	-1,741	6,34E-74	-1,205	1,78E-03	-1,148	5,01E-04
PA4156	fvbA	-1,929	7,99E-122	-2,151	4,07E-03		
PA4159	fepB	-1,195	1,17E-19	-1,246	9,24E-03		
PA4168	fpvB	-1,162	2,89E-33	-1,103	2,74E-03		
PA4175	piv	-1,795	1,01E-12	-2,515	3,21E-04		
PA4195	-	-4,136	2,32E-131	-1,223	1,49E-03	-4,699	2,16E-03
PA4211	phzB1	-2,653	8,31E-21	-1,546	4,64E-03	-1,628	4,04E-03
PA4218	ampP	-3,747	2,86E-300	-1,878	1,70E-02	-2,065	9,32E-03
PA4219	ampO	-3,684	3,02E-108	-7,729	4,77E-01		
PA4220	fptB	-3,827	1,98E-170	-1,566	9,36E-01	-4,327	3,92E-01
PA4221	fptA	-4,206	0	-3,159	1,05E-04	-4,510	1,64E-06
PA4222	pchI	-4,122	2,54E-116	-2,453	7,67E-04	-3,929	2,64E-05
PA4223	pchH	-4,3	2,48E-257	-2,621	2,25E-04	-3,592	5,53E-04
PA4224	pchG	-4,382	1,02E-235	-1,446	1,74E-03	-1,636	1,30E-03
PA4225	pchF	-4,406	7,46E-282	-2,872	1,45E-04	-3,640	1,51E-05
PA4226	pchE	-4,404	2,88E-194	-2,749	1,74E-04	-4,191	4,12E-06
PA4228	pchD	-3,397	0	-1,929	2,41E-04	-3,336	2,10E-06
PA4230	pchB	-3,946	0	-3,037	7,45E-06	-5,317	4,90E-07
PA4231	pchA	-3,818	9,10E-271	-2,796	1,14E-04	-5,055	1,32E-04

Table R4. Expression values from transcriptomic and proteomic analysis of Co-dependent proteins that have been down-regulated in the presence of Co²⁺. Several genes belonging to different functional networks were identified: linked to PCH biosynthesis (blue), related to the quinolone-based intracellular signalling (PQS) of the *Quorum sensing* (green), involved in oxydo-reduction reactions (brown), in the sulfur/cysteine metabolism (orange), and in the type VI secretion system (red). See text for more details.

On the opposite, only three genes are found significantly up-regulated (log2 ratio > 1 and a p-value < 0,02) in the transcriptome and proteome analyses (Table R5): PA1297, PA1298 and PA2691. These proteins could have a role in Co²⁺ transport, in the efflux or regulation, being involved in metal resistance. PA1298 is the homolog of RcnR in *P. aeruginosa*, a transcriptional regulator. In interaction with Co²⁺ or Ni²⁺, RcnR controls the expression of RcnA, a transporter involved in the efflux of Ni and Co cations, thus in Co²⁺ and Ni²⁺ detoxification (Rodrigue et al., 2005). Therefore RcnR plays a role in both metal homeostasis. The PA1297 promoter is located in the same intergenic region of PA1298, and even if we could think it might be the homolog of RcnA in this pathogen, we can just confirm that it is another Co-dependent protein that may be involved in Co²⁺ efflux, supported by the match to InterPro signature evidence used in automatic assertion (Jones et

al., 2014), proposing this protein as a cation transmembrane transporter. PA2691 is a protein hypothetically involved in oxydo-reduction process.

Up-regulated proteins						
Transcriptome			Proteome			
PAO1 wt			PAO1 wt		$\Delta pchR$	
ID	log2 fold change	p-value	log2 ratio	p-value	log2 ratio	p-value
PA1297	3,930	1,23E-164	2,270	7,11E-03	-1,14	5,05E-02
PA1298	3,370	5,06E-121	3,890	7,05E-04	-	-
PA2691	3,740	1,69E-113	2,290	6,63E-05	-	-

Table R5. Expression values from transcriptomic and proteomic analysis of Co-dependent proteins that have been up-regulated in presence of Co^{2+} . Genes theoretically involved in metal transport are marked in light purple. See text for more details.

Discussion

Pyoverdine (PVD) and pyochelin (PCH) siderophores are involved in iron homeostasis, which maintenance is crucial for the cells survival. Fe is an essential nutriment involved in many biological processes, such as energy production and stabilization of protein structures, as well as oxido-reduction reactions (Heldal et al., 1985), although, this metal at high concentrations has a toxic effect by producing Reactive Oxygen Species (ROS) *via* the Fenton reaction (Rizvi et al., 2015), causing damage to the macromolecular components of the cells, including DNA and proteins (Imlay et al., 1988; Nunoshiba et al., 1999; Aisen et al., 2001).

It should be pointed out that PVD and PCH are able to chelate a large range of different metals (Ag^+ , Al^{3+} , Cd^{2+} , Co^{2+} , Cr^{2+} , Cu^{2+} , Eu^{3+} , Ga^{3+} , Hg^{2+} , Mn^{2+} , Ni^{2+} , Pb^{2+} , Sn^{2+} , Tb^{3+} , Tl^+ and Zn^{2+}), even though they have a preference for ferric iron (Fe^{3+}) (Braud et al., 2009a, 2009b). Most of them in complex with the siderophores PVD or PCH can bind FpvA or FptA binding sites with different affinities even though only a few will accumulate in the bacteria. It was shown that these siderophores play also a role in the mechanism of metal resistance, protecting bacteria against toxic effects of heavy metals by chelating and sequestering them in the extracellular medium (Braud et al., 2010). During this thesis, we have revisited these interactions between the PVD and PCH with biological metals, in order to check if these siderophores could have some biological roles in the acquisition of biological metals other than iron.

We found that the production of PVD is completely repressed by Fe^{3+} and at 60% by 150 μM of Co^{2+} , while the PCH production is totally repressed by Fe^{3+} and Co^{2+} , and at 40% by 150 μM of Ni^{2+} . We have seen a strong repression, but none of the metals tested (Fe^{3+} , Co^{2+} , Ni^{2+} , Mn^{2+} , Cu^{2+} and Zn^{2+}) induced significantly the production of PVD or PCH, which contrast to the results previously published. P. Visca has published that PCH production in *P. aeruginosa* is repressed by 10 μM Fe^{3+} , Co^{2+} and 100 μM of Ni^{2+} or Cu^{2+} (Visca *et al.*, 1992), and our group that PVD production is induced by 10 μM Cu^{2+} , Mn^{2+} and Ni^{2+} (Braud et al., 2009b; Braud et al., 2010). Moreover, exposure to 10 mM Cu^{2+} up-regulates genes involved in the synthesis of PVD and down-regulates those involved in the synthesis of PCH (Teitzel *et al.*, 2006). Induction of siderophores synthesis in presence of others metals than iron has also been reported for different other bacteria (Huyer and Page, 1988; Hofte *et al.*, 1993; Hu and Boyer, 1996; Kershaw *et al.*, 2005).

Concerning the transport, only Fe^{3+} was transported *via* PVD/FpvA/FpvB into *P. aeruginosa* cells, but regarding the PCH pathway, Fe and also Co^{2+} have been transported specifically *via* PCH/FptA, and no other biological metal tested. More precisely our data show for Co^{2+} two different type of transport: one, which is PCH/FptA dependent and the second probably due to diffusion across porins. When Co^{2+} was in the presence of PCH its intracellular concentration decreased in *P. aeruginosa* cells and the remaining transport was PCH/FptA dependent, suggesting a PCH-independent transport is probably due to diffusion via porines and the PCH-dependent transport occurs via FptA. Therefore, PCH has also a role in biological metal resistance and this was observed also with our data for Zn^{2+} . Such a role in metal resistance has already been reported previously by our group for PVD and PCH in the presence of different toxic metals (Braud et al., 2010).

The protecting role of PVD and PCH may be useful for this pathogen during the infection event. Complex mechanisms have evolved illustrating the longstanding battle between pathogens and hosts in the process of bacterial infection, a co-evolution during generations. Therefore, they have developed mechanism to protect themselves against the other to increase their fitness and survival. In this context, transition metals are important for bacteria as well as for the host's cells, and the equilibrium and metal concentration into the cells and the environment can determine the rate of survival of both. One of the mechanisms used by the host consists to engulf bacteria with toxic concentrations of some metals, a mechanism called 'brass dagger'. Mammalian cells are capable of imbibed pathogen bacteria into the phagosome and increase inside the concentration of Cu^{2+} and Zn^{2+} , with the aim of killing bacteria due to their toxicity. Cu can be highly toxic due to its high oxidative potential, increasing the reactive oxygen species (ROS) (Rizvi et al., 2015), and it is classified by the Irving-William series as a metal with strong affinity for biomolecules, able to compete and displace other transition metal form the molecule 'blocking' their correct function (Waldron and Robinson, 2009). Zn is part of 6% of all proteins of bacteria (Andreini et al., 2006) and plays catalytic and structural roles (Maret, 2011), but as Cu, it is a metal with high affinity for biological molecules. Their presence in excess, in combination with ROS produced by NADPH oxidase in the membrane of the phagosome, cause bacterial death (German et al., 2013; Djoko et al., 2015). In respond, several bacterial pathogens produce periplasmic or membrane-associated Cu and Zn superoxide dismutases, which protect infectious bacteria from oxy-radical damage

(Battistoni, 2003), and in this context, we propose that PVD and PCH could play a role in the bacterial survival by increasing their metal resistance, sequestering these metals out of the cells or decreasing their transport through the bacterial membrane across the porines, thus its intracellular concentration.

The metal ion transport is one of the mechanisms that bacteria control to maintain the metal homeostasis and avoid their excess into the cells. The proteins involved in Co^{2+} transport (uptake or efflux) in *P. aeruginosa* have not been widely studied and they have still to be identified. Our proteomic data indicate a possible role of PA1298 in Co homeostasis in *P. aeruginosa*, which theoretically correspond to the transcriptional regulator RcnR, and PA1297 a transmembrane transporter, sharing the same intergenic region than PA1298.

As we mentioned above, the case of Co^{2+} in the PCH pathway is different to the other biological metals. If PCH protects bacteria against the excess of Co^{2+} by decreasing its intracellular concentration when the metal is in complex with PCH, why is $\text{PCH}_2\text{-Co}$ specifically recognized and transported by FptA, like $\text{PCH}_2\text{-Fe}$? Is there a biological reason under this transport?

The intracellular Fe^{2+} controls *via* Fur the expression of both pathways, PVD and PCH. This repression by Fe^{2+} and Fur involves a Fur-Fe complex interacting with the DNA (Fur box) of the different PCH and PVD operons, repressing the gene expression. In the PCH pathway, the Fur boxes are present in all promoters of PCH operons, involved in the synthesis (*pchDCBA*, *pchEFGHI*), transport (*fptAB(CX)*) and regulation (*pchR*).

In vitro, we saw that Fur was able to bind Co^{2+} , and the complex was able to bind to the Fur box of *pvdS* and to the promoter region containing the Fur box of *pchD*. The *pchD* promoter contains two 'Fur box' overlapped, one of them to control the expression of *pchR* and the other *pchD* expression. If we assume that binding of Fur to the Fur boxes is due to the protein activation, Co^{2+} should activate Fur and repress *pchR* expression. However, *mCherry-pchR* expression analysis in the presence of Fe^{3+} , Co^{2+} , Ni^{2+} , Cu^{2+} and Zn^{2+} showed that only Fe^{3+} repressed *pchR* expression, and not Co^{2+} or the other metals. Therefore, Co^{2+} seems not able to activate Fur, and the repression effect observed with this metal on the PCH genes expression involves a different mechanism of action as for Fe^{3+} . These results may indicate that in the Fur-Co complex is not able to bind in an efficient way to DNA and repress the expression of the genes.

Concerning the positive auto-regulation loop of regulation of the PCH pathway, the proteome and transcriptome analysis shown that in the $\Delta pchR$ strain (i) some networks linked to PCH production, like sulfur/cysteine metabolism, oxydo-reduction, and *Quorum sensing* networks were down-regulated, and moreover they are not directly regulated by Co^{2+} , but probably through the regulation of PCH production; and (ii) the transcription and expression of all PCH genes (except *pchR* and *pchC*, not detected) were strongly repressed (transcriptome: $-3.5 > \log_2 \text{ ratio} > -4.5$; and proteome: $-1.8 > \log_2 \text{ ratio} > -3.2$). This last observation was also supported by the experiments of expression plasmids showing that no reporter expression was produced when the PchR box was not present in the promoter region. These results confirm that PchR is essential (responsible) for the expression of all PCH genes. PCH₂-Fe once in the cytoplasm, interacts with PchR and the formed complex PchR-PCH-Fe activates the expression of the proteins of the PCH pathway (Michel et al., 2005). We have shown using the fluorescent characteristics of the tryptophans present in PchR that this regulator can bind PCH-Co but with a slightly lower affinity than for PCH-Fe, $K_{d \text{ PCH-Co}} = 13,95 \pm 3,37 \mu\text{M}$ and $K_{d \text{ PCH-Fe}} = 5,82 \pm 2,84 \mu\text{M}$. To see if PCH-Co is able to render PchR active and activate the expression of the PCH pathway, we monitored the expression of a reporter (mCherry) gene under the effect of the *pchD* promoter region containing a Fur box and a PchR box, or just the Fur box. We saw no differences in the expression in presence of Co^{2+} when just the Fur box was present, but when both PchR and Fur boxes were present, 5 μM of Co^{2+} repressed mCherry expression. According to these results and since we have shown that Co^{2+} does not affect the Fur activity, we propose that the presence of PCH₂-Co in the bacterial periplasm of *P. aeruginosa* involves an increase of PchR-PCH-Co formation and probably, as a consequence, a decrease of PchR-PCH-Fe complexes, which are the only able to activate the transcription of PCH pathway. See Fig. D1. The repression effect on PCH genes could be due to the inability of PchR-PCH-Co complex to bind to the PchR boxes, or because PchR-PCH-Co binds to the PchR boxes in a not efficient way to induce the gene expression as observed with PchR-PCH-Fe. It would be interesting to carry out EMSA assays to investigate this question. We have preliminary results of the specific binding between PchR and the PchR box in the presence of the effector PCH₂-Fe (Fig. S3), but since the binding was unspecific in the presence or absence of PCH₂-Fe, these data were inconclusive. It would be important to improve the purification of MBP-PchR performing a third chromatography of gel filtration, because several proteins that bind

naturally to the DNA were found in the MBP-PchR purified solution by mass spectrometry (Table S4).

Concerning the uptake of PCH₂-Co, the competition experiments with PCH-⁵⁵Fe complexes demonstrated that PCH₂-Co can enter in competition with PCH₂-Fe during the transport and consequently on FptA binding site. Braud et al., calculated the affinity of both complexes to FptA binding site, and in fact they had almost the same values, $K_{i\text{PCH}_2\text{-Co}} = 14,6 \text{ nM}$ and $K_{i\text{PCH}_2\text{-Fe}} = 13,6 \text{ nM}$ (Braud, et al, 2009).

Fe and Co are very similar metals and it has been previously shown that both can interfere in the ligand binding site of certain proteins replacing one for the other by competition, and promoting an improper functioning of the protein. This can happen due to both metals have the same biological relevant oxidation states (2+/3+) and similar radii, which facilitate their interference (Okamoto and Eltis, 2011). As previously described for the formation of Fe-S clusters, where IscU can incorporate Co and transfers it to apo-targets (Ranquet et al., 2007), Co can also take the place of Fe in the PCH pathway, by interacting with PCH and the formed PCH₂-Co complex can then interact with FptA and PchR and probably also with FptX since PCH₂-Co reaches the bacterial cytoplasm (Fig. D1). These data suggest also that PCH₂-Co must have the same size and geometry as PCH₂-Fe allowing that way an interaction with PchR, FptA and FptX.

These results indicate that the Co²⁺ transport *via* PVD and PCH may have no biological significance, and both siderophores do not contribute to increase the intracellular concentrations of all metals tested (Fe²⁺, Co²⁺, Ni²⁺, Mn²⁺, Zn²⁺, Cu²⁺), only for Fe²⁺ in the PVD pathway and for Fe²⁺ and Co²⁺ in the PCH pathway. These data show how a metal like Co can pollute and parasitize the PCH pathway (Fig. D1), and also indicate that it is not because a siderophore-dependent uptake is seen for a metal that this uptake has a biological significance.

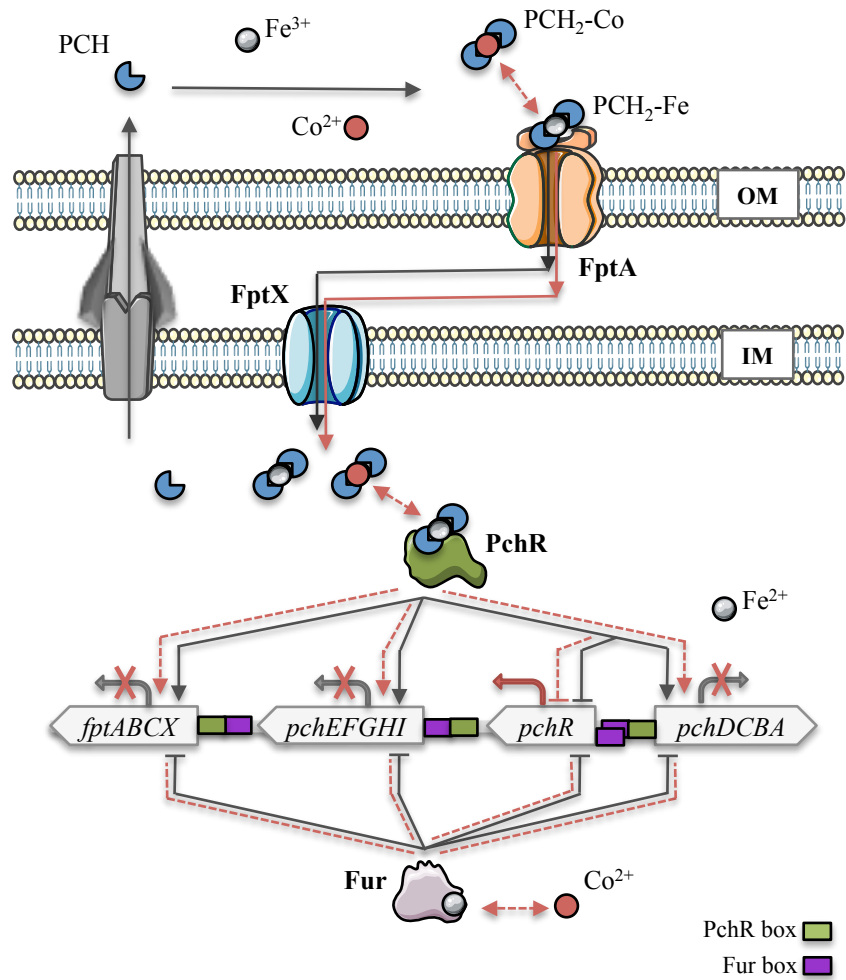


Figure D1. Schematic interactions proposed between Co and the PCH iron uptake pathway, interfering at the level of the PCH₂-Fe transport and also in the regulation mechanism of the PCH genes, involving PchR and Fur transcriptional regulators. See text for more details.

Supplementary material

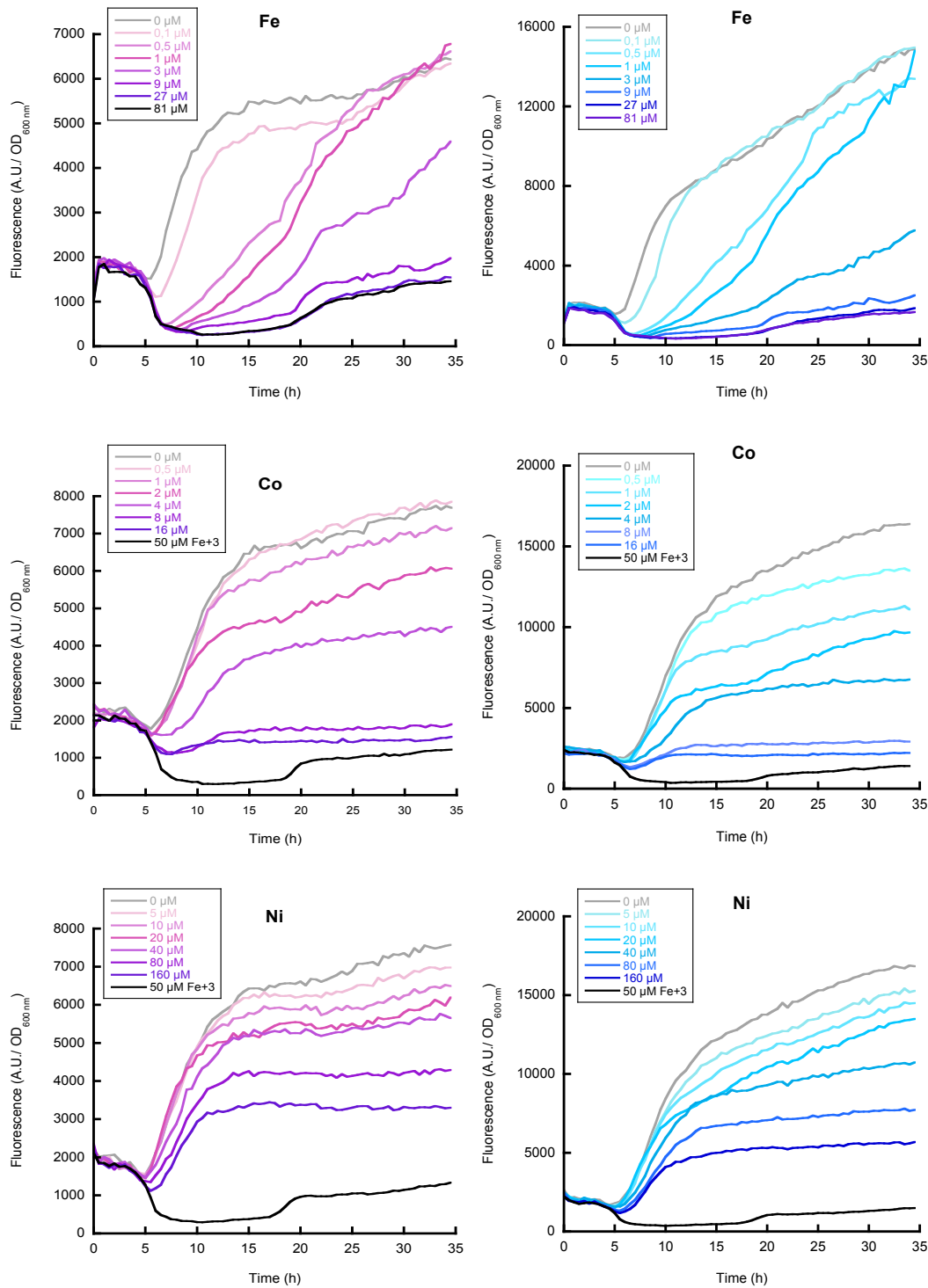


Figure S1. *PchA* (pink) and *FptX* (blue) expression in *pchA-mCherry* and *fptX-mCherry* cells respectively, grown in CAA medium, in presence of different concentrations of FeCl₃, CoCl₂, NiCl₂, CuCl₂, MnCl₂, and ZnCl₂ added in the culture medium at the beginning of growth. The data represented here are the mCherry fluorescence in function of the incubation time, plotted against the time of growth. The measures: fluorescence (excitation 610 nm/emission 570 nm) and OD_{600 nm} were done using the spectrophotometer plate reader TECAN.

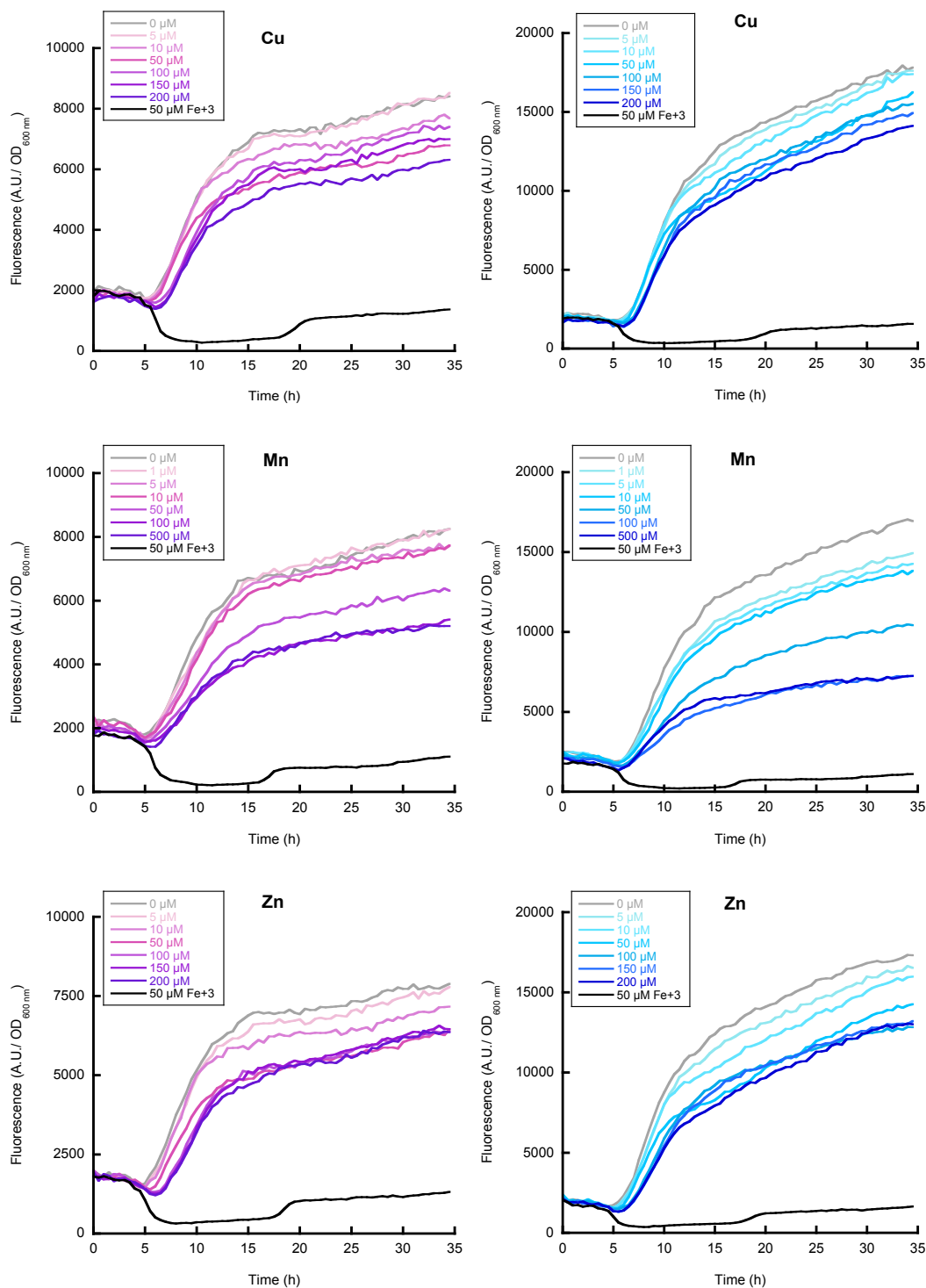


Figure S1. PchA (pink) and FptX (blue) expression in *pchA-mCherry* and *fptX-mCherry* cells respectively, grown in CAA medium, in presence of different concentrations of FeCl₃, CoCl₂, NiCl₂, CuCl₂, MnCl₂, and ZnCl₂ added in the culture medium at the beginning of growth. The data represented here are the mCherry fluorescence in function of the incubation time, plotted against the time of growth. The measures: fluorescence (excitation 610 nm/emission 570 nm) and OD_{600 nm} were done using the spectrophotometer plate reader TECAN.

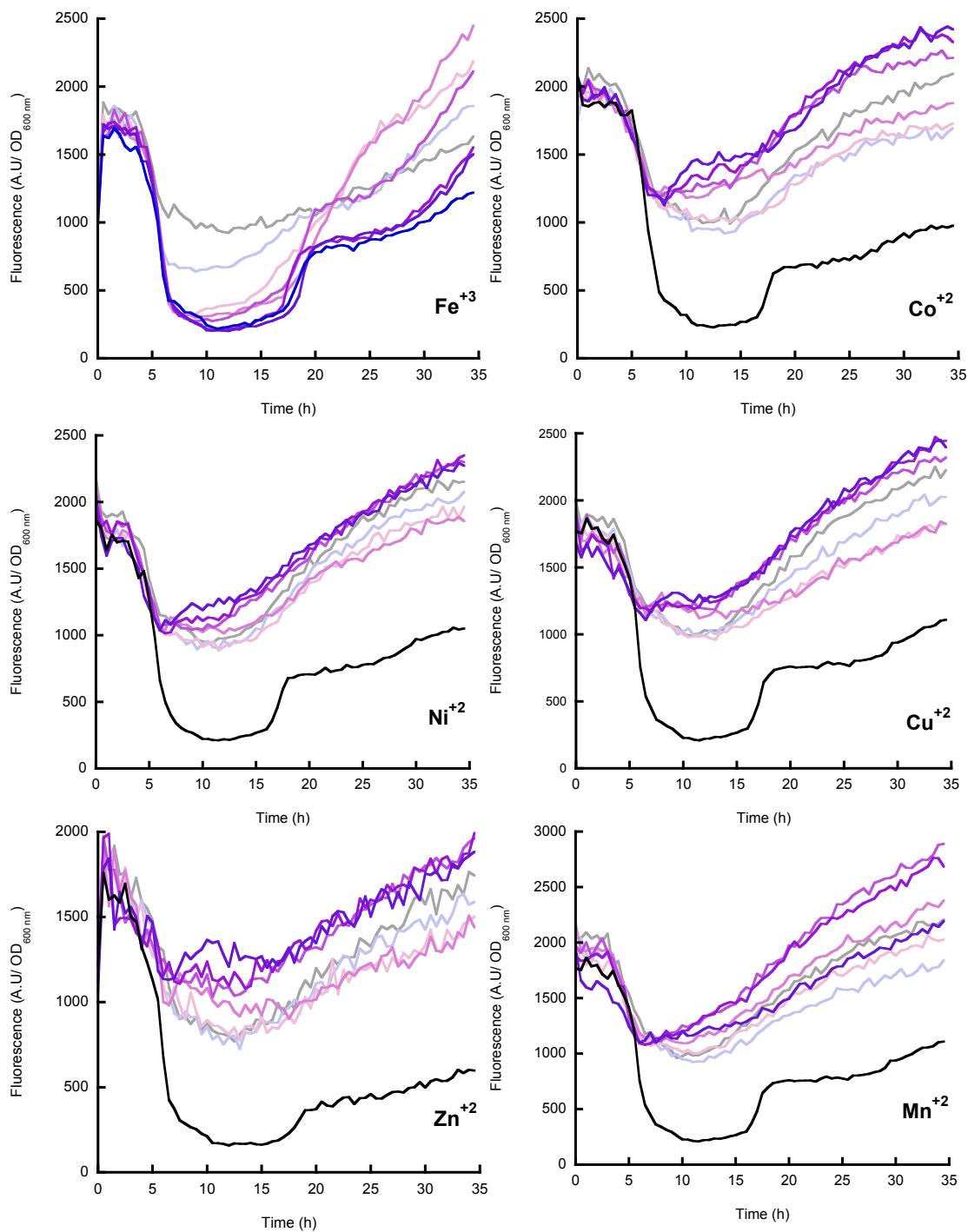


Figure S2. PchR expression in *mCherry-pchR* cells grown in CAA medium, in presence of different concentrations of FeCl₃, CoCl₂, NiCl₂, CuCl₂, MnCl₂, and ZnCl₂ added in the culture medium at the beginning of growth. The data represented here are the mCherry fluorescence in function of the incubation time, plotted against the time of growth. The measures: fluorescence (excitation 610 nm/emission 570 nm) and OD_{600 nm} were done using the spectrophotometer plate reader TECAN. The concentrations of each metal used were the same of the previous Figure SM1. In this representation, the colour darkens at increasing metal concentration.

Strains	C. Ref.	Description	Ref.
PAO1 <i>wt</i>	n° 459	ATCC15692. <i>P. aeruginosa</i> wild-type strain	DSMZ
<i>ΔpvdFApchBAΔfptA</i>	n° 61 (234)	Deletion of <i>pvdF</i> , <i>pchB</i> , <i>pchA</i> and <i>fptA</i> genes	Reimmann
<i>ΔpvdFApchA</i>	PAS283	Deletion of <i>pvdF</i> and <i>pchA</i> genes in PAO1 459	Gasser et al., 2015
<i>pvdJ-mCherry</i>	PAS245	PAO1; mCherry fused to 3' of <i>pvdJ</i>	Cunrath et al., 2014
<i>pchA-mCherry</i>	PAS193	Derivate of PAO1 <i>wt</i> ; <i>pchAmcherry</i> chromosomally integrated	Cunrath et al., 2014
<i>fptX-mCherry</i>	PAS210	Derivate of PAO1 <i>wt</i> ; <i>fptXmcherry</i> chromosomally integrated	Cunrath et al., 2014
<i>mCherry-pchR</i>	PAS208	Derivate of PAO1 <i>wt</i> ; <i>mcherrypchR</i> chromosomally integrated	Cunrath et al., 2014
<i>ΔpchR</i>	PAS387	Deletion of <i>pchR</i> in PAO1 strain 459	Fechter
<i>ΔpvdS</i>	PAS386	Deletion of <i>pvdS</i> in PAO1 strain 459	Fechter
<i>E. coli</i> DH5a	-	Strain with pME7180 plasmid carrying <i>MBP</i> added to the 5' <i>pchR</i> under the effect of the lac promoter induced by IPTG	Michel et al., 2005
<i>E. coli</i> HB101	n° 56	Helper strain carrying pME487	Reimmann
<i>E. coli</i> Top10	-	F- <i>mcrA</i> Δ(<i>mrr</i> - <i>hsdRMS</i> - <i>mcrBC</i>) φ80lacZΔM15 ΔlacX74 nupG recA1 araD139 Δ(<i>ara-leu</i>)7697 galE15 galK16 rpsL(StrR) endA1 λ	Invitrogen
Plasmids			
pSEVA631 <i>pchD_fur-mCherry</i>	pAYC6	<i>pchD</i> promoter containing only the Fur box fused to mCherry ORF	This study
pSEVA631_ <i>pchD_Fur PchR-mCherry</i>	pAYC5	<i>pchD</i> promoter containing the Fur box and PchR box fused to mCherry ORF	This study
pSEVA631 <i>PvdS-mCherry</i>	pPF3	<i>pvdS</i> promoter containing the Fur box fused to mCherry ORF	This study
pSEVA631	244	Low copy plasmid for <i>E. coli</i> / <i>Pseudomonas spp.</i>	Martinez Garcia et al. 2015
pLG3	154	Expression vector carrying mCherry sequence	Guillon et al., 2013

Table S1. Bacterial strains used in the different experiments of this study.

Collection	Primers	Sequences (5' → 3')
PchR box & Fur box		
1256	<i>pchD</i> . Fur Box. Fwd	CAAAGAATTCGCCGCCGCCAATGATAATAAATCTCATTTC
1257	<i>pchD</i> . Fur Box. Rev	CCATGTTATCCTCCTCGCCCTTGCTCACCATGCGATCTCCGTGGATGCGG
1258	<i>pchD</i> . PchR Box & Fur Box. Fwd	CAAAGAATTCGACAAAGCGCCCTGCACTCCG
1259	<i>pchD</i> . PchR Box & Fur Box. Rev	CATGTTATCCTCCTCGCCCTTGCTCACCATGCGATCTCCGTGGATGCG
1290	<i>pvdS</i> large Fur box Fwd	CAAAGAATTCGAAACGCCGAAGAATTTCTCCCTC
1291	<i>pvdS</i> Fur box Rev	GAAGGCATAA CTGGAACCCT CGATGGTGAG CAAGGGCGAG GAGGATAACA TGG
1262	mCherry Fwd	GTGAGCAAGGGCGAGGAGGATAACATG
1263	mCherry Rev	CTCCAAGCTTTTACTTGTACAGCTCGTCCATGCCGC
EMSA		
1043	Fwd.32p-PchRbox	GCGGAGATGGACAAAGCGCCCTGC
1044	Fwd.32p-PchRnobox	CGCGGGCTTGCGCGGTCCCT
1045	Rev.32p	GCGATCTCCGTGGATGCGGTGCGATTGCC

Table S2. Primers used in this study.

Gene	Promoter boxes	Promoter sequence	Genome location	Plasmid collection
<i>pchD</i>	PchR box, Fur box	5'GACAAAGCGCCCTGCACTCCGCCCTG CAGCGAATGAA AAAGCCCCGCAATCGAAA AGGCGGGGCTTGCGCGGT CCCTGCCGCCGCCCAAT TGATAATAAATCTCA TTTCCCAAC AATGGCAATCGACCGCATCCACGGAGATCGCATG 3'	4742278 – 4742426 [+]	pAYC5
	Fur box	5'GCCGCCGCCCAAT TGATAATAAATCTCA TTTCCCAACAA TGGCAATCGACCGCATCCACGGAGATCGCATG 3'	4742356 – 4742426 [+]	pAYC6
<i>pvdS</i>	Fur box	5' GAAACGCCGAAGAATTTCTCCCTCCATCATTTCGAGCG GCTATTTGCCAGCATGCGGACCATTACGAATAAAGGT GAGATTGGTTATTTCTTCGTAAT TGACAATACATTATCATTCA ACATATTTGTTGCGCCATGT GTG GGTCTTACCCACCGCCAGTGTCTGCAGCCCCCTCCGCA GCAAGGTGATTCCATG 3'	2721978 – 2722177 [+]	pPF3

Table S3. Promoter regions cloned into pSEVA631 for the expression analysis.

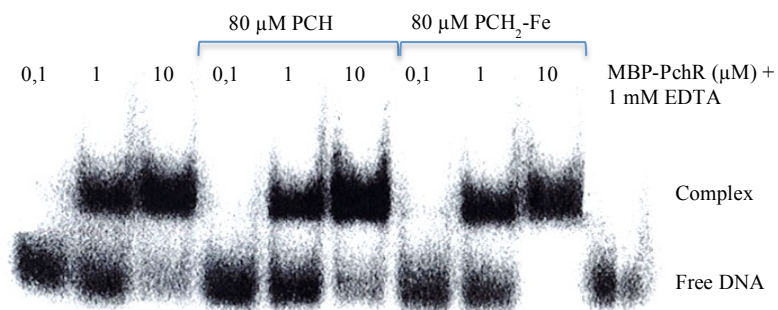


Figure S3. Electrophoresis mobility shift assay (EMSA). Purified MBP-PchR recognition to the *pchD* promoter containing the PchR box.

Protein description	Protein_set_score
Regulatory protein PchR <i>P. aeruginosa</i> PAO1	2948,43
Maltose-binding periplasmic protein MBP <i>E. coli</i>	1740,2
Tryptophanase	1487,2
D-tagatose-1,6-bisphosphate aldolase subunit GatZ	1076,5
Outer membrane protein	1140,95
D-tagatose-1,6-bisphosphate aldolase subunit GatZ	1120,33
Aerobic glycerol-3-phosphate dehydrogenase	1298,6
Outer membrane protein F	1016,05
Glycerol kinase	1328,58
Glycerol kinase	1288,65
4-deoxy-L-threo-5-hexosulose-uronate ketol-isomerase	866,07
30S ribosomal protein S5	862,71
Lactose operon repressor	854,28
50S ribosomal protein L5	849,25

Table S4. Proteins detected into the purified MBP-PchR sample. nanoLC-MSMS RESULTS: proteins. Database = SwissProt (updated each month) with the "Bacteria" sub-taxonomy. Mascot Score: Mascot is the algorithm used for database searching (probability score: the higher it is, the more probable is the presence of a given protein in the sample)

Materials and methods

1. Growth culture media

For 1 L of Lysogeny Broth (LB) (Difco), nutritionally rich medium, add 20 g of LB in bi-distilled water and then autoclave.

For 1 L of Casamino acids (CAA), iron restricted medium, add:

5 g Casamino Acids [Difco. BD: 223050]

1.46 g KH_2PO_4 (136.09 g / mol) [Carlo Erba: 361507]

0.25 $\text{MgSO}_4 \cdot 7\text{H}_2\text{O}$ (248.48 g / mol) [Merck: 105886]

Solubilize these components in pre-heated bi-distilled water and autoclave the final solution.

2. Biological metals

The metals FeCl_3 , CoCl_2 , CuCl_2 , NiCl_2 , ZnCl_2 from PURATREM™ had a higher purity than 99%. They were used to prepare 1M stocks in 0,1 M HCl. These stock solutions were then diluted in Tris 50 mM pH 8.

3. Pyoverdine (PVD) and pyochelin (PCH) extraction and quantification

Cell culture

PAO1-*wt* cells were pre-incubated in 5 ml of LB medium during 24 h, washed twice in 2 volumes of CAA, and incubated overnight (O/N) in this medium. 10 ml of CAA (in 50 ml Falcon) were then inoculated at an OD = 0.1, and the cells grown for 24h in the presence of different concentrations (0 μM ; 1,5 μM ; 15 μM and 150 μM) of Fe^{+3} , Co^{+2} , Ni^{+2} , Cu^{+2} , Mn^{+2} and Zn^{+2} . All incubations were performed at 30 °C with agitation (220 rpm).

PVD and PCH extraction

The OD_{600 nm} was taken, to report the concentration of siderophores in function on the amount of cells. Since *P. aeruginosa* cells produce and export siderophores to the extracellular medium to chelate iron, the detection of siderophores takes place in the supernatant. Cells were centrifuged (5 min, 10 000 rpm) and aliquots of 200 μl from supernatants were distributed in a 96 well plates (Greiner, PS flat-bottomed microplate) to estimate the PVD concentration by measuring the OD at 400 nm, using the TECAN Infinite® M200 microplate reader. The measure was performed in triplicate. PCH extraction is more complex. Aliquots of 1 ml from the supernatant were acidified

with nitric acid HNO₃ to pH 3-4 in order to dissociate iron from PCH. The solution was supplemented with 1/2 volumes of dichloromethane CH₂Cl₂ 100%, mixed, and the organic phase, containing the dichloromethane and the PCH, was finally extracted carefully (bottom phase). This step was repeated. The quantification was performed by measuring the absorbance at 320 nm. All experiments were done in triplicate.

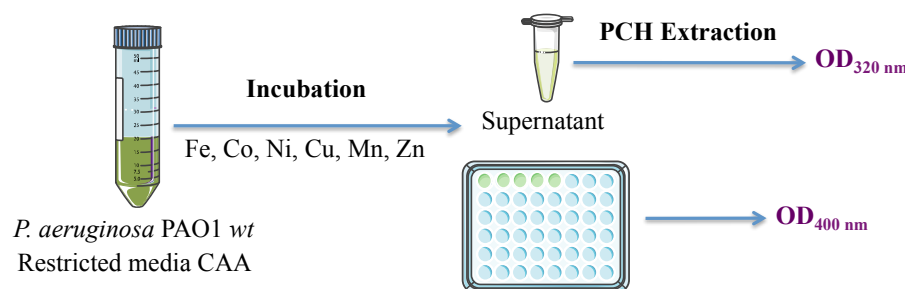


Figure M1. Schematic representation of siderophore extraction and quantification. See text for more information. PAO1 *wt* cells in CAA were incubated 24 h in presence of different biological metals, and then aliquots from the supernatant were taken to measure the PVD (OD_{400 nm}) and the PVD (OD_{320 nm} after an extraction in CH₂Cl₂).

The concentration in molarity of each siderophore was calculated based on the Lambert-Beer law $OD = \epsilon cl$, where 'l' is the path length of the cuvette (1 cm) and 'c' the concentration of the siderophore. $\epsilon_{PVD} = 19000 \text{ M}^{-1} \cdot \text{cm}^{-1}$, and $\epsilon_{PCH} = 4300 \text{ M}^{-1} \cdot \text{cm}^{-1}$.

4. PvdJ, PchA and FptX expression in presence of biological metals

To study the expression of different proteins belonging to the PVD and PCH iron uptake pathway, the genes *pvdJ* (PVD biosynthesis) *pchA* (PCH biosynthesis) and *fptX* (PCH₂-Fe transport across the inner membrane) have been tagged to mCherry in the laboratory by Dr. Olivier Cunrath, being the mCherry sequence integrated into the chromosomal DNA, at the 5' of the genes, to obtain PAO1 *pvdJ-mCherry*, *pchA-mCherry* and *fptX-mCherry* strains (Table S1).

Cell culture and metal incubation

These strains were incubated in LB Broth medium O/N, washed twice in 2 volumes of CAA medium and incubated during 16 h in CAA. Then the cultures were diluted to an OD₆₀₀ = 0,01 in CAA, aliquoted 200 µl/well in a 96 well plate (Greiner, PS flat-bottomed microplate), and incubated in presence of different concentration of Fe⁺³, Co⁺², Ni⁺², Cu⁺², Mn⁺² and Zn⁺² (10 µl of

metal solution for each sample/well). The range of concentration for each metal changed in function of their effect, although they were initially tested in a range of concentration between 0.5 μM to 200 μM . All conditions were performed in technical and biological triplicates. The incubation of the 96 well plate was performed in the TECAN Infinite® M200 microplate reader. The fluorescence intensity of mCherry signal (excitation/emission wavelengths 570 nm / 610 nm) and the $\text{OD}_{600 \text{ nm}}$ were monitored each 30 min during 35h, at 30 °C with agitation. At last, the values of fluorescence corresponding to the mCherry signal were represented as a function of bacterial growth ($\text{OD}_{600 \text{ nm}}$) and plotted against the time of incubation.

5. Detection of metals transported by PCH by Inductively Coupled Plasma Atomic Emission Spectroscopy (ICP-AES)

Preparation of PCH-metal complexes

The PCH used was synthesized according to previously published protocol in Zamri and Abdallah, 2000. For this experiment, PCH was diluted in methanol 100% to prepare a stock at 20 mM. The remaining PCH solution was kept at -20 °C during one week maximum.

The complexes siderophore-metal were generated by mixing the PCH solution with FeCl_3 , CoCl_2 , NiCl_2 , and ZnCl_2 in methanol in a molar ratio of 2:1 for PCH:metal, and 1:1 for PVD:Fe . They were incubated during 15 min at room temperature (RT), and diluted with Tris HCl 50 mM pH 8 to a final concentration of 4 mM (Fig. M3).

Kinetic

Concerning the PCH pathway, *P. aeruginosa* $\Delta\text{pvdF}\Delta\text{pchA}$ strain, unable to produce PVD and PCH, and $\Delta\text{pvdF}\Delta\text{pchA}\Delta\text{fptA}$ strain, unable to produce any siderophore and with no expression of the outer membrane transporter FptA, were incubated in 5 ml of LB Broth medium at 30 °C and 220 rpm during 24 h. Then they were washed twice in 2 volumes of CAA, and cultured 16 h at 30 °C in agitation. Concerning the PVD pathway the strains used were $\Delta\text{pvdF}\Delta\text{pchA}$ and $\Delta\text{pvdF}\Delta\text{pchA}\Delta\text{fpvA}\Delta\text{fpvB}$, without the FpvA and FpvB transporters expressed.

The cell cultures (samples) were diluted to obtain the $\text{OD}_{600 \text{ nm}} = 1.5$ in CAA in a volume of 10 ml (in 50 ml Falcon tubes), and incubated 15 min at 30 °C. 10 μl of PCH₂-metal or of the metal alone were added to the samples, to a final concentration of 4 μM , and at this point the kinetic starts. All conditions were done in triplicated for each time, t_0 , t_{15} , and t_{30} min (Fig. M2). After the addition

of PCH₂-metal and metal alone, the samples at t₀ were placed on ice and centrifuged at 4 °C to discard the supernatant. The samples at t₁₅ and t₃₀ were incubated at 30 °C with agitation and after the incubation times, the same process as for the t₀ is repeated. Then the bacterial pellets were washed with ultra-pure water and dried at 50 °C during 48 h. The cells were mineralized by the addition of 1 ml of nitric acid (HNO₃) 70%, and incubated at RT during 72 h. They were shaken very carefully, incubated again for 2 h, and H₂O was added to dilute the HNO₃ to 1%. These solutions were incubated for 24 h at RT. Finally, the supernatants were filtered (0,22 μm) and kept at 4 °C in the dark until the ICP-AES measures, carried out by the ICP-AES platform (ECPM, Strasbourg) by Pascale Ronot. The results were then analysed, at the following wavelengths (nm) depending on the metal: Co (228.62), Cu (327.40), Fe (238.20), Mn (257,61), Ni (231.60), and Zn (213.86).

Solutions in Tris 50mM pH8:
 8mM PCH (diluted in methanol)
 4mM Metal

Each tube: 10 ml CAA at OD_{600 nm} = 1,5 + 10μl PCH₂-metal

In presence of each metal → 3 times of incubation (t₀, t_{15 min} and t_{30 min}). 3 replicas

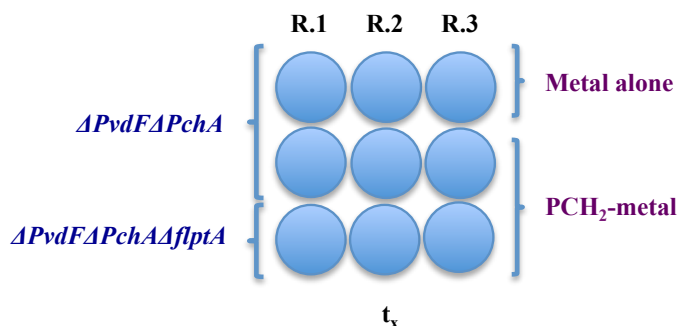


Figure M2. Scheme of all conditions prepared for the metal detection by ICP-AES. The blue circles represent the falcon tubes used. 'R.n' represents the number of the replica for each incubation time. 't_x' represents a specific incubation time: t₀, t_{15 min} and t_{30 min}.

6. Inhibition of siderophore-⁵⁵Fe transport by siderophore-metal competition

We studied the inhibition of PVD-iron and PCH-iron uptake by PVD and PCH in complex with other biological metals.

⁵⁵FeCl₃ was obtained from Perkin Elmer Life and Analytical Sciences (Billerica, MA, USA) with a specific activity of 10.18 Ci/g for a concentration of 71.1 mM.

PCH₂-metal and PVD-metal complexes formation

To generate the complexes, siderophore and metal were mixed at a ratio 20:1 (PCH:metal) and 4:1 (PVD:metal), to ensure that all the metal is complexed with the siderophore. For each siderophore, three different complexes were prepared: siderophore-⁵⁵Fe at 20 μM, siderophore-metal at 20 μM and siderophore-metal at 200 μM to obtain an excess of 10 equivalents compared to the siderophore-⁵⁵Fe. The necessary volumes of siderophore and metal stocks solutions were mixed in methanol and incubated for 15 min at RT. Then Tris HCl 50 mM pH 8 was added to adjust the volume to the required concentration.

Cell culture preparation

PAO1 *ΔpvdFΔpchA* and *ΔpvdFΔpchAΔfptA* (Table S1) were pre-incubated in 5 ml of LB O/N at 30 °C with agitation (220 rpm), washed by 2 volumes of CAA and incubated at 30 °C during 24 h. Each strain was then diluted to an OD_{600 nm} of 0,1 in 10 ml of CAA, and incubated for 16 h. They were washed in 1 volume of Tris HCl 50 mM pH 8 and the OD was adjusted to 1. 1 ml of the cell cultures was added in each tube required for the experiment (Fig. M3). Two different tubes were prepared for the each condition to prepare the negative controls. The negative controls were supplemented with 10 μl of CCCP 20 mM and incubated for 10 minutes before the addition of the siderophore-metal complexes, and the other tubes kept at 37 °C until metal addition. CCCP (Sigma) is a protonophore that disrupt the proton gradient by carrying protons across a membrane, inhibiting the transporters that use the proton-motive force, as FpvA or FptA. It was used in the negative control, since this proton gradient is required for the active transport of siderophores.

Conditions

Strains and Conditions for PCH₂-⁵⁵Fe and PCH-metal competition (Fig. M4):

ΔpvdFΔpchA + 200 nM PCH₂-Fe (no competition)

ΔpvdFΔpchBAΔfptA + 200 nM PCH₂-Fe (negative control)

ΔpvdFΔpchA + 200 nM PCH₂-Fe + 200 nM PCH₂-metal (competition with other PCH₂-metal at the same concentration)

ΔpvdFΔpchA + 200 nM PCH₂-Fe + 2 μM PCH₂-metal (competition with other PCH₂-metal at 10-fold excess)

+CCCP at 200 μM as a negative control.

Strains and Conditions for PVD-⁵⁵Fe and PVD-metal competition:

ΔpvdFΔpchA + 200 nM PVD-Fe

ΔpvdFΔpchA + 200 nM PVD-Fe + 200 nM PVD-metal

ΔpvdFΔpchA + 200 nM PVD-Fe + 2 μM PVD-metal

+CCCP at 200 μ M as a negative control.

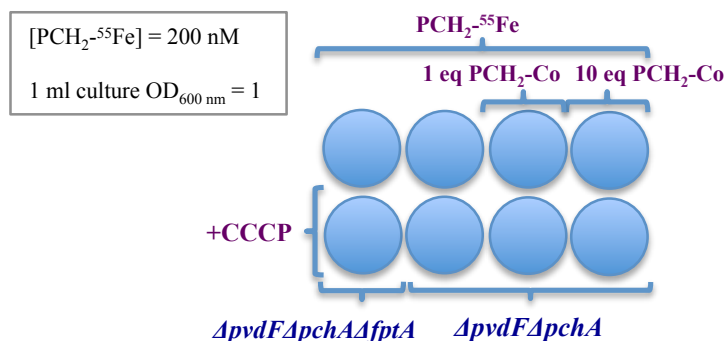


Figure M3. Scheme showing all conditions tested for this competition experiment using Co. Circles represent the 50 ml Falcon tubes. See text for more information.

Kinetic of transport and ⁵⁵Fe measure

10 μ l of PCH₂-metal or PVD-metal complexes were added and the kinetic started. To measure the concentration of ⁵⁵Fe that has been transported into the cells, 100 μ l aliquots were taken at different incubation times: t₀, t₃, t₆, t₉, t₁₂, t₁₅, and t₃₀ (min) and added to 100 μ l of cold (4 °C) Tris HCl 50 mM pH 8 to stop iron transport. At the end of the kinetic the cells were centrifuged, the supernatant discarded, and 900 μ l of liquid scintillator was added to each tube containing the pellets. As positive control, liquid scintillator was also added to 5 μ l PCH₂-⁵⁵Fe alone at 200 nM. After 1 h of incubation in the dark, the ⁵⁵Fe was measured by liquid scintillation counting, 3H / 10' (results obtained were in dpm, disintegrations per minute).

7. Proteome

Cell culture and sample preparation

PAO1-*wt*, *ΔpvdFΔpchA* and *ΔpchR* strains were pre-incubated in LB Broth medium O/N at 30 °C, washed twice in 2 volumes of CAA and incubated at 30 °C in CAA during 16 h. The cells were diluted in 10 ml of CAA to the OD_{600 nm} = 0.1. Three conditions were tested: one control without metal, the second with 10 μ M of Fe and the third with 10 μ M of Co (50 μ M of Co in the case of *ΔpvdFΔpchA*). All samples were incubated during 8 h at 30 °C in agitation (220 rpm). Then 5.10⁸ cells (corresponding to 0.5 ml of cell at OD_{600 nm} = 1) were centrifuged at 4 °C and the pellet sent

to the Dirk Bumman's group (Basel, Switzerland) to perform Shotgun proteomic. Each condition was prepared in triplicate.

8. MBP-PchR purification

Cell culture and sample preparation

One single colony of *E. coli DH5 α -pME7180* (Table S1), containing the recombinant protein PchR (Michel et al., 2005) tagged with MBP at the N-terminal domain, was pre-incubated O/N in LB Broth medium supplemented with 100 μ g/ml of ampicillin at 37 °C with agitation (220 rpm). 1 L of LB medium + ampicillin 100 μ g/ml was inoculated at this pre-culture to obtain OD_{600 nm} = 0,05. The culture was incubated at 30 °C until the OD_{600 nm} \approx 0,8, and then 0,3 mM of IPTG was then added to allow the overexpression of MBP-PchR. After 2 h 15 min of incubation at 30 °C the cell culture was centrifuged to remove the supernatant and the pellet was stored at -80 °C.

The cellular pellet was thawed on ice, weight, and 20 ml of lysis solution (50 mM pH 7,5 Tris HCl supplemented with 1 tablet of cOmpleteTM EDTA-free protease inhibitor) was added. The mixture was vortexed and homogenised using a Potter-Elvehjem. The cells were disrupted by sonication (3 times, 30 s each time, at pulse of 70% of amplitude) and the lysate was ultracentrifuged at 4 °C during 15 min at 40 k to pellet all membranes or cell fractions.

Note: All chromatographies performed to purify the protein MBP-PchR were carried out using the ÄKTA System, and all buffers have to be prepared in MilliQ[®] H₂O, filtered (0,22 μ m) and degased before use.

Affinity chromatography

The column used was MBPTrap HP 5ml, which allows the affinity purification of recombinant proteins tagged with maltose binding protein (MBP) (Table M1).

The column was washed by ethanol and MilliQ H₂O, and equilibrated with Buffer A1 (Table M3) before the sample injection. The supernatant obtained after ultracentrifugation was diluted 2X with Buffer A1, injected into the ÄKTA system through a filter of 0,22 μ m, and loaded onto the column at a flow rate of 2 ml/min. The MBP-PchR protein was eluted by addition of Buffer B1 containing maltose (flow rate of 2 ml/min). The composition of the eluates was analysed on a polyacrylamide gel and the fractions containing the MBP-PchR (band at 75 KDa, the size of MBP-PchR) were

dialyzed in Buffer A2 (Table M1) using a dialysis cassette from Thermo Fisher O/N at 4 °C, to decrease the NaCl concentration.

Anionic exchange chromatography

We performed a second chromatography using the Mono QTM 5/50 GL 1ml column to improve the purification. The column was first cleaned with 2 M NaCl and 1 M NaOH, before equilibration with Buffer A2. The sample was injected and the PchR-MBP eluted by increasing the NaCl concentration until 1 M with the Buffer B2. The eluates of different fractions were analysed by polyacrylamide gel and the MBP-PchR then dialysed in Buffer A3 (Table M1), O/N at 4 °C. The flow rate used onto this column was 0,5 ml/min.

MBP-PchR quantification

The absorbance of the purified MBP-PchR sample was measured by NanoDropTM, and its concentration calculated using its ϵ ($8,97 \times 10^4 \text{ M}^{-1} \cdot \text{cm}^{-1}$) and MW (72,66 KDa), obtained in ExPASy ProtParam tool.

Buffers	Chromatography	Columns	Composition of buffer
<i>Buffer A1</i>	Affinity	MBPTrap HP 5 ml (GE Healthcare)	20 mM pH 7,5 Tris HCl, 600 mM NaCl, 1 mM EDTA, 1 mM DTT, 5 % Glycerol
<i>Buffer B1</i>	Affinity	MBPTrap HP 5 ml (GE Healthcare)	20 mM pH 7,5 Tris HCl, 600 mM NaCl, 1 mM EDTA, 1 mM DTT, 5 % Glycerol, 10 mM Maltose
<i>Buffer A2</i>	Anionic Exchange	Mono Q TM 5/50 GL 1 ml (GE Healthcare)	20 mM pH 7,5 Tris HCl, 100 mM NaCl, 1 mM EDTA, 1 mM DTT, 5 % Glycerol
<i>Buffer B2</i>	Anionic Exchange	Mono Q TM 5/50 GL 1 ml (GE Healthcare)	20 mM pH 7,5 Tris HCl, 1 M NaCl, 1 mM EDTA, 1 mM DTT, 5 % Glycerol
<i>Buffer A3</i>	Dialysis		20 mM Tris HCl pH 7,5, 300 mM NaCl, 1 mM DTT, 1 mM β -mercaptoethanol, 10 % Glycerol

Table M1. Buffers used for the purification of the MBP-PchR fusion protein. All of them had to be filtered and degased before use.

9. Binding between MBP-PchR and PCH₂-metal

We adapted the protocol from Lin et al., 2013 to study the binding between MBP PchR and different ligands: PCH₂-metal, metal, apo-PCH. Metals tested: Fe, Co, Ni, Cu, Mn and Zn.

Samples preparation

The PCH-metal complexes were generated by mixing the PCH solution at 20 mM with FeCl₃, CoCl₂, NiCl₂, and ZnCl₂ in methanol in a molar ratio of 2:1 (PCH:metal), to obtain a final concentration of 500 μM. They were incubated during 15 min at RT, and finally Tris HCl 50 mM pH 8 was added to adjust the volume to the desired concentration. They were prepared just before the binding experiment. Apo-PCH was prepared by adding EDTA (1:1) to avoid any metal binding to the siderophore.

1 ml of 10 μg/ml of purified MBP-PchR was prepared in the assay buffer (20 mM HEPES pH 7.5 and 40 mM NaCl), and incubated with 10 mM of DTT at 25 °C for 10 min.

Fluorescence measurements and K_d

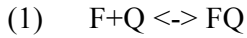
Fluorescence measurements were carried out with a spectrofluorometer Fluorolog®. Excitation was set at 280 nm to measure the fluorescence emitted by the tryptophans of MBP-PchR. The emission spectra were recorded in the range 290–480 nm, with a slit-width of 5 and 10 nm for excitation and emission, respectively. All measures were carried out at 25 °C under gentle agitation.

1 μl of ligand at 500 μM (apo-PCH, metal or PCH-metal) was added to the PchR sample and the solution incubated for 2 min at RT just before the fluorescence measurements. Then, 1 μl of the same ligand was added again to the same sample to increase the ligand concentration 0.5 μM. The solution was incubated for 2 min at RT before its fluorescence measurements. This step was repeated until test all concentrations needed. The concentrations vary. See results in Figures R6, R7 and R8.

Tryptophan emits usually at 340 nm. The binding of MBP-PchR to its ligands should induce a conformational change and thus a change in the fluorescence emission of tryptophans. K_d was determined by plotting the relative fluorescence intensity (F₀/F) of MBP-PchR against the concentration of the ligand. 'F₀/F' is the ratio between the initial MBP-PchR emission fluorescence (F₀) divided by the fluorescence emitted after the addition of the ligand (F), at 340 nm. The data were fitted to a linear regression from which a K_d value was calculated.

K_d calculation:

To calculate the K_d we followed the Stern-Volmer equation (Stern and Volmer, 1919):



‘F’ is the fluorophore, MBP-PchR in this case, and ‘Q’ the quencher that corresponds to the ligand. The Stern-Volmer constant K_{sv} is equivalent to K_a (association constant), which can be derived from the equation (1):

$$(2) \quad [FQ] / [F] [Q] = K_{sv} = K_a$$

‘[FQ]’ is the concentration of the quencher + fluorophore, ‘[F]’ the free fluorophore concentration, and ‘[Q]’ the quencher concentration. The total fluorophore ($[F]_0$) will be then:

$$(3) \quad [F]_0 = [F] + [FQ]$$

From this equation (3) and the equation (2), K_a can be calculated:

$$(4) \quad K_a = [FQ] / [F] [Q] - 1 / [Q] \Rightarrow [FQ] / [F] = 1 + K_a [Q]$$

If we assume the [F] is proportionated to the intensity of fluorescence:

$$(5) \quad [FQ] / [F] = F_0 / F = 1 + K_a [Q]$$

If the relative fluorescence (F_0 / F) is plotted against the [Q], and as K_d is the dissociation constant, it means it is the reverse reaction than K_a :

$$(6) \quad K_d = 1 / K_a$$

Controls: Fluorescence emission of different concentrations of all metals and PCH-metals used was recorded in the absence of MBP-PchR proteins as a negative control. Also the fluorescence emission of MBP-PchR were measured each 30 min during the time of experiment to verify that there was not a degradation of the protein.

10. Construction of expression plasmids carrying PchR box & Fur box

We have constructed expression vectors containing the PCH operons promoters carrying the DNA specific recognition sequences for the transcriptional repressor Fur and the transcriptional activator PchR. To obtain the expression vectors, we used the pSEVA631 plasmid (Standard European Vector Architecture), and we cloned the promoters of the *pchD* and *pvdS* genes fused to *mCherry*, to quantify the level of expression controlled by the regulatory boxes present in the promoters (Fig. M4).

All vectors were obtained from two steps of PCRs followed by an enzymatic restriction and ligation. In the first step of PCR, mCherry sequence was amplified from the plasmid pLG3 as template, by the primers listed in the Table S2. The reverse primer allowed the insertion of a restriction site *HindIII*. The *pchD* and *pvdS* promoters carrying a PchR box and a Fur box, or only the Fur box sequence (Table S3) was amplified from the *P. aeruginosa* PAO1 genome using the primers listed in the Table S2, inserting a *EcoRI* restriction site at the 5' extremity of all sequences. Then by another step of PCRs, the mCherry sequence was fused to the 3' extremity of all DNA promoter sequence amplified, to obtain the different promoter-mCherry sequences. The forward primer specific for each promoter sequence and the reverse primer used for the mCherry amplification were used to amplify these constructions. The fusion was possible because the reverse primer of all promoter fragments amplified contained in their 3' extremity a homolog sequence of 30 nt to the first 30 nt of mCherry sequence. Then the different promoter-mCherry sequences were integrated in the pSEVA631 vector after enzymatic restriction using *EcoRI* and *HindIII*, and ligation by T4 ligase, generating the plasmids pAYC5, pAYC6, or pPF3 (Table S1). pSEVA631 containing only the mCherry sequence was constructed to use it as a control. All final vector sequences were verified, including the control vector (without the presence of any promoter sequence) by the 'supreme Sanger sequencing service' of GATC Biotech.

***P. aeruginosa* transformation**

Transformed *E. coli* Top10 with the plasmids pAYC5, pAYC6, or pPF3, and the helper strain HB101/pME487 (Table S1) were incubated O/N at 37 °C, whereas the *P. aeruginosa* strains to be mutated (PAO1-wt, $\Delta pvdF\Delta pchA$, and $\Delta PchR$) were incubated at 43 °C, to weaken the restriction system of the recipient. Then *P. aeruginosa* PAO1 strain, the *E. coli* TOP10 and the HB101 were mixed (1:1:1), deposited as a drop on a LB agar plate, and incubated at 37 °C during 3 h. Cells were taken, diluted and spread in a LB plated supplemented with 10 µg/ml of chloramphenicol + 30 µM of gentamicin. The resulted colonies are cells that have integrated the expression plasmid.

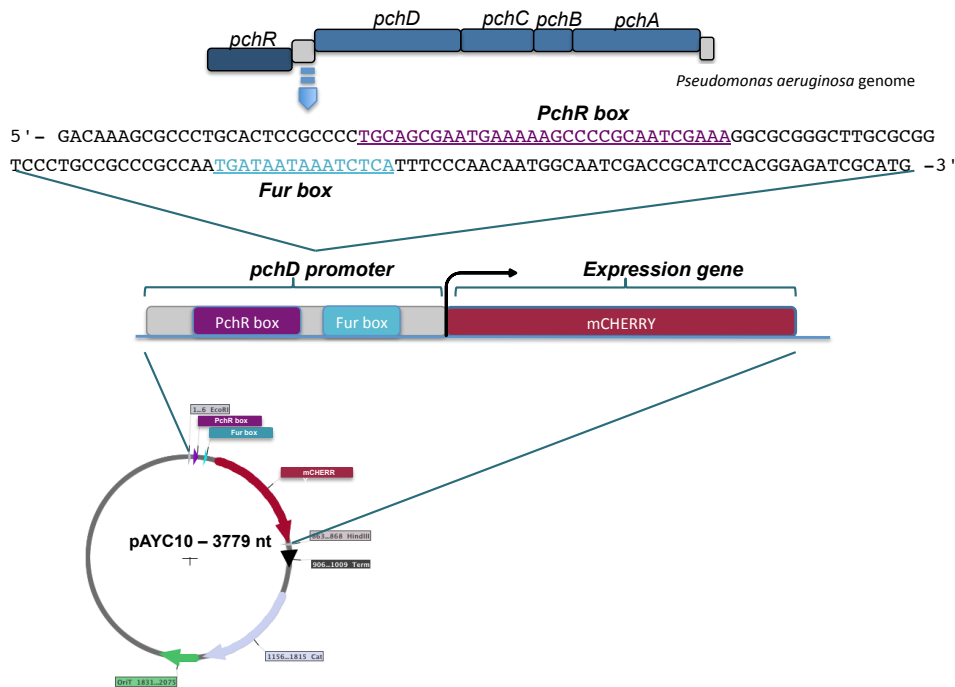


Figure M4. Construction of the expression vector pAYC5. See text for more details.

The experimental procedure for the expression analysis was the same as described in ‘Cell culture and metal incubation’ of the section ‘4. PvdJ, PchA and FptX expression in presence of biological metals’. PAO1 wt cells containing these plasmids were incubated without metal, in presence of 0,5 μ M of Co or Fe, and in presence of 5 μ M of Co or Fe.

11. Specific recognition of MBP-PchR to the PchR box, by electrophoresis mobility shift assay (EMSA)

ATP, [γ - 32 P]- 3000Ci/mmol 10mCi/ml Lead, 100 μ Ci

DNA sequences

Two fragments of the *pchD* promoter were amplified by PCR using the *P. aeruginosa* PAO1 genome as template and using Phusion polymerase: one fragment containing the PchR box established by Michel et al., 2015, using the *primers* Fwd.32p-PchRbox which hybridizes 34 bp before the PchR box, and the Rev.32p; a second fragment, which does not carry the PchR box, using the *primers* Fwd.32p-PchRnobox and Rev.32p (Table S2).

Radiolabeling

Both DNA fragments were radiolabeled with ATP γ - ^{32}P at 10 mCi/ml by incubation with T4 polynucleotide kinase (PNK) during 1 h at 37 °C, and purified by micro Bio-Spin chromatography columns from Bio-Rad. For the band shift analysis we used 10.000 counts per minute (cpm) of labelled DNA per condition.

EMSA

Radioactive DNA fragments, with and without the PchR box were incubated with different concentrations of MBP-PchR and in presence of PCH₂-Fe, PCH or Fe in buffer analysis (20 mM HEPES, 40 mM NaCl). All samples were incubated during 30 min at 30 °C, loaded into a native 6 % acrylamide gel, and run at 235 V during 2 h 30 min. TBE buffer at pH8 (70 mM Tris, 90 mM boric acid and 5 mM EDTA) was used as gel and electrode buffer. The gel was pre-run for at least 30 min before loading samples. Then the gel was dried, and the radioactive bands were revealed using the phosphor imaging system 'Typhoon'.



Conclusions

PVD and PCH are two siderophores produced by *P. aeruginosa* in order to get access to iron, a biological metal considered as an essential nutriment. During this thesis we obtained major results concerning the molecular mechanisms regulating the expression of the different proteins involved in these two pathways. Moreover, we have also shown how Co, a biological metal, interferes with iron uptake involving the siderophore PCH.

We have highlighted the differences in the molecular mechanisms involved in the expression of both pathways, PVD and PCH. Both systems utilize positive auto-regulation loops: the sigma/anti-sigma factor for PVD (PvdS/FpvI/FpvR) and the AraC-type regulator PchR for PCH. Both pathways are also negatively regulated by the transcriptional repressor Fur. All these regulators work together, allowing *P. aeruginosa* to switch from one pathway to another depending on the environment and iron concentrations. Under strongly iron-depleted conditions, PVD is produced mostly independently of the positive auto-regulation loop, whereas PCH production still requires PCH-Fe interaction with PchR. This mechanism results in a lower production of PCH, being PVD the predominant produced siderophore. When iron concentration increases slightly, both positive auto-regulation modes become important. Nevertheless, Fur represses more tightly *pvdS* expression than *pchR*, making the PVD production decrease more quickly than the PCH production. In iron-replete conditions, both pathways are repressed by Fur. In the case of the PCH pathway, Fur is able to compete with PchR and bind the Fur box, as well as the PchR box and consequently completely repress the expression of the PCH pathway.

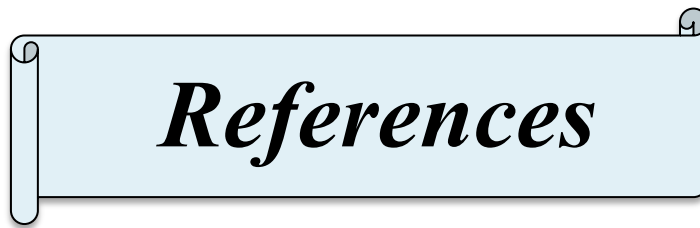
In the frame of this thesis, we were able to show that among the different biological metal tested, only Co had a significant effect on the proteins expression of both PVD and PCH pathways, but these effects were significantly stronger on the PCH pathway compared to the PVD one: PCH production was affected in an equivalent manner by Fe^{3+} and Co^{2+} , and at a lower level by the presence of Ni^{2+} .

We have also shown that Co is transported efficiently and specifically by FptA, the ferri-PCH outer membrane transporter. Due to some similarities between Fe and Co (similar radii, oxidation states, molecular weight, and probably similar tridimensional interaction of $\text{PCH}_2\text{-Fe}$ complex compared to $\text{PCH}_2\text{-Co}$), Co can interfere with Fe at the level of transport (FptA) and regulation (PchR), having an impacting on the expression of the PCH pathway and promoting a repression effect. Therefore, the uptake of Co observed *via* the PCH pathway does not mean that this uptake has a biological significance. The Co transport observed is probably due to a contamination of PCH pathway by Co, which is able to inhibit the Fe uptake.

We saw that the presence of Co in the bacterial growth media decreases the expression of the genes under the control of PchR, the transcriptional regulator that is essential for the PCH genes expression, and also that PCH₂-Co interacts with PchR with an affinity close to the affinity for PCH₂-Fe. We propose that this effect of Co on the expression of the proteins belonging to the PCH pathway may be due to an inability of PchR-PCH-Co complex to bind to the PchR boxes, even though another possibility is that PchR-Pch-Co binds to the PchR boxes in a way not efficient enough to induce the gene expression as observed with PchR-PCH-Fe.

Moreover, PchR seems to have a more complex activity as initially thought, by affecting also the expression of several networks linked to the PCH production, like sulfur/cysteine metabolism, oxydo-reduction and *Quorum sensing*. This network of regulation *via* PchR and the importance of sulfur/cysteine metabolism for PCH biosynthesis let us suggest that the energetic cost of the biosynthesis of this siderophore is not much lower than the PVD, as it has been thought.

In addition, our study using proteomic and transcriptomic approaches highlighted as well other genes than those of the PCH pathway, regulated by the presence of Co, like T6SS, RcnR and RcnA or the non-coding RNA, ErsA.



References

Ackerley, D.F., Caradoc-Davies, T.T., and Lamont, I.L. (2003). Substrate specificity of the nonribosomal peptide synthetase PvdD from *Pseudomonas aeruginosa*. *J. Bacteriol.* *185*, 2848–2855.

Adler, C., Corbalán, N.S., Seyedsayamdost, M.R., Pomares, M.F., de Cristóbal, R.E., Clardy, J., Kolter, R., and Vincent, P.A. (2012). Catecholate siderophores protect bacteria from pyochelin toxicity. *PLoS ONE* *7*.

Adrait, A., Jacquamet, L., Le Pape, L., Gonzalez de Peredo, A., Aberdam, D., Hazemann, J.L., Latour, J.M., and Michaud-Soret, I. (1999). Spectroscopic and saturation magnetization properties of the manganese- and cobalt-substituted Fur (ferric uptake regulation) protein from *Escherichia coli*. *Biochemistry (Mosc.)* *38*, 6248–6260.

Aisen, P., Enns, C., and Wessling-Resnick, M. (2001). Chemistry and biology of eukaryotic iron metabolism. *Int. J. Biochem. Cell Biol.* *33*, 940–959.

Albrecht-Gary, A.-M., Blanc, S., Rochel, N., Ocaktan, A.Z., and Abdallah, M.A. (1994). Bacterial iron transport: coordination properties of pyoverdine PaA, a peptidic siderophore of *Pseudomonas aeruginosa*. *Inorg. Chem.* *33*, 6391–6402.

Alexander, J.W. (2009). History of the medical use of silver. *Surg. Infect.* *10*, 289–292.

Ambrosi, C., Tiburzi, F., Imperi, F., Putignani, L., and Visca, P. (2005). Involvement of AlgQ in transcriptional regulation of pyoverdine genes in *Pseudomonas aeruginosa* PAO1. *J. Bacteriol.* *187*, 5097–5107.

de Amorim, G.C., Prochnicka-Chalufour, A., Delepelaire, P., Lefèvre, J., Simenel, C., Wandersman, C., Delepierre, M., and Izadi-Pruneyre, N. (2013). The structure of HasB reveals a new class of TonB protein fold. *PLoS One* *8*, e58964.

Andreini, C., Banci, L., Bertini, I., and Rosato, A. (2006). Counting the zinc-proteins encoded in the human genome. *J. Proteome Res.* *5*, 196–201.

Andreini, C., Bertini, I., Cavallaro, G., Holliday, G.L., and Thornton, J.M. (2008). Metal ions in biological catalysis: from enzyme databases to general principles. *J. Biol. Inorg. Chem. JBIC Publ. Soc. Biol. Inorg. Chem.* *13*, 1205–1218.

Andrews, S.C., Robinson, A.K., and Rodríguez-Quiñones, F. (2003). Bacterial iron homeostasis. *FEMS Microbiol. Rev.* *27*, 215–237.

Argüello, J.M., González-Guerrero, M., and Raimunda, D. (2011). Bacterial transition metal P(1B)-ATPases: transport mechanism and roles in virulence. *Biochemistry (Mosc.)* *50*, 9940–9949.

Argüello, J.M., Raimunda, D., and González-Guerrero, M. (2012). Metal transport across biomembranes: emerging models for a distinct chemistry. *J. Biol. Chem.* *287*, 13510–13517.

Axelsen, K.B., and Palmgren, M.G. (1998). Evolution of substrate specificities in the P-type ATPase superfamily. *J. Mol. Evol.* *46*, 84–101.

Balasubramanian, D., Schneper, L., Kumari, H., and Mathee, K. (2013). A dynamic and intricate regulatory network determines *Pseudomonas aeruginosa* virulence. *Nucleic Acids Res.* *41*, 1–20.

- Balasubramanian, D., Kumari, H., Jaric, M., Fernandez, M., Turner, K.H., Dove, S.L., Narasimhan, G., Lory, S., and Mathee, K. (2014). Deep sequencing analyses expands the *Pseudomonas aeruginosa* AmpR regulon to include small RNA-mediated regulation of iron acquisition, heat shock and oxidative stress response. *Nucleic Acids Res.* *42*, 979–998.
- Balasubramanian, R., Kenney, G.E., and Rosenzweig, A.C. (2011). Dual pathways for copper uptake by methanotrophic bacteria. *J. Biol. Chem.* *286*, 37313–37319.
- Barbier, M., Damron, F.H., Bielecki, P., Suárez-Diez, M., Puchałka, J., Albertí, S., Dos Santos, V.M., and Goldberg, J.B. (2014). From the environment to the host: re-wiring of the transcriptome of *Pseudomonas aeruginosa* from 22°C to 37°C. *PLoS One* *9*, e89941.
- Barken, K.B., Pamp, S.J., Yang, L., Gjermansen, M., Bertrand, J.J., Klausen, M., Givskov, M., Whitchurch, C.B., Engel, J.N., and Tolker-Nielsen, T. (2008). Roles of type IV pili, flagellum-mediated motility and extracellular DNA in the formation of mature multicellular structures in *Pseudomonas aeruginosa* biofilms. *Environ. Microbiol.* *10*, 2331–2343.
- Barker, K.D., Barkovits, K., and Wilks, A. (2012). Metabolic flux of extracellular heme uptake in *Pseudomonas aeruginosa* is driven by the iron-regulated heme oxygenase (HemO). *J. Biol. Chem.* *287*, 18342–18350.
- Bassford, P.J., and Kadner, R.J. (1977). Genetic analysis of components involved in vitamin B12 uptake in *Escherichia coli*. *J. Bacteriol.* *132*, 796–805.
- Battersby, A.R., and Sheng, Z.C. (1982). Preparation and spectroscopic properties of CoIII-isobacteriochlorins: relationship to the cobalt-containing proteins from *Desulphovibrio gigas* and *D. desulphuricans*. *J. Chem. Soc. Chem. Commun.* *0*, 1393–1394.
- Battistoni, A. (2003). Role of prokaryotic Cu,Zn superoxide dismutase in pathogenesis. *Biochem. Soc. Trans.* *31*, 1326–1329.
- Beare, P.A., For, R.J., Martin, L.W., and Lamont, I.L. (2003). Siderophore-mediated cell signalling in *Pseudomonas aeruginosa*: divergent pathways regulate virulence factor production and siderophore receptor synthesis. *Mol. Microbiol.* *47*, 195–207.
- Beinert, H., Holm, R.H., and Münck, E. (1997). Iron-sulfur clusters: nature's modular, multipurpose structures. *Science* *277*, 653–659.
- Bhakta, M.N., and Wilks, A. (2006). The mechanism of heme transfer from the cytoplasmic heme binding protein PhuS to the delta-regioselective heme oxygenase of *Pseudomonas aeruginosa*. *Biochemistry (Mosc.)* *45*, 11642–11649.
- Billings, N., Millan, M., Caldara, M., Rusconi, R., Tarasova, Y., Stocker, R., and Ribbeck, K. (2013). The extracellular matrix Component Psl provides fast-acting antibiotic defense in *Pseudomonas aeruginosa* biofilms. *PLoS Pathog.* *9*, e1003526.
- Bjarnsholt, T. (2013). The role of bacterial biofilms in chronic infections. *APMIS. Suppl.* 1–51.
- Blériot, C., Effantin, G., Lagarde, F., Mandrand-Berthelot, M.-A., and Rodrigue, A. (2011). RcnB is a periplasmic protein essential for maintaining intracellular Ni and Co concentrations in *Escherichia coli*. *J. Bacteriol.* *193*, 3785–3793.

- Borths, E.L., Locher, K.P., Lee, A.T., and Rees, D.C. (2002). The structure of Escherichia coli BtuF and binding to its cognate ATP binding cassette transporter. *Proc. Natl. Acad. Sci. U. S. A.* *99*, 16642–16647.
- Boukhalfa, H., and Crumbliss, A.L. (2002). Chemical aspects of siderophore mediated iron transport. *Biometals Int. J. Role Met. Ions Biol. Biochem. Med.* *15*, 325–339.
- Branda, S.S., Vik, S., Friedman, L., and Kolter, R. (2005). Biofilms: the matrix revisited. *Trends Microbiol.* *13*, 20–26.
- Brandel, J., Humbert, N., Elhabiri, M., Schalk, I.J., Mislin, G.L.A., and Albrecht-Gary, A.-M. (2012). Pyochelin, a siderophore of *Pseudomonas aeruginosa*: Physicochemical characterization of the iron(III), copper(II) and zinc(II) complexes. *Dalton Trans.* *41*, 2820–2834.
- Braud, A., Hannauer, M., Mislin, G.L.A., and Schalk, I.J. (2009a). The *Pseudomonas aeruginosa* pyochelin-iron uptake pathway and its metal specificity. *J. Bacteriol.* *191*, 3517–3525.
- Braud, A., Hoegy, F., Jezequel, K., Lebeau, T., and Schalk, I.J. (2009b). New insights into the metal specificity of the *Pseudomonas aeruginosa* pyoverdine-iron uptake pathway. *Environ. Microbiol.* *11*, 1079–1091.
- Braud, A., Geoffroy, V., Hoegy, F., Mislin, G.L.A., and Schalk, I.J. (2010). Presence of the siderophores pyoverdine and pyochelin in the extracellular medium reduces toxic metal accumulation in *Pseudomonas aeruginosa* and increases bacterial metal tolerance. *Environ. Microbiol. Rep.* *2*, 419–425.
- Braun, V., and Hantke, K. (2011). Recent insights into iron import by bacteria. *Curr. Opin. Chem. Biol.* *15*, 328–334.
- Braymer, J.J., and Giedroc, D.P. (2014). Recent developments in copper and zinc homeostasis in bacterial pathogens. *Curr. Opin. Chem. Biol.* *19*, 59–66.
- Brennan, B.A., Alms, G., Nelson, M.J., Durney, L.T., and Scarrow, R.C. (1996). Nitrile Hydratase from *Rhodococcus rhodochrous* J1 Contains a Non-Corrin Cobalt Ion with Two Sulfur Ligands. *J. Am. Chem. Soc.* *118*, 9194–9195.
- Brillet, K., Journet, L., Célia, H., Paulus, L., Stahl, A., Pattus, F., and Cobessi, D. (2007). A β strand lock exchange for signal transduction in TonB-dependent transducers on the basis of a common structural motif. *structure* *15*, 1383–1391.
- Brillet, K., Ruffenach, F., Adams, H., Journet, L., Gasser, V., Hoegy, F., Guillon, L., Hannauer, M., Page, A., and Schalk, I.J. (2012). An ABC transporter with two periplasmic binding proteins involved in iron acquisition in *Pseudomonas aeruginosa*. *ACS Chem. Biol.* *7*, 2036–2045.
- Brock, J.H., Williams, P.H., Licéaga, J., and Wooldridge, K.G. (1991). Relative availability of transferrin-bound iron and cell-derived iron to aerobactin-producing and enterochelin-producing strains of *Escherichia coli* and to other microorganisms. *Infect. Immun.* *59*, 3185–3190.
- Buchanan, S.K., Smith, B.S., Venkatramani, L., Xia, D., Esser, L., Palnitkar, M., Chakraborty, R., van der Helm, D., and Deisenhofer, J. (1999). Crystal structure of the outer membrane active transporter FepA from *Escherichia coli*. *Nat. Struct. Biol.* *6*, 56–63.

Budzikiewicz, H. (2004). Siderophores of the Pseudomonadaceae sensu stricto (fluorescent and non-fluorescent *Pseudomonas* spp.). *Fortschritte Chem. Org. Naturstoffe Prog. Chem. Org. Nat. Prod. Progres Dans Chim. Subst. Org. Nat.* 87, 81–237.

Cadioux, N., Bradbeer, C., Reeger-Schneider, E., Köster, W., Mohanty, A.K., Wiener, M.C., and Kadner, R.J. (2002). Identification of the periplasmic cobalamin-binding protein BtuF of *Escherichia coli*. *J. Bacteriol.* 184, 706–717.

Cantin, A.M., Hartl, D., Konstan, M.W., and Chmiel, J.F. (2015). Inflammation in cystic fibrosis lung disease: Pathogenesis and therapy. *J. Cyst. Fibros.* 14, 419–430.

Capdevila, D.A., Wang, J., and Giedroc, D.P. (2016). Bacterial strategies to maintain zinc metallostasis at the host-pathogen interface. *J. Biol. Chem.* jbc.R116.742023.

Carmeli, Y., Troillet, N., Eliopoulos, G.M., and Samore, M.H. (1999). Emergence of antibiotic-resistant *Pseudomonas aeruginosa*: comparison of risks associated with different antipseudomonal agents. *Antimicrob. Agents Chemother.* 43, 1379–1382.

Cass, L.G., and Wilcox, G. (1986). Mutations in the *araC* regulatory gene of *Escherichia coli* B/r that affect repressor and activator functions of AraC protein. *J. Bacteriol.* 166, 892–900.

Celia, H., Noinaj, N., Zakharov, S.D., Bordignon, E., Botos, I., Santamaria, M., Barnard, T.J., Cramer, W.A., Lloubes, R., and Buchanan, S.K. (2016). Structural insight into the role of the Ton complex in energy transduction. *Nature* 538, 60–65.

Cézard, C., Farvacques, N., and Sonnet, P. (2015). Chemistry and biology of pyoverdines, *Pseudomonas* primary siderophores. *Curr. Med. Chem.* 22, 165–186.

Chaloupka, R., Courville, P., Veyrier, F., Knudsen, B., Tompkins, T.A., and Cellier, M.F.M. (2005). Identification of functional amino acids in the Nramp family by a combination of evolutionary analysis and biophysical studies of metal and proton cotransport in vivo. *Biochemistry (Mosc.)* 44, 726–733.

Champion, O.L., Karlyshev, A., Cooper, I.A.M., Ford, D.C., Wren, B.W., Duffield, M., Oyston, P.C.F., and Titball, R.W. (2011). *Yersinia pseudotuberculosis* *mntH* functions in intracellular manganese accumulation, which is essential for virulence and survival in cells expressing functional Nramp1. *Microbiol. Read. Engl.* 157, 1115–1122.

Chaturvedi, K.S., Hung, C.S., Giblin, D.E., Urushidani, S., Austin, A.M., Dinauer, M.C., and Henderson, J.P. (2014). Cupric yersiniabactin is a virulence-associated superoxide dismutase mimic. *ACS Chem. Biol.* 9, 551–561.

Chen, Y., Jurkevitch, E., Bar-Ness, E., and Hadar, Y. (1994). Stability Constants of Pseudobactin Complexes with Transition Metals. *Soil Sci. Soc. Am. J.* 58, 390–396.

Chen, Y., Yuan, M., Mohanty, A., Yam, J.K.H., Liu, Y., Chua, S.L., Nielsen, T.E., Tolker-Nielsen, T., Givskov, M., Cao, B., et al. (2015). Multiple diguanylate cyclase-coordinated regulation of pyoverdine synthesis in *Pseudomonas aeruginosa*. *Environ. Microbiol. Rep.* 7, 498–507.

Cherrier, M.V., Martin, L., Cavazza, C., Jacquamet, L., Lemaire, D., Gaillard, J., and Fontecilla-Camps, J.C. (2005). Crystallographic and spectroscopic evidence for high affinity binding of

FeEDTA(H₂O)- to the periplasmic nickel transporter NikA. *J. Am. Chem. Soc.* *127*, 10075–10082.

Cherrier, M.V., Cavazza, C., Bochot, C., Lemaire, D., and Fontecilla-Camps, J.C. (2008). Structural characterization of a putative endogenous metal chelator in the periplasmic nickel transporter NikA. *Biochemistry (Mosc.)* *47*, 9937–9943.

Cherrier, M.V., Girgenti, E., Amara, P., Iannello, M., Marchi-Delapierre, C., Fontecilla-Camps, J.C., Ménage, S., and Cavazza, C. (2012). The structure of the periplasmic nickel-binding protein NikA provides insights for artificial metalloenzyme design. *J. Biol. Inorg. Chem. JBIC Publ. Soc. Biol. Inorg. Chem.* *17*, 817–829.

Chimento, D.P., Mohanty, A.K., Kadner, R.J., and Wiener, M.C. (2003). Substrate-induced transmembrane signaling in the cobalamin transporter BtuB. *Nat. Struct. Biol.* *10*, 394–401.

Chirpich, T.P., Zappia, V., Costilow, R.N., and Barker, H.A. (1970). Lysine 2,3-Aminomutase PURIFICATION AND PROPERTIES OF A PYRIDOXAL PHOSPHATE AND S-ADENOSYLMETHIONINE-ACTIVATED ENZYME. *J. Biol. Chem.* *245*, 1778–1789.

Chivers, P.T., and Sauer, R.T. (1999). NikR is a ribbon-helix-helix DNA-binding protein. *Protein Sci. Publ. Protein Soc.* *8*, 2494–2500.

Chivers, P.T., Benanti, E.L., Heil-Chapdelaine, V., Iwig, J.S., and Rowe, J.L. (2012). Identification of Ni-(L-His)₂ as a substrate for NikABCDE-dependent nickel uptake in *Escherichia coli*. *Met. Integr. Biometal Sci.* *4*, 1043–1050.

Clément, E., Mesini, P.J., Pattus, F., and Schalk, I.J. (2004). The binding mechanism of pyoverdine with the outer membrane receptor FpvA in *Pseudomonas aeruginosa* is dependent on its iron-loaded status. *Biochemistry (Mosc.)* *43*, 7954–7965.

Cobessi, D., Celia, H., and Pattus, F. (2005). Crystal Structure at High Resolution of Ferric-pyochelin and its Membrane Receptor FptA from *Pseudomonas aeruginosa*. *J. Mol. Biol.* *352*, 893–904.

Coggan, K.A., and Wolfgang, M.C. (2012). Global regulatory pathways and cross-talk control *Pseudomonas aeruginosa* environmental lifestyle and virulence phenotype. *Curr. Issues Mol. Biol.* *14*, 47–70.

Colvin, K.M., Gordon, V.D., Murakami, K., Borlee, B.R., Wozniak, D.J., Wong, G.C.L., and Parsek, M.R. (2011). The pel polysaccharide can serve a structural and protective role in the biofilm matrix of *Pseudomonas aeruginosa*. *PLoS Pathog.* *7*, e1001264.

Cornelis, P. (2010). Iron uptake and metabolism in pseudomonads. *Appl. Microbiol. Biotechnol.* *86*, 1637–1645.

Cornelis, P., and Dingemans, J. (2013). *Pseudomonas aeruginosa* adapts its iron uptake strategies in function of the type of infections. *Front. Cell. Infect. Microbiol.* *3*.

Cox, C.D. (1980). Iron uptake with ferripyochelin and ferric citrate by *Pseudomonas aeruginosa*. *J. Bacteriol.* *142*, 581–587.

Cox, C.D., and Adams, P. (1985). Siderophore activity of pyoverdine for *Pseudomonas aeruginosa*.

Infect. Immun. *48*, 130–138.

Cox, C.D., Rinehart, K.L., Moore, M.L., and Cook, J.C. (1981). Pyochelin: novel structure of an iron-chelating growth promoter for *Pseudomonas aeruginosa*. Proc. Natl. Acad. Sci. *78*, 4256–4260.

Coy, M., and Neilands, J.B. (1991). Structural dynamics and functional domains of the fur protein. Biochemistry (Mosc.) *30*, 8201–8210.

Crosa, J.H. (1997). Signal transduction and transcriptional and posttranscriptional control of iron-regulated genes in bacteria. Microbiol. Mol. Biol. Rev. MMBR *61*, 319–336.

Crosa, J.H., and Walsh, C.T. (2002). Genetics and assembly line enzymology of siderophore biosynthesis in bacteria. Microbiol. Mol. Biol. Rev. MMBR *66*, 223–249.

Cuiv, P.O., Clarke, P., and O’Connell, M. (2006). Identification and characterization of an iron-regulated gene, *chtA*, required for the utilization of the xenosiderophores aerobactin, rhizobactin 1021 and schizokinen by *Pseudomonas aeruginosa*. Microbiology *152*, 945–954.

Cunliffe, H.E., Merriman, T.R., and Lamont, I.L. (1995). Cloning and characterization of *pvdS*, a gene required for pyoverdine synthesis in *Pseudomonas aeruginosa*: PvdS is probably an alternative sigma factor. J. Bacteriol. *177*, 2744–2750.

Cunrath, O., Gasser, V., Hoegy, F., Reimann, C., Guillon, L., and Schalk, I.J. (2014). A cell biological view of the siderophore pyochelin iron uptake pathway in *Pseudomonas aeruginosa*. Environ. Microbiol. *17*, 171–185.

Cunrath, O., Geoffroy, V.A., and Schalk, I.J. (2016). Metallome of *Pseudomonas aeruginosa*: a role for siderophores. Environ. Microbiol. *18*, 3258–3267.

Da, R., P, H., Ms, G., and T, E. (2006). Comparative and functional genomic analysis of prokaryotic nickel and cobalt uptake transporters: evidence for a novel group of ATP-binding cassette transporters. J. Bacteriol. *188*, 317–327.

Dalecki, A.G., Haeili, M., Shah, S., Speer, A., Niederweis, M., Kutsch, O., and Wolschendorf, F. (2015). Disulfiram and Copper Ions Kill Mycobacterium tuberculosis in a Synergistic Manner. Antimicrob. Agents Chemother. *59*, 4835–4844.

De Pina, K., Desjardin, V., Mandrand-Berthelot, M.A., Giordano, G., and Wu, L.F. (1999). Isolation and characterization of the *nikR* gene encoding a nickel-responsive regulator in *Escherichia coli*. J. Bacteriol. *181*, 670–674.

Dean, C.R., and Poole, K. (1993). Expression of the ferric enterobactin receptor (PfeA) of *Pseudomonas aeruginosa*: involvement of a two-component regulatory system. Mol. Microbiol. *8*, 1095–1103.

Deligianni, E., Pattison, S., Berrar, D., Ternan, N.G., Haylock, R.W., Moore, J.E., Elborn, S.J., and Dooley, J.S.G. (2010). *Pseudomonas aeruginosa* cystic fibrosis isolates of similar RAPD genotype exhibit diversity in biofilm forming ability in vitro. BMC Microbiol. *10*, 38.

Demange, P., Wendenbaum, S., Linget, C., Mertz, C., Cung, M.T., Dell, A., and Abdallah, M.A. (1990). Bacterial siderophores: structure and NMR assignment of pyoverdins Pa, siderophores of

Pseudomonas aeruginosa ATCC 15692. *Biol. Met.* 3, 155–170.

Dieppois, G., Ducret, V., Caille, O., and Perron, K. (2012). The transcriptional regulator CzcR modulates antibiotic resistance and Quorum Sensing in *Pseudomonas aeruginosa*. *PLoS ONE* 7.

Djoko, K.Y., Goytia, M.M., Donnelly, P.S., Schembri, M.A., Shafer, W.M., and McEwan, A.G. (2015a). Copper(II)-Bis(Thiosemicarbazonato) complexes as antibacterial agents: insights into their mode of action and potential as therapeutics. *Antimicrob. Agents Chemother.* 59, 6444–6453.

Djoko, K.Y., Ong, C.Y., Walker, M.J., and McEwan, A.G. (2015b). Copper and zinc toxicity and its role in innate immune defense against bacterial pathogens. *J. Biol. Chem.* jbc.R115.647099.

Donlan, R.M. (2002). Biofilms: microbial life on surfaces. *Emerg. Infect. Dis.* 8, 881–890.

D’Orazio, M., Mastropasqua, M.C., Cerasi, M., Pacello, F., Consalvo, A., Chirullo, B., Mortensen, B., Skaar, E.P., Ciavardelli, D., Pasquali, P., et al. (2015). The capability of *Pseudomonas aeruginosa* to recruit zinc under conditions of limited metal availability is affected by inactivation of the ZnuABC transporter. *Met. Integr. Biometal Sci.* 7, 1023–1035.

Duhme, A.-K., Hider, R.C., Naldrett, M.J., and Pau, R.N. (1998). The stability of the molybdenum-azotochelin complex and its effect on siderophore production in *Azotobacter vinelandii*. *JBIC J. Biol. Inorg. Chem.* 3, 520–526.

Dumas, Z., Ross-Gillespie, A., and Kümmerli, R. (2013). Switching between apparently redundant iron-uptake mechanisms benefits bacteria in changeable environments. *Proc. Biol. Sci.* 280, 20131055.

Dupont, C.L., Grass, G., and Rensing, C. (2011). Copper toxicity and the origin of bacterial resistance--new insights and applications. *Met. Integr. Biometal Sci.* 3, 1109–1118.

Edgar, R.J., Xu, X., Shirley, M., Konings, A.F., Martin, L.W., Ackerley, D.F., and Lamont, I.L. (2014). Interactions between an anti-sigma protein and two sigma factors that regulate the pyoverdine signaling pathway in *Pseudomonas aeruginosa*. *BMC Microbiol.* 14.

Eitinger, T., Suhr, J., Moore, L., and Smith, J.A.C. (2005). Secondary transporters for nickel and cobalt ions: theme and variations. *Biometals Int. J. Role Met. Ions Biol. Biochem. Med.* 18, 399–405.

Ellison, M.L., Farrow, J.M., Farrow, J.M., Parrish, W., Danell, A.S., and Pesci, E.C. (2013). The transcriptional regulator Np20 is the zinc uptake regulator in *Pseudomonas aeruginosa*. *PLoS One* 8, e75389.

English, B.K., and Gaur, A.H. (2010). The use and abuse of antibiotics and the development of antibiotic resistance. *Adv. Exp. Med. Biol.* 659, 73–82.

Escolar, L., Pérez-Martín, J., and Lorenzo, V. de (1999). Opening the iron box: transcriptional metalloregulation by the Fur Protein. *J. Bacteriol.* 181, 6223–6229.

Evers, A., Hancock, R.D., Martell, A.E., and Motekaitis, R.J. (1989). Metal ion recognition in ligands with negatively charged oxygen donor groups. Complexation of iron(III), gallium(III), indium(III), aluminum(III), and other highly charged metal ions. *Inorg. Chem.* 28, 2189–2195.

- Fan, B., and Rosen, B.P. (2002). Biochemical characterization of CopA, the *Escherichia coli* Cu(I)-translocating P-type ATPase. *J. Biol. Chem.* *277*, 46987–46992.
- Feinbaum, R.L., Urbach, J.M., Liberati, N.T., Djonovic, S., Adonizio, A., Carvunis, A.-R., and Ausubel, F.M. (2012). Genome-wide identification of *Pseudomonas aeruginosa* virulence-related genes using a *Caenorhabditis elegans* infection model. *PLoS Pathog.* *8*.
- Fillat, M.F. (2014). The FUR (ferric uptake regulator) superfamily: diversity and versatility of key transcriptional regulators. *Arch. Biochem. Biophys.* *546*, 41–52.
- Flemming, H.-C., and Wingender, J. (2010). The biofilm matrix. *Nat. Rev. Microbiol.* *8*, 623–633.
- Folschweiller, N., Gallay, J., Vincent, M., Abdallah, M.A., Pattus, F., and Schalk, I.J. (2002). The interaction between pyoverdinin and its outer membrane receptor in *Pseudomonas aeruginosa* leads to different conformers: a time-resolved fluorescence study. *Biochemistry (Mosc.)* *41*, 14591–14601.
- Fournier, C., Smith, A., and Delepelaire, P. (2011). Haem release from haemopexin by HxuA allows *Haemophilus influenzae* to escape host nutritional immunity. *Mol. Microbiol.* *80*, 133–148.
- Frangipani, E., Visaggio, D., Heeb, S., Kaefer, V., Cámara, M., Visca, P., and Imperi, F. (2014). The Gac/Rsm and cyclic-di-GMP signalling networks coordinately regulate iron uptake in *Pseudomonas aeruginosa*. *Environ. Microbiol.* *16*, 676–688.
- Fuchs, R., Schäfer, M., Geoffroy, V., and Meyer, J.M. (2001). Siderotyping--a powerful tool for the characterization of pyoverdines. *Curr. Top. Med. Chem.* *1*, 31–57.
- Fukushima, T., Allred, B.E., Sia, A.K., Nichiporuk, R., Andersen, U.N., and Raymond, K.N. (2013). Gram-positive siderophore-shuttle with iron-exchange from Fe-siderophore to apo-siderophore by *Bacillus cereus* YxeB. *Proc. Natl. Acad. Sci. U. S. A.* *110*, 13821–13826.
- Funken, H., Knapp, A., Vasil, M.L., Wilhelm, S., Jaeger, K.-E., and Rosenau, F. (2011). The lipase LipA (PA2862) but not LipC (PA4813) from *Pseudomonas aeruginosa* influences regulation of pyoverdinin production and expression of the sigma factor PvdS. *J. Bacteriol.* *193*, 5858–5860.
- Gaille, C., Kast, P., and Haas, D. (2002). Salicylate biosynthesis in *Pseudomonas aeruginosa*. Purification and characterization of PchB, a novel bifunctional enzyme displaying isochorismate pyruvate-lyase and chorismate mutase activities. *J. Biol. Chem.* *277*, 21768–21775.
- Ganne, G., Brillet, K., Basta, B., Roche, B., Hoegy, F., Gasser, V., and Schalk, I.J. (2017). Iron release from the siderophore pyoverdinin in *Pseudomonas aeruginosa* involves three new actors: FpvC, FpvG, and FpvH. *ACS Chem. Biol.* *12*, 1056–1065.
- Gasser, V., Guillon, L., Cunrath, O., and Schalk, I.J. (2015). Cellular organization of siderophore biosynthesis in *Pseudomonas aeruginosa*: Evidence for siderosomes. *J. Inorg. Biochem.* *148*, 27–34.
- Gasser, V., Baco, E., Cunrath, O., August, P.S., Perraud, Q., Zill, N., Schleberger, C., Schmidt, A., Paulen, A., Bumann, D., et al. (2016). Catechol siderophores repress the pyochelin pathway and activate the enterobactin pathway in *Pseudomonas aeruginosa*: an opportunity for siderophore-antibiotic conjugates development: Ability of *P. aeruginosa* to acquire iron via catechols. *Environ. Microbiol.* *18*, 819–832.

German, N., Doyscher, D., and Rensing, C. (2013). Bacterial killing in macrophages and amoeba: do they all use a brass dagger? *Future Microbiol.* 8, 1257–1264.

Gessard, C. (1984). Classics in infectious diseases. On the blue and green coloration that appears on bandages. by Carle Gessard (1850-1925). *Rev. Infect. Dis.* 6 *Suppl* 3, S775-776.

Ghssein, G., Brutesco, C., Ouerdane, L., Fojcik, C., Izaute, A., Wang, S., Hajjar, C., Lobinski, R., Lemaire, D., Richaud, P., et al. (2016). Biosynthesis of a broad-spectrum nicotianamine-like metallophore in *Staphylococcus aureus*. *Science* 352, 1105–1109.

Giedroc, D.P., and Arunkumar, A.I. (2007). Metal sensor proteins: nature's metalloregulated allosteric switches. *Dalton Trans. Camb. Engl.* 2003 3107–3120.

Gilbreath, J.J., West, A.L., Pich, O.Q., Carpenter, B.M., Michel, S., and Merrell, D.S. (2012). Fur activates expression of the 2-oxoglutarate oxidoreductase genes (oorDABC) in *Helicobacter pylori*. *J. Bacteriol.* 194, 6490–6497.

Girard, G., and Bloemberg, G.V. (2008). Central role of quorum sensing in regulating the production of pathogenicity factors in *Pseudomonas aeruginosa*. *Future Microbiol.* 3, 97–106.

Gogada, R., Singh, S.S., Lunavat, S.K., Pamarthi, M.M., Rodrigue, A., Vadivelu, B., Phanithi, P.-B., Gopala, V., and Apte, S.K. (2015). Engineered *Deinococcus radiodurans* R1 with NiCoT genes for bioremoval of trace cobalt from spent decontamination solutions of nuclear power reactors. *Appl. Microbiol. Biotechnol.* 99, 9203–9213.

Goodman, A.L., Kulasekara, B., Rietsch, A., Boyd, D., Smith, R.S., and Lory, S. (2004). A signaling network reciprocally regulates genes associated with acute infection and chronic persistence in *Pseudomonas aeruginosa*. *Dev. Cell* 7, 745–754.

Grass, G., Otto, M., Fricke, B., Haney, C.J., Rensing, C., Nies, D.H., and Munkelt, D. (2005a). FieF (YiiP) from *Escherichia coli* mediates decreased cellular accumulation of iron and relieves iron stress. *Arch. Microbiol.* 183, 9–18.

Grass, G., Fricke, B., and Nies, D.H. (2005b). Control of expression of a periplasmic nickel efflux pump by periplasmic nickel concentrations. *Biometals Int. J. Role Met. Ions Biol. Biochem. Med.* 18, 437–448.

Greenwald, J., Hoegy, F., Nader, M., Journet, L., Mislin, G.L.A., Graumann, P.L., and Schalk, I.J. (2007). Real time fluorescent resonance energy transfer visualization of ferric pyoverdine uptake in *Pseudomonas aeruginosa*. A role for ferrous iron. *J. Biol. Chem.* 282, 2987–2995.

Greenwald, J., Nader, M., Celia, H., Gruffaz, C., Geoffroy, V., Meyer, J.M., Schalk, I.J., and Pattus, F. (2009). FpvA bound to non-cognate pyoverdines: molecular basis of siderophore recognition by an iron transporter. *Mol Microbiol* 72, 1246–1259.

Greenwood, N., and Earnshaw, A. (1997). Chemistry of elements, 2nd edition. Butterworth-Heinemann.

Guarner, F., and Malagelada, J.-R. (2003). Gut flora in health and disease. *Lancet Lond. Engl.* 361, 512–519.

Guerinot, M.L. (1994). Microbial iron transport. *Annu. Rev. Microbiol.* 48, 743–772.

- Guerra, A.J., and Giedroc, D.P. (2012). Metal site occupancy and allosteric switching in bacterial metal sensor proteins. *Arch. Biochem. Biophys.* *519*, 210–222.
- Guillon, L., Altenburger, S., Graumann, P.L., and Schalk, I.J. (2013). Deciphering protein dynamics of the siderophore pyoverdine pathway in *Pseudomonas aeruginosa*. *PloS One* *8*, e79111.
- Haas, H., Eisendle, M., and Turgeon, B.G. (2008). Siderophores in fungal physiology and virulence. *Annu. Rev. Phytopathol.* *46*, 149–187.
- Hannauer, M., Barda, Y., Mislin, G.L.A., Shanzer, A., and Schalk, I.J. (2010a). The ferrichrome uptake pathway in *Pseudomonas aeruginosa* involves an iron release mechanism with acylation of the siderophore and recycling of the modified desferrichrome. *J. Bacteriol.* *192*, 1212–1220.
- Hannauer, M., Yeterian, E., Martin, L.W., Lamont, I.L., and Schalk, I.J. (2010b). An efflux pump is involved in secretion of newly synthesized siderophore by *Pseudomonas aeruginosa*. *FEBS Lett.* *584*, 4751–4755.
- Hannauer, M., Braud, A., Hoegy, F., Ronot, P., Boos, A., and Schalk, I.J. (2012). The PvdRT-OpmQ efflux pump controls the metal selectivity of the iron uptake pathway mediated by the siderophore pyoverdine in *Pseudomonas aeruginosa*. *Environ. Microbiol.* *14*, 1696–1708.
- Harding, R.A., and Royt, P.W. (1990). Acquisition of iron from citrate by *Pseudomonas aeruginosa*. *J Gen Microbiol* *136*, 1859–1867.
- Haritha, A., Rodrigue, A., and Mohan, P.M. (2008). A comparative analysis of metal transportomes from metabolically versatile *Pseudomonas*. *BMC Res. Notes* *1*, 88.
- Harrison, J.J., Ceri, H., and Turner, R.J. (2007). Multimetal resistance and tolerance in microbial biofilms. *Nat. Rev. Microbiol.* *5*, 928–938.
- Harrison, J.J., Tremaroli, V., Stan, M.A., Chan, C.S., Vacchi-Suzzi, C., Heyne, B.J., Parsek, M.R., Ceri, H., and Turner, R.J. (2009). Chromosomal antioxidant genes have metal ion-specific roles as determinants of bacterial metal tolerance. *Environ. Microbiol.* *11*, 2491–2509.
- Hedde, J., Scott, D.J., Unzai, S., Park, S.-Y., and Tame, J.R.H. (2003). Crystal structures of the liganded and unliganded nickel-binding protein NikA from *Escherichia coli*. *J. Biol. Chem.* *278*, 50322–50329.
- Heinrichs, D.E., and Poole, K. (1993). Cloning and sequence analysis of a gene (pchR) encoding an AraC family activator of pyochelin and ferripyochelin receptor synthesis in *Pseudomonas aeruginosa*. *J. Bacteriol.* *175*, 5882–5889.
- Heinrichs, D.E., and Poole, K. (1996). PchR, a regulator of ferripyochelin receptor gene (fptA) expression in *Pseudomonas aeruginosa*, functions both as an activator and as a repressor. *J. Bacteriol.* *178*, 2586–2592.
- Heldal, M., Norland, S., and Tumyr, O. (1985). X-ray microanalytic method for measurement of dry matter and elemental content of individual bacteria. *Appl. Environ. Microbiol.* *50*, 1251–1257.
- Helmann, J.D. (2002). The extracytoplasmic function (ECF) sigma factors. *Adv. Microb. Physiol.* *46*, 47–110.

- Herbig, A.F., and Helmann, J.D. (2002). Metal ion uptake and oxidative stress. 405–414.
- Hernlem, B.J., Vane, L.M., and Sayles, G.D. (1996). Stability constants for complexes of the siderophore desferrioxamine B with selected heavy metal cations. *Inorganica Chim. Acta* 244, 179–184.
- Hider, R.C., and Kong, X. (2010). Chemistry and biology of siderophores. *Nat. Prod. Rep.* 27, 637–657.
- Hobman, J.L., and Crossman, L.C. (2015). Bacterial antimicrobial metal ion resistance. *J. Med. Microbiol.* 64, 471–497.
- Hodgkinson, V., and Petris, M.J. (2012). Copper homeostasis at the host-pathogen interface. *J. Biol. Chem.* 287, 13549–13555.
- Hood, M.I., and Skaar, E.P. (2012). Nutritional immunity: transition metals at the pathogen–host interface. *Nat. Rev. Microbiol.* 10, 525–537.
- Horsburgh, M.J., Wharton, S.J., Karavolos, M., and Foster, S.J. (2002). Manganese: elemental defence for a life with oxygen. *Trends Microbiol.* 10, 496–501.
- Hu, X., and Boyer, G.L. (1996). Siderophore-mediated aluminum uptake by *Bacillus megaterium* ATCC 19213. *Appl. Environ. Microbiol.* 62, 4044–4048.
- Imlay, J.A., Chin, S.M., and Linn, S. (1988). Toxic DNA damage by hydrogen peroxide through the Fenton reaction in vivo and in vitro. *Science* 240, 640–642.
- Imperi, F., and Visca, P. (2013). Subcellular localization of the pyoverdine biogenesis machinery of *Pseudomonas aeruginosa*: a membrane-associated “siderosome.” *FEBS Lett.* 587, 3387–3391.
- Imperi, F., Tiburzi, F., and Visca, P. (2009). Molecular basis of pyoverdine siderophore recycling in *Pseudomonas aeruginosa*. *Proc. Natl. Acad. Sci. U. S. A.* 106, 20440–20445.
- Irving, H., and Williams, R.J.P. (1948). Order of stability of metal complexes. *Nature* 162, 162746a0.
- Itoh, N., Morinaga, N., and Kouzai, T. (1994). Purification and characterization of a novel metal-containing nonheme bromoperoxidase from *Pseudomonas putida*. *Biochim. Biophys. Acta* 1207, 208–216.
- Jackson, K.D., Starkey, M., Kremer, S., Parsek, M.R., and Wozniak, D.J. (2004). Identification of *psl*, a locus encoding a potential exopolysaccharide that is essential for *Pseudomonas aeruginosa* PAO1 biofilm formation. *J. Bacteriol.* 186, 4466–4475.
- Jayaseelan, S., Ramaswamy, D., and Dharmaraj, S. (2014). Pyocyanin: production, applications, challenges and new insights. *World J. Microbiol. Biotechnol.* 30, 1159–1168.
- Jimenez, P.N., Koch, G., Thompson, J.A., Xavier, K.B., Cool, R.H., and Quax, W.J. (2012). The multiple signaling systems regulating virulence in *Pseudomonas aeruginosa*. *Microbiol. Mol. Biol. Rev. MMBR* 76, 46–65.
- Jones, P., Binns, D., Chang, H.-Y., Fraser, M., Li, W., McAnulla, C., McWilliam, H., Maslen, J., Mitchell, A., Nuka, G., et al. (2014). InterProScan 5: genome-scale protein function classification.

Bioinforma. Oxf. Engl. *30*, 1236–1240.

Kaluarachchi, H., Chan Chung, K.C., and Zamble, D.B. (2010). Microbial nickel proteins. *Nat. Prod. Rep.* *27*, 681–694.

Kammler, M., Schön, C., and Hantke, K. (1993). Characterization of the ferrous iron uptake system of *Escherichia coli*. *J. Bacteriol.* *175*, 6212–6219.

Kaneko, Y., Thoendel, M., Olakanmi, O., Britigan, B.E., and Singh, P.K. (2007). The transition metal gallium disrupts *Pseudomonas aeruginosa* iron metabolism and has antimicrobial and antibiofilm activity. *J. Clin. Invest.* *117*, 877–888.

Karatan, E., and Watnick, P. (2009). Signals, regulatory networks, and materials that build and break bacterial biofilms. *Microbiol. Mol. Biol. Rev. MMBR* *73*, 310–347.

Kehres, D.G., and Maguire, M.E. (2003). Emerging themes in manganese transport, biochemistry and pathogenesis in bacteria. *FEMS Microbiol. Rev.* *27*, 263–290.

Kenney, G.E., and Rosenzweig, A.C. (2012). Chemistry and biology of the copper chelator methanobactin. *ACS Chem. Biol.* *7*, 260–268.

Kiraly, O., Gong, G., Olipitz, W., Muthupalani, S., and Engelward, B.P. (2015). Inflammation-induced cell proliferation potentiates DNA damage-induced mutations in vivo. *PLoS Genet.* *11*.

Klein, J.S., and Lewinson, O. (2011). Bacterial ATP-driven transporters of transition metals: physiological roles, mechanisms of action, and roles in bacterial virulence. *Met. Integr. Biometal Sci.* *3*, 1098–1108.

Kloepper, J.W., Leong, J., Teintze, M., and Schroth, M.N. (1980). Enhanced plant growth by siderophores produced by plant growth-promoting rhizobacteria. *Nature* *286*, 885–886.

Kobayashi, M., and Shimizu, S. (1999). Cobalt proteins. *Eur. J. Biochem.* *261*, 1–9.

Komeda, H., Kobayashi, M., and Shimizu, S. (1997). A novel transporter involved in cobalt uptake. *Proc. Natl. Acad. Sci. U. S. A.* *94*, 36–41.

Krewulak, K.D., and Vogel, H.J. (2008). Structural biology of bacterial iron uptake. *Biochim. Biophys. Acta BBA - Biomembr.* *1778*, 1781–1804.

Lamont, I.L., Beare, P.A., Ochsner, U., Vasil, A.I., and Vasil, M.L. (2002). Siderophore-mediated signaling regulates virulence factor production in *Pseudomonas aeruginosa*. *Proc. Natl. Acad. Sci. U. S. A.* *99*, 7072–7077.

Lamont, I.L., and Martin, L.W. (2003). Identification and characterization of novel pyoverdine synthesis genes in *Pseudomonas aeruginosa*. *Microbiol. Read. Engl.* *149*, 833–842.

Leach, L.H., and Lewis, T.A. (2006). Identification and characterization of *Pseudomonas* membrane transporters necessary for utilization of the siderophore pyridine-2,6-bis(thiocarboxylic acid) (PDTC). *Microbiol. Read. Engl.* *152*, 3157–3166.

Leach, L.H., Morris, J.C., and Lewis, T.A. (2007). The role of the siderophore pyridine-2,6-bis(thiocarboxylic acid) (PDTC) in zinc utilization by *Pseudomonas putida* DSM 3601. *Biometals Int. J. Role Met. Ions Biol. Biochem. Med.* *20*, 717–726.

- Lebrette, H., Iannello, M., Fontecilla-Camps, J.C., and Cavazza, C. (2013). The binding mode of Ni-(L-His)₂ in NikA revealed by X-ray crystallography. *J. Inorg. Biochem.* *121*, 16–18.
- Lee, J., and Zhang, L. (2015). The hierarchy quorum sensing network in *Pseudomonas aeruginosa*. *Protein Cell* *6*, 26–41.
- Lefèvre, J., Delepelaire, P., Delepierre, M., and Izadi-Pruneyre, N. (2008). Modulation by substrates of the interaction between the HasR outer membrane receptor and its specific TonB-like protein, HasB. *J. Mol. Biol.* *378*, 840–851.
- Lemire, J., Mailloux, R., Auger, C., Whalen, D., and Appanna, V.D. (2010). *Pseudomonas fluorescens* orchestrates a fine metabolic-balancing act to counter aluminium toxicity. *Environ. Microbiol.* *12*, 1384–1390.
- Lemire, J.A., Harrison, J.J., and Turner, R.J. (2013). Antimicrobial activity of metals: mechanisms, molecular targets and applications. *Nat. Rev. Microbiol.* *11*, 371–384.
- Létoffé, S., Nato, F., Goldberg, M.E., and Wandersman, C. (1999). Interactions of HasA, a bacterial haemophore, with haemoglobin and with its outer membrane receptor HasR. *Mol. Microbiol.* *33*, 546–555.
- Lewinson, O., Lee, A.T., and Rees, D.C. (2009). A P-type ATPase importer that discriminates between essential and toxic transition metals. *Proc. Natl. Acad. Sci. U. S. A.* *106*, 4677–4682.
- Lewis, T.A., Cortese, M.S., Sebat, J.L., Green, T.L., Lee, C.H., and Crawford, R.L. (2000). A *Pseudomonas stutzeri* gene cluster encoding the biosynthesis of the CCl₄-dechlorination agent pyridine-2,6-bis(thiocarboxylic acid). *Environ. Microbiol.* *2*, 407–416.
- Li, Y., and Zamble, D.B. (2009). Nickel Homeostasis and Nickel Regulation: An Overview. *Chem. Rev.* *109*, 4617–4643.
- Lill, R. (2009). Function and biogenesis of iron-sulphur proteins. *Nature* *460*, 831–838.
- Lin, H., Fischbach, M.A., Liu, D.R., and Walsh, C.T. (2005). In vitro characterization of salmochelin and enterobactin trilactone hydrolases IroD, IroE, and Fes. *J. Am. Chem. Soc.* *127*, 11075–11084.
- Lin, P.-C., Youard, Z.A., and Reimann, C. (2013). In vitro-binding of the natural siderophore enantiomers pyochelin and enantiopyochelin to their AraC-type regulators PchR in *Pseudomonas*. *Biometals Int. J. Role Met. Ions Biol. Biochem. Med.* *26*, 1067–1073.
- Lisher, J.P., and Giedroc, D.P. (2013). Manganese acquisition and homeostasis at the host-pathogen interface. *Front. Cell. Infect. Microbiol.* *3*, 91.
- Lister, P.D., Wolter, D.J., and Hanson, N.D. (2009). Antibacterial-resistant *Pseudomonas aeruginosa*: clinical impact and complex regulation of chromosomally encoded resistance mechanisms. *Clin. Microbiol. Rev.* *22*, 582–610.
- Liu, P.V. (1974). Extracellular toxins of *Pseudomonas aeruginosa*. *J. Infect. Dis.* *130*, S94–S99.
- Liu, P.V., and Shokrani, F. (1978). Biological activities of pyochelins: iron-chelating agents of *Pseudomonas aeruginosa*. *Infect. Immun.* *22*, 878–890.

- Liu, T., Ramesh, A., Ma, Z., Ward, S.K., Zhang, L., George, G.N., Talaat, A.M., Sacchettini, J.C., and Giedroc, D.P. (2007). CsoR is a novel Mycobacterium tuberculosis copper-sensing transcriptional regulator. *Nat. Chem. Biol.* *3*, 60–68.
- Llamas, M.A., Sparrius, M., Kloet, R., Jimenez, C.R., Vandenbroucke-Grauls, C., and Bitter, W. (2006). The heterologous siderophores ferrioxamine B and ferrichrome activate signaling pathways in *Pseudomonas aeruginosa*. *J Bacteriol* *188*, 1882–1891.
- Llamas, M.A., Mooij, M.J., Sparrius, M., Vandenbroucke-Grauls, C.M., Ratledge, C., and Bitter, W. (2008). Characterization of five novel *Pseudomonas aeruginosa* cell-surface signalling systems. *Mol Microbiol* *67*, 458–472.
- Llamas, M.A., Imperi, F., Visca, P., and Lamont, I.L. (2014). Cell-surface signaling in *Pseudomonas*: stress responses, iron transport, and pathogenicity. *FEMS Microbiol. Rev.* *38*, 569–597.
- Lutkenhaus, J.F. (1977). Role of a major outer membrane protein in *Escherichia coli*. *J. Bacteriol.* *131*, 631–637.
- Lyczak, J.B., Cannon, C.L., and Pier, G.B. (2002). Lung Infections Associated with Cystic Fibrosis. *Clin. Microbiol. Rev.* *15*, 194–222.
- Ma, Z., Jacobsen, F.E., and Giedroc, D.P. (2009). Metal transporters and metal sensors: how coordination chemistry controls bacterial metal homeostasis. *Chem. Rev.* *109*, 4644–4681.
- Macomber, L., and Imlay, J.A. (2009). The iron-sulfur clusters of dehydratases are primary intracellular targets of copper toxicity. *Proc. Natl. Acad. Sci. U. S. A.* *106*, 8344–8349.
- Madigan, M.T. (2012). *Brock biology of microorganisms* (San Francisco Benjamin Cummings).
- Mahren, S., Schnell, H., and Braun, V. (2005). Occurrence and regulation of the ferric citrate transport system in *Escherichia coli* B, *Klebsiella pneumoniae*, *Enterobacter aerogenes*, and *Photobacterium luminescens*. *Arch. Microbiol.* *184*, 175–186.
- Maity, A., and Teets, T.S. (2016). Main group lewis acid-mediated transformations of transition-metal hydride complexes. *Chem. Rev.* *116*, 8873–8911.
- Mandal, A.K., Cheung, W.D., and Argüello, J.M. (2002). Characterization of a thermophilic P-type Ag⁺/Cu⁺-ATPase from the extremophile *Archaeoglobus fulgidus*. *J. Biol. Chem.* *277*, 7201–7208.
- Maret, W. (2011). Metals on the move: zinc ions in cellular regulation and in the coordination dynamics of zinc proteins. *Biometals Int. J. Role Met. Ions Biol. Biochem. Med.* *24*, 411–418.
- Martínez-García, E., Aparicio, T., Goñi-Moreno, A., Fraile, S., and de Lorenzo, V. (2015). SEVA 2.0: an update of the Standard European Vector Architecture for de-/re-construction of bacterial functionalities. *Nucleic Acids Res.* *43*, D1183-1189.
- Mastropasqua, M.C., D’Orazio, M., Cerasi, M., Pacello, F., Gismondi, A., Canini, A., Canuti, L., Consalvo, A., Ciavardelli, D., Chirullo, B., et al. (2017). Growth of *Pseudomonas aeruginosa* in zinc poor environments is promoted by a nicotianamine-related metallophore. *Mol. Microbiol.* *106*, 543–561.

McGowan, J.E. (2006). Resistance in nonfermenting gram-negative bacteria: multidrug resistance to the maximum. *Am. J. Infect. Control* 34, S29-37-73.

McMorran, B.J., Merriman, M.E., Rombel, I.T., and Lamont, I.L. (1996). Characterisation of the *pvdE* gene which is required for pyoverdine synthesis in *Pseudomonas aeruginosa*. *Gene* 176, 55–59.

McPhee, J.B., Tamber, S., Bains, M., Maier, E., Gellatly, S., Lo, A., Benz, R., and Hancock, R.E.W. (2009). The major outer membrane protein OprG of *Pseudomonas aeruginosa* contributes to cytotoxicity and forms an anaerobically regulated, cation-selective channel. *FEMS Microbiol. Lett.* 296, 241–247.

Meneely, K.M., Luo, Q., Dhar, P., and Lamb, A.L. (2013). Lysine221 is the general base residue of the isochorismate synthase from *Pseudomonas aeruginosa* (PchA) in a reaction that is diffusion limited. *Arch. Biochem. Biophys.* 538, 49–56.

Meyer, J.M. (1992). Exogenous siderophore-mediated iron uptake in *Pseudomonas aeruginosa*: possible involvement of porin OprF in iron translocation. *J Gen Microbiol* 138, 951–958.

Meyer, J.M. (2000). Pyoverdines: pigments, siderophores and potential taxonomic markers of fluorescent *Pseudomonas* species. *Arch. Microbiol.* 174, 135–142.

Meyer, J.-M. (2010). Pyoverdine siderophores as taxonomic and phylogenetic markers. In *Pseudomonas*, (Springer, Dordrecht), pp. 201–233.

Meyer, J.M., and Abdallah, M.A. (1978). The fluorescent pigment of *Pseudomonas fluorescens*: biosynthesis, purification and physicochemical properties. *Microbiology* 107, 319–328.

Meyer, J.M., Stintzi, A., Coulanges, V., Shivaji, S., Voss, J.A., Taraz, K., and Budzikiewicz, H. (1998). Siderotyping of fluorescent pseudomonads: characterization of pyoverdines of *Pseudomonas fluorescens* and *Pseudomonas putida* strains from Antarctica. *Microbiol. Read. Engl.* 144 (Pt 11), 3119–3126.

Meyer, J.-M., Geoffroy, V.A., Baida, N., Gardan, L., Izard, D., Lemanceau, P., Achouak, W., and Palleroni, N.J. (2002). Siderophore typing, a powerful tool for the identification of fluorescent and nonfluorescent pseudomonads. *Appl. Environ. Microbiol.* 68, 2745–2753.

Michel, L., González, N., Jagdeep, S., Nguyen-Ngoc, T., and Reimmann, C. (2005). PchR-box recognition by the AraC-type regulator PchR of *Pseudomonas aeruginosa* requires the siderophore pyochelin as an effector. *Mol. Microbiol.* 58, 495–509.

Michel, L., Bachelard, A., and Reimmann, C. (2007). Ferripyochelin uptake genes are involved in pyochelin-mediated signalling in *Pseudomonas aeruginosa*. *Microbiology* 153, 1508–1518.

Miethke, M., and Marahiel, M.A. (2007). Siderophore-based iron acquisition and pathogen control. *Microbiol. Mol. Biol. Rev. MMBR* 71, 413–451.

Mikkelsen, H., McMullan, R., and Filloux, A. (2011). The *Pseudomonas aeruginosa* Reference Strain PA14 Displays Increased Virulence Due to a Mutation in *ladS*. *PLOS ONE* 6, e29113.

Minagawa, S., Inami, H., Kato, T., Sawada, S., Yasuki, T., Miyairi, S., Horikawa, M., Okuda, J., and Gotoh, N. (2012). RND type efflux pump system MexAB-OprM of *pseudomonas aeruginosa*

selects bacterial languages, 3-oxo-acyl-homoserine lactones, for cell-to-cell communication. *BMC Microbiol.* *12*, 70.

Mislin, G.L.A., Hoegy, F., Cobessi, D., Poole, K., Rognan, D., and Schalk, I.J. (2006). Binding properties of pyochelin and structurally related molecules to FptA of *Pseudomonas aeruginosa*. *J Mol Biol* *357*, 1437–1448.

Monosson, E. (2012). *Evolution in a Toxic World: How Life Responds to Chemical Threats* (Island Press).

Moore, S.J., Mayer, M.J., Biedendieck, R., Deery, E., and Warren, M.J. (2014). Towards a cell factory for vitamin B12 production in *Bacillus megaterium*: bypassing of the cobalamin riboswitch control elements. *New Biotechnol.* *31*, 553–561.

Mossialos, D., Ochsner, U., Baysse, C., Chablain, P., Pirnay, J.-P., Koedam, N., Budzikiewicz, H., Fernández, D.U., Schäfer, M., Ravel, J., et al. (2002). Identification of new, conserved, non-ribosomal peptide synthetases from fluorescent pseudomonads involved in the biosynthesis of the siderophore pyoverdine. *Mol. Microbiol.* *45*, 1673–1685.

Mulrooney, S.B., and Hausinger, R.P. (2003). Nickel uptake and utilization by microorganisms. *FEMS Microbiol. Rev.* *27*, 239–261.

Nadal-Jimenez, P., Koch, G., Reis, C.R., Muntendam, R., Raj, H., Jeronimus-Stratingh, C.M., Cool, R.H., and Quax, W.J. (2014). PvdP is a tyrosinase that drives maturation of the pyoverdine chromophore in *Pseudomonas aeruginosa*. *J. Bacteriol.* *196*, 2681–2690.

Nagar, E., and Schwarz, R. (2015). To be or not to be planktonic? Self-inhibition of biofilm development. *Environ. Microbiol.* *17*, 1477–1486.

Neubauer, U., Nowack, B., Furrer, G., and Schulin, R. (2000). Heavy metal sorption on clay minerals affected by the siderophore desferrioxamine B. *Environ. Sci. Technol.* *34*, 2749–2755.

Neumann, W., Hadley, R.C., and Nolan, E.M. (2017). Transition metals at the host-pathogen interface: how *Neisseria* exploit human metalloproteins for acquiring iron and zinc. *Essays Biochem.* *61*, 211–223.

Nieminen, T., Ukonmaanaho, L., Rausch, N., and Shoty, W. (2007). Biogeochemistry of nickel and its release into the environment. *Met Ions Life Sci* *2*, 1–29.

Nies, D.H. (1995). The cobalt, zinc, and cadmium efflux system CzcABC from *Alcaligenes eutrophus* functions as a cation-proton antiporter in *Escherichia coli*. *J. Bacteriol.* *177*, 2707–2712.

Nies, D.H. (1999). Microbial heavy-metal resistance. *Appl. Microbiol. Biotechnol.* *51*, 730–750.

Nikaido, H., and Pagès, J.-M. (2012). Broad specificity efflux pumps and their role in multidrug resistance of Gram negative bacteria. *FEMS Microbiol. Rev.* *36*, 340–363.

Nikaido, H., and Takatsuka, Y. (2009). Mechanisms of RND multidrug efflux pumps. *Biochim. Biophys. Acta* *1794*, 769–781.

Noinaj, N., Guillier, M., Barnard, T.J., and Buchanan, S.K. (2010). TonB-dependent transporters: regulation, structure, and function. *Annu. Rev. Microbiol.* *64*, 43–60.

Nunoshiba, T., Obata, F., Boss, A.C., Oikawa, S., Mori, T., Kawanishi, S., and Yamamoto, K. (1999). Role of iron and superoxide for generation of hydroxyl radical, oxidative DNA lesions, and mutagenesis in *Escherichia coli*. *J. Biol. Chem.* *274*, 34832–34837.

Ó Cuív, P., Clarke, P., Lynch, D., and O’Connell, M. (2004). Identification of *rhtX* and *fptX*, novel genes encoding proteins that show homology and function in the utilization of the siderophores rhizobactin 1021 by *Sinorhizobium meliloti* and pyochelin by *Pseudomonas aeruginosa*, respectively. *J. Bacteriol.* *186*, 2996–3005.

Ochsner, U.A., Vasil, A.I., and Vasil, M.L. (1995). Role of the ferric uptake regulator of *Pseudomonas aeruginosa* in the regulation of siderophores and exotoxin A expression: purification and activity on iron-regulated promoters. *J. Bacteriol.* *177*, 7194–7201.

Ochsner, U.A., Johnson, Z., Lamont, I.L., Cunliffe, H.E., and Vasil, M.L. (1996). Exotoxin A production in *Pseudomonas aeruginosa* requires the iron-regulated *pvdS* gene encoding an alternative sigma factor. *Mol. Microbiol.* *21*, 1019–1028.

Ochsner, U.A., Johnson, Z., and Vasil, M.L. (2000). Genetics and regulation of two distinct haem-uptake systems, *phu* and *has*, in *Pseudomonas aeruginosa*. *Microbiol. Read. Engl.* *146 (Pt 1)*, 185–198.

Ochsner, U.A., Wilderman, P.J., Vasil, A.I., and Vasil, M.L. (2002). GeneChip expression analysis of the iron starvation response in *Pseudomonas aeruginosa*: identification of novel pyoverdine biosynthesis genes. *Mol. Microbiol.* *45*, 1277–1287.

Odermatt, A., Suter, H., Krapf, R., and Solioz, M. (1993). Primary structure of two P-type ATPases involved in copper homeostasis in *Enterococcus hirae*. *J. Biol. Chem.* *268*, 12775–12779.

Okamoto, S., and Eltis, L.D. (2011). The biological occurrence and trafficking of cobalt. *Metallomics* *3*, 963–970.

O’Neill, M.J., and Wilks, A. (2013). The *P. aeruginosa* heme binding protein *PhuS* is a heme oxygenase titratable regulator of heme uptake. *ACS Chem. Biol.* *8*, 1794–1802.

Osman, D., and Cavet, J.S. (2008). Copper homeostasis in bacteria. *Adv. Appl. Microbiol.* *65*, 217–247.

Outten, C.E., and O’Halloran, T.V. (2001). Femtomolar sensitivity of metalloregulatory proteins controlling zinc homeostasis. *Science* *292*, 2488–2492.

Palmer, L.D., and Skaar, E.P. (2016). Transition metals and virulence in bacteria. *Annu. Rev. Genet.* *50*, 67–91.

Pascual, J., Lucena, T., Ruvira, M.A., Giordano, A., Gambacorta, A., Garay, E., Arahall, D.R., Pujalte, M.J., and Macián, M.C. (2012). *Pseudomonas litoralis* sp. nov., isolated from Mediterranean seawater. *Int. J. Syst. Evol. Microbiol.* *62*, 438–444.

Pechère, J.-C., and Köhler, T. (1999). Patterns and modes of beta-lactam resistance in *Pseudomonas aeruginosa*. *Clin. Microbiol. Infect. Off. Publ. Eur. Soc. Clin. Microbiol. Infect. Dis.* *5 Suppl 1*, S15–S18.

Pederick, V.G., Eijkelkamp, B.A., Begg, S.L., Ween, M.P., McAllister, L.J., Paton, J.C., and

- McDevitt, C.A. (2015). ZnuA and zinc homeostasis in *Pseudomonas aeruginosa*. *Sci. Rep.* *5*, 13139.
- Perry, R.D., and Fetherston, J.D. (2011). Yersiniabactin iron uptake: mechanisms and role in *Yersinia pestis* pathogenesis. *Microbes Infect.* *13*, 808–817.
- Piddock, L.J.V. (2006). Multidrug-resistance efflux pumps - not just for resistance. *Nat. Rev. Microbiol.* *4*, 629–636.
- Poole, K., Young, L., and Neshat, S. (1990). Enterobactin-mediated iron transport in *Pseudomonas aeruginosa*. *J. Bacteriol.* *172*, 6991–6996.
- Porcheron, G., Garénaux, A., Proulx, J., Sabri, M., and Dozois, C.M. (2013). Iron, copper, zinc, and manganese transport and regulation in pathogenic Enterobacteria: correlations between strains, site of infection and the relative importance of the different metal transport systems for virulence. *Front. Cell. Infect. Microbiol.* *3*.
- Postle, K., and Larsen, R.A. (2007). TonB-dependent energy transduction between outer and cytoplasmic membranes. *Biometals Int. J. Role Met. Ions Biol. Biochem. Med.* *20*, 453–465.
- Potvin, E., Sanschagrín, F., and Levesque, R.C. (2008). Sigma factors in *Pseudomonas aeruginosa*. *FEMS Microbiol. Rev.* *32*, 38–55.
- Pugsley, A.P., and Schnaitman, C.A. (1978). Identification of three genes controlling production of new outer membrane pore proteins in *Escherichia coli* K-12. *J. Bacteriol.* *135*, 1118–1129.
- Ragsdale, S.W. (2009). Nickel-based Enzyme Systems. *J. Biol. Chem.* *284*, 18571–18575.
- Randaccio, L., Geremia, S., Demitri, N., and Wuerges, J. (2010). Vitamin B12: unique metalorganic compounds and the most complex vitamins. *Mol. Basel Switz.* *15*, 3228–3259.
- Ranquet, C., Ollagnier-de-Choudens, S., Loiseau, L., Barras, F., and Fontecave, M. (2007). Cobalt stress in *Escherichia coli*. The effect on the iron-sulfur proteins. *J. Biol. Chem.* *282*, 30442–30451.
- Rasamiravaka, T., Labtani, Q., Duez, P., and El Jaziri, M. (2015). The formation of biofilms by *Pseudomonas aeruginosa*: a review of the natural and synthetic compounds interfering with control mechanisms.
- Ravel, J., and Cornelis, P. (2003). Genomics of pyoverdine-mediated iron uptake in pseudomonads. *Trends Microbiol.* *11*, 195–200.
- Raymond, K.N., Dertz, E.A., and Kim, S.S. (2003). Enterobactin: An archetype for microbial iron transport. *Proc. Natl. Acad. Sci. U. S. A.* *100*, 3584–3588.
- Reddy, D.V., Rothmund, S., Shenoy, B.C., Carey, P.R., and Sönnichsen, F.D. (1998). Structural characterization of the entire 1.3S subunit of transcarboxylase from *Propionibacterium shermanii*. *Protein Sci. Publ. Protein Soc.* *7*, 2156–2163.
- Reimann, C. (2012). Inner-membrane transporters for the siderophores pyochelin in *Pseudomonas aeruginosa* and enantio-pyochelin in *Pseudomonas fluorescens* display different enantioselectivities. *Microbiol. Read. Engl.* *158*, 1317–1324.
- Reimann, C., Serino, L., Beyeler, M., and Haas, D. (1998). Dihydroaeruginosic acid synthetase

and pyochelin synthetase, products of the pchEF genes, are induced by extracellular pyochelin in *Pseudomonas aeruginosa*. *Microbiol. Read. Engl.* *144 (Pt 11)*, 3135–3148.

Reimann, C., Patel, H.M., Serino, L., Barone, M., Walsh, C.T., and Haas, D. (2001). Essential PchG-dependent reduction in pyochelin biosynthesis of *Pseudomonas aeruginosa*. *J. Bacteriol.* *183*, 813–820.

Rensing, C., Fan, B., Sharma, R., Mitra, B., and Rosen, B.P. (2000). CopA: An *Escherichia coli* Cu(I)-translocating P-type ATPase. *Proc. Natl. Acad. Sci. U. S. A.* *97*, 652–656.

Ringel, M.T., Dräger, G., and Brüser, T. (2016). PvdN enzyme catalyzes a periplasmic pyoverdine modification. *J. Biol. Chem.* *291*, 23929–23938.

Rizvi, A., Rizvi, G., and Naseem, I. (2015). Calcitriol induced redox imbalance and DNA breakage in cells sharing a common metabolic feature of malignancies: Interaction with cellular copper (II) ions leads to the production of reactive oxygen species. *Tumour Biol. J. Int. Soc. Oncodevelopmental Biol. Med.* *36*, 3661–3668.

Roderick, S.L., and Matthews, B.W. (1993). Structure of the cobalt-dependent methionine aminopeptidase from *Escherichia coli*: a new type of proteolytic enzyme. *Biochemistry (Mosc.)* *32*, 3907–3912.

Rodionov, D.A., Hebbeln, P., Gelfand, M.S., and Eitinger, T. (2006). Comparative and functional genomic analysis of prokaryotic nickel and cobalt uptake transporters: evidence for a novel group of ATP-binding cassette transporters. *J. Bacteriol.* *188*, 317–327.

Rodrigue, A., Effantin, G., and Mandrand-Berthelot, M.A. (2005). Identification of rcnA (yohM), a nickel and cobalt resistance gene in *Escherichia coli*. *J. Bacteriol.* *187*, 2912–2916.

Rodrigue, A., Quentin, Y., Lazdunski, A., Méjean, V., and Foglino, M. (2000). Two-component systems in *Pseudomonas aeruginosa*: why so many? *Trends Microbiol.* *8*, 498–504.

Rowe, J.L., Starnes, G.L., and Chivers, P.T. (2005). Complex transcriptional control links NikABCDE-dependent nickel transport with hydrogenase expression in *Escherichia coli*. *J. Bacteriol.* *187*, 6317–6323.

Ruer, S., Stender, S., Filloux, A., and de Bentzmann, S. (2007). Assembly of fimbrial structures in *Pseudomonas aeruginosa*: functionality and specificity of chaperone-usher machineries. *J. Bacteriol.* *189*, 3547–3555.

Rui, H., Rivera, M., and Im, W. (2012). Protein dynamics and ion traffic in bacterioferritin. *Biochemistry (Mosc.)* *51*, 9900–9910.

Ruiz, R., Marqués, S., and Ramos, J.L. (2003). Leucines 193 and 194 at the N-terminal domain of the XylS protein, the positive transcriptional regulator of the TOL meta-cleavage pathway, are involved in dimerization. *J. Bacteriol.* *185*, 3036–3041.

Ryder, C., Byrd, M., and Wozniak, D.J. (2007). Role of polysaccharides in *Pseudomonas aeruginosa* biofilm development. *Curr. Opin. Microbiol.* *10*, 644–648.

Saecker, R.M., Record, M.T., and deHaseth, P.L. (2011). Mechanism of bacterial transcription initiation: RNA polymerase - promoter binding, isomerization to initiation-competent open

complexes, and initiation of RNA synthesis. *J. Mol. Biol.* *412*, 754–771.

Santos, S.P., Mitchell, E.P., Franquelim, H.G., Castanho, M.A.R.B., Abreu, I.A., and Romão, C.V. (2015). Dps from *Deinococcus radiodurans*: oligomeric forms of Dps1 with distinct cellular functions and Dps2 involved in metal storage. *FEBS J.* *282*, 4307–4327.

Schalk, I.J. (2008). Metal trafficking via siderophores in Gram-negative bacteria: specificities and characteristics of the pyoverdine pathway. *J. Inorg. Biochem.* *102*, 1159–1169.

Schalk, I.J., and Guillon, L. (2013a). Fate of ferrisiderophores after import across bacterial outer membranes: different iron release strategies are observed in the cytoplasm or periplasm depending on the siderophore pathways. *Amino Acids* *44*, 1267–1277.

Schalk, I.J., and Guillon, L. (2013b). Pyoverdine biosynthesis and secretion in *Pseudomonas aeruginosa*: implications for metal homeostasis. *Environ. Microbiol.* *15*, 1661–1673.

Schalk, I.J., Hennard, C., Dugave, C., Poole, K., Abdallah, M.A., and Pattus, F. (2001). Iron-free pyoverdinin binds to its outer membrane receptor FpvA in *Pseudomonas aeruginosa*: a new mechanism for membrane iron transport. *Mol. Microbiol.* *39*, 351–360.

Schalk, I.J., Abdallah, M.A., and Pattus, F. (2002). Recycling of pyoverdinin on the FpvA receptor after ferric pyoverdinin uptake and dissociation in *Pseudomonas aeruginosa*. *Biochemistry (Mosc.)* *41*, 1663–1671.

Schalk, I.J., Hannauer, M., and Braud, A. (2011). New roles for bacterial siderophores in metal transport and tolerance. *Environ. Microbiol.* *13*, 2844–2854.

Schalk, I.J., Mislin, G.L.A., and Brillet, K. (2012). Structure, function and binding selectivity and stereoselectivity of siderophore-iron outer membrane transporters. *Curr. Top. Membr.* *69*, 37–66.

Schleif, R. (2003). AraC protein: a love-hate relationship. *BioEssays News Rev. Mol. Cell. Dev. Biol.* *25*, 274–282.

Schmitt, M.P. (2002). Analysis of a DtxR-like metalloregulatory protein, MntR, from *Corynebacterium diphtheriae* that controls expression of an ABC metal transporter by an Mn(2+)-dependent mechanism. *J. Bacteriol.* *184*, 6882–6892.

Schramm, E., Mende, J., Braun, V., and Kamp, R.M. (1987). Nucleotide sequence of the colicin B activity gene *cba*: consensus pentapeptide among TonB-dependent colicins and receptors. *J. Bacteriol.* *169*, 3350–3357.

Schreiber, K., Boes, N., Eschbach, M., Jaensch, L., Wehland, J., Bjarnsholt, T., Givskov, M., Hentzer, M., and Schobert, M. (2006). Anaerobic survival of *Pseudomonas aeruginosa* by pyruvate fermentation requires an Usp-type stress protein. *J. Bacteriol.* *188*, 659–668.

Seebach, D., Müller, H.M., Bürger, H.M., and Plattner, D.A. (1992). The triolide of (R)-3-hydroxybutyric acid—direct preparation from polyhydroxybutyrate and formation of a crown estercarbonyl complex with Na ions. *Angew. Chem. Int. Ed. Engl.* *31*, 434–435.

Serino, L., Reimann, C., Visca, P., Beyeler, M., Chiesa, V.D., and Haas, D. (1997). Biosynthesis of pyochelin and dihydroaeruginic acid requires the iron-regulated *pchDCBA* operon in *Pseudomonas aeruginosa*. *J. Bacteriol.* *179*, 248–257.

- Silby, M.W., Winstanley, C., Godfrey, S.A.C., Levy, S.B., and Jackson, R.W. (2011). *Pseudomonas* genomes: diverse and adaptable. *FEMS Microbiol. Rev.* *35*, 652–680.
- Silva, J.J.R.F. da, and Williams, R.J.P. (2001). *The biological chemistry of the elements: the inorganic chemistry of life* (Oxford, New York: Oxford University Press).
- Silver, S., and Phung, L.T. (1996). Bacterial heavy metal resistance: new surprises. *Annu. Rev. Microbiol.* *50*, 753–789.
- Smith, R.L., Banks, J.L., Snively, M.D., and Maguire, M.E. (1993). Sequence and topology of the CorA magnesium transport systems of *Salmonella typhimurium* and *Escherichia coli*. Identification of a new class of transport protein. *J. Biol. Chem.* *268*, 14071–14080.
- Solioz, M., Abicht, H.K., Mermod, M., and Mancini, S. (2010). Response of gram-positive bacteria to copper stress. *J. Biol. Inorg. Chem. JBIC Publ. Soc. Biol. Inorg. Chem.* *15*, 3–14.
- Stewart, P.S., and Costerton, J.W. (2001). Antibiotic resistance of bacteria in biofilms. *Lancet Lond. Engl.* *358*, 135–138.
- Stintzi, A., Evans, K., Meyer, J.M., and Poole, K. (1998). Quorum-sensing and siderophore biosynthesis in *Pseudomonas aeruginosa*: lasR/lasI mutants exhibit reduced pyoverdine biosynthesis. *FEMS Microbiol. Lett.* *166*, 341–345.
- Stojiljkovic, I., and Hantke, K. (1995). Functional domains of the *Escherichia coli* ferric uptake regulator protein (Fur). *Mol. Gen. Genet. MGG* *247*, 199–205.
- Stover, C.K., Pham, X.Q., Erwin, A.L., Mizoguchi, S.D., Warrenner, P., Hickey, M.J., Brinkman, F.S.L., Hufnagle, W.O., Kowalik, D.J., Lagrou, M., et al. (2000). Complete genome sequence of *Pseudomonas aeruginosa* PAO1, an opportunistic pathogen. *Nature* *406*, 959–964.
- Strateva, T., and Yordanov, D. (2009). *Pseudomonas aeruginosa* - a phenomenon of bacterial resistance. *J. Med. Microbiol.* *58*, 1133–1148.
- Suh, S.-J., Runyen-Janecky, L.J., Maleniak, T.C., Hager, P., MacGregor, C.H., Zielinski-Mozny, N.A., Phibbs, P.V., and West, S.E.H. (2002). Effect of vfr mutation on global gene expression and catabolite repression control of *Pseudomonas aeruginosa*. *Microbiol. Read. Engl.* *148*, 1561–1569.
- Sutherland, I.W. (2001). The biofilm matrix--an immobilized but dynamic microbial environment. *Trends Microbiol.* *9*, 222–227.
- Teitzel, G.M., Geddie, A., De Long, S.K., Kirisits, M.J., Whiteley, M., and Parsek, M.R. (2006). Survival and growth in the presence of elevated copper: transcriptional profiling of copper-stressed *Pseudomonas aeruginosa*. *J. Bacteriol.* *188*, 7242–7256.
- Thelander, L., Gräslund, A., and Thelander, M. (1983). Continual presence of oxygen and iron required for mammalian ribonucleotide reduction: possible regulation mechanism. *Biochem. Biophys. Res. Commun.* *110*, 859–865.
- Tilles, G., and Wallach, D. (1996). [History of the treatment of syphilis with mercury: five centuries of uncertainty and toxicity]. *Rev. Hist. Pharm.* *44*, 347–351.
- Tobes, R., and Ramos, J.L. (2002). AraC-XylS database: a family of positive transcriptional

regulators in bacteria. *Nucleic Acids Res.* *30*, 318–321.

Totter, S., Harvie, D.R., and Robinson, N.J. (2005). Understanding how cells allocate metals using metal sensors and metallochaperones. *Acc. Chem. Res.* *38*, 775–783.

Tseng, C.-F., Burger, A., Mislin, G.L.A., Schalk, I.J., Yu, S.S.-F., Chan, S.I., and Abdallah, M.A. (2006). Bacterial siderophores: the solution stoichiometry and coordination of the Fe(III) complexes of pyochelin and related compounds. *JBIC J. Biol. Inorg. Chem.* *11*, 419–432.

Tsuji, A., Kaneko, Y., Takahashi, K., Ogawa, M., and Goto, S. (1982). The effects of temperature and pH on the growth of eight enteric and nine glucose non-fermenting species of gram-negative rods. *Microbiol. Immunol.* *26*, 15–24.

Valdebenito, M., Crumbliss, A.L., Winkelmann, G., and Hantke, K. (2006). Environmental factors influence the production of enterobactin, salmochelin, aerobactin, and yersiniabactin in *Escherichia coli* strain Nissle 1917. *Int. J. Med. Microbiol. IJMM* *296*, 513–520.

Vander Wauven, C., Piérard, A., Kley-Raymann, M., and Haas, D. (1984). *Pseudomonas aeruginosa* mutants affected in anaerobic growth on arginine: evidence for a four-gene cluster encoding the arginine deiminase pathway. *J. Bacteriol.* *160*, 928–934.

Venturi, V., Weisbeek, P., and Koster, M. (1995). Gene regulation of siderophore-mediated iron acquisition in *Pseudomonas*: not only the Fur repressor. *Mol. Microbiol.* *17*, 603–610.

Vinckx, T., Matthijs, S., and Cornelis, P. (2008). Loss of the oxidative stress regulator OxyR in *Pseudomonas aeruginosa* PAO1 impairs growth under iron-limited conditions. *FEMS Microbiol. Lett.* *288*, 258–265.

Visca, P., Colotti, G., Serino, L., Verzili, D., Orsi, N., and Chiancone, E. (1992). Metal regulation of siderophore synthesis in *Pseudomonas aeruginosa* and functional effects of siderophore-metal complexes. *Appl. Environ. Microbiol.* *58*, 2886–2893.

Visca, P., Leoni, L., Wilson, M.J., and Lamont, I.L. (2002). Iron transport and regulation, cell signalling and genomics: lessons from *Escherichia coli* and *Pseudomonas*. *Mol. Microbiol.* *45*, 1177–1190.

Wakeman, C.A., and Skaar, E.P. (2012). Metalloregulation of Gram-positive pathogen physiology. *Curr. Opin. Microbiol.* *15*, 169–174.

Waldron, K.J., and Robinson, N.J. (2009). How do bacterial cells ensure that metalloproteins get the correct metal? *Nat. Rev. Microbiol.* *7*, 25–35.

Weinberg, E.D. (1997). The *Lactobacillus* anomaly: total iron abstinence. *Perspect. Biol. Med.* *40*, 578–583.

Wilderman, P.J., Vasil, A.I., Johnson, Z., Wilson, M.J., Cunliffe, H.E., Lamont, I.L., and Vasil, M.L. (2001). Characterization of an endoprotease (PrpL) encoded by a PvdS-regulated gene in *Pseudomonas aeruginosa*. *Infect. Immun.* *69*, 5385–5394.

Wilderman, P.J., Sowa, N.A., FitzGerald, D.J., FitzGerald, P.C., Gottesman, S., Ochsner, U.A., and Vasil, M.L. (2004). Identification of tandem duplicate regulatory small RNAs in *Pseudomonas aeruginosa* involved in iron homeostasis. *Proc. Natl. Acad. Sci. U. S. A.* *101*, 9792–9797.

Yao, H., Jepkorir, G., Lovell, S., Nama, P.V., Weeratunga, S., Battaile, K.P., and Rivera, M. (2011). Two distinct ferritin-like molecules in *Pseudomonas aeruginosa*: the product of the *bfrA* gene is a bacterial ferritin (FtnA) and not a bacterioferritin (Bfr). *Biochemistry (Mosc.)* *50*, 5236–5248.

Yarza, P., Ludwig, W., Euzéby, J., Amann, R., Schleifer, K.-H., Glöckner, F.O., and Rosselló-Móra, R. (2010). Update of the All-Species Living Tree Project based on 16S and 23S rRNA sequence analyses. *Syst. Appl. Microbiol.* *33*, 291–299.

Yeterian, E., Martin, L.W., Guillon, L., Journet, L., Lamont, I.L., and Schalk, I.J. (2010). Synthesis of the siderophore pyoverdine in *Pseudomonas aeruginosa* involves a periplasmic maturation. *Amino Acids* *38*, 1447–1459.

Youard, Z.A., and Reimmann, C. (2010). Stereospecific recognition of pyochelin and enantio-pyochelin by the PchR proteins in fluorescent pseudomonads. *Microbiology* *156*, 1772–1782.

Youard, Z.A., Wenner, N., and Reimmann, C. (2011). Iron acquisition with the natural siderophore enantiomers pyochelin and enantio-pyochelin in *Pseudomonas* species. *Biometals Int. J. Role Met. Ions Biol. Biochem. Med.* *24*, 513–522.

Zamri, A., and Abdallah, M. (2000). An Improved Stereocontrolled Synthesis of Pyochelin, Siderophore of *Pseudomonas aeruginosa* and *Burkholderia cepacia*. *Tetrahedron* *56*, 249–256.

Zannoni, D., Borsetti, F., Harrison, J.J., and Turner, R.J. (2008). The bacterial response to the chalcogen metalloids Se and Te. *Adv. Microb. Physiol.* *53*, 1–72.

Zeth, K. (2012). Dps biomineralizing proteins: multifunctional architects of nature. *Biochem. J.* *445*, 297–311.

Zhang, Y.-B., Monchy, S., Greenberg, B., Mergeay, M., Gang, O., Taghavi, S., and van der Lelie, D. (2009). ArsR arsenic-resistance regulatory protein from *Cupriavidus metallidurans* CH34. *Antonie Van Leeuwenhoek* *96*, 161–170.

Zhu, M., Valdebenito, M., Winkelmann, G., and Hantke, K. (2005). Functions of the siderophore esterases IroD and IroE in iron-salmochelin utilization. *Microbiol. Read. Engl.* *151*, 2363–2372.

Bacterial siderophores: structure and NMR assignment of pyoverdin Pa, siderophores of *Pseudomonas aeruginosa* ATCC 15692.

Web links:

BIFTM program:

<http://www.bif.kit.edu/58.php>

Chemspider:

<http://www.chemspider.com/Chemical-Structure.16738332.html>

European Centre for Disease Prevention and Control (ECDC), 2014:
<https://ecdc.europa.eu/sites/portal/files/media/en/publications/Publications/antimicrobial-resistance-europe-2014.pdf>

P. aeruginosa database:
www.pseudomonas.com

Uniprot:
www.uniprot.org

RCBS protein data bank:
<http://www.rcsb.org/pdb/explore.do?structureId=1xkw>

Note: The illustrations elements used to create the homemade figures of this Thesis were obtained and modified from Servier Medical Art by Servier (<https://smart.servier.com/>).

RÉSUMÉ DE THÈSE

Rôle des voies d'import du fer impliquant des sidérophores dans l'homéostasie de métaux biologiques autres que le fer chez *Pseudomonas aeruginosa*

Ana Yaiza Carballido López

Introduction

Pseudomonas aeruginosa est une bactérie à Gram-négatif, pathogène et opportuniste, responsable de nombreuses et sévères infections chez l'homme. Ce microorganisme comme la quasi totalité des organismes vivants a besoin de fer pour sa croissance ainsi que d'autres métaux biologiques comme le zinc, le cuivre, le nickel, le manganèse, le cobalt, le molybdène, le vanadium. Ces métaux sont impliqués dans de nombreux processus biologiques important pour la survie cellulaire. Mais à fortes concentrations, ces métaux deviennent souvent toxiques, produisant un stress oxydatif dans le cas du Fe, du Cu et du Co (Valko et al., 2005) ou interagissant avec des cibles non spécifiques (Foster et al. , 2014). Il est donc nécessaire pour les cellules bactériennes de finement réguler l'import de ces métaux biologiques dans le cytoplasme bactérien (ou l'homéostasie de ces métaux) pour éviter une carence ou une concentration trop élevée pouvant être toxique.

A ce jour, c'est essentiellement l'homéostasie du fer qui a été étudiée chez les bactéries, les autres métaux ont suscité nettement moins d'intérêt. Malgré l'importance du fer pour la croissance bactérienne, ce métal, est paradoxalement très peu biodisponible en présence d'oxygène et à pH physiologique, car il précipite sous forme d'hydroxyde ferrique. Pour accéder au fer, les bactéries produisent et sécrètent des sidérophores, qui sont des molécules de poids moléculaire de 200 à 2000 Da se caractérisant par une très forte affinité pour le fer. *P. aeruginosa* produit deux sidérophores majeurs, la pyoverdine (PVD) et la pyochelin (PCH) (Cornelis et al., 2009; Cornelis, 2010; Hider et Kong, 2010). Les sidérophores jouent un rôle clé dans l'acquisition du fer chez les bactéries et ceci dans n'importe quel environnement que se soit durant une infection ou par exemple dans la rhizosphère. Il a été montré également, que les sidérophores sont impliqués dans la tolérance des bactéries vis à vis à des métaux lourds, en diminuant l'accumulation de ces métal par diffusion dans les bactéries (Braud et al., 2010; Schalk et al., 2011). Certaines données préliminaires dans la littérature suggèrent aussi que les sidérophores pourraient jouer un rôle dans l'import d'autres métaux biologiques que le fer.

Objectif

Nous avons dans un premier temps mieux caractérisés ces mécanismes de régulation de l'expression des protéines impliquées dans les voies d'import du fer *via* les sidérophores PVD et PCH (protéines de synthèse de sidérophores et protéines impliquées dans l'import des complexes PVD-Fe et PCH-Fe) dans le cadre de la réponse au stress ferrique.

Dans un second temps, nous avons étudié le rôle des sidérophores PVD et PCH dans l'homéostasie des métaux biologiques autre que le fer chez *P. aeruginosa*, aussi bien dans des conditions de carences en ces métaux que dans des conditions de stress du à la présence de fortes concentrations de ces métaux. Plus particulièrement nous avons essayé d'identifier si la PVD ou la PCH pouvait être impliqué dans l'import d'un autre métal biologique que le fer. Ensuite, nous avons essayé de mieux comprendre les mécanismes moléculaires impliqués dans la régulation de l'expression des voies PVD et PCH (c'est-à-dire dans l'expression des protéines de biosynthèses de ces sidérophores et les protéines impliquées dans l'import des complexes PVD-métal ou PCH-métal) en présence de métaux biologiques autre que le fer. Nous avons essayé d'identifier si d'autres métaux pouvaient jouer un rôle dans ces mécanismes de régulation et la capacité des complexes PVD-métal ou PCH-métal à interagir avec les régulateurs transcriptionnels.

Résultats

1.- Mécanismes de régulation des voies PVD et PCH

En conditions de carence en fer, l'expression des protéines impliquées dans les voies PVD et PCH est activée et de ce fait la production de sidérophores également. Cette régulation implique pour la voie PVD deux facteurs sigmas (FpvI et PvdS) et un facteur anti-sigma (FpvR), et pour la voie PCH un régulateur PchR de la famille des régulateurs AraC. Dans les deux cas, une boucle d'auto-activation avait été identifiée : la PVD et la PCH sont indispensables pour l'activation de ces voies, ce qui permet d'éviter leur synthèse lorsque la bactérie n'est plus capable d'importer ces sidérophores. Lorsque la bactérie a acquis suffisamment de fer, les voies PVD et PCH sont réprimées par le régulateur Fur. Ces mécanismes de régulation permettent de donner une image instantanée de l'expression des deux sidérophores dans des cas extrêmes (forte concentration en fer, ou forte carence), mais ne donne pas d'indication sur la dynamique de ces régulations, lors de variations des conditions de carence, ou lors de la présence de compétiteurs (sidérophores produits par d'autres organismes).

Durant cette thèse, nous avons étudié plus en détail l'expression de ces deux voies afin de mieux comprendre cette dynamique. Ainsi, nous avons démontré que la PVD n'est pas indispensable à sa propre synthèse en cas de forte carence en fer, c'est-à-dire la boucle d'auto-activation n'est pas indispensable dans ces conditions. Le rôle de la boucle d'auto-activation permet en fait de répondre plus finement aux variations de la concentration en fer. Par des expériences de FACS, nous avons montré qu'en cas de forte carence en fer, cette boucle permet d'augmenter beaucoup plus rapidement l'expression de PVD. Par délétion de certaines protéines de la voie de biosynthèse de la PVD, et suivie de l'expression des différents protagonistes (qRT-PCR, ou fusion des protéines à des rapporteurs fluorescents), nous avons également montré que lorsque la carence en fer est moindre, cette boucle prend plus d'importance dans la régulation de l'expression de la PVD, et contribue à diminuer plus rapidement la production de PVD lorsque les conditions sont plus favorables.

Nous avons également montré que la voie PCH est moins réactive que la voie PVD aux variations de concentration en fer. Si la boucle d'auto-activation de la voie PCH est bien indispensable dans la plupart des situations, l'expression de la voie PCH diminue plus lentement que celle de la PVD par exemple.

Enfin la régulation des voies PVD et PCH par Fur n'est pas non plus identique. Cette régulation s'exerce plus rapidement sur la voie PVD que sur la voie PCH, contribuant à différencier l'expression de ces deux voies en fonction des situations en fer.

Au final, en condition de faible carence en fer, la cellule privilégie l'expression du sidérophore PCH, alors que la PVD est beaucoup plus rapidement synthétisée en cas de carence en fer plus prononcée. Par ailleurs, la présence de sidérophores compétiteurs (sidérophores produits par d'autres bactéries) affecte prioritairement l'expression de la PCH, par inhibition de la boucle d'auto-activation, alors que la voie PVD reste active. Cela permet à la cellule d'avoir un sidérophore fonctionnel (PVD), même en présence de bactéries compétitrices. Enfin, ces résultats indiquent aussi que le piratage de ces voies par d'autres métaux puisse perturber plus fortement la voie PCH que la voie PVD. L'ensemble de ces données sera publié dans un article en cours de rédaction.

2.- Sidérophores PVD et PCH et l'homéostasie des métaux biologiques autres que le fer

En utilisant des protéines de fusion entre mCherry et différentes protéines des voies PVD et PCH (introduction du gène de la protéine fluorescente au niveau du chromosome) et en dosant la production de sidérophores dans les milieux de culture de *P. aeruginosa* nous avons pu mettre en évidence que seul le Co^{2+} réprimait l'expression de la voie PVD, mais avec un impact atténué comparé au fer. Aucun effet n'a été observé pour tous les autres métaux biologiques testés. Concernant la voie PCH, une répression équivalente de l'expression de la voie PCH et de la production de ce sidérophore a été observée pour le Fer et le Co^{2+} . Un effet atténué mais allant dans le même sens a été observé pour le Ni^{2+} et les autres métaux : $\text{Fe}^{3+} \approx \text{Co}^{2+} > \text{Ni}^{2+} > \text{Mn}^{2+} \gg \text{Cu}^{2+} = \text{Zn}^{2+}$. Ces premiers résultats semblaient indiquer que la PCH pouvait jouer un rôle dans l'homéostasie du Co^{2+} et éventuellement du Ni^{2+} ou Mn^{2+} .

Dans un second temps, nous avons dosé l'import de fer, de Co^{2+} , de Ni^{2+} et de Mn^{2+} par la voie PCH chez *P. aeruginosa* par une approche utilisant l'ICP-AES (Plasma à couplage inductif couplé à la spectrométrie d'émission atomique). Cette étude a montré effectivement un transport du Co^{2+} dépendant de la PCH chez *P. aeruginosa*. Pour le Ni^{2+} et le Mn^{2+} aucun transport significatif n'a été mis en évidence. Nous avons également montré que le Co^{2+} entrainait en compétition avec le fer dans des expériences de transport de fer radioactif (^{55}Fe) via la PCH chez *P. aeruginosa*. Ces différentes approches ont permis de démontrer clairement que la PCH était capable de transporter dans les cellules de *P. aeruginosa* le fer et le Co^{2+} .

PchR est le régulateur cytoplasmique qui active la transcription des gènes codants pour les différentes protéines de la voie PCH (protéines de synthèse de la PCH et d'import de la PCH en complexe avec le fer). L'import du complexe PCH-Fe dans le cytoplasme de la bactérie permet d'activer le régulateur PchR en formant un complexe PchR-PCH-Fe, se liant ensuite aux promoteurs des gènes de la voie PCH. Nous avons surexprimé et purifié PchR et étudié sa capacité à interagir avec la PCH en complexe avec le Co^{2+} . Ces expériences de liaisons ont été réalisées en suivant les changements de l'émission de fluorescence des tryptophanes de la protéine PchR. L'étude a montré que PCH-Co pouvait interagir avec le régulateur PchR mais avec une affinité moindre comparée à celle du complexe PCH-Fe. Cette interaction entre PCH-Co et PchR est en accord avec les effets observés du Co^{2+} sur l'expression de la voie PCH.

A fin de mieux comprendre l'homéostasie du Co^{2+} chez *P. aeruginosa* et la possible implication du sidérophore PCH, nous avons également réalisé des études protéomiques ou nous avons

comparé le protéome d'une part de cellules de *P. aeruginosa* cultivées en présence et en absence de fer ou de Co et d'autre part le protéome de cellules sauvages avec celui d'un mutant *pchR*. Cette seconde étude devait permettre d'identifier les protéines dont la transcription est sous l'effet du régulateur transcriptionnel PchR. Ces études protéomiques ont été réalisées en collaboration avec le laboratoire de Dirk Bumann du Biozentrum à Bâle.

La présence de Co^{2+} a moduler l'expression des protéines de la voie PCH, mais aussi d'autres protéines comme la pompe d'efflux Ni/Co dont l'expression a été augmentée.

La suppression du gène *pchR* induit la répression des gènes impliqués dans l'import de soufre, impliqué dans la synthèse de la cystéine, un métabolite précurseur dans la biosynthèse de PCH, et des gènes codant pour les enzymes impliquées dans la dégradation des molécules organo-soufrées. La PCH étant une molécule organo-soufrée, il est possible que ces enzymes soient impliquées dans la dégradation de la PCH. Nous avons également observé une répression de gènes d'enzymes impliquées dans les procédés d'oxydo-réduction. La PCH peut induire un stress oxydatif pouvant expliquer l'exigence d'enzymes protectrices.

Conclusion

Toutes nos données indiquent clairement que le Co^{2+} peut être transporté dans les cellules de *P. aeruginosa* par le sidérophore PCH. Lorsque ce métal est présent en excès, il réprime l'expression des protéines de la voie PCH et la production de PCH probablement du à l'interaction avec le régulateur PchR. Toutes ces données sont en accords avec les données de la première partie de cette thèse (mécanisme de régulation de l'expression de la voie PCH) et indiquent que la PCH joue un rôle dans l'homéostasie du Co^{2+} . Malheureusement pour l'instant nous n'avons pas pu démontrer que ce transport du Co^{2+} par la PCH avait une signification biologique et n'était pas un transport parasite avec le Co^{2+} entrant juste en compétition avec le fer. En effet, la concentration de Co^{2+} nécessaire à la vie de *P. aeruginosa* étant beaucoup plus faible que pour le fer, il est très difficile d'évaluer l'importance biologique de ce transport du Co^{2+} par la PCH. Néanmoins tous nos résultats permettent de comprendre comment le Co^{2+} interagit avec la PCH d'écrite à ce jour comme transportant uniquement le fer dans les cellules de *P. aeruginosa*.

Rôle des voies d'import du fer impliquant des sidérophores dans l'homéostasie de métaux biologiques autres que le fer chez *Pseudomonas aeruginosa*

Les métaux biologiques jouent un rôle clé en tant que cofacteurs, contribuant à la structuration des macromolécules et catalysant les réactions biochimiques dans les cellules. Ils sont nécessaires pour une croissance bactérienne optimale mais deviennent toxiques lorsqu'ils sont présents en excès. Par conséquent, l'homéostasie de ces métaux doit être finement régulée, et tout déséquilibre dans leur concentration pourrait affecter la viabilité cellulaire. Lors de cette thèse nous avons investigué les mécanismes moléculaires impliqués dans l'homéostasie du Fe chez *Pseudomonas aeruginosa*, en étudiant les deux principaux sidérophores produits par cette bactérie, pyoverdine (PVD) et pyochéline (PCH). Avec notre approche, nous avons identifié des nouveaux mécanismes de régulation des voies d'acquisition du fer par PVD et PCH. Nous avons également étudié comment d'autres métaux biologiques peuvent interférer avec ces voies, et le Co a montré une forte propension à pirater et à polluer la voie PCH.

- Mots-clés: Métal, homéostasie, cobalt, fer, pyochéline, pyoverdine, *P. aeruginosa*, régulation.

Biological metals (Fe, Zn, Co, Ni, Mn, Cu) play a key role by acting as co-factors, contributing to macromolecule structuration, and catalyzing biochemical reactions into the cells. They are required for optimal bacterial growth but also become toxic when present in excess. Consequently, the homeostasis of these metals has to be finely regulated, and any disequilibrium in their concentration into bacteria could affect cell viability. We have further investigated the molecular mechanisms implicated in Fe homeostasis in *Pseudomonas aeruginosa* involving the two major siderophores produced by this bacterium, pyoverdine (PVD) and pyochelin (PCH). With our approach we identified new regulation mechanisms of both PVD and PCH pathways. In parallel, we have also investigated how other biological metals than Fe can interfere with these iron uptake pathways. Our data showed a strong propensity of Co to pirate and pollute the PCH iron uptake pathway.

- Keywords: Metal, homeostasis, cobalt, iron, pyochelin, pyoverdine, *P. aeruginosa*, regulation.